

# Color in Wiki

20170628

# Contents

<b>1</b>	<b>Color Space</b>	<b>1</b>
1.1	CIE 1931 color space . . . . .	1
1.1.1	Tristimulus values . . . . .	1
1.1.2	Meaning of $X$ , $Y$ and $Z$ . . . . .	2
1.1.3	CIE standard observer . . . . .	2
1.1.4	CIE xy chromaticity diagram and the CIE xyY color space . . . . .	4
1.1.5	Definition of the CIE XYZ color space . . . . .	4
1.1.6	See also . . . . .	7
1.1.7	References . . . . .	7
1.1.8	Further reading . . . . .	8
1.1.9	External links . . . . .	8
1.2	CIE 1960 color space . . . . .	8
1.2.1	Background . . . . .	9
1.2.2	Relation to CIE XYZ . . . . .	9
1.2.3	Relation to CIELUV . . . . .	9
1.2.4	References . . . . .	10
1.2.5	External links . . . . .	10
1.3	CIE 1964 color space . . . . .	10
1.3.1	Chromaticity and color difference . . . . .	10
1.3.2	References . . . . .	10
1.4	CIELUV . . . . .	10
1.4.1	Historical background . . . . .	11
1.4.2	$XYZ \rightarrow CIELUV$ and $CIELUV \rightarrow XYZ$ conversions . . . . .	11
1.4.3	Cylindrical representation (CIELCH) . . . . .	12
1.4.4	Color and hue difference . . . . .	12
1.4.5	See also . . . . .	12
1.4.6	References . . . . .	12
1.4.7	External links . . . . .	12
1.5	LMS color space . . . . .	12
1.5.1	$XYZ$ to LMS . . . . .	12
1.5.2	See also . . . . .	13
1.5.3	References . . . . .	13

1.6	Lab color space . . . . .	13
1.6.1	Advantages . . . . .	14
1.6.2	Differentiation . . . . .	15
1.6.3	CIELAB . . . . .	15
1.6.4	CIELAB-CIEXYZ conversions . . . . .	16
1.6.5	Hunter Lab . . . . .	16
1.6.6	Cylindrical representation: CIELCh or CIEHLC . . . . .	17
1.6.7	See also . . . . .	18
1.6.8	References . . . . .	18
1.6.9	External links . . . . .	18
1.7	CIECAM02 . . . . .	20
1.7.1	Viewing conditions . . . . .	20
1.7.2	Parameter decision table . . . . .	20
1.7.3	Chromatic adaptation . . . . .	21
1.7.4	Appearance correlates . . . . .	22
1.7.5	References . . . . .	23
1.7.6	External links . . . . .	23
1.8	Primary color . . . . .	24
1.8.1	Biological basis . . . . .	24
1.8.2	History . . . . .	25
1.8.3	Examples . . . . .	25
1.8.4	See also . . . . .	27
1.8.5	References . . . . .	27
1.9	Cone cell . . . . .	27
1.9.1	Types . . . . .	28
1.9.2	Structure . . . . .	28
1.9.3	Diseases . . . . .	29
1.9.4	Color afterimage . . . . .	29
1.9.5	See also . . . . .	29
1.9.6	References . . . . .	30
1.9.7	External links . . . . .	30
1.10	Spectral sensitivity . . . . .	30
1.10.1	See also . . . . .	31
1.10.2	References . . . . .	31
<b>2</b>	<b>RGB Color Gamut</b>	<b>32</b>
2.1	Planck's law . . . . .	32
2.1.1	Introduction . . . . .	32
2.1.2	Different forms . . . . .	33
2.1.3	Derivation . . . . .	34
2.1.4	Physics . . . . .	36
2.1.5	Properties . . . . .	40

2.1.6	History . . . . .	42
2.1.7	See also . . . . .	47
2.1.8	References . . . . .	47
2.1.9	External links . . . . .	54
2.2	Planckian locus . . . . .	54
2.2.1	The Planckian locus in the XYZ color space . . . . .	54
2.2.2	Correlated color temperature . . . . .	55
2.2.3	References . . . . .	56
2.2.4	External links . . . . .	56
2.3	Planck–Einstein relation . . . . .	56
2.3.1	Spectral forms . . . . .	57
2.3.2	de Broglie relation . . . . .	57
2.3.3	Bohr’s frequency condition . . . . .	57
2.3.4	References . . . . .	57
2.3.5	Cited bibliography . . . . .	58
2.4	Standard illuminant . . . . .	58
2.4.1	CIE illuminants . . . . .	58
2.4.2	White point . . . . .	62
2.4.3	References . . . . .	62
2.4.4	External links . . . . .	64
2.5	Black body . . . . .	64
2.5.1	Definition . . . . .	64
2.5.2	Idealizations . . . . .	64
2.5.3	Realizations . . . . .	65
2.5.4	Radiative cooling . . . . .	67
2.5.5	See also . . . . .	68
2.5.6	References . . . . .	68
2.5.7	External links . . . . .	71
2.6	Illuminant D65 . . . . .	71
2.6.1	History . . . . .	71
2.6.2	Definition . . . . .	72
2.6.3	Why 6504 K? . . . . .	72
2.6.4	References . . . . .	72
2.6.5	External links . . . . .	73
2.7	RGB color space . . . . .	73
2.7.1	Intuition . . . . .	73
2.7.2	Applications . . . . .	74
2.7.3	Specifications . . . . .	74
2.7.4	See also . . . . .	74
2.7.5	References . . . . .	74
2.7.6	External links . . . . .	74

2.8	sRGB	74
2.8.1	The sRGB gamut	74
2.8.2	The sRGB transfer function (“gamma”)	75
2.8.3	Specification of the transformation	75
2.8.4	Theory of the transformation	76
2.8.5	Viewing environment	76
2.8.6	Usage	77
2.8.7	See also	77
2.8.8	References	77
2.8.9	External links	78
2.9	rg chromaticity	78
2.9.1	Conversion between RGB and rg chromaticity	78
2.9.2	Pixel-Based Photometric Invariance	78
2.9.3	RGB Color specification System	80
2.9.4	Conversion xyY color system	81
2.9.5	See also	81
2.9.6	References	81
2.10	Adobe RGB color space	81
2.10.1	Historical background	82
2.10.2	Specifications	82
2.10.3	Comparison to sRGB	83
2.10.4	See also	83
2.10.5	References	83
2.10.6	External links	84
2.11	Wide-gamut RGB color space	84
2.11.1	References	84
2.12	ProPhoto RGB color space	84
2.12.1	Development	85
2.12.2	ProPhoto RGB (ROMM RGB) Encoding Primaries	85
2.12.3	Viewing Environment	85
2.12.4	Encoding Function	85
2.12.5	References	85
2.12.6	External links	85
2.13	scRGB	86
2.13.1	Encoding	86
2.13.2	Usage	86
2.13.3	Origin of sc in scRGB	86
2.13.4	See also	86
2.13.5	References	86
2.13.6	External links	87
2.14	DCI-P3	87

2.14.1 History . . . . .	87
2.14.2 System colorimetry . . . . .	87
2.14.3 References . . . . .	87
2.15 Rec. 709 . . . . .	88
2.15.1 Technical details . . . . .	88
2.15.2 See also . . . . .	89
2.15.3 References . . . . .	89
2.15.4 External links . . . . .	90
2.16 Rec. 2020 . . . . .	90
2.16.1 Technical details . . . . .	90
2.16.2 Implementations . . . . .	91
2.16.3 Rec. 2100 . . . . .	92
2.16.4 See also . . . . .	92
2.16.5 References . . . . .	92
2.16.6 External links . . . . .	94
2.17 Rec. 2100 . . . . .	94
2.17.1 Resolution . . . . .	94
2.17.2 Frame rate . . . . .	94
2.17.3 Digital representation . . . . .	94
2.17.4 System colorimetry . . . . .	95
2.17.5 Luma coefficients . . . . .	95
2.17.6 Signal formats . . . . .	95
2.17.7 Optical Transfer functions . . . . .	95
2.17.8 See also . . . . .	95
2.17.9 References . . . . .	95
2.17.10 External links . . . . .	95
<b>3 Text and image sources, contributors, and licenses</b>	<b>96</b>
3.1 Text . . . . .	96
3.2 Images . . . . .	99
3.3 Content license . . . . .	102

# Chapter 1

## Color Space

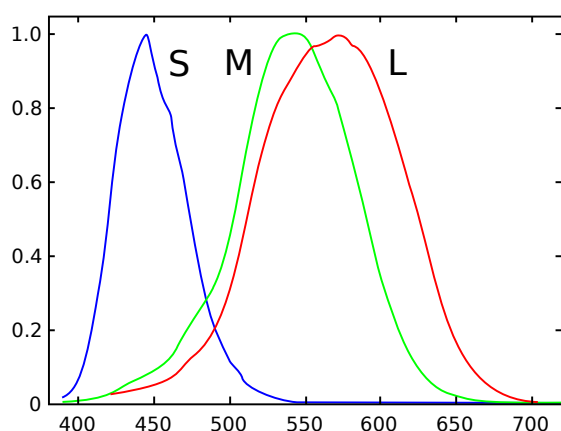
### 1.1 CIE 1931 color space

The **CIE 1931 color spaces** were the first defined quantitative links between physical pure colors (i.e. wavelengths) in the electromagnetic **visible spectrum**, and physiological perceived colors in human **color vision**. The mathematical relationships that define these color spaces are essential tools for **color management**, important when dealing with color inks, illuminated displays, and recording devices such as digital cameras.

The **CIE 1931 RGB color space** and **CIE 1931 XYZ color space** were created by the International Commission on Illumination (CIE) in 1931.<sup>[1][2]</sup> They resulted from a series of experiments done in the late 1920s by William David Wright<sup>[3]</sup> and John Guild.<sup>[4]</sup> The experimental results were combined into the specification of the CIE RGB color space, from which the CIE XYZ color space was derived.

The CIE 1931 color spaces are still widely used, as is the 1976 **CIELUV** color space.

#### 1.1.1 Tristimulus values



*The normalized spectral sensitivity of human cone cells of short-, middle- and long-wavelength types.*

The **human eye** with normal vision has three kinds of cone cells, which sense light, with spectral sensitivity

peaks in short (*S*, 420 nm–440 nm), middle (*M*, 530 nm–540 nm), and long (*L*, 560 nm–580 nm) wavelengths. These cone cells underlie human color perception under medium- and high-brightness conditions (in very dim light, **color vision** diminishes, and the low-brightness, monochromatic “night-vision” receptors, called **rod cells**, take over). Thus, three parameters, corresponding to levels of stimulus of the three types of cone cells, can in principle describe any color sensation. Weighting a total light power spectrum by the individual spectral sensitivities of the three types of cone cells gives three effective stimulus values; these three values make up a tristimulus specification of the objective color of the light spectrum. The three parameters, denoted *S*, *M*, and *L*, can be indicated using a 3-dimensional space, called **LMS color space**, which is one of many color spaces which have been devised to help quantify **human color vision**.

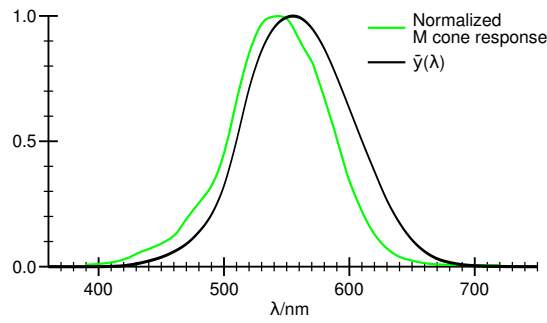
A color space maps a range of physically produced colors (from mixed light, **pigments**, etc.) to an objective description of color sensations registered in the eye, typically in terms of tristimulus values, but not usually in the LMS space defined by the cone spectral sensitivities. The **tristimulus values** associated with a color space can be conceptualized as amounts of three **primary colors** in a tri-chromatic **additive color model**. In some color spaces, including LMS and XYZ spaces, the primary colors used are not real colors, in the sense that they cannot be generated with any light spectrum.

The CIE XYZ color space encompasses all color sensations that an average person can experience. That is why CIE XYZ (Tristimulus values) is a device invariant color representation.<sup>[5]</sup> It serves as a standard reference against which many other color spaces are defined. A set of color-matching functions, like the spectral sensitivity curves of the LMS space but not restricted to be nonnegative sensitivities, associates physically produced light spectra with specific tristimulus values.

Consider two light sources made up of different mixtures of various wavelengths. Such light sources may appear to be the same color; this effect is called **metamerism**. Such light sources have the same apparent color to an observer when they produce the same tristimulus values, no matter what the spectral power distributions of the sources are.

Most wavelengths stimulate two or all three types of cone cell, because the spectral sensitivity curves of the three types of cone cells overlap. Certain tristimulus values are thus physically impossible (for instance LMS tristimulus values that are non-zero for the M component, and zero for both L and S). Furthermore, LMS tristimulus values for pure spectral colors would, in any normal trichromatic additive color space (e.g. RGB color spaces), imply negative values for at least one of the three primaries, since the chromaticity would be outside the color triangle defined by the primary colors. To avoid these negative RGB values, and to have one component that describes the perceived brightness, “imaginary” primary colors and corresponding color-matching functions have been formulated. The resulting tristimulus values are defined by the CIE 1931 color space, in which they are denoted  $X$ ,  $Y$ , and  $Z$ .<sup>[6]</sup> In XYZ space, all combinations of nonnegative coordinates are meaningful, but many such as the primary locations  $[1, 0, 0]$ ,  $[0, 1, 0]$ , and  $[0, 0, 1]$  correspond to imaginary colors outside the space of possible LMS coordinates; imaginary colors do not correspond to any spectral distribution of wavelengths, so have no physical reality.

## 1.1.2 Meaning of $X$ , $Y$ and $Z$



A comparison between a typical normalised M cone's spectral sensitivity and the CIE 1931 luminosity function for a standard observer in photopic vision.

When judging the relative luminance (brightness) of different colors in well-lit situations, humans tend to perceive light within the green parts of the spectrum as brighter than red or blue light of equal power. The luminosity function that describes the perceived brightnesses of different wavelengths is thus roughly analogous to the spectral sensitivity of M cones.

The CIE model capitalises on this fact by defining  $Y$  as luminance.  $Z$  is quasi-equal to blue stimulation, or the S cone response, and  $X$  is a mix (a linear combination) of cone response curves chosen to be nonnegative. The XYZ tristimulus values are thus analogous to, but different from, the LMS cone responses of the human eye. Defining  $Y$  as luminance has the useful result that for any given  $Y$  value, the XZ plane will contain all possible

chromaticities at that luminance.

The unit of the tristimulus values  $X$ ,  $Y$ , and  $Z$  is often arbitrarily chosen so that  $Y = 1$  or  $Y = 100$  is the brightest white that a color display supports. The corresponding whitepoint values for  $X$  and  $Z$  can then be inferred using the standard illuminants.

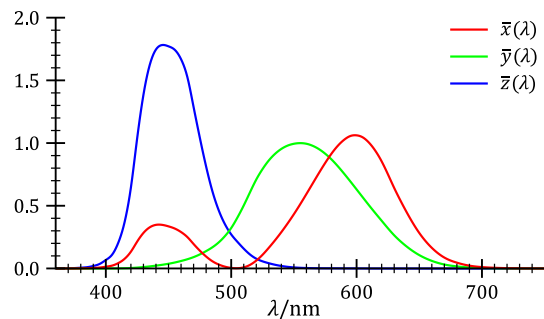
## 1.1.3 CIE standard observer

Due to the distribution of cones in the eye, the tristimulus values depend on the observer's field of view. To eliminate this variable, the CIE defined a color-mapping function called the **standard (colorimetric) observer**, to represent an average human's chromatic response within a  $2^\circ$  arc inside the fovea. This angle was chosen owing to the belief that the color-sensitive cones resided within a  $2^\circ$  arc of the fovea. Thus the *CIE 1931 Standard Observer* function is also known as the *CIE 1931  $2^\circ$  Standard Observer*. A more modern but less-used alternative is the *CIE 1964  $10^\circ$  Standard Observer*, which is derived from the work of Stiles and Burch,<sup>[7]</sup> and Speranskaya.<sup>[8]</sup>

For the  $10^\circ$  experiments, the observers were instructed to ignore the central  $2^\circ$  spot. The 1964 Supplementary Standard Observer function is recommended when dealing with more than about a  $4^\circ$  field of view. Both standard observer functions are discretized at 5 nm wavelength intervals from 380 nm to 780 nm and distributed by the CIE.<sup>[9]</sup> All corresponding values have been calculated from experimentally obtained data using interpolation. The standard observer is characterized by three *color matching functions*.

The derivation of the CIE standard observer from color matching experiments is given below, after the description of the CIE RGB space.

## Color matching functions



The CIE standard observer color matching functions.

The CIE's **color matching functions**  $\bar{x}(\lambda)$ ,  $\bar{y}(\lambda)$  and  $\bar{z}(\lambda)$  are the numerical description of the chromatic response of the *observer* (described above). They can be thought of as the spectral sensitivity curves of three linear light detectors yielding the CIE tristimulus values  $X$ ,

$Y$  and  $Z$ . Collectively, these three functions are known as the CIE standard observer.<sup>[10]</sup>

Other observers, such as for the CIE RGB space or other RGB color spaces, are defined by other sets of three color-matching functions, and lead to tristimulus values in those other spaces.

### Computing XYZ From Spectral Data

**Emissive Case** The tristimulus values for a color with a spectral radiance  $L_{e,\Omega,\lambda}$  are given in terms of the standard observer by:

$$X = \int_{\lambda} L_{e,\Omega,\lambda}(\lambda) \bar{x}(\lambda) d\lambda,$$

$$Y = \int_{\lambda} L_{e,\Omega,\lambda}(\lambda) \bar{y}(\lambda) d\lambda,$$

$$Z = \int_{\lambda} L_{e,\Omega,\lambda}(\lambda) \bar{z}(\lambda) d\lambda.$$

where  $\lambda$  is the wavelength of the equivalent monochromatic light (measured in nanometers), and the standard limits of the integral are  $\lambda \in [380, 780]$ .

The values of  $X$ ,  $Y$ , and  $Z$  are bounded if the radiance spectrum  $L_{e,\Omega,\lambda}$  is bounded.

**Reflective and Transmissive Cases** The reflective and transmissive cases are very similar to the emissive case, with a few differences. The spectral radiance  $L_{e,\Omega,\lambda}$  is replaced by the spectral reflectance (or transmittance)  $S(\lambda)$  of the object being measured, multiplied by the spectral power distribution of the illuminant  $I(\lambda)$ .

$$X = \frac{K}{N} \int_{\lambda} S(\lambda) I(\lambda) \bar{x}(\lambda) d\lambda,$$

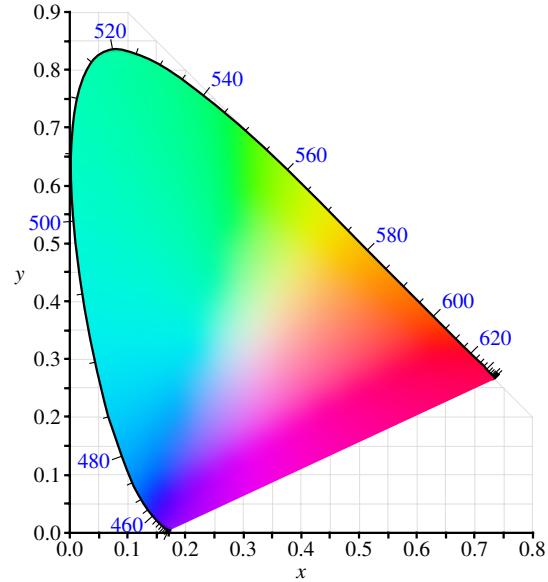
$$Y = \frac{K}{N} \int_{\lambda} S(\lambda) I(\lambda) \bar{y}(\lambda) d\lambda,$$

$$Z = \frac{K}{N} \int_{\lambda} S(\lambda) I(\lambda) \bar{z}(\lambda) d\lambda,$$

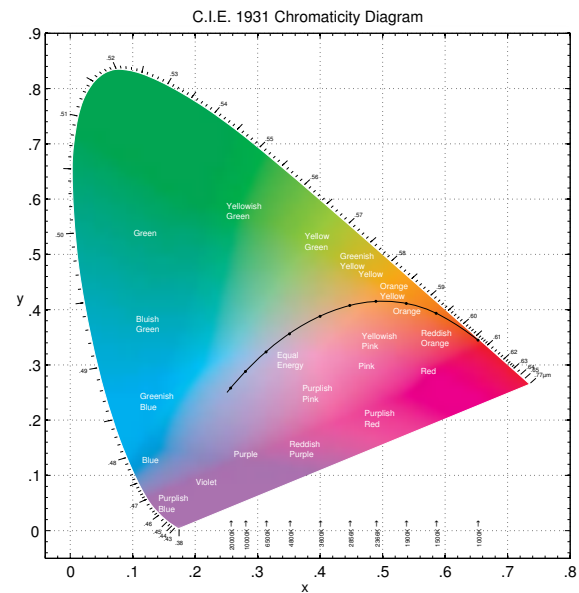
where

$$N = \int_{\lambda} I(\lambda) \bar{y}(\lambda) d\lambda,$$

$K$  is a scaling factor (usually 1 or 100), and  $\lambda$  is the wavelength of the equivalent monochromatic light (measured in nanometers), and the standard limits of the integral are  $\lambda \in [380, 780]$ .



The CIE 1931 color space chromaticity diagram. The outer curved boundary is the spectral (or monochromatic) locus, with wavelengths shown in nanometers. Note that the colors your screen displays in this image are specified using sRGB, so the colors outside the sRGB gamut are not displayed properly. Depending on the color space and calibration of your display device, the sRGB colors may not be displayed properly either. This diagram displays the maximally saturated bright colors that can be produced by a computer monitor or television set.



The CIE 1931 color space chromaticity diagram rendered in terms of the colors of lower saturation and value than those displayed in the diagram above that can be produced by pigments, such as those used in printing. The color names are from the Munsell color system.

### 1.1.4 CIE xy chromaticity diagram and the CIE xyY color space

Since the **human eye** has three types of color sensors that respond to different ranges of **wavelengths**, a full plot of all visible colors is a three-dimensional figure. However, the concept of color can be divided into two parts: brightness and **chromaticity**. For example, the color white is a bright color, while the color grey is considered to be a less bright version of that same white. In other words, the chromaticity of white and grey are the same while their brightness differs.

The CIE XYZ color space was deliberately designed so that the  $Y$  parameter is a measure of the **luminance** of a color. The chromaticity of a color is then specified by the two derived parameters  $x$  and  $y$ , two of the three normalized values being functions of all three **tristimulus** values  $X$ ,  $Y$ , and  $Z$ :

$$\begin{aligned}x &= \frac{X}{X + Y + Z} \\y &= \frac{Y}{X + Y + Z} \\z &= \frac{Z}{X + Y + Z} = 1 - x - y\end{aligned}$$

The derived color space specified by  $x$ ,  $y$ , and  $Y$  is known as the CIE xyY color space and is widely used to specify colors in practice.

The  $X$  and  $Z$  tristimulus values can be calculated back from the chromaticity values  $x$  and  $y$  and the  $Y$  tristimulus value:

$$\begin{aligned}X &= \frac{Y}{y}x, \\Z &= \frac{Y}{y}(1 - x - y).\end{aligned}$$

The figure on the right shows the related chromaticity diagram. The outer curved boundary is the *spectral locus*, with wavelengths shown in nanometers. Note that the chromaticity diagram is a tool to specify how the human eye will experience light with a given spectrum. It cannot specify colors of objects (or printing inks), since the chromaticity observed while looking at an object depends on the light source as well.

Mathematically the colors of the chromaticity diagram occupy a region of the real projective plane.

The chromaticity diagram illustrates a number of interesting properties of the CIE XYZ color space:

- The diagram represents all of the chromaticities visible to the average person. These are shown in color and this region is called the **gamut** of human vision. The gamut of all visible chromaticities

on the CIE plot is the tongue-shaped or horseshoe-shaped figure shown in color. The curved edge of the gamut is called the *spectral locus* and corresponds to monochromatic light (each point representing a pure hue of a single wavelength), with wavelengths listed in nanometers. The straight edge on the lower part of the gamut is called the **line of purples**. These colors, although they are on the border of the gamut, have no counterpart in monochromatic light. Less saturated colors appear in the interior of the figure with white at the center.

- It is seen that all visible chromaticities correspond to non-negative values of  $x$ ,  $y$ , and  $z$  (and therefore to non-negative values of  $X$ ,  $Y$ , and  $Z$ ).
- If one chooses any two points of color on the chromaticity diagram, then all the colors that lie in a straight line between the two points can be formed by mixing these two colors. It follows that the gamut of colors must be **convex** in shape. All colors that can be formed by mixing three sources are found inside the triangle formed by the source points on the chromaticity diagram (and so on for multiple sources).
- An equal mixture of two equally bright colors will not generally lie on the midpoint of that **line segment**. In more general terms, a distance on the CIE xy chromaticity diagram does not correspond to the degree of difference between two colors. In the early 1940s, **David MacAdam** studied the nature of visual sensitivity to **color differences**, and summarized his results in the concept of a **MacAdam ellipse**. Based on the work of MacAdam, the **CIE 1960**, **CIE 1964**, and **CIE 1976** color spaces were developed, with the goal of achieving perceptual uniformity (have an equal distance in the color space correspond to equal differences in color). Although they were a distinct improvement over the CIE 1931 system, they were not completely free of distortion.
- It can be seen that, given three real sources, these sources cannot cover the gamut of human vision. Geometrically stated, there are no three points within the gamut that form a triangle that includes the entire gamut; or more simply, the gamut of human vision is not a triangle.
- Light with a **flat power spectrum** in terms of wavelength (equal power in every 1 nm interval) corresponds to the point  $(x, y) = (1/3, 1/3)$ .

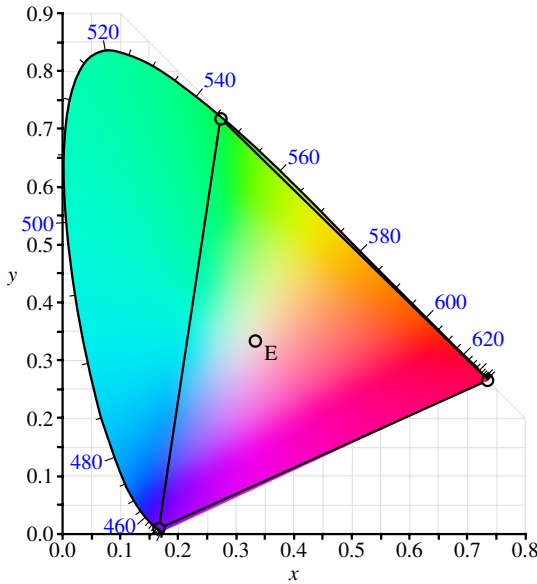
### 1.1.5 Definition of the CIE XYZ color space

#### CIE RGB color space

The CIE RGB color space is one of many RGB color spaces, distinguished by a particular set of monochro-

matic (single-wavelength) primary colors.

In the 1920s, W. David Wright<sup>[3]</sup> and John Guild<sup>[4]</sup> independently conducted a series of experiments on human sight which laid the foundation for the specification of the CIE XYZ color space. Wright carried out trichromatic color matching experiments with ten observers. Guild actually conducted his experiments with seven observers.

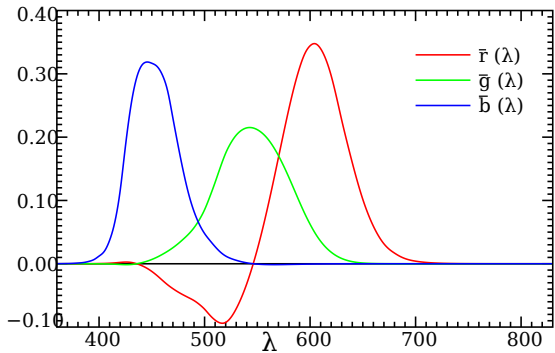


*Gamut of the CIE RGB primaries and location of primaries on the CIE 1931 xy chromaticity diagram.*

The experiments were conducted by using a circular split screen (a bipartite field) 2 degrees in diameter, which is the angular size of the human fovea. On one side of the field a *test* color was projected and on the other side, an observer-adjustable color was projected. The adjustable color was a mixture of three *primary* colors, each with fixed **chromaticity**, but with adjustable **brightness**.

The observer would alter the brightness of each of the three primary beams until a match to the test color was observed. Not all test colors could be matched using this technique. When this was the case, a variable amount of one of the primaries could be added to the test color, and a match with the remaining two primaries was carried out with the variable color spot. For these cases, the amount of the primary added to the test color was considered to be a negative value. In this way, the entire range of human color perception could be covered. When the test colors were monochromatic, a plot could be made of the amount of each primary used as a function of the wavelength of the test color. These three functions are called the *color matching functions* for that particular experiment.

Although Wright and Guild's experiments were carried out using various primaries at various intensities, and although they used a number of different observers, all of their results were summarized by the standardized CIE RGB color matching functions  $\bar{r}(\lambda)$ ,  $\bar{g}(\lambda)$ , and  $\bar{b}(\lambda)$ , obtained using three monochromatic primaries at stan-



*The CIE 1931 RGB color matching functions. The color matching functions are the amounts of primaries needed to match the monochromatic test color at the wavelength shown on the horizontal scale.*

dardized wavelengths of 700 nm (red), 546.1 nm (green) and 435.8 nm (blue). The color matching functions are the amounts of primaries needed to match the monochromatic test primary. These functions are shown in the plot on the right (CIE 1931). Note that  $\bar{r}(\lambda)$  and  $\bar{g}(\lambda)$  are zero at 435.8 nm,  $\bar{r}(\lambda)$  and  $\bar{b}(\lambda)$  are zero at 546.1 nm and  $\bar{g}(\lambda)$  and  $\bar{b}(\lambda)$  are zero at 700 nm, since in these cases the test color is one of the primaries. The primaries with wavelengths 546.1 nm and 435.8 nm were chosen because they are easily reproducible monochromatic lines of a mercury vapor discharge. The 700 nm wavelength, which in 1931 was difficult to reproduce as a monochromatic beam, was chosen because the eye's perception of color is rather unchanging at this wavelength, and therefore small errors in wavelength of this primary would have little effect on the results.

The color matching functions and primaries were settled upon by a CIE special commission after considerable deliberation.<sup>[11]</sup> The cut-offs at the short- and long-wavelength side of the diagram are chosen somewhat arbitrarily; the human eye can actually see light with wavelengths up to about 810 nm, but with a sensitivity that is many thousand times lower than for green light. These color matching functions define what is known as the "1931 CIE standard observer". Note that rather than specify the brightness of each primary, the curves are normalized to have constant area beneath them. This area is fixed to a particular value by specifying that

$$\int_0^\infty \bar{r}(\lambda) d\lambda = \int_0^\infty \bar{g}(\lambda) d\lambda = \int_0^\infty \bar{b}(\lambda) d\lambda.$$

The resulting normalized color matching functions are then scaled in the r:g:b ratio of 1:4.5907:0.0601 for source luminance and 72.0962:1.3791:1 for source radiance to reproduce the true color matching functions. By proposing that the primaries be standardized, the CIE established an international system of objective color notation.

Given these scaled color matching functions, the RGB

tristimulus values for a color with a spectral power distribution  $S(\lambda)$  would then be given by:

$$R = \int_0^\infty S(\lambda) \bar{r}(\lambda) d\lambda,$$

$$G = \int_0^\infty S(\lambda) \bar{g}(\lambda) d\lambda,$$

$$B = \int_0^\infty S(\lambda) \bar{b}(\lambda) d\lambda.$$

These are all inner products and can be thought of as a projection of an infinite-dimensional spectrum to a three-dimensional color.

### Grassmann's law

One might ask: "Why is it possible that Wright and Guild's results can be summarized using different primaries and different intensities from those actually used?" One might also ask: "What about the case when the test colors being matched are not monochromatic?" The answer to both of these questions lies in the (near) linearity of human color perception. This linearity is expressed in Grassmann's law.

The CIE RGB space can be used to define chromaticity in the usual way: The chromaticity coordinates are  $r$  and  $g$  where:

$$r = \frac{R}{R + G + B},$$

$$g = \frac{G}{R + G + B}.$$

### Construction of the CIE XYZ color space from the Wright–Guild data

The sRGB gamut (*left*) and visible gamut under D65 illumination (*right*) projected within the CIExyZ color space.  $X$  and  $Z$  are the horizontal axes;  $Y$  is the vertical axis.

The sRGB gamut (*left*) and visible gamut under D65 illumination (*right*) projected within the CIExyY color space.  $x$  and  $y$  are the horizontal axes;  $Y$  is the vertical axis.

Having developed an RGB model of human vision using the CIE RGB matching functions, the members of the special commission wished to develop another color space that would relate to the CIE RGB color space. It was assumed that Grassmann's law held, and the new space would be related to the CIE RGB space by a linear transformation. The new space would be defined in terms of three new color matching functions  $\bar{x}(\lambda)$ ,  $\bar{y}(\lambda)$ , and  $\bar{z}(\lambda)$  as described above. The new color space would be chosen to have the following desirable properties:

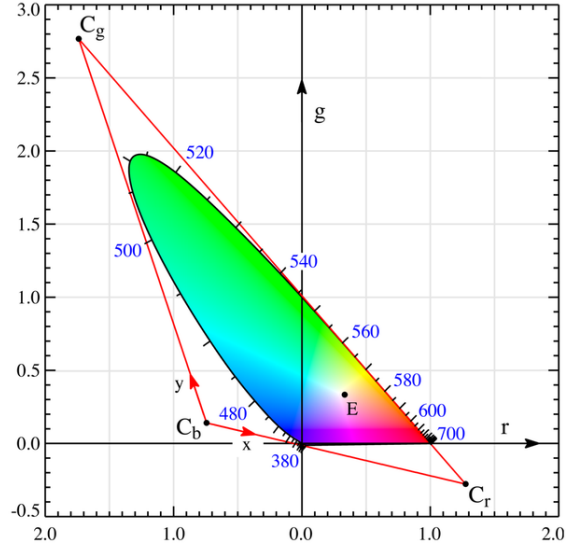


Diagram in CIE rg chromaticity space showing the construction of the triangle specifying the CIE XYZ color space. The triangle  $Cb-Cg-Cr$  is just the  $xy = (0, 0), (0, 1), (1, 0)$  triangle in CIE xy chromaticity space. The line connecting  $Cb$  and  $Cr$  is the alychne. Notice that the spectral locus passes through  $rg = (0, 0)$  at 435.8 nm, through  $rg = (0, 1)$  at 546.1 nm and through  $rg = (1, 0)$  at 700 nm. Also, the equal energy point ( $E$ ) is at  $rg = xy = (1/3, 1/3)$ .

1. The new color matching functions were to be everywhere greater than or equal to zero. In 1931, computations were done by hand or slide rule, and the specification of positive values was a useful computational simplification.
2. The  $\bar{y}(\lambda)$  color matching function would be exactly equal to the photopic luminous efficiency function  $V(\lambda)$  for the "CIE standard photopic observer".<sup>[12]</sup> The luminance function describes the variation of perceived brightness with wavelength. The fact that the luminance function could be constructed by a linear combination of the RGB color matching functions was not guaranteed by any means but might be expected to be nearly true due to the near-linear nature of human sight. Again, the main reason for this requirement was computational simplification.
3. For the constant energy white point, it was required that  $x = y = z = 1/3$ .
4. By virtue of the definition of chromaticity and the requirement of positive values of  $x$  and  $y$ , it can be seen that the gamut of all colors will lie inside the triangle  $[1, 0], [0, 0], [0, 1]$ . It was required that the gamut fill this space practically completely.
5. It was found that the  $\bar{z}(\lambda)$  color matching function could be set to zero above 650 nm while remaining within the bounds of experimental error. For computational simplicity, it was specified that this would be so.

In geometrical terms, choosing the new color space amounts to choosing a new triangle in  $rg$  chromaticity space. In the figure above-right, the  $rg$  chromaticity coordinates are shown on the two axes in black, along with the gamut of the 1931 standard observer. Shown in red are the CIE  $xy$  chromaticity axes which were determined by the above requirements. The requirement that the XYZ coordinates be non-negative means that the triangle formed by  $C_r$ ,  $C_g$ ,  $C_b$  must encompass the entire gamut of the standard observer. The line connecting  $C_r$  and  $C_b$  is fixed by the requirement that the  $\bar{y}(\lambda)$  function be equal to the luminance function. This line is the line of zero luminance, and is called the alychne. The requirement that the  $\bar{z}(\lambda)$  function be zero above 650 nm means that the line connecting  $C_g$  and  $C_r$  must be tangent to the gamut in the region of  $K_r$ . This defines the location of point  $C_r$ . The requirement that the equal energy point be defined by  $x = y = 1/3$  puts a restriction on the line joining  $C_b$  and  $C_g$ , and finally, the requirement that the gamut fill the space puts a second restriction on this line to be very close to the gamut in the green region, which specifies the location of  $C_g$  and  $C_b$ . The above described transformation is a linear transformation from the CIE RGB space to XYZ space. The standardized transformation settled upon by the CIE special commission was as follows:

The numbers in the conversion matrix below are exact, with the number of digits specified in CIE standards.<sup>[11]</sup>

$$\begin{bmatrix} X \\ Y \\ Z \end{bmatrix} = \frac{1}{b_{21}} \begin{bmatrix} b_{11} & b_{12} & b_{13} \\ b_{21} & b_{22} & b_{23} \\ b_{31} & b_{32} & b_{33} \end{bmatrix} \begin{bmatrix} R \\ G \\ B \end{bmatrix} = \frac{1}{0.176,97} \begin{bmatrix} 0.490,00 \\ 0.176,97 \\ 0.000,0 \end{bmatrix}$$

Tristimulus Value of Color Representation

$$\begin{bmatrix} R \\ G \\ B \end{bmatrix} = \begin{bmatrix} 0.310,00 & 0.200,00 \\ 0.812,40 & 0.910,630 \\ 0.010,000 & 0.990,00 \end{bmatrix} \begin{bmatrix} X \\ Y \\ Z \end{bmatrix}$$

Device Independent Color Representation

While the above matrix is exactly specified in standards, going the other direction uses an inverse matrix that is not exactly specified, but is approximately:

$$\begin{bmatrix} R \\ G \\ B \end{bmatrix} = \begin{bmatrix} 0.418,47 & -0.158,66 & -0.082,835 \\ -0.091,169 & 0.252,43 & 0.015,708 \\ 0.000,920,90 & -0.002,549,8 & 0.178,60 \end{bmatrix} \cdot \begin{bmatrix} X \\ Y \\ Z \end{bmatrix}$$

The integrals of the XYZ color matching functions must all be equal by requirement 3 above, and this is set by the integral of the photopic luminous efficiency function by requirement 2 above. The tabulated sensitivity curves have a certain amount of arbitrariness in them. The shapes of the individual  $X$ ,  $Y$  and  $Z$  sensitivity curves can be measured with a reasonable accuracy. However, the overall luminosity curve (which in fact is a weighted sum of these three curves) is subjective, since it involves asking a test person whether two light sources have the same brightness, even if they are in completely different colors. Along the same lines, the relative magnitudes of the  $X$ ,  $Y$ , and  $Z$  curves are arbitrary. Furthermore, one could define a valid color space with an  $X$  sensitivity curve that has twice the amplitude. This new color space would have a different shape. The sensitivity curves in the CIE 1931 and 1964 XYZ color spaces are scaled to have equal areas under the curves.

## 1.1.6 See also

- Trichromacy
- Imaginary color
- Lab color space
- Standard illuminant, the definition of white point used by CIE and commonly shown in color space diagrams as E, D50 or D65

## 1.1.7 References

- [1] CIE (1932). *Commission internationale de l'Eclairage proceedings, 1931*. Cambridge: Cambridge University Press.
- [2] Smith, Thomas; Guild, John (1931–32). “The C.I.E. colorimetric standards and their use”. *Transactions of the Optical Society*. **33** (3): 73–134. doi:10.1088/1475-4878/33/3/301.
- [3] Wright, William David (1928). “A re-determination of the trichromatic coefficients of the spectral colors”. *Transactions of the Optical Society*. **30** (4): 141–164. doi:10.1088/1475-4878/30/4/301.
- [4] Guild, J. (1932). “The colorimetric properties of the spectrum”. *Philosophical Transactions of the Royal Society of London. Series A, Containing Papers of a Mathematical or Physical Character*. **230**: 149–187. JSTOR 91229. doi:10.1098/rsta.1932.0005.
- [5] Stiles, W. S.; Birch, J. M. (1959). “N.P.L. Colour-matching Investigation: Final Report (1958)”. *Optica Acta*. **6** (1): 1–26. doi:10.1080/713826267.
- [6] Hunt, R. W. (1998). *Measuring Colour* (3rd ed.). England: Fountain Press. ISBN 0-86343-387-1.. See pgs. 39–46 for the basis in human eye physiology of three-component color models, and 54–57 for chromaticity coordinates.
- [7] Speranskaya, N. I. (1959). “Determination of spectrum color co-ordinates for twenty seven normal observers”. *Optics and Spectroscopy*. **7**: 424–428.
- [8] Fairman, H. S.; Brill, M. H.; Hemmendinger, H. (February 1997). “How the CIE 1931 Color-Matching Functions Were Derived from the Wright–Guild Data”. *Color Research and Application*. **22** (1): 11–23. doi:10.1002/(SICI)1520-6378(199702)22:1<11::AID-COL4>3.0.CO;2-7. and Fairman, H. S.; Brill, M. H.;

- Hemmendinger, H. (August 1998). “Erratum: How the CIE 1931 Color-Matching Functions Were Derived from the Wright–Guild Data”. *Color Research and Application*. **23** (4): 259–259. doi:10.1002/(SICI)1520-6378(199808)23:4<259::AID-COL18>3.0.CO;2-7.
- [12] CIE (1926). *Commission internationale de l'éclairage proceedings, 1924*. Cambridge: Cambridge University Press. Note that the 1924 luminous efficiency function seriously underestimates sensitivity at wavelengths below 460 nm, and has been supplemented with newer and more accurate luminosity curves; see Luminosity function#Improvements to the standard.
- Calculation from the original experimental data of the CIE 1931 RGB standard observer spectral chromaticity co-ordinates and color matching functions
  - Colorimetric data useful for calculation, in various file formats
  - Colorlab MATLAB toolbox for color science computation and accurate color reproduction. It includes CIE standard tristimulus colorimetry and transformations to a number of non-linear color appearance models (CIE Lab, CIE CAM, etc.).

### 1.1.8 Further reading

- Broadbent, Arthur D. (August 2004). “A critical review of the development of the CIE1931 RGB color-matching functions”. *Color Research & Applications*. **29** (4): 267–272. doi:10.1002/col.20020. This article describes the development of the CIE1931 chromaticity coordinates and color-matching functions starting from the initial experimental data of W. D. Wright and J. Guild. Sufficient information is given to allow the reader to reproduce and verify the results obtained at each stage of the calculations and to analyze critically the procedures used. Unfortunately, some of the information required for the coordinate transformations was never published and the appended tables provide likely versions of that missing data.
- Trezona, Pat W. (2001). “Derivation of the 1964 CIE 10° XYZ Colour-Matching Functions and Their Applicability in Photometry”. *Color Research and Application*. **26** (1): 67–75. doi:10.1002/1520-6378(200102)26:1<67::AID-COL7>3.0.CO;2-4.
- Wright, William David (2007). “Golden Jubilee of Colour in the CIE—The Historical and Experimental Background to the 1931 CIE System of Colorimetry”. In Schanda, János. *Colorimetry*. Wiley Interscience. pp. 9–24. ISBN 978-0-470-04904-4. doi:10.1002/9780470175637.ch2. (originally published by the Society of Dyers and Colourists, Bradford, 1981.)

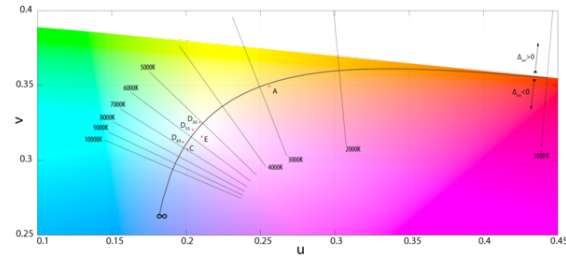
### 1.1.9 External links

- Introduction to Colour Science, William Andrew Steer.
- efg's Color Chromaticity Diagrams Lab Report and Delphi source
- CIE Color Space, Gernot Hoffmann
- Annotated downloadable data tables, Andrew Stockman and Lindsay T. Sharpe.

## 1.2 CIE 1960 color space

This article is about an obsolete version of the CIE color space. For the video color model, see YUV.

The **CIE 1960 color space** (“CIE 1960 UCS”, var-



*The Planckian locus on the MacAdam (u, v) chromaticity diagram. The normals are lines of equal correlated color temperature.*

iously expanded *Uniform Color Space*, *Uniform Color Scale*, *Uniform Chromaticity Scale*, *Uniform Chromaticity Space*) is another name for the (u, v) chromaticity space devised by David MacAdam.<sup>[1]</sup>

The CIE 1960 UCS does not define a luminance or lightness component, but the Y tristimulus value of the XYZ color space or a lightness index similar to W\* of the CIE 1964 color space are sometimes used.<sup>[2]</sup>

Today, the CIE 1960 UCS is mostly used to calculate correlated color temperature, where the isothermal lines are perpendicular to the Planckian locus. As a uniform chromaticity space, it has been superseded by the CIE 1976 UCS.

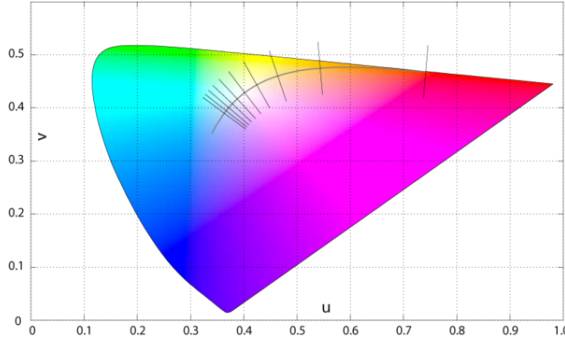
### 1.2.1 Background

Judd determined that a more uniform color space could be found by a simple projective transformation of the CIEXYZ tristimulus values:<sup>[3]</sup>

$$\begin{pmatrix} "R" \\ "G" \\ "B" \end{pmatrix} = \begin{pmatrix} 3.1956 & 2.4478 & -0.1434 \\ -2.5455 & 7.0492 & 0.9963 \\ 0.0000 & 0.0000 & 1.0000 \end{pmatrix} \begin{pmatrix} X \\ Y \\ Z \end{pmatrix}$$

(Note: What we have called “G” and “B” here are not the G and B of the CIE 1931 color space and in fact are “colors” that do not exist at all.)

Judd was the first to employ this type of transformation, and many others were to follow. Converting this RGB space to chromaticities one finds<sup>[4]</sup>



*Judd’s UCS, with the Planckian locus and the isotherms from 1,000K to 10,000K, perpendicular to the locus. Judd then translated these isotherms back into the CIEXYZ color space. (The colors used in this illustration are illustrative only and do not correspond to the true colors represented by the respective points.)*

$$u = \frac{0.4661x + 0.1593y}{y - 0.15735x + 0.2424}$$

$$v = \frac{0.6581y}{y - 0.15735x + 0.2424}$$

or equivalently (for comparative purposes with the equations to follow):

$$u = \frac{5.5932x + 1.9116y}{12y - 1.882x + 2.9088}$$

$$v = \frac{7.8972y}{12y - 1.882x + 2.9088}$$

MacAdam simplified Judd’s UCS for computational purposes:

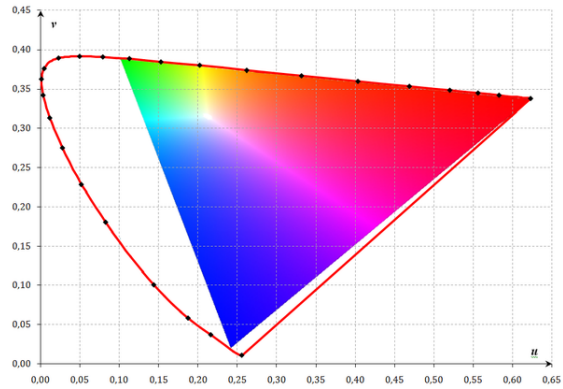
$$u = \frac{4x}{12y - 2x + 3}$$

$$v = \frac{6y}{12y - 2x + 3}$$

The Colorimetry committee of the CIE considered MacAdam’s proposal at its 14th Session in Brussels for use in situations where more perceptual uniformity was desired than the (x,y) chromaticity space,<sup>[5]</sup> and officially adopted it as the standard UCS the next year.<sup>[6]</sup>

### 1.2.2 Relation to CIE XYZ

U, V, and W can be found from X, Y, and Z using:



*The CIE 1960 UCS, also known as the MacAdam (u,v) chromaticity diagram. Colors outside the colored triangle cannot be represented on most computer screens.*

$$U = \frac{2}{3}X$$

$$V = Y$$

$$W = \frac{1}{2}(-X + 3Y + Z)$$

Going the other way:

$$X = \frac{3}{2}U$$

$$Y = V$$

$$Z = \frac{3}{2}U - 3V + 2W$$

We then find the chromaticity variables as:

$$u = \frac{U}{U + V + W} = \frac{4X}{X + 15Y + 3Z}$$

$$v = \frac{V}{U + V + W} = \frac{6Y}{X + 15Y + 3Z}$$

We can also convert from  $u$  and  $v$  to  $x$  and  $y$ :

$$x = \frac{3u}{2u - 8v + 4}$$

$$y = \frac{2v}{2u - 8v + 4}$$

### 1.2.3 Relation to CIELUV

$$u' = u$$

$$v' = \frac{3}{2}v$$

## 1.2.4 References

- [1] MacAdam, David Lewis (August 1937). “Projective transformations of I.C.I. color specifications”. *JOSA*. **27** (8): 294–299. doi:10.1364/JOSA.27.000294.
- [2] Arun N. Netravali, Barry G. Haskell (1986). *Digital Pictures: Representation, Compression, and Standards* (2E ed.). Springer. p. 288. ISBN 0-306-42195-X.
- [3] Judd, Deane B. (January 1935). “A Maxwell Triangle Yielding Uniform Chromaticity Scales”. *JOSA*. **25** (1): 24–35. doi:10.1364/JOSA.25.000024. An important application of this coordinate system is its use in finding from any series of colors the one most resembling a neighboring color of the same brilliance, for example, the finding of the nearest color temperature for a neighboring non-Planckian stimulus. The method is to draw the shortest line from the point representing the non-Planckian stimulus to the Planckian locus.
- [4] OSA Committee on Colorimetry (November 1944). “Quantitative data and methods for colorimetry”. *JOSA*. **34** (11): 633–688. (recommended reading)
- [5] CIE (January 1960). “Brussels Session of the International Commission on Illumination”. *JOSA*. **50** (1): 89–90. The use of the following chromaticity diagram is provisionally recommended whenever a diagram yielding color spacing perceptually more nearly uniform than the (xy) diagram is desired. The chromaticity diagram is produced by plotting  $4X/(X + 15Y + 3Z)$  as abscissa and  $6Y/(X + 15Y + 3Z)$  as ordinate, in which X, Y, and Z are the tristimulus values corresponding to the 1931 CIE Standard Observer and Coordinate System.
- [6] CIE (1960). “Publication No. 004: Proceedings of the CIE Session 1959 in Bruxelles”. 14th Session. Brussels. p. 36. lcontribution= ignored ([help](#))

## 1.2.5 External links

- Free Windows utility to generate chromaticity diagrams. Delphi source included.

## 1.3 CIE 1964 color space

The **CIE 1964 ( $U^*$ ,  $V^*$ ,  $W^*$ ) color space**, also known as **CIEUVW**, is based on the **CIE 1960 UCS**:<sup>[1]</sup>

$U^* = 13W^*(u - u_0)$ ,    $V^* = 13W^*(v - v_0)$ ,    $W^* = 25Y^{1/3}$   
 where  $(u_0, v_0)$  is the white point and  $Y$  is the luminous tristimulus value of the object. The asterisks in the exponent indicates that the variable represent a more perceptually uniform color space than its predecessor (compare with **CIELAB**).

Wyszecki invented the UVW color space in order to be able to calculate color differences without having to hold

the luminance constant. He defined a lightness index  $W^*$  by simplifying expressions suggested earlier by Ladd and Pinney,<sup>[2]</sup> and Glasser *et al.*<sup>[3]</sup> The chromaticity components  $U^*$  and  $V^*$  are defined such that the white point maps to the origin, as in Adams chromatic valence color spaces. This arrangement has the benefit of being able to express the loci of chromaticities with constant saturation simply as  $(U^*)^2 + (V^*)^2 = C$  for a constant  $C$ . Furthermore, the chromaticity axes are scaled by the lightness “so as to account for the apparent increase or decrease in saturation when the lightness index is increased or decreased, respectively, and the chromaticity  $(u, v)$  is kept constant”.<sup>[4]</sup>

## 1.3.1 Chromaticity and color difference

The chromaticity co-efficients were chosen “on the basis of the spacing of the Munsell system. A lightness difference  $\Delta W = 1$  is assumed to correspond to a chromatic-ness difference  $\sqrt{\Delta U^2 + \Delta V^2} = 13$  (approximately).”<sup>[4]</sup>

With the co-efficients thus selected, the color difference in CIEUVW is simply the Euclidean distance:

$$\Delta E_{\text{CIEUVW}} = \sqrt{(\Delta U^*)^2 + (\Delta V^*)^2 + (\Delta W^*)^2}$$

## 1.3.2 References

- [1] Janos Schanda (2007). *Colorimetry: Understanding the CIE System*. Wiley Interscience. p. 81.
- [2] Ladd, J.H.; Pinney, J.E. (September 1955). “Empirical relationships with the Munsell Value scale”. *Proceedings of the Institute of Radio Engineers*. **43** (9): 1137. doi:10.1109/JRPROC.1955.277892.
- [3] Glasser, L.G.; A.H. McKinney; C.D. Reilly; P.D. Schnelle (October 1958). “Cube-root color coordinate system”. *JOSA*. **48** (10): 736–740. doi:10.1364/JOSA.48.000736.
- [4] Wyszecki, Günther (November 1963). “Proposal for a New Color-Difference Formula”. *Journal of the Optical Society of America*. *JOSA*. **53** (11): 1318–1319. doi:10.1364/JOSA.53.001318. Note: The asterisks are not used in the paper.

## 1.4 CIELUV

In colorimetry, the **CIE 1976 ( $L^*$ ,  $u^*$ ,  $v^*$ ) color space**, commonly known by its abbreviation **CIELUV**, is a color space adopted by the **International Commission on Illumination** (CIE) in 1976, as a simple-to-compute transformation of the 1931 CIE XYZ color space, but which attempted perceptual uniformity. It is extensively used for applications such as computer graphics which deal with colored lights. Although additive mixtures of different colored lights will fall on a line in CIELUV’s uniform

chromaticity diagram (dubbed the *CIE 1976 UCS*), such additive mixtures will not, contrary to popular belief, fall along a line in the CIELUV color space unless the mixtures are constant in **lightness**.

### 1.4.1 Historical background

The sRGB gamut (*left*) and visible gamut under D65 illumination (*right*) plotted within the CIELUV color space.  $u$  and  $v$  are the horizontal axes;  $L$  is the vertical axis.

CIELUV is an Adams chromatic valence color space, and is an update of the CIE 1964 ( $U^*$ ,  $V^*$ ,  $W^*$ ) color space (CIEUVW). The differences include a slightly modified **lightness** scale, and a modified uniform chromaticity scale in which one of the coordinates,  $v'$ , is 1.5 times as large as  $v$  its 1960 predecessor. CIELUV and CIELAB were adopted simultaneously by the CIE when no clear consensus could be formed behind only one or the other of these two color spaces.

CIELUV uses Judd-type (translational) **white point adaptation** (in contrast with CIELAB, which uses a “wrong” von Kries transform).<sup>[1]</sup> This can produce useful results when working with a single illuminant, but can predict imaginary colors (i.e., outside the spectral locus) when attempting to use it as a **chromatic adaptation transform**.<sup>[2]</sup> The translational adaptation transform used in CIELUV has also been shown to perform poorly in predicting corresponding colors.<sup>[3]</sup>

### 1.4.2 XYZ → CIELUV and CIELUV → XYZ conversions

For typical images,  $u^*$  and  $v^*$  range  $\pm 100$ . By definition,  $0 \leq L^* \leq 100$ .

#### The forward transformation

CIELUV is based on CIEUVW and is another attempt to define an encoding with uniformity in the perceptibility of color differences.<sup>[4]</sup> The non-linear relations for  $L^*$ ,  $u^*$ , and  $v^*$  are given below:<sup>[4]</sup>

$$L^* = \begin{cases} \left(\frac{29}{3}\right)^3 Y/Y_n, & Y/Y_n \leq \left(\frac{6}{29}\right)^3 \\ 116(Y/Y_n)^{1/3} - 16, & Y/Y_n > \left(\frac{6}{29}\right)^3 \end{cases}$$

$$u^* = 13L^* \cdot (u' - u'_n)$$

$$v^* = 13L^* \cdot (v' - v'_n)$$

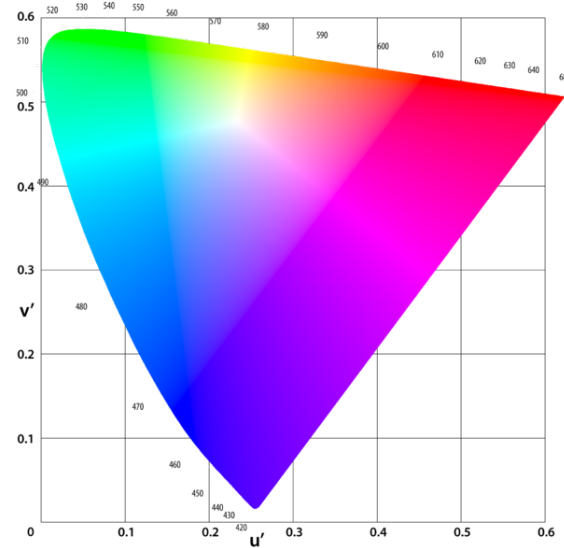
The quantities  $u'n$  and  $v'n$  are the  $(u', v')$  chromaticity coordinates of a “specified white object” – which may be termed the **white point** – and  $Y_n$  is its luminance. In reflection mode, this is often (but not always) taken as the

$(u', v')$  of the perfect reflecting diffuser under that illuminant. (For example, for the  $2^\circ$  observer and standard illuminant C,  $u'n = 0.2009$ ,  $v'n = 0.4610$ .) Equations for  $u'$  and  $v'$  are given below:<sup>[5][6]</sup>

$$u' = \frac{4X}{X + 15Y + 3Z} = \frac{4x}{-2x + 12y + 3}$$

$$v' = \frac{9Y}{X + 15Y + 3Z} = \frac{9y}{-2x + 12y + 3}$$

#### The reverse transformation



$(u', v')$  chromaticity diagram, also known as the *CIE 1976 UCS* (uniform chromaticity scale) diagram.

The transformation from  $(u', v')$  to  $(x, y)$  is:<sup>[6]</sup>

$$x = \frac{9u'}{6u' - 16v' + 12}$$

$$y = \frac{4v'}{6u' - 16v' + 12}$$

The transformation from CIELUV to XYZ is performed as follows:<sup>[6]</sup>

$$u' = \frac{u^*}{13L^*} + u'_n$$

$$v' = \frac{v^*}{13L^*} + v'_n$$

$$Y = \begin{cases} Y_n \cdot L^* \cdot \left(\frac{3}{29}\right)^3, & L^* \leq 8 \\ Y_n \cdot \left(\frac{L^* + 16}{116}\right)^3, & L^* > 8 \end{cases}$$

$$X = Y \cdot \frac{9u'}{4v'}$$

$$Z = Y \cdot \frac{12 - 3u' - 20v'}{4v'}$$

### 1.4.3 Cylindrical representation (CIELCH)

The sRGB gamut (*left*) and visible gamut under D65 illumination (*right*) plotted within the CIELCHuv color space.  $L$  is the vertical axis;  $C$  is the cylinder radius;  $h$  is the angle around the circumference.

The cylindrical version of CIELUV is known as CIE LCh<sub>uv</sub> (or CIE HLC<sub>uv</sub>), where  $C^*uv$  is the chroma and  $huv$  is the hue.<sup>[6]</sup>

$$C_{uv}^* = \sqrt{(u^*)^2 + (v^*)^2}$$

$$h_{uv} = \text{atan2}(v^*, u^*),$$

where atan2 function, a “two-argument arctangent”, computes the polar angle from a Cartesian coordinate pair.

Furthermore, the saturation correlate can be defined as:

$$s_{uv} = \frac{C^*}{L^*} = 13\sqrt{(u' - u'_n)^2 + (v' - v'_n)^2}$$

Similar correlates of chroma and hue, but not saturation, exist for CIELAB. See Colorfulness for more discussion on saturation.

### 1.4.4 Color and hue difference

The color difference can be calculated using the Euclidean distance of the  $(L^*, u^*, v^*)$  coordinates.<sup>[6]</sup> It follows that a chromaticity distance of  $\sqrt{(\Delta u')^2 + (\Delta v')^2} = 1/13$  corresponds to the same  $\Delta E^*uv$  as a lightness difference of  $\Delta L^* = 1$ , in direct analogy to CIEUVW.

The Euclidean metric can also be used in CIELCH, with that component of  $\Delta E^*uv$  attributable to difference in hue as<sup>[4]</sup>  $\Delta H^* = \sqrt{C_{uv}^* C_{uv}^* 2 \sin(\Delta h/2)}$ , where  $\Delta h = h_2 - h_1$ .

### 1.4.5 See also

- YUV

### 1.4.6 References

- [1] Judd, Deane B. (January 1940). “Hue saturation and lightness of surface colors with chromatic illumination”. *JOSA*. **30** (1): 2–32. doi:10.1364/JOSA.30.000002.
- [2] Mark D Fairchild, *Color Appearance Models*. Reading, MA: Addison-Wesley, 1998.
- [3] D. H. Alman, R. S. Berns, G. D. Snyder, and W. A. Larson, “Performance testing of color difference metrics using a color-tolerance dataset.” *Color Research and Application*, **21**:174-188 (1989).

- [4] Schanda, János (2007). *Colorimetry: Understanding the CIE System*. Wiley Interscience. pp. 61–64. ISBN 978-0-470-04904-4. As 24/116 is not a simple ratio, in some publications the 6/29 ratio is used, in others the approximate value of 0.008856 (used in earlier editions of CIE 15). Similarly some authors prefer to use instead of 841/108 the expression  $(1/3)\times(29/6)^2$  or the approximate value of 7.787, or instead of 16/116 the ratio 4/29.

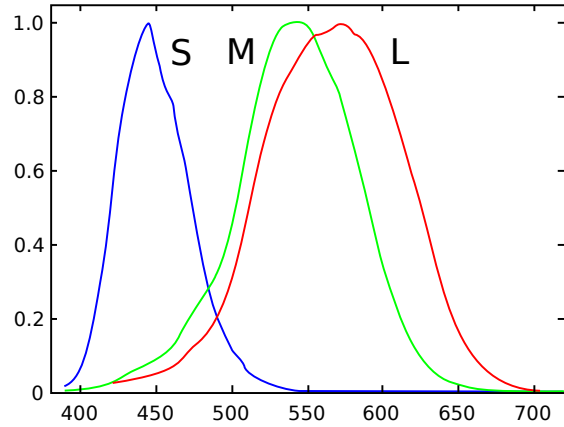
- [5] *Colorimetry*, second edition: CIE publication 15.2. Vienna: Bureau Central CIE, 1986.

- [6] Poynton, Charles (2003). *Digital Video and HDTV*. Morgan-Kaufmann. p. 226. ISBN 1-55860-792-7.

### 1.4.7 External links

- Chromaticity diagrams, including the CIE 1931, CIE 1960, CIE 1976

## 1.5 LMS color space



Normalized responsivity spectra of human cone cells, S, M, and L types

**LMS** is a color space represented by the response of the three types of cones of the human eye, named after their responsivity (sensitivity) at long, medium and short wavelengths.

It is common to use the LMS color space when performing chromatic adaptation (estimating the appearance of a sample under a different illuminant). It's also useful in the study of color blindness, when one or more cone types are defective.

### 1.5.1 XYZ to LMS

Typically, colors to be adapted chromatically will be specified in a color space other than LMS. The chromatic adaptation matrix in the von Kries transform method, however, expects the LMS color space. Since colors in any color space can, by definition, be transformed to the

XYZ color space, only one additional transformation matrix is required to transform colors from the XYZ color space to the LMS color space.

Since the LMS color space is supposed to model the complex human color perception, no single, “objective” transformation matrix between XYZ and LMS exists[ref ?]. Instead, various **Color Appearance Models (CAMs)** offer various *Chromatic Adaptation Transform (CAT)* matrices **M** as part of their modeling of human color perception.

The CAT matrices for some CAMs in terms of **CIEXYZ** coordinates are presented here.

## Notes

- All **tristimulus values** are normally calculated using the **CIE 1931 2° standard colorimetric observer**.<sup>[1]</sup>
- Unless specified otherwise, the CAT matrices are normalized (the elements in a row add up to unity) so the tristimulus values for an equal-energy illuminant ( $X=Y=Z$ ), like **CIE Illuminant E**, produce equal LMS values.<sup>[1]</sup>

## Hunt, RLAB

The **Hunt** and **RLAB** color appearance models use the **Hunt-Pointer-Estevez** transformation matrix (MHPE) for conversion from **CIE XYZ** to LMS.<sup>[1][2]</sup> This is the transformation matrix which was originally used in conjunction with the *von Kries transform* method, and is therefore also called **von Kries** transformation matrix ( $M_{\text{vonKries}}$ ).

## CIECAM97s, LLAB

The original **CIECAM97s** color appearance model uses the **Bradford** transformation matrix (MBFD) (as does the **LLAB** color appearance model).<sup>[1]</sup> This is a “spectrally sharpened” transformation matrix (i.e. the L and M cone response curves are narrower and more distinct from each other). The Bradford transformation matrix was supposed to work in conjunction with a modified von Kries transform method which introduced a small non-linearity in the S (blue) channel. However, outside of CIECAM97s and LLAB this is often neglected and the Bradford transformation matrix is used in conjunction with the linear von Kries transform method, explicitly so in ICC profiles.<sup>[3]</sup>

$$\begin{bmatrix} L \\ M \\ S \end{bmatrix} = \begin{bmatrix} 0.8951 & 0.2664 & -0.1614 \\ -0.7502 & 1.7135 & 0.0367 \\ 0.0389 & -0.0685 & 1.0296 \end{bmatrix} \begin{bmatrix} X \\ Y \\ Z \end{bmatrix}$$

A revised version of CIECAM97s switches back to a linear transform method and introduces a corresponding transformation matrix ( $\text{MCAT}_{97s}$ ).<sup>[4]</sup>

$$\begin{bmatrix} L \\ M \\ S \end{bmatrix} = \begin{bmatrix} 0.8562 & 0.3372 & -0.1934 \\ -0.8360 & 1.8327 & 0.0033 \\ 0.0357 & -0.0469 & 1.0112 \end{bmatrix} \begin{bmatrix} X \\ Y \\ Z \end{bmatrix}$$

## CIECAM02

**CIECAM02** is the successor to CIECAM97s; its transformation matrix (MCAT<sub>02</sub>) is:<sup>[1]</sup>

$$\begin{bmatrix} L \\ M \\ S \end{bmatrix} = \begin{bmatrix} 0.7328 & 0.4296 & -0.1624 \\ -0.7036 & 1.6975 & 0.0061 \\ 0.0030 & 0.0136 & 0.9834 \end{bmatrix} \begin{bmatrix} X \\ Y \\ Z \end{bmatrix}$$

## 1.5.2 See also

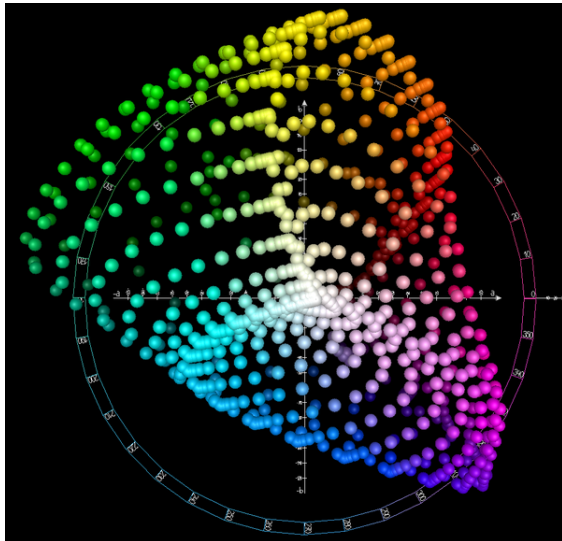
- Color balance
- Color vision
- Luminosity function
- Trichromacy

## 1.5.3 References

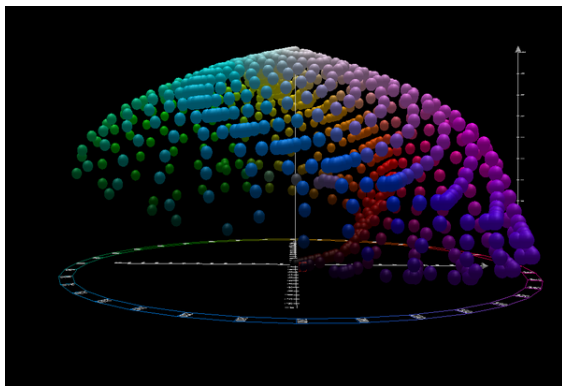
- [1] Fairchild, Mark D. (2005). *Color Appearance Models* (2E ed.). Wiley Interscience. ISBN 978-0-470-01216-1.
- [2] Moroney, Nathan; Fairchild, Mark D.; Hunt, Robert W.G.; Li, Changjun; Luo, M. Ronnier; Newman, Todd (November 12, 2002). “The CIECAM02 Color Appearance Model” (PDF). *IS&T/SID Tenth Color Imaging Conference*. Scottsdale, Arizona: The Society for Imaging Science and Technology. ISBN 0-89208-241-0.
- [3] Specification ICC.1:2010 (Profile version 4.3.0.0). Image technology colour management — Architecture, profile format, and data structure, Annex E.3, pp. 102.
- [4] Fairchild, Mark D. (2001). “A Revision of CIECAM97s for Practical Applications” (PDF). *Color Research & Applications*. Wiley Interscience. **26**: 13.

## 1.6 Lab color space

The **Lab** color space describes mathematically all perceptible colors in the three dimensions **L** for lightness and **a** and **b** for the color opponents green-red and blue-yellow. The terminology “Lab” originates from the Hunter 1948 color space.<sup>[1][2]</sup> Nowadays “Lab” is frequently mis-used as abbreviation for **CIEL\*a\*b\*** 1976 color space (also CIELAB); the asterisks/stars distinguish the CIE version from Hunter’s original version. The difference from the Hunter Lab coordinates is that the CIELAB coordinates are created by a cube root transformation of the CIE XYZ color data, while the Hunter Lab coordinates are the result of a square root transformation. Other, less common examples of color spaces with Lab



CIELAB color space top view



CIELAB color space front view

representations make use of the CIE 1994 color difference and the CIE 2000 color difference.

The Lab color space exceeds the gamuts of the RGB and CMYK color models (for example, ProPhoto RGB includes about 90% all perceivable colors). One of the most important attributes of the Lab model is device independence. This means that the colors are defined independent of their nature of creation or the device they are displayed on. The Lab color space is used when graphics for print have to be converted from RGB to CMYK, as the Lab gamut includes both the RGB and CMYK gamut. Also it is used as an interchange format between different devices as for its device independency. The space itself is a three-dimensional real number space, that contains an infinite number of possible representations of colors. However, in practice, the space is usually mapped onto a three-dimensional integer space for device-independent digital representation, and for these reasons, the  $L^*$ ,  $a^*$ , and  $b^*$  values are usually absolute, with a pre-defined range. The lightness,  $L^*$ , represents the darkest black at  $L^* = 0$ , and the brightest white at  $L^* = 100$ . The color channels,  $a^*$  and  $b^*$ , will represent true neutral gray val-

ues at  $a^* = 0$  and  $b^* = 0$ . The red/green opponent colors are represented along the  $a^*$  axis, with green at negative  $a^*$  values and red at positive  $a^*$  values. The yellow/blue opponent colors are represented along the  $b^*$  axis, with blue at negative  $b^*$  values and yellow at positive  $b^*$  values. The scaling and limits of the  $a^*$  and  $b^*$  axes will depend on the specific implementation of Lab color, as described below, but they often run in the range of  $\pm 100$  or  $-128$  to  $+127$  (signed 8-bit integer).

Both the Hunter and the 1976 CIELAB color spaces were derived from the prior “master” space CIE 1931 XYZ color space, which can predict which spectral power distributions will be perceived as the same color (see metamerism), but which is not particularly perceptually uniform.<sup>[3]</sup> Strongly influenced by the Munsell color system, the intention of both “Lab” color spaces is to create a space that can be computed via simple formulas from the XYZ space but is more perceptually uniform than XYZ.<sup>[4]</sup> *Perceptually uniform* means that a change of the same amount in a color value should produce a change of about the same visual importance. When storing colors in limited precision values, this can improve the reproduction of tones. Both Lab spaces are relative to the white point of the XYZ data they were converted from. Lab values do not define absolute colors unless the white point is also specified. Often, in practice, the white point is assumed to follow a standard and is not explicitly stated (e.g., for “absolute colorimetric” rendering intent, the International Color Consortium  $L^*a^*b^*$  values are relative to CIE standard illuminant D50, while they are relative to the unprinted substrate for other rendering intents).<sup>[5]</sup>

The lightness correlate in CIELAB is calculated using the cube root of the relative luminance.

### 1.6.1 Advantages

Unlike the RGB and CMYK color models, Lab color is designed to approximate human vision. It aspires to perceptual uniformity, and its  $L$  component closely matches human perception of lightness, although it does not take the Helmholtz–Kohlrausch effect into account. Thus, it can be used to make accurate color balance corrections by modifying output curves in the  $a$  and  $b$  components, or to adjust the lightness contrast using the  $L$  component. In RGB or CMYK spaces, which model the output of physical devices rather than human visual perception, these transformations can be done only with the help of appropriate blend modes in the editing application.

Because the Lab space is larger than the gamut of computer displays and printers and because the visual step-widths are relatively different to the color area, a bitmap image represented as Lab requires more data per pixel to obtain the same precision as an RGB or CMYK bitmap. In the 1990s, when computer hardware and software were limited to storing and manipulating mostly 8-bit/channel

bitmaps, converting an RGB image to Lab and back was a very lossy operation. With 16-bit/channel and floating-point support now common, the loss due to quantization is negligible.

Copyright and license-free: as it is fully mathematically defined, the CIELAB model is public domain, it is in all respects freely usable and integrable (also systematic Lab / HLC color value tables).

A big portion of the Lab coordinate space cannot be generated by spectral distributions, it therefore falls outside the human vision and such Lab values are not “colors”.

## 1.6.2 Differentiation

Some specific uses of the abbreviation in software, literature etc.

- In **Adobe Photoshop**, image editing using “Lab mode” is CIELAB D50.<sup>[6][7]</sup>
- In **Affinity Photo**, Lab editing is achieved by changing the document’s Colour Format to “Lab (16 bit)”
- In **ICC profiles**, the “Lab color space” used as a profile connection space is CIELAB D50.<sup>[5]</sup>
- In **TIFF** files, the CIELAB color space may be used.<sup>[8]</sup>
- In **PDF** documents, the “Lab color space” is CIELAB.<sup>[9][10]</sup>
- In Digital Color Meter on **OS X**, it is described as “L\*a\*b\*”
- In the open source non-destructive-editing software **RawTherapee**, an entire tab with many controls is dedicated to the CIE Color Appearance Model

## 1.6.3 CIELAB

The **sRGB** gamut (*left*) and visible gamut under D65 illumination (*right*) plotted within the CIELAB color space.  $a$  and  $b$  are the horizontal axes;  $L$  is the vertical axis.

**CIE L\*a\*b\* (CIELAB)** is a color space specified by the International Commission on Illumination (French *Commission internationale de l'éclairage*, hence its *CIE* initialism). It describes all the colors visible to the human eye and was created to serve as a device-independent model to be used as a reference.

The three coordinates of CIELAB represent the lightness of the color ( $L^* = 0$  yields black and  $L^* = 100$  indicates diffuse white; specular white may be higher), its position between red/magenta and green ( $a^*$ , negative values indicate green while positive values indicate magenta) and

its position between yellow and blue ( $b^*$ , negative values indicate blue and positive values indicate yellow). The asterisk (\*) after  $L$ ,  $a$  and  $b$  are pronounced *star* and are part of the full name, since they represent  $L^*$ ,  $a^*$  and  $b^*$ , to distinguish them from Hunter’s  $L$ ,  $a$ , and  $b$ , described below.

Since the  $L^*a^*b^*$  model is a three-dimensional model, it can be represented properly only in a three-dimensional space.<sup>[11]</sup> Two-dimensional depictions include chromaticity diagrams: sections of the **color solid** with a fixed lightness. It is crucial to realize that the visual representations of the full **gamut** of colors in this model are never accurate; they are there just to help in understanding the concept.

Because the red-green and yellow-blue opponent channels are computed as differences of lightness transformations of (putative) cone responses, CIELAB is a chromatic value color space.

A related color space, the CIE 1976 ( $L^*$ ,  $u^*$ ,  $v^*$ ) color space (a.k.a. **CIELUV**), preserves the same  $L^*$  as  $L^*a^*b^*$  but has a different representation of the chromaticity components. CIELAB and CIELUV can also be expressed in cylindrical form (CIELCH<sup>[12]</sup> and **CIELCH<sub>uv</sub>**, respectively), with the chromaticity components replaced by correlates of **chroma** and **hue**.

Since CIELAB and CIELUV, the CIE has been incorporating an increasing number of **color appearance phenomena** into their models, to better model color vision. These **color appearance models**, of which CIELAB is a simple example,<sup>[13]</sup> culminated with **CIECAM02**.

## Perceptual differences

This topic is covered in more detail at **Color difference**.

The nonlinear relations for  $L^*$ ,  $a^*$ , and  $b^*$  are intended to mimic the nonlinear response of the eye. Furthermore, uniform changes of components in the  $L^*a^*b^*$  color space aim to correspond to uniform changes in perceived color, so the relative perceptual differences between any two colors in  $L^*a^*b^*$  can be approximated by treating each color as a point in a three-dimensional space (with three components:  $L^*$ ,  $a^*$ ,  $b^*$ ) and taking the Euclidean distance between them.<sup>[14]</sup>

## RGB and CMYK conversions

There are no simple formulas for conversion between **RGB** or **CMYK** values and  $L^*a^*b^*$ , because the RGB and CMYK color models are device-dependent. The RGB or CMYK values first must be transformed to a specific **absolute color space**, such as **sRGB** or **Adobe RGB**. This adjustment will be device-dependent, but the resulting data from the transform will be device-independent, allowing data to be transformed to the **CIE 1931** color space and then transformed into  $L^*a^*b^*$ .

### Range of coordinates

As mentioned previously, the  $L^*$  coordinate ranges from 0 to 100. The possible range of  $a^*$  and  $b^*$  coordinates is independent of the color space that one is converting from, since the conversion below uses X and Y, which come from RGB.

### 1.6.4 CIELAB-CIEXYZ conversions

#### Forward transformation

$$\begin{aligned} L^* &= 116 f\left(\frac{Y}{Y_n}\right) - 16 \\ a^* &= 500 \left( f\left(\frac{X}{X_n}\right) - f\left(\frac{Y}{Y_n}\right) \right) \\ b^* &= 200 \left( f\left(\frac{Y}{Y_n}\right) - f\left(\frac{Z}{Z_n}\right) \right) \end{aligned}$$

where

$$\begin{aligned} f(t) &= \begin{cases} \sqrt[3]{t} & \text{if } t > \delta^3 \\ \frac{t}{3\delta^2} + \frac{4}{29} & \text{otherwise} \end{cases} \\ \delta &= \frac{6}{29} \end{aligned}$$

Here,  $X_n$ ,  $Y_n$  and  $Z_n$  are the **CIE XYZ** tristimulus values of the reference white point (the subscript n suggests “normalized”). Under **Illuminant D65** with normalization  $Y = 100$ , the values are

$$\begin{aligned} X_n &= 95.047, \\ Y_n &= 100.000, \\ Z_n &= 108.883 \end{aligned}$$

The division of the domain of the  $f$  function into two parts was done to prevent an infinite slope at  $t = 0$ . The function  $f$  was assumed to be linear below some  $t = t_0$ , and was assumed to match the  $t^{1/3}$  part of the function at  $t_0$  in both value and slope. In other words:

$$\begin{aligned} t_0^{1/3} &= mt_0 + c && \text{(value) in (match)} \\ \frac{1}{3}t_0^{-2/3} &= m && \text{(slope) in (match)} \end{aligned}$$

The intercept  $f(0) = c$  was chosen so that  $L^*$  would be 0 for  $Y = 0$ :  $c = 16/116 = 4/29$ . The above two equations can be solved for  $m$  and  $t_0$ :

$$\begin{aligned} m &= \frac{1}{3}\delta^{-2} = 7.787037\dots \\ t_0 &= \delta^3 = 0.008856\dots \end{aligned}$$

where  $\delta = 6/29$ .<sup>[15]</sup>

#### Reverse transformation

The reverse transformation is most easily expressed using the inverse of the function  $f$  above:

$$\begin{aligned} X &= X_n f^{-1} \left( \frac{L^* + 16}{116} + \frac{a^*}{500} \right) \\ Y &= Y_n f^{-1} \left( \frac{L^* + 16}{116} \right) \\ Z &= Z_n f^{-1} \left( \frac{L^* + 16}{116} - \frac{b^*}{200} \right) \end{aligned}$$

where

$$f^{-1}(t) = \begin{cases} t^3 & \text{if } t > \delta \\ 3\delta^2(t - \frac{4}{29}) & \text{otherwise} \end{cases}$$

and where  $\delta = 6/29$ .

### 1.6.5 Hunter Lab

**L** is a correlate of lightness, and is computed from the  $Y$  tristimulus value using Priest's approximation to Munsell value:

$$L = 100\sqrt{Y/Y_n}$$

where  $Y_n$  is the  $Y$  tristimulus value of a specified white object. For surface-color applications, the specified white object is usually (though not always) a hypothetical material with unit reflectance that follows **Lambert's law**. The resulting **L** will be scaled between 0 (black) and 100 (white); roughly ten times the Munsell value. Note that a medium lightness of 50 is produced by a luminance of 25, since  $100\sqrt{25/100} = 100 \cdot 1/2$

**a** and **b** are termed **opponent color axes**. **a** represents, roughly, Redness (positive) versus Greenness (negative). It is computed as:

$$a = K_a \left( \frac{X/X_n - Y/Y_n}{\sqrt{Y/Y_n}} \right)$$

where  $K_a$  is a coefficient that depends upon the illuminant (for D65,  $K_a$  is 172.30; see approximate formula below) and  $X_n$  is the  $X$  tristimulus value of the specified white object.

The other opponent color axis, **b**, is positive for yellow colors and negative for blue colors. It is computed as:

$$b = K_b \left( \frac{Y/Y_n - Z/Z_n}{\sqrt{Y/Y_n}} \right)$$

where  $K_b$  is a coefficient that depends upon the illuminant (for D65,  $K_b$  is 67.20; see approximate formula below) and  $Z_n$  is the  $Z$  tristimulus value of the specified white object.<sup>[16]</sup>

Both  $a$  and  $b$  will be zero for objects that have the same chromaticity coordinates as the specified white objects (i.e., achromatic, grey, objects).

The name for the system is an attribution to Richard S. Hunter.

#### Approximate formulas for $K_a$ and $K_b$

In the previous version of the Hunter *Lab* color space,  $K_a$  was 175 and  $K_b$  was 70. Hunter Associates Lab discovered that better agreement could be obtained with other color difference metrics, such as CIELAB (see above) by allowing these coefficients to depend upon the illuminants. Approximate formulae are:

$$K_a \approx \frac{175}{198.04} (X_n + Y_n)$$

$$K_b \approx \frac{70}{218.11} (Y_n + Z_n)$$

which result in the original values for Illuminant  $C$ , the original illuminant with which the *Lab* color space was used.

#### As an Adams chromatic valence space

Adams chromatic valence color spaces are based on two elements: a (relatively) uniform lightness scale, and a (relatively) uniform chromaticity scale.<sup>[17]</sup> If we take as the uniform lightness scale Priest's approximation to the Munsell Value scale, which would be written in modern notation:

$$L = 100\sqrt{Y/Y_n}$$

and, as the uniform chromaticity coordinates:

$$c_a = \frac{X/X_n}{Y/Y_n} - 1 = \frac{X/X_n - Y/Y_n}{Y/Y_n}$$

$$c_b = k_e \left( 1 - \frac{Z/Z_n}{Y/Y_n} \right) = k_e \frac{Y/Y_n - Z/Z_n}{Y/Y_n}$$

where  $k_e$  is a tuning coefficient, we obtain the two chromatic axes:

$$a = K \cdot L \cdot c_a = K \cdot 100 \frac{X/X_n - Y/Y_n}{\sqrt{Y/Y_n}}$$

and

$$b = K \cdot L \cdot c_b = K \cdot 100 k_e \frac{Y/Y_n - Z/Z_n}{\sqrt{Y/Y_n}}$$

which is identical to the Hunter *Lab* formulas given above if we select  $K = K_a/100$  and  $k_e = K_b/K_a$ . Therefore, the Hunter Lab color space is an Adams chromatic valence color space.

#### 1.6.6 Cylindrical representation: CIELCh or CIEHLC

The sRGB gamut (*left*) and visible gamut under D65 illumination (*right*) plotted within the CIELChab color space.  $L$  is the vertical axis;  $C$  is the cylinder radius;  $h$  is the angle around the circumference.

The CIELCh color space is a CIELab cube color space, where instead of Cartesian coordinates  $a^*$ ,  $b^*$ , the cylindrical coordinates  $C^*$  (chroma, relative saturation) and  $h^\circ$  (hue angle, angle of the hue in the CIELab color wheel) are specified. The CIELab lightness  $L^*$  remains unchanged.

The conversion of  $a^*$  and  $b^*$  to  $C^*$  and  $h^\circ$  is done using the following formulas:

$$C^* = \sqrt{a^{*2} + b^{*2}}, \quad h^\circ = \arctan \left( \frac{b^*}{a^*} \right)$$

Conversely, given the polar coordinates, conversion to Cartesian coordinates is achieved with:

$$a^* = C^* \cos(h^\circ), \quad b^* = C^* \sin(h^\circ)$$

The LCh color space is not the same as the HSV, HSL or HSB color spaces, although their values can also be interpreted as a base color, saturation and lightness of a color. The LCh values are a polar coordinate transformation of what is technically defined RGB cube color space. LCh is still perceptually uniform.

Further,  $H$  and  $h$  are not identical, because HSL space uses as primary colors the three additive primary colors red, green, blue ( $H = 0, 120, 240^\circ$ ). Instead, the LCh system uses the four physiological elementary colors yellow, green, blue and red ( $h = 90, 180, 270, 360^\circ$ ). Regardless the angle  $h$ ,  $C = 0$  means the achromatic colors, that is, the gray axis.

The simplified spellings LCh, LCH and HLC are common, but the latter presents a different order. HCL color space (Hue-Chroma-Luminance) on the other hand is a commonly used alternative name for the L\*C\*h(uv) color space, also known as the *cylindrical representation* or *polar CIELUV*.

### 1.6.7 See also

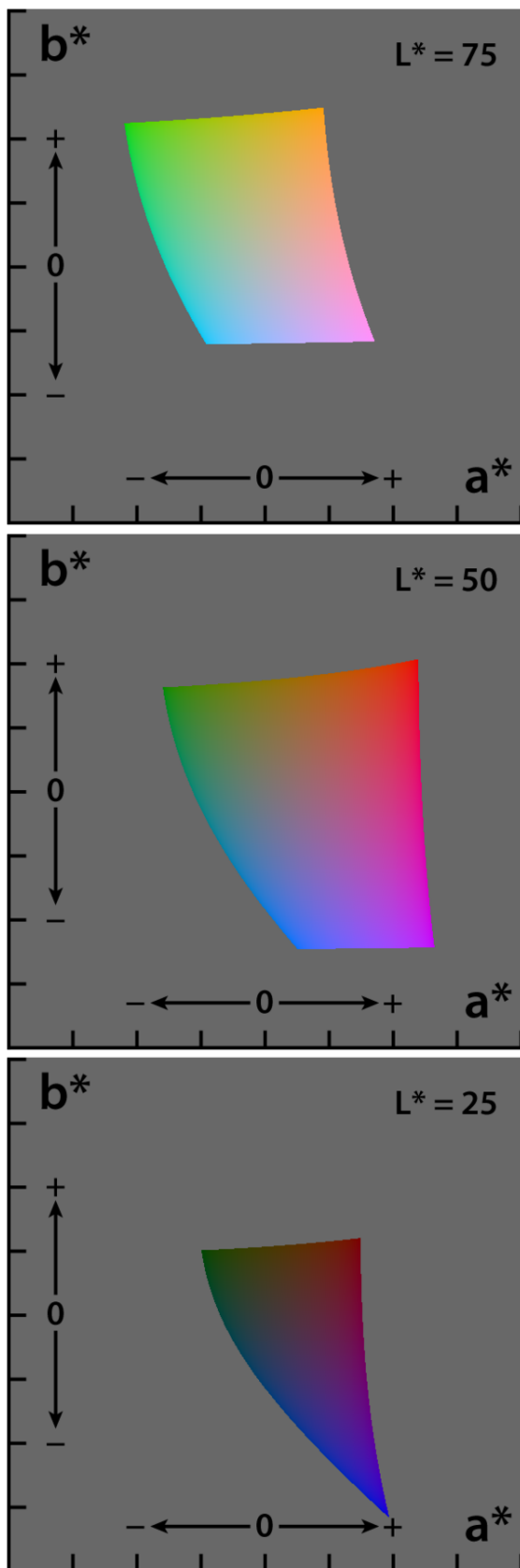
- Color theory
- HSL and HSV
- RGB color model
- CMYK color model
- CIECAM02
- HCL color space

### 1.6.8 References

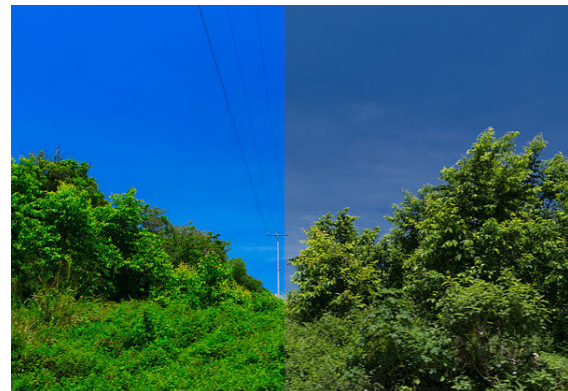
- [1] Hunter, Richard Sewall (July 1948). “Photoelectric Color-Difference Meter”. *JOSA*. **38** (7): 661. (Proceedings of the Winter Meeting of the Optical Society of America)
- [2] Hunter, Richard Sewall (December 1948). “Accuracy, Precision, and Stability of New Photo-electric Color-Difference Meter”. *JOSA*. **38** (12): 1094. (Proceedings of the Thirty-Third Annual Meeting of the Optical Society of America)
- [3] A discussion and proposed improvement, Bruce Lindbloom
- [4] Explanation of this history, Bruce MacEvoy
- [5] International Color Consortium, *Specification ICC.1:2004-10 (Profile version 4.2.0.0) Image technology colour management — Architecture, profile format, and data structure*, (2006).
- [6] Margulis, Dan (2006). *Photoshop Lab Color: The Canyon Conundrum and Other Adventures in the Most Powerful Colorspace*. Berkeley, Calif. : London: Peachpit ; Pearson Education. ISBN 0-321-35678-0.
- [7] The Lab Color Mode in Photoshop, Adobe TechNote 310838
- [8] *TIFF: Revision 6.0* Adobe Developers Association, 1992
- [9] Color Consistency and Adobe Creative Suite
- [10] Adobe Acrobat Reader 4.0 User Guide “The color model Acrobat Reader uses is called CIELAB...”
- [11] 3D representations of the  $L^*a^*b^*$  gamut, Bruce Lindbloom.
- [12] CIE-L\*C\*h Color Scale
- [13] Fairchild, Mark D. (2005). “Color and Image Appearance Models”. *Color Appearance Models*. John Wiley and Sons. p. 340. ISBN 0-470-01216-1.
- [14] Jain, Anil K. (1989). *Fundamentals of Digital Image Processing*. New Jersey, United States of America: Prentice Hall. pp. 68, 71, 73. ISBN 0-13-336165-9.
- [15] János Schanda (2007). *Colorimetry*. Wiley-Interscience. p. 61. ISBN 978-0-470-04904-4.
- [16] Hunter Labs (1996). “Hunter Lab Color Scale”. *Insight on Color* **8** 9 (August 1–15, 1996). Reston, VA, USA: Hunter Associates Laboratories.
- [17] Adams, E.Q. (1942). “X-Z planes in the 1931 I.C.I. system of colorimetry”. *JOSA*. **32** (3): 168–173. doi:10.1364/JOSA.32.000168.

### 1.6.9 External links

- Demonstrative color conversion applet
- CIELAB Color Space by Gernot Hoffmann, includes explanations of  $L^*a^*b^*$  conversion formulae, graphical depictions of various gamuts plotted in  $L^*a^*b^*$  space, and PostScript code for performing the color transformations.
- Color Differences
- LAB Color Spaces with MATLAB
- Convert Rgb to Lab

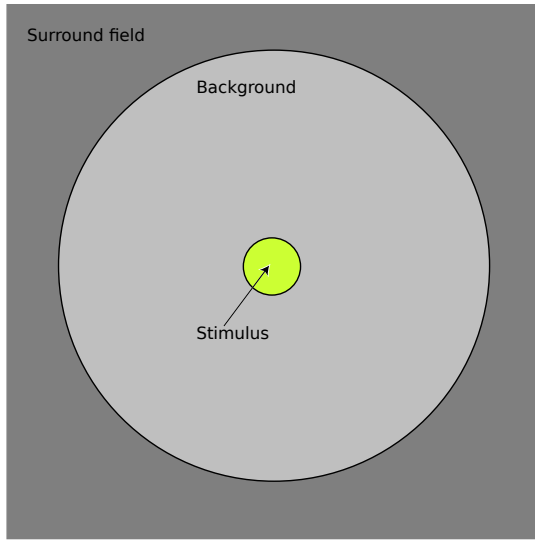


The CIE 1976 ( $L^*$ ,  $a^*$ ,  $b^*$ ) color space (CIELAB), showing only colors that fit within the sRGB gamut (and can therefore be displayed on a typical computer display). Each axis of each square ranges from -128 to 128.



An example of color enhancement using LAB color mode in Photoshop. The left side of the photo is enhanced, while the right side is normal.

## 1.7 CIECAM02



*Observing field model. Not drawn to scale.*

In colorimetry, **CIECAM02** is the color appearance model published in 2002 by the International Commission on Illumination (CIE) Technical Committee 8-01 (*Color Appearance Modelling for Color Management Systems*) and the successor of **CIECAM97s**.<sup>[1]</sup>

The two major parts of the model are its chromatic adaptation transform, **CIECAT02**, and its equations for calculating mathematical correlates for the six technically defined dimensions of color appearance: brightness (luminance), lightness, colorfulness, chroma, saturation, and hue.

Brightness is the subjective appearance of how bright an object appears given its surroundings and how it is illuminated. Lightness is the subjective appearance of how light a color appears to be. Colorfulness is the degree of difference between a color and grey. Chroma is the colorfulness relative to the brightness of another color that appears white under similar viewing conditions. This allows for the fact that a surface of a given chroma displays increasing colorfulness as the level of illumination increases. Saturation is the colorfulness of a color relative to its own brightness. Hue is the degree to which a stimulus can be described as similar to or different from stimuli that are described as red, green, blue, and yellow, the so-called unique hues. The colors that make up an object's appearance are best described in terms of lightness and chroma when talking about the colors that make up the object's surface, and it in terms of brightness, saturation and colorfulness when talking about the light that is emitted by or reflected off the object.

CIECAM02 takes for its input the tristimulus values of the stimulus, the tristimulus values of an adapting white point, adapting background, and surround luminance information, and whether or not observers are discounting

the illuminant (color constancy is in effect). The model can be used to predict these appearance attributes or, with forward and reverse implementations for distinct viewing conditions, to compute corresponding colors.

CIECAM02 is used in Windows Vista's Windows Color System.<sup>[2]</sup>

### 1.7.1 Viewing conditions

The inner circle is the *stimulus*, from which the tristimulus values should be measured in CIE XYZ using the 2° standard observer. The intermediate circle is the *proximal field*, extending out another 2°. The outer circle is the *background*, reaching out to 10°, from which the relative luminance ( $Y_b$ ) need be measured. If the proximal field is the same color as the background, the background is considered to be adjacent to the stimulus. Beyond the circles which comprise the *display field* (*display area*, *viewing area*) is the *surround field* (or *peripheral area*), which can be considered to be the entire room. The totality of the proximal field, background, and surround is called the *adapting field* (the field of view that supports adaptation—extends to the limit of vision).<sup>[3]</sup>

When referring to the literature, it is also useful to be aware of the difference between the terms *adopted white point* (the computational *white point*) and the *adapted white point* (the observer white point).<sup>[4]</sup> The distinction may be important in mixed mode illumination, where psychophysical phenomena come into play. This is a subject of research.

### 1.7.2 Parameter decision table

CIECAM02 defines three surround(ing)s – average, dim, and dark – with associated parameters defined here for reference in the rest of this article.<sup>[5]</sup>

- $SR = Lsw / Ldw$ : ratio of the absolute luminance of the *reference white* (white point) measured in the surround field to the display area. The 0.2 coefficient derives from the “gray world” assumption (~18%–20% reflectivity). It tests whether the surround luminance is darker or brighter than medium gray.
- $F$ : factor determining degree of adaptation
- $c$ : impact of surrounding
- $Nc$ : chromatic induction factor

For intermediate conditions, these values can be linearly interpolated.<sup>[5]</sup>

The absolute luminance of the adapting field, which is a quantity that will be needed later, should be measured

with a photometer. If one is not available, it can be calculated using a reference white:

$$L_A = \frac{E_w}{\pi} \frac{Y_b}{Y_w} = \frac{L_W Y_b}{Y_w}$$

where  $Y_b$  is the relative luminance of background, the  $E_w = \pi L W$  is the illuminance of the reference white in lux,  $LW$  is the absolute luminance of the reference white in  $\text{cd}/\text{m}^2$ , and  $Y_w$  is the relative luminance of the reference white in the adapting field. If unknown, the adapting field can be assumed to have average reflectance ("gray world" assumption):  $L_A = LW / 5$ .

*Note:* Care should be taken not to confuse  $LW$ , the absolute luminance of the reference white in  $\text{cd}/\text{m}^2$ , and  $L_w$  the red cone response in the LMS color space.

### 1.7.3 Chromatic adaptation

#### Summary

1. Convert to the "spectrally sharpened" CAT02 LMS space to prepare for adaptation. *Spectral sharpening* is the transformation of the tristimulus values into new values that would have resulted from a sharper, more concentrated set of spectral sensitivities. It is argued that this aids color constancy, especially in the blue region.(Compare Finlayson et al. 94, Spectral Sharpening:Sensor Transformations for Improved Colour Constancy)
2. Perform chromatic adaptation using CAT02 (also known as the "modified CMCCAT2000 transform").
3. Convert to an LMS space closer to the cone fundamentals. It is argued that predicting perceptual attribute correlates is best done in such spaces.<sup>[5]</sup>
4. Perform post-adaptation cone response compression.

#### CAT02

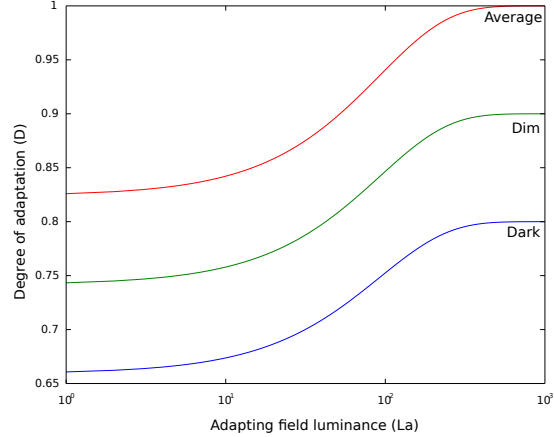
Given a set of tristimulus values in XYZ, the corresponding LMS values can be determined by the MCAT02 transformation matrix (calculated using the CIE 1931 2° standard colorimetric observer).<sup>[1]</sup> The sample color in the *test* illuminant is:

$$\begin{bmatrix} L \\ M \\ S \end{bmatrix} = \mathbf{M}_{\text{CAT02}} \begin{bmatrix} X \\ Y \\ Z \end{bmatrix}, \quad \mathbf{M}_{\text{CAT02}} = \begin{bmatrix} 0.7328 & 0.4296 \\ -0.7036 & 1.6975 \\ 0.0030 & 0.0136 \end{bmatrix}$$

Once in LMS, the white point can be adapted to the desired degree by choosing the parameter  $D$ .<sup>[3]</sup> For the general CAT02, the corresponding color in the reference illuminant is:

$$\begin{aligned} L_c &= \left( \frac{Y_w}{Y_{wr}} D + 1 - D \right) L \\ M_c &= \left( \frac{Y_w}{Y_{wr}} M_{wr} D + 1 - D \right) M \\ S_c &= \left( \frac{Y_w}{Y_{wr}} S_{wr} D + 1 - D \right) S \end{aligned}$$

where the  $Y_w / Y_{wr}$  factor accounts for the two illumi-



nants having the same chromaticity but different reference whites.<sup>[6]</sup> The subscripts indicate the cone response for white under the test ( $w$ ) and reference illuminant ( $wr$ ). The degree of adaptation (discounting)  $D$  can be set to zero for no adaptation (stimulus is considered self-luminous) and unity for complete adaptation (color constancy). In practice, it ranges from 0.65 to 1.0, as can be seen from the diagram. Intermediate values can be calculated by:<sup>[5]</sup>

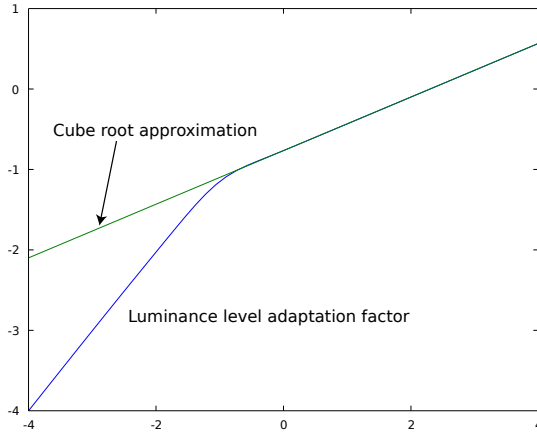
$$D = F \left( 1 - \frac{1}{3.6} e^{-(L_A + 42)/92} \right)$$

where surround  $F$  is as defined above and  $LA$  is the adapting field luminance in  $\text{cd}/\text{m}^2$ .<sup>[1]</sup>

In CIECAM02, the reference illuminant has equal energy  $L_{wr} = M_{wr} = S_{wr} = 100$  and the reference white is the perfect reflecting diffuser (i.e., unity reflectance, and  $Y_{wr} = 100$ ) hence:

$$\begin{aligned} L_c &= \left( \frac{Y_w}{L_w} D + 1 - D \right) L \\ M_c &= \left( \frac{Y_w}{M_w} D + 1 - D \right) M \\ S_c &= \left( \frac{Y_w}{S_w} D + 1 - D \right) S \end{aligned}$$

Furthermore, if the reference white in both illuminants have the  $Y$  tristimulus value ( $Y_{wr} = Y_w$ ) then:



*log-log plot of FL vs. LA (LA ranges from  $10^{-4}$  to  $10^4$ , FL ranges from  $10^{-4}$  to 10). The cube root approximation of FL is  $0.1715LA^{1/3}$*

$$L_c = \left( \frac{L_{wr}}{L_w} D + 1 - D \right) L$$

$$M_c = \left( \frac{M_{wr}}{M_w} D + 1 - D \right) M$$

$$S_c = \left( \frac{S_{wr}}{S_w} D + 1 - D \right) S$$

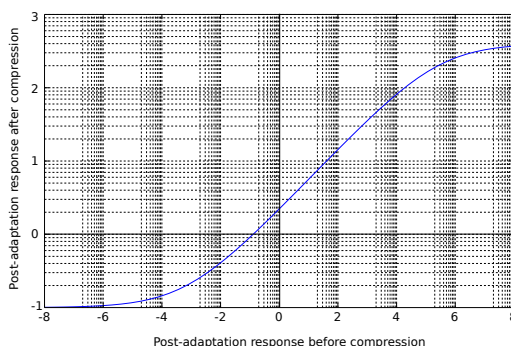
### Post-adaptation

After adaptation, the cone responses are converted to the Hunt–Pointer–Estévez space by going to XYZ and back:<sup>[5]</sup>

$$\begin{bmatrix} L' \\ M' \\ S' \end{bmatrix} = \mathbf{M}_H \begin{bmatrix} X_c \\ Y_c \\ Z_c \end{bmatrix} = \mathbf{M}_H \mathbf{M}_{CAT02}^{-1} \begin{bmatrix} L_c \\ M_c \\ S_c \end{bmatrix}$$

$$\mathbf{M}_H = \begin{bmatrix} 0.38971 & 0.68898 & -0.07868 \\ -0.22981 & 1.18340 & 0.04641 \\ 0.00000 & 0.00000 & 1.00000 \end{bmatrix}$$

Finally, the response is compressed based on the general



*log L'a vs. log L' for LA = 200 (FL = 1)*

alized Michaelis–Menten equation (as depicted aside):<sup>[5]</sup>

$$k = \frac{1}{5L_A + 1}$$

$$F_L = \frac{1}{5} k^4 (5L_A) + \frac{1}{10} (1 - k^4)^2 (5L_A)^{1/3}$$

FL is the luminance level adaptation factor.

$$L'_a = \frac{400(F_L L'/100)^{0.42}}{27.13 + (F_L L'/100)^{0.42}} + 0.1$$

$$M'_a = \frac{400(F_L M'/100)^{0.42}}{27.13 + (F_L M'/100)^{0.42}} + 0.1$$

$$S'_a = \frac{400(F_L S'/100)^{0.42}}{27.13 + (F_L S'/100)^{0.42}} + 0.1$$

As previously mentioned, if the luminance level of the background is unknown, it can be estimated from the absolute luminance of the white point as  $LA = LW / 5$  using the “medium gray” assumption. (The expression for FL is given in terms of  $5LA$  for convenience.) In photopic conditions, the luminance level adaptation factor (FL) is proportional to the cube root of the luminance of the adapting field (LA). In scotopic conditions, it is proportional to LA (meaning no luminance level adaptation). The photopic threshold is roughly  $LW = 1$  (see FL–LA graph above).

### 1.7.4 Appearance correlates

CIECAM02 defines correlates for yellow-blue, red-green, brightness, and colorfulness. Let us make some preliminary definitions.

$$C_1 = L'_a - M'_a$$

$$C_2 = M'_a - S'_a$$

$$C_3 = S'_a - L'_a$$

The **correlate for red–green (a)** is the magnitude of the departure of  $C_1$  from the criterion for unique yellow ( $C_1 = C_2 / 11$ ), and the **correlate for yellow–blue (b)** is based on the mean of the magnitude of the departures of  $C_1$  from unique red ( $C_1 = C_2$ ) and unique green ( $C_1 = C_3$ ).<sup>[3]</sup>

$$a = C_1 - \frac{1}{11} C_2 = L'_a - \frac{12}{11} M'_a + \frac{1}{11} S'_a$$

$$b = \frac{1}{2} (C_2 - C_1 + C_1 - C_3) / 4.5 = \frac{1}{9} (L'_a + M'_a - 2S'_a)$$

The 4.5 factor accounts for the fact that there are fewer cones at shorter wavelengths (the eye is less sensitive to blue). The order of the terms is such that b is positive for yellowish colors (rather than blueish).

The **hue angle (h)** can be found by converting the rectangular coordinate (a, b) into polar coordinates:

$$h = \angle(a, b), (0 < h < 360^\circ)$$

To calculate the eccentricity ( $e_t$ ) and hue composition ( $H$ ), determine which quadrant the hue is in with the aid of the following table. Choose  $i$  such that  $h_i \leq h' < h_{i+1}$ , where  $h' = h$  if  $h > h_1$  and  $h' = h + 360^\circ$  otherwise.

$$H = H_i + \frac{100(h' - h_i)/e_i}{(h' - h_i)/e_i + (h_{i+1} - h')/e_{i+1}}$$

$$e_t = \frac{1}{4} [\cos(\frac{\pi}{180}h + 2) + 3.8]$$

(This is not exactly the same as the eccentricity factor given in the table.)

Calculate the achromatic response  $A$ :

$$A = (2L'_a + M'_a + \frac{1}{20}S'_a - 0.305)N_{bb}$$

where

$$N_{bb} = N_{cb} = 0.725n^{-0.2}$$

$$n = Y_b/Y_w$$

The correlate of **lightness** is

$$J = 100(A/A_w)^{cz}$$

where  $c$  is the impact of surround (see above), and

$$z = 1.48 + \sqrt{n}$$

The correlate of **brightness** is

$$Q = (4/c) \sqrt{\frac{1}{100} J} (A_w + 4) F_L^{1/4}$$

Then calculate a temporary quantity  $t$ ,

$$t = \frac{\frac{50.000}{13} N_c N_{cb} e_t \sqrt{a^2 + b^2}}{L'_a + M'_a + \frac{21}{20} S'_a}$$

The correlate of **chroma** is

$$C = t^{0.9} \sqrt{\frac{1}{100} J} (1.64 - 0.29^n)^{0.73}$$

The correlate of **colorfulness** is

$$M = C \cdot F_L^{1/4}$$

The correlate of **saturation** is

$$s = 100\sqrt{M/Q}$$

## 1.7.5 References

- [1] Fairchild, Mark D.; Luo, M. R.; Hunt, R. W. G. (August 2000). “A Revision of CIECAM97s for Practical Applications” (PDF). *Color Research & Applications*. Wiley Interscience. **25** (4): 260–266. doi:10.1002/1520-6378(200008)25:4<260::AID-COL6>3.0.CO;2-9. The CIECAM97s model was adopted by the CIE in 1997 for color imaging applications. It includes forward and reverse modes. Some problems in using this model were found in recent field trials. This article suggests revision to the model in two respects: (a) to make the lightness (J) zero when the Y tristimulus value is zero, under all surround conditions; (b) to modify the chromatic induction factor (Nc) from 1.10 to 0.95 for the dim surround condition. To avoid confusion, it is suggested that the revised version of the model be designated CAM97s2. The article also describes an alternative mode to achieve a more nearly exact reversibility between the forward and reverse modes.
- [2] “Windows Color System: The Next Generation Color Management System”. Microsoft white paper. September 13, 2005.
- [3] Schanda, János (2007). “The Future of Colorimetry in the CIE: Color Appearance”. *Colorimetry: Understanding the CIE System*. Wiley Interscience. p. 359. ISBN 978-0-470-04904-4.
- [4] Westland, Stephen; Ripamonti, Caterina (2004). *Computational Colour Science Using MATLAB*. John Wiley & Sons. ISBN 0-470-84562-7.
- [5] Moroney, Nathan; Fairchild, Mark D.; Hunt, Robert W.G.; Li, Changjun; Luo, M. Ronnier; Newman, Todd (November 12, 2002). “The CIECAM02 Color Appearance Model” (PDF). *IS&T/SID Tenth Color Imaging Conference*. Scottsdale, Arizona: The Society for Imaging Science and Technology. ISBN 0-89208-241-0.
- [6] Hunt, Robert W. G.; Changjun Li; M. Ronnier Luo (February 2005). “Chromatic Adaptation Transforms”. *Color Research & Applications*. Wiley Interscience. **30** (1): 69. doi:10.1002/col.20085. Chromatic adaptation transforms (CATs) have appeared in different forms. The reasons for these forms, and the relationships between them, are described. The factors governing which type of CAT should be used in different applications are explained
- CIE TC 8-01 (2004). *A Color appearance model for color management systems*. Publication 159. Vienna: CIE Central Bureau. ISBN 3-901906-29-0.
- Fairchild, Mark D. (2004-11-09). “Color Appearance Models: CIECAM02 and Beyond” (PDF). IS&T/SID 12th Color Imaging Conference. Retrieved 2008-02-11.

## 1.7.6 External links

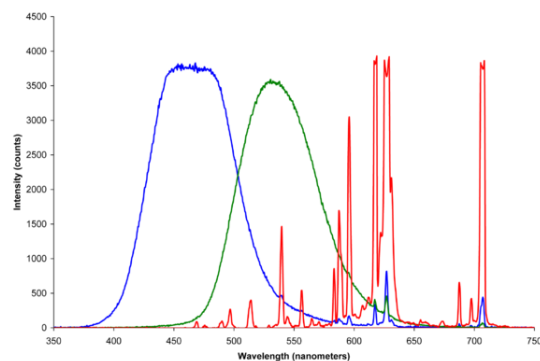
- Excel spreadsheet with forward and inverse examples, by Eric Walowit and Grit O'Brien

- Experimental Implementation of the CIECAM02 Color Appearance Model in a Photoshop Compatible Plug-in (Windows Only), by Cliff Rames.
- Notes on the CIECAM02 Colour Appearance Model. Source code in C of the forward and reverse transforms, by Billy Biggs.
- CIECAM02 Java applet, by Nathan Moroney

## 1.8 Primary color

This article is about colors. For other uses, see Primary Colors.

A set of **primary colors** is a small, arbitrary set of



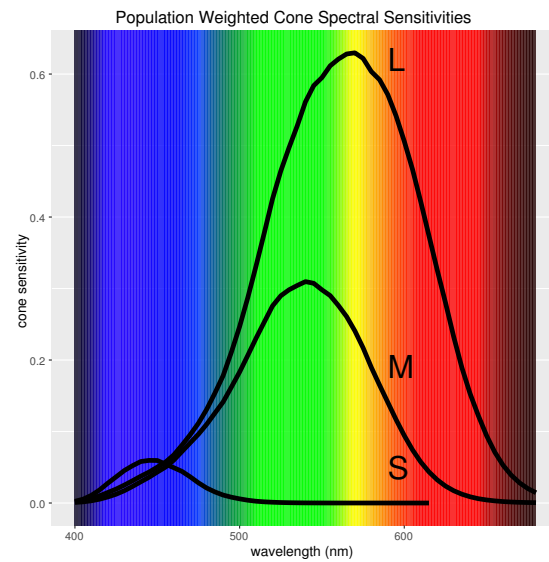
*The emission spectra of the three phosphors that define the additive primary colors of a CRT color video display. Other electronic color display technologies (LCD, Plasma display, OLED) have analogous sets of primaries with different emission spectra.*

pigmented physical media, lights or purely abstract elements of a mathematical colorspace model. Distinct colors from a larger gamut can be specified in terms of a mixture of primary colors which facilitates technological applications such as painting, electronic displays and printing. Any small set of pigments or lights are “imperfect” physical primary colors in that they cannot be mixed to yield all possible colors that can be perceived by the human color vision system. The abstract (or “imaginary”) primaries X, Y and Z of the CIEXYZ colorspace can be mathematically summed to specify essentially all colors that can be perceived but these primaries cannot be physically realized due to the underlying structure and overlapping spectral sensitivities of each of the human cone photoreceptors.<sup>[1]</sup> The precise set of primary colors that are used in a specific color application depend on gamut requirements as well as application-specific constraints such as cost, power consumption, lightfastness, mixing behavior etc.

In an *additive* set of colors, as in coincident projected lights or in **electronic visual displays**, the primary colors normally used are red, green and blue (but the precise visible light spectra for each color can vary significantly). In a *subtractive* set of colors, as in mixing of pigments

or dyes for printing, the colors magenta, yellow and cyan are normally used.<sup>[2]</sup> See **RGB color model**, and **CMYK color model** for more on these popular sets of primary colors.

### 1.8.1 Biological basis



*Population weighted cone spectral sensitivities*

Primary colors are not a fundamental property of light but are related to the color vision system in animals. The human eye normally contains only three types of color photoreceptors (L, M and S) that are associated with specialized **cone cells**. Each photoreceptor responds to different ranges of the visible electromagnetic spectrum and there is no single wavelength that stimulates only one photoreceptor type. Humans and other species with three such types of color photoreceptor are known as **trichromats**. In spite of color being a complex psychophysical response to electromagnetic radiation, controlled color matching experiments (e.g., CIE 1931) have essentially mapped all possible colors the eye can see in terms of the response of each of the three color photoreceptors, which correspond to the three dimensions of **CIEXYZ**. **Color appearance** models like **CIECAM02** describe color more generally in six dimensions and can be used to predict how colors appear in different viewing conditions.

Most **placental mammals** other than primates have only two types of color photoreceptor and are therefore **dichromats** while birds and marsupials are **tetrachromats** with four color photoreceptor types. There is no currently peer reviewed scholarly work that has confirmed the existence of a functional human tetrachromat though they are suspected to exist.<sup>[3]</sup> It may seem that the primary colors of an animal’s vision system corresponds to the number of color photoreceptor types but the mere presence of “extra” photoreceptor types does not directly imply that they are being used functionally. Demonstrating im-

proved spectral discrimination in any animal can be difficult since complex sets of neurons affect color perception in ways that are generally difficult to interrogate.<sup>[4]</sup>

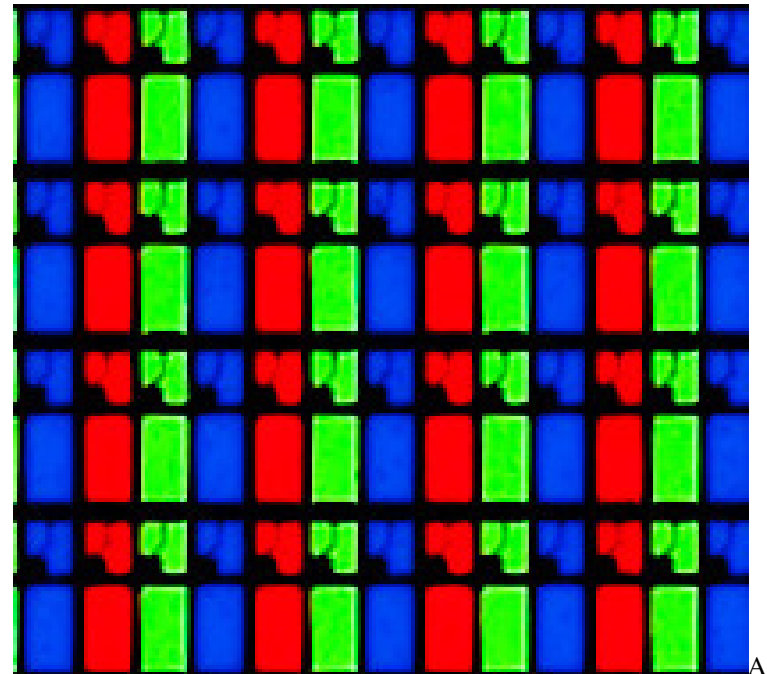
## 1.8.2 History

Before the nature of colorimetry and visual physiology were well understood a number of color models assigned primary colors to different hues (e.g. the RYB model). Scientists such as Thomas Young, James Clerk Maxwell and Hermann von Helmholtz expressed various opinions about what should be the three primary colors to describe the three primary color sensations of the eye.<sup>[5]</sup> Young originally proposed red, green and violet, and Maxwell changed violet to blue; Helmholtz proposed “a slightly purplish red, a vegetation-green, slightly yellowish, and an ultramarine-blue.<sup>[6]</sup> In modern understanding, human cone cells do not correspond precisely to a specific set of primary colors, as each cone type responds to a relatively broad range of wavelengths.

## 1.8.3 Examples



A self-portrait by Anders Zorn clearly showing a four pigment palette of what are thought to be white, yellow ochre, red vermilion and black pigments.<sup>[7]</sup>



photograph of the red, green and blue pixels of an LCD display.



The cyan, magenta, yellow and black (key) (CMYK) inks found in an inkjet printer that can be used for color photographic reproduction.

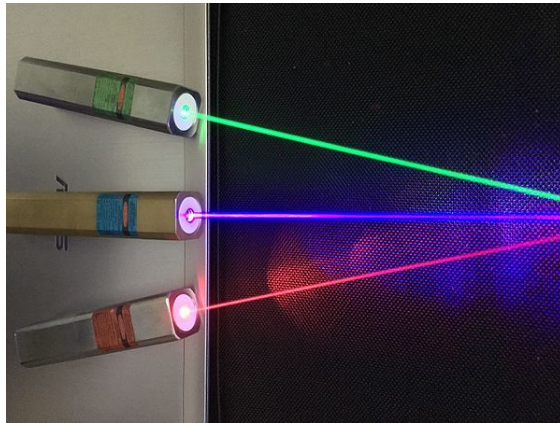
## Limited palettes in visual art

There are hundreds of commercially available pigments for visual artists to use and mix (in various media such as oil, watercolor, acrylic and pastel). A common approach is to use just a limited palette of pigments (often between four and eight) that can be physically mixed to any color that the artist desires in the final work. There are no spe-

cific set of pigments that are primary colors, the choice of pigment depends entirely on the artist's subjective preference of subject and style of art as well as material considerations like lightfastness and mixing heuristics. Contemporary classical realists have often advocated that a limited palette of white, red, yellow and black pigment (often described as the "Zorn palette") is sufficient for compelling work.<sup>[8]</sup>

### RGB for electronic displays

Main articles: Additive color and RGB color model  
Media that combine emitted lights to create the sensation



The *RGB color Laser diodes*

of a range of colors are using the **additive color** system. The primary colors used in most electronic displays are typically saturated red, green and blue light.<sup>[9]</sup>

The exact colors chosen for the primaries are a technological compromise between the available **phosphors** (including considerations such as cost and power usage) and the need for large **color triangle** to allow a large gamut of colors. The **ITU-R BT.709-5/sRGB** primaries are typical. Additive mixing of red and green light produces shades of **yellow**, **orange**, or **brown**.<sup>[10]</sup> Mixing green and blue produces shades of **cyan**, and mixing red and blue produces shades of **purple**, including **magenta**. Mixing nominally equal proportions of the additive primaries results in shades of **grey** or **white**; the **color space** that is generated is called an **RGB color space**. The experiments used to derive the **CIE 1931** colorspace used **monochromatic** primary colored lights with the (arbitrary) wavelengths of 435.8 nm (violet), 546.1 nm (green) and 700 nm (red) due to the convenience they afforded to the experimental work.

**Recent developments** Some recent TV and computer displays are starting to include yellow as a fourth primary color, often in a four-point square pixel area, so as to achieve brighter pure yellows and a larger color gamut.<sup>[11]</sup> Even the four-primary technology does not yet reach the range of colors that the human eye can see

from light reflected by illuminated surfaces (as defined by the sample-based estimate called the **Pointer Gamut**<sup>[12]</sup>), with 4-primary LED prototypes providing typically about 87% and 5-primary prototypes about 95%. Several firms, including Samsung and Mitsubishi, have demonstrated LED displays with five or six "primaries", or color LED point light sources per pixel.<sup>[13][14]</sup> A recent academic literature review claims a gamut of 99% can be achieved with 5-primary LED technology.<sup>[15]</sup> While technology for achieving a wider gamut appears to be within reach, other issues remain; for example, affordability, dynamic range, and brilliance. In addition, there exists hardly any source material recorded in this wider gamut, nor is it currently possible to recover this information from existing visual media. Regardless, industry is still exploring a wide variety of "primary" active light sources (per pixel) with the goal of matching the capability of human color perception within a broadly affordable price. One example of a potentially affordable but yet unproven active light hybrid places an LED screen over a plasma light screen, each with different "primaries". Because both LED and plasma technologies are many decades old (plasma pixels going back to the 1960s), both have become so affordable that they could be combined.

### CMYK color model or four-color printing

Main article: **CMYK color model**

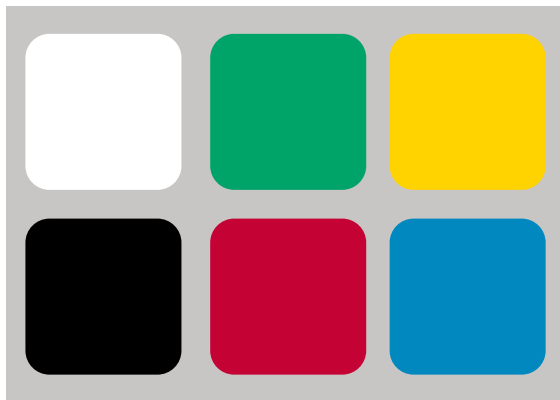
In the printing industry, the **subtractive primaries** **cyan**, **magenta** and **yellow** are applied together in varying amounts for useful gamuts. An additional **key ink** (short-hand for the **key printing plate** that impressed the artistic detail of an image, usually in black ink.<sup>[16]</sup>) is also usually used since it is difficult to mix a dark enough black ink using the other three inks as well as other practical considerations such as cost and ink bleed. Before the color names **cyan** and **magenta** were in common use, these primaries were often known as blue-green and purple or in some pop art circles as blue and red, respectively, and their exact color has changed over time with access to new pigments and technologies.<sup>[17]</sup>

### Psychological primaries

Main article: **Opponent process**

See also: **Natural Color System** and **Unique hues**

The **opponent process** is a color theory that states that the **human visual system** interprets information about **color** by processing signals from **cones** and **rods** in an antagonistic manner. The three types of cones have some overlap in the **wavelengths of light** to which they respond, so it is more efficient for the visual system to record **differences** between the responses of cones, rather than each type of cone's individual response. The opponent color theory



*Approximations within the sRGB gamut to the “aim colors” of the Natural Color System, a model based on the opponent process theory of color vision.*

suggests that there are three opponent channels: red versus green, blue versus yellow and black versus white.<sup>[18]</sup> Responses to one color of an opponent channel are antagonistic to those of the other color. The theory states that the particular colors considered by an observer to be uniquely representative of the concepts red, yellow, green, blue, white and black might be called “psychological primary colors”, because any other color could be described in terms of some combination of these.

#### 1.8.4 See also

- Color vision

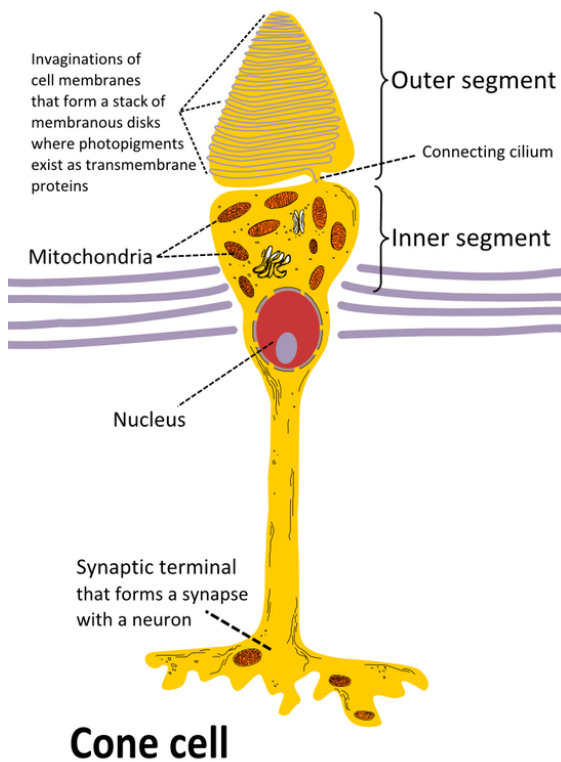
#### 1.8.5 References

- [1] Bruce MacEvoy. “Do ‘Primary’ Colors Exist?” (Material Trichromacy section). *Handprint*. Accessed 10 August 2007.
- [2] Matthew Luckiesh (1915). *Color and Its Applications*. D. Van Nostrand company. pp. 58, 221.
- [3] Greenwood, Veronique. “The Humans With Super Human Vision”. *Discover Magazine*. Kalmbach Publishing Co. Retrieved 29 September 2016.
- [4] Morrison, Jessica (23 January 2014). “Mantis shrimp’s super colour vision debunked”. *Nature*. doi:10.1038/nature.2014.14578.
- [5] Edward Albert Sharpey-Schäfer (1900). *Text-book of physiology*. 2. Y. J. Pentland. p. 1107.
- [6] Alfred Daniell (1904). *A text book of the principles of physics*. Macmillan and Co. p. 575.
- [7] Nyholm, Arvid (1914). “Anders Zorn: The Artist and the Man”. *Fine Arts Journal*. 31 (4): 469. doi:10.2307/25587278.
- [8] Gurney. “The Zorn Palette”. *Gurney Journey*. Retrieved 27 September 2016.
- [9] Thomas D. Rossing & Christopher J. Chiaverina (1999). *Light science: physics and the visual arts*. Birkhäuser. p. 178. ISBN 978-0-387-98827-6.
- [10] “Some Experiments on Color”, *Nature* 111, 1871, in John William Strutt (Lord Rayleigh) (1899). *Scientific Papers*. University Press.
- [11] Garvey, Jude (2010-01-20). “Sharp four primary color TVs enable over one trillion colors”. gizmag.com.
- [12] M. R. Pointer (1980). “The Gamut of Real Surface Colours”. *Color Research and Application*. John Wiley & Sons, Inc. 5 (3): 145–155. doi:10.1002/col.5080050308.
- [13] Chih-Cheng Chan; Guo-Feng Wei; Hui Chu-Ke; Sheng-Wen Cheng; Shih-Chang Chu; Ming-Sheng Lai; Arex Wang; Shmuel Roth; Oded Ben David; Moshe Ben Chorin; Dan Eliav; Ilan Ben David (1999). *Development of Multi-Primary Color LCD*. AU Optronics, Science-Based Industrial Park, Hsin-Chu, Taiwan; Genoa Color Technologies, Herzlia, Israel.
- [14] Thomas Rossing; Christopher J Chiaverina (24 September 1999). *Light Science: Physics and the Visual Arts*. Springer Science & Business Media. pp. 178-. ISBN 978-0-387-98827-6.
- [15] Abhinav Priya (2011), *Five-Primary Color LCD* (PDF), Cochin University of Science and Technology, Department of Electronics Engineering, p. 2
- [16] Frank S. Henry (1917). *Printing for School and Shop: A Textbook for Printers’ Apprentices, Continuation Classes, and for General use in Schools*. John Wiley & Sons.
- [17] Ervin Sidney Ferry (1921). *General Physics and Its Application to Industry and Everyday Life*. John Wiley & Sons.
- [18] Michael Foster (1891). *A Text-book of physiology*. Lea Bros. & Co. p. 921.

## 1.9 Cone cell

**Cone cells**, or **cones**, are one of three types of photoreceptor cells in the retina of mammalian eyes (e.g. the human eye). They are responsible for **color vision** and function best in relatively bright **light**, as opposed to **rod cells**, which work better in dim light. Cone cells are densely packed in the **fovea centralis**, a 0.3 mm diameter rod-free area with very thin, densely packed cones which quickly reduce in number towards the periphery of the retina. There are about six to seven million cones in a human eye and are most concentrated towards the **macula**.<sup>[1]</sup> The commonly cited figure of six million cone cells in the human eye was found by Osterberg in 1935.<sup>[2]</sup> Oyster’s textbook (1999)<sup>[3]</sup> cites work by Curcio et al. (1990) indicating an average close to 4.5 million cone cells and 90 million rod cells in the human retina.<sup>[4]</sup>

Cones are less sensitive to light than the rod cells in the retina (which support vision at low light levels), but allow the perception of colour. They are also able to per-



*Cone cell structure*

ceive finer detail and more rapid changes in images, because their response times to stimuli are faster than those of rods.<sup>[5]</sup> Cones are normally one of the three types, each with different pigment, namely: S-cones, M-cones and L-cones. Each cone is therefore sensitive to visible wavelengths of light that correspond to short-wavelength, medium-wavelength and long-wavelength light.<sup>[6]</sup> Because humans usually have three kinds of cones with different photopsins, which have different response curves and thus respond to variation in colour in different ways, we have **trichromatic vision**. Being **colour blind** can change this, and there have been some verified reports of people with four or more types of cones, giving them **tetrachromat**ic vision.<sup>[7][8][9]</sup> The three pigments responsible for detecting light have been shown to vary in their exact chemical composition due to genetic mutation; different individuals will have cones with different color sensitivity. Destruction of the cone cells from disease would result in blindness.

### 1.9.1 Types

Humans normally have three types of cones. The first responds the most to light of long wavelength, peaking at about 560 nm ; this type is sometimes designated **L** for long. The second type responds the most to light of medium-wavelength, peaking at 530 nm, and is abbreviated **M** for medium. The third type responds the most to short-wavelength light, peaking at 420 nm, and is desig-

nated **S** for short. The three types have peak wavelengths near 564–580 nm, 534–545 nm, and 420–440 nm, respectively, depending on the individual.<sup>[10][11]</sup> The difference in the signals received from the three cone types allows the brain to perceive a continuous range of colours, through the **opponent process of colour vision**. (Rod cells have a peak sensitivity at 498 nm, roughly halfway between the peak sensitivities of the S and M cones.)

All of the receptors contain the protein **photopsin**, with variations in its conformation causing differences in the optimum wavelengths absorbed.

The colour yellow, for example, is perceived when the L cones are stimulated slightly more than the M cones, and the colour red is perceived when the L cones are stimulated significantly more than the M cones. Similarly, blue and violet hues are perceived when the S receptor is stimulated more. Cones are most sensitive to light at wavelengths around 420 nm. However, the lens and cornea of the human eye are increasingly absorptive to shorter wavelengths, and this sets the short wavelength limit of human-visible light to approximately 380 nm, which is therefore called 'ultraviolet' light. People with **aphakia**, a condition where the eye lacks a lens, sometimes report the ability to see into the ultraviolet range.<sup>[12]</sup> At moderate to bright light levels where the cones function, the eye is more sensitive to yellowish-green light than other colors because this stimulates the two most common (M and L) of the three kinds of cones almost equally. At lower light levels, where only the rod cells function, the sensitivity is greatest at a blueish-green wavelength.

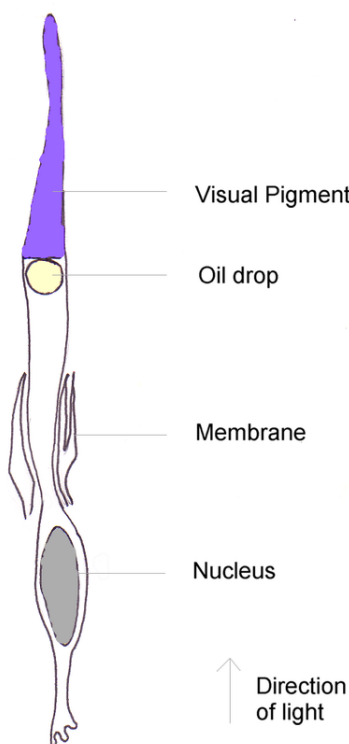
Cones also tend to possess a significantly elevated visual acuity because each cone cell has a lone connection to the optic nerve, therefore, the cones have an easier time telling that two stimuli are isolated. Separate connectivity is established in the **inner plexiform layer** so that each connection is parallel.<sup>[13]</sup>

While it has been discovered that there exists a mixed type of **bipolar cells** that bind to both rod and cone cells, bipolar cells still predominantly receive their input from cone cells.<sup>[13]</sup>

### 1.9.2 Structure

Cone cells are somewhat shorter than rods, but wider and tapered, and are much less numerous than rods in most parts of the retina, but greatly outnumber rods in the **fovea**. Structurally, cone cells have a **cone-like shape** at one end where a pigment filters incoming light, giving them their different response curves. They are typically 40–50  $\mu\text{m}$  long, and their diameter varies from 0.5 to 4.0  $\mu\text{m}$ , being smallest and most tightly packed at the center of the eye at the **fovea**. The S cone spacing is slightly larger than the others.<sup>[14]</sup>

**Photobleaching** can be used to determine cone arrangement. This is done by exposing dark-adapted retina to a



*Bird, reptilian, and monotreme cone cells.*

certain wavelength of light that paralyzes the particular type of cone sensitive to that wavelength for up to thirty minutes from being able to dark-adapt making it appear white in contrast to the grey dark-adapted cones when a picture of the retina is taken. The results illustrate that S cones are randomly placed and appear much less frequently than the M and L cones. The ratio of M and L cones varies greatly among different people with regular vision (e.g. values of 75.8% L with 20.0% M versus 50.6% L with 44.2% M in two male subjects).<sup>[15]</sup>

Like rods, each cone cell has a synaptic terminal, an inner segment, and an outer segment as well as an interior nucleus and various mitochondria. The synaptic terminal forms a synapse with a neuron such as a bipolar cell. The inner and outer segments are connected by a cilium.<sup>[5]</sup> The inner segment contains organelles and the cell's nucleus, while the outer segment, which is pointed toward the back of the eye, contains the light-absorbing materials.<sup>[5]</sup>

Like rods, the outer segments of cones have invaginations of their cell membranes that create stacks of membranous disks. Photopigments exist as transmembrane proteins within these disks, which provide more surface area for light to affect the pigments. In cones, these disks are attached to the outer membrane, whereas they are pinched off and exist separately in rods. Neither rods nor cones divide, but their membranous disks wear out and are worn off at the end of the outer segment, to be consumed and

recycled by phagocytic cells.

The response of cone cells to light is also directionally nonuniform, peaking at a direction that receives light from the center of the pupil; this effect is known as the Stiles–Crawford effect.

### 1.9.3 Diseases

One of the diseases related to cone cells present in retina is retinoblastoma. Retinoblastoma is a rare cancer of the retina, caused by the mutation of both copies of retinoblastoma genes (RB1). Most cases of retinoblastoma occur during early childhood.<sup>[16]</sup> One or both eyes may be affected. The protein encoded by RB1 regulates a signal transduction pathway while controlling the cell cycle progression as normally. Retinoblastoma seems to originate in cone precursor cells present in the retina that consist of natural signalling networks which restrict cell death and promote cell survival after losing the RB1, or having both the RB1 copies mutated. It has been found that TRB2 which is a transcription factor specifically affiliated with cones is essential for rapid reproduction and existence of the retinoblastoma cell.<sup>[16]</sup> A drug that can be useful in the treatment of this disease is MDM2 (murine double minute 2) gene. Knockdown studies have shown that the MDM2 gene silences ARF-induced apoptosis in retinoblastoma cells and that MDM2 is necessary for the survival of cone cells.<sup>[16]</sup> It is unclear at this point why the retinoblastoma in humans is sensitive to RB1 inactivation.

The pupil may appear white or have white spots. A white glow in the eye is often seen in photographs taken with a flash, instead of the typical “red eye” from the flash, and the pupil may appear white or distorted. Other symptoms can include crossed eyes, double vision, eyes that do not align, eye pain and redness, poor vision or differing iris colours in each eye. If the cancer has spread, bone pain and other symptoms may occur.<sup>[16][17]</sup>

### 1.9.4 Color afterimage

Sensitivity to a prolonged stimulation tends to decline over time, leading to neural adaptation. An interesting effect occurs when staring at a particular color for a minute or so. Such action leads to an exhaustion of the cone cells that respond to that color - resulting in the afterimage. This vivid color aftereffect can last for a minute or more.<sup>[18]</sup>

### 1.9.5 See also

- Cone dystrophy
- Disc shedding
- Double cones

- RG color space
- Tetrachromacy
- Melanopsin

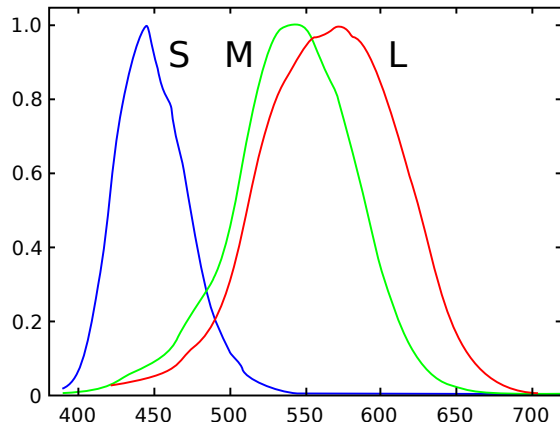
## 1.9.6 References

- [1] “The Rods and Cones of the Human Eye”.
- [2] Osterberg, G. (1935). “Topography of the layer of rods and cones in the human retina”. *Acta Ophthalmol. Suppl.* 13 (6): 1–102.
- [3] Oyster, C. W. (1999). *The human eye: structure and function*. Sinauer Associates.
- [4] Curcio, C.A.; Sloan, K.R.; Kalina, R.E.; Hendrickson, A.E. (Feb 1990). “Human photoreceptor topography.”. *J Comp Neurol.* 292 (4): 497–523. PMID 2324310. doi:10.1002/cne.902920402.
- [5] Kandel, E.R.; Schwartz, J.H; Jessell, T. M. (2000). *Principles of Neural Science* (4th ed.). New York: McGraw-Hill. pp. 507–513.
- [6] Schacter, Gilbert, Wegner, “Psychology”, New York: Worth Publishers, 2009.
- [7] Jameson, K. A.; Highnote, S. M. & Wasserman, L. M. (2001). “Richer colour experience in observers with multiple photopigment opsin genes” (PDF). *Psychonomic Bulletin and Review*. 8 (2): 244–261. PMID 11495112. doi:10.3758/BF03196159.
- [8] “You won't believe your eyes: The mysteries of sight revealed”. The Independent. 7 March 2007.
- [9] Mark Roth (September 13, 2006). “Some women may see 100,000,000 colours, thanks to their genes”. Pittsburgh Post-Gazette.
- [10] Wyszecki, Günther; Stiles, W.S. (1981). *Colour Science: Concepts and Methods, Quantitative Data and Formulae* (2nd ed.). New York: Wiley Series in Pure and Applied Optics. ISBN 0-471-02106-7.
- [11] R. W. G. Hunt (2004). *The Reproduction of Colour* (6th ed.). Chichester UK: Wiley-IS&T Series in Imaging Science and Technology. pp. 11–12. ISBN 0-470-02425-9.
- [12] *Let the light shine in: You don't have to come from another planet to see ultraviolet light* EducationGuardian.co.uk, David Hambling (May 30, 2002)
- [13] Strettoi, E; Novelli, E; Mazzoni, F; Barone, I; Damiani, D (Jul 2010). “Complexity of retinal cone bipolar cells.”. *Progress in retinal and eye research*. 29 (4): 272–83. PMC 2878852. PMID 20362067. doi:10.1016/j.preteyeres.2010.03.005.
- [14] Brian A. Wandell (1995). “Foundations of Vision”.
- [15] Roorda A.; Williams D.R. (1999). “The arrangement of the three cone classes in the living human eye”. *Nature*. 397 (6719): 520–522. PMID 10028967. doi:10.1038/17383.
- [16] Skinner, Mhairi (2009). “Tumorigenesis: Cone cells set the stage”. *Nature Reviews Cancer*. 9: 534. doi:10.1038/nrc2710.
- [17] “Retinoblastoma”. A.D.A.M. Medical Encyclopedia.
- [18] Schacter, Daniel L. *Psychology: the second edition*. Chapter 4.9.

## 1.9.7 External links

- Cell Centered Database – Cone cell
- Webvision's *Photoreceptors*
- NIF Search – Cone Cell via the Neuroscience Information Framework
- Model and image of cone cell

## 1.10 Spectral sensitivity



*Spectral sensitivities (normalized responsivity spectra) of human cone cells, S, M, and L types*

**Spectral sensitivity** is the relative efficiency of detection, of light or other signal, as a function of the frequency or wavelength of the signal.

In **visual neuroscience**, spectral sensitivity is used to describe the different characteristics of the photopigments in the rod cells and cone cells in the **retina** of the eye. It is known that the rod cells are more suited to **scotopic vision** and cone cells to **photopic vision**, and that they differ in their sensitivity to different wavelengths of light.<sup>[2][3]</sup> It has been established that the maximum spectral sensitivity of the human eye under daylight conditions is at a wavelength of 555nm, while at night the peak shifts to 507 nm.<sup>[4]</sup>

In **photography**, film and sensors are often described in terms of their spectral sensitivity, to supplement their characteristic curves that describe their **responsivity**.<sup>[5]</sup> A database of camera spectral sensitivity is created and its space analyzed.<sup>[6]</sup> For **X-ray** films, the spectral sensitivity

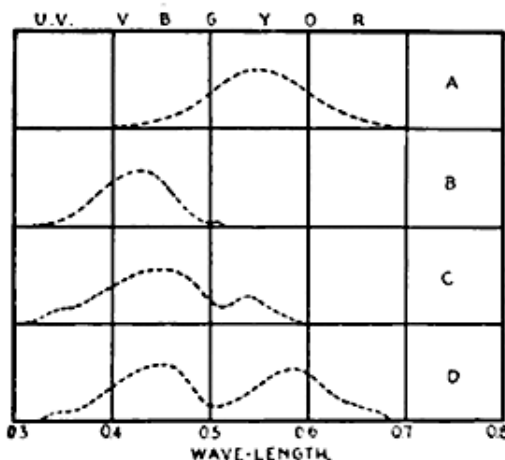


**Fig. 102 — Approximate spectral sensibilities of;** A, eye; B, ordinary photographic emulsion; C, orthochromatic; D, panchromat.

1916 plot of “spectral sensibilities.” The author also uses the more modern term “spectral sensitivity” in the same book.<sup>[1]</sup>

is chosen to be appropriate to the phosphors that respond to X-rays, rather than being related to human vision.<sup>[7]</sup>

In sensor systems, where the output is easily quantified, the **responsivity** can be extended to be wavelength dependent, incorporating the spectral sensitivity. When the sensor system is linear, its spectral sensitivity and spectral responsivity can both be decomposed with similar basis functions.<sup>[8]</sup> When a system’s responsivity is a fixed monotonic nonlinear function, that nonlinearity can be estimated and corrected for, to determine the spectral sensitivity from spectral input–output data via standard linear methods.<sup>[9]</sup>

The responses of the rod and cone cells of the retina, however, have a very context-dependent (coupled) nonlinear response, which complicates the analysis of their spectral sensitivities from experimental data.<sup>[10]</sup> In spite of these complexities, however, the conversion of light energy spectra to the effective stimulus, the excitation of the photopigment, is quite linear, and linear characterizations such as spectral sensitivity are therefore quite useful in describing many properties of color vision.<sup>[11]</sup>

Spectral sensitivity is sometimes expressed as a **quantum efficiency**, that is, as probability of getting a quantum reaction, such as a captured electron, to a quantum of light, as a function of wavelength.<sup>[12]</sup> In other contexts, the spectral sensitivity is expressed as the relative response per light energy, rather than per quantum, normalized to a peak value of 1, and a quantum efficiency is used to calibrate the sensitivity at that peak wavelength.<sup>[13]</sup> In some linear applications, the spectral sensitivity may be expressed as a **spectral responsivity**, with units such as amperes per watt.<sup>[14][15][16]</sup>

### 1.10.1 See also

- Frequency response

### 1.10.2 References

- [1] Matthew Luckiesh (1916). *Light and shade and their applications*. D. Van Nostrand Company.
- [2] Michael Levine (2000). *Fundamentals of Sensation and Perception* (3rd ed.). Oxford University Press.
- [3] Steven H. Schwartz (2004). *Visual Perception: A Clinical Orientation*. McGraw-Hill Professional. ISBN 0-07-141187-9.
- [4] Gross, Herbert; Blechinger, Fritz; Achtner, Bertram (2008). Gross, Herbert H., ed. *Handbook of optical systems*. 4. Weinheim, Germany: WILEY-VCH. p. 40. ISBN 978-3-527-40380-6.
- [5] Michael Langford (1998). *Advanced Photography*. Focal Press. ISBN 0-240-51486-4.
- [6] Jun Jiang; Dengyu Liu; Jinwei Gu & Sabine Süsstrunk (2013). *What is the space of spectral sensitivity functions for digital color cameras?*. IEEE. ISBN 978-1-4673-5053-2.
- [7] John Ball & Tony Price (1995). *Chesneys’ Radiographic Imaging*. Blackwell Publishing. ISBN 0-632-03901-9.
- [8] Glenn E. Healey; Steven A. Shafer & Lawrence B. Wolff (1992). *Physics-Based Vision*. A. K. Peters Ltd. ISBN 0-86720-295-5.
- [9] Steven K. Shevell (2003). *The Science of Color*. Elsevier. ISBN 0-444-51251-9.
- [10] S. N. Archer (1999). *Adaptive mechanisms in the ecology of vision*. Springer. ISBN 0-7923-5319-6.
- [11] Arne Valberg (1995). *Light Vision Color*. John Wiley and Sons. ISBN 0-470-84902-9.
- [12] M. H. F. Wilkinson & F. Schut (1998). *Digital Image Analysis of Microbes: Imaging, Morphometry, Fluorometry and Motility Techniques and Applications*. John Wiley and Sons. ISBN 0-471-97440-4.
- [13] Peter G. J. Barten (1999). *Contrast Sensitivity of the Human Eye and Its Effects on Image Quality*. SPIE Press. ISBN 0-8194-3496-5.
- [14] Matt Young (1993). *Optics and lasers: including fibers and optical waveguides*. Springer. ISBN 3-540-65741-X.
- [15] Stephen A. Dyer (2001). *Survey of Instrumentation and Measurement*. Wiley-IEEE. ISBN 0-471-39484-X.
- [16] Robert B. Northrop (2004). *Analysis and Application of Analog Electronic Circuits to Biomedical Instrumentation*. CRC Press. ISBN 0-8493-2143-3.

# Chapter 2

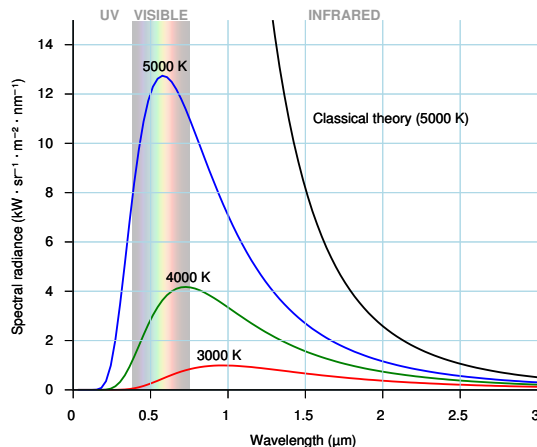
## RGB Color Gamut

### 2.1 Planck's law

Not to be confused with Planck relation.

See also: Black body radiation and Thermal radiation

**Planck's law** describes the spectral density of electro-



Planck's law (colored curves) accurately described black body radiation and resolved the **ultraviolet catastrophe** (black curve).

magnetic radiation emitted by a **black body** in thermal equilibrium at a given temperature  $T$ . The law is named after Max Planck, who proposed it in 1900. It is a pioneering result of modern physics and quantum theory.

The spectral radiance of a body,  $B\nu$ , describes the amount of energy it gives off as radiation of different frequencies. It is measured in terms of the power emitted per unit area of the body, per unit solid angle that the radiation is measured over, per unit frequency. Planck showed that the spectral radiance of a body for frequency  $\nu$  at absolute temperature  $T$  is given by

$$B_\nu(\nu, T) = \frac{2h\nu^3}{c^2} \frac{1}{e^{\frac{h\nu}{k_B T}} - 1}$$

where  $k_B$  the Boltzmann constant,  $h$  the Planck constant, and  $c$  the speed of light in the medium, whether material or vacuum.<sup>[1][2][3]</sup> The spectral radiance can also be measured per unit wavelength  $\lambda$  instead of per unit frequency. In this case, it is given by

$$B_\lambda(\lambda, T) = \frac{2hc^2}{\lambda^5} \frac{1}{e^{\frac{hc}{\lambda k_B T}} - 1}$$

The law may also be expressed in other terms, such as the number of photons emitted at a certain wavelength, or the energy density in a volume of radiation. The SI units of  $B\nu$  are  $\text{W}\cdot\text{sr}^{-1}\cdot\text{m}^{-2}\cdot\text{Hz}^{-1}$ , while those of  $B\lambda$  are  $\text{W}\cdot\text{sr}^{-1}\cdot\text{m}^{-3}$ .

In the limit of low frequencies (i.e. long wavelengths), Planck's law tends to the Rayleigh–Jeans law, while in the limit of high frequencies (i.e. small wavelengths) it tends to the Wien approximation.

Max Planck developed the law in 1900 with only empirically determined constants, and later showed that, expressed as an energy distribution, it is the unique stable distribution for radiation in thermodynamic equilibrium.<sup>[4]</sup> As an energy distribution, it is one of a family of thermal equilibrium distributions which include the Bose–Einstein distribution, the Fermi–Dirac distribution and the Maxwell–Boltzmann distribution.

### 2.1.1 Introduction

Every physical body spontaneously and continuously emits electromagnetic radiation. Near thermodynamic equilibrium, the emitted radiation is nearly described by Planck's law. Because of its dependence on temperature, Planck radiation is said to be thermal radiation. The higher the temperature of a body the more radiation it emits at every wavelength. Planck radiation has a maximum intensity at a specific wavelength that depends on the temperature. For example, at room temperature (~300 K), a body emits thermal radiation that is mostly infrared and invisible. At higher temperatures the amount of infrared radiation increases and can be felt as heat, and the body glows visibly red. At even higher temperatures, a body is dazzlingly bright yellow or blue-white and emits significant amounts of short wavelength radiation, including ultraviolet and even x-rays. The surface of the sun (~6000 K) emits large amounts of both infrared and ultraviolet radiation; its emission is peaked in the visible spectrum.

Planck radiation is the greatest amount of radiation that any body at thermal equilibrium can emit from its surface, whatever its chemical composition or surface structure.<sup>[5]</sup> The passage of radiation across an interface between media can be characterized by the emissivity of the interface (the ratio of the actual radiance to the theoretical Planck radiance), usually denoted by the symbol  $\varepsilon$ . It is in general dependent on chemical composition and physical structure, on temperature, on the wavelength, on the angle of passage, and on the polarization.<sup>[6]</sup> The emissivity of a natural interface is always between  $\varepsilon = 0$  and 1.

A body that interfaces with another medium which both has  $\varepsilon = 1$  and absorbs all the radiation incident upon it, is said to be a black body. The surface of a black body can be modelled by a small hole in the wall of a large enclosure which is maintained at a uniform temperature with opaque walls that, at every wavelength, are not perfectly reflective. At equilibrium, the radiation inside this enclosure follows Planck's law, and so will the radiation coming out of the small hole.

Just as the Maxwell–Boltzmann distribution is the unique maximum entropy energy distribution for a gas of material particles at thermal equilibrium, so is Planck's distribution for a gas of photons.<sup>[7][8]</sup> By contrast to a material gas where the masses and number of particles play a role, the spectral radiance, pressure and energy density of a photon gas at thermal equilibrium are entirely determined by the temperature.

If the photon gas is not Planckian, the second law of thermodynamics guarantees that interactions (between photons and other particles or even, at sufficiently high temperatures, between the photons themselves) will cause the photon energy distribution to change and approach the Planck distribution. In such an approach to thermodynamic equilibrium, photons are created or annihilated in the right numbers and with the right energies to fill the cavity with a Planck distribution until they reach the equilibrium temperature. It is as if the gas is a mixture of sub-gases, one for every band of wavelengths, and each sub-gas eventually attains the common temperature.

The quantity  $B\nu(\nu, T)$  is the spectral radiance as a function of temperature and frequency. It has units of  $\text{W}\cdot\text{m}^{-2}\cdot\text{sr}^{-1}\cdot\text{Hz}^{-1}$  in the SI system. An infinitesimal amount of power  $B\nu(\nu, T) \cos \theta dA d\Omega d\nu$  is radiated in the direction described by the angle  $\theta$  from the surface normal from infinitesimal surface area  $dA$  into infinitesimal solid angle  $d\Omega$  in an infinitesimal frequency band of width  $d\nu$  centered on frequency  $\nu$ . The total power radiated into any solid angle is the integral of  $B\nu(\nu, T)$  over those three quantities, and is given by the Stefan–Boltzmann law. The spectral radiance of Planckian radiation from a black body has the same value for every direction and angle of polarization, and so the black body is said to be a Lambertian radiator.

## 2.1.2 Different forms

Planck's law can be encountered in several forms depending on the conventions and preferences of different scientific fields. The various forms of the law for spectral radiance are summarized in the table below. Forms on the left are most often encountered in experimental fields, while those on the right are most often encountered in theoretical fields.

These distributions represent the spectral radiance of blackbodies—the power emitted from the emitting surface, per unit projected area of emitting surface, per unit solid angle, per spectral unit (frequency, wavelength, wavenumber or their angular equivalents). Since the radiance is isotropic (i.e. independent of direction), the power emitted at an angle to the normal is proportional to the projected area, and therefore to the cosine of that angle as per Lambert's cosine law, and is unpolarized.

### Correspondence between spectral variable forms

Different spectral variables require different corresponding forms of expression of the law. In general, one may not convert between the various forms of Planck's law simply by substituting one variable for another, because this would not take into account that the different forms have different units. Wavelength and frequency units are reciprocal.

Corresponding forms of expression are related because they express one and the same physical fact: for a particular physical spectral increment, a corresponding particular physical energy increment is radiated.

This is so whether it is expressed in terms of an increment of frequency,  $d\nu$ , or, correspondingly, of wavelength,  $d\lambda$ . Introduction of a minus sign can indicate that an increment of frequency corresponds with decrement of wavelength. For the above corresponding forms of expression of the spectral radiance, one may use an obvious expansion of notation, temporarily for the present calculation only. Then, for a particular spectral increment, the particular physical energy increment may be written

$$B_\lambda(\lambda, T) d\lambda = -B_\nu(\nu(\lambda), T) d\nu, \text{ which leads to } B_\lambda(\lambda, T) = -\frac{d\nu}{d\lambda} B_\nu(\nu(\lambda), T).$$

Also,  $\nu(\lambda) = c/\lambda$ , so that  $d\nu/d\lambda = -c/\lambda^2$ . Substitution gives the correspondence between the frequency and wavelength forms, with their different dimensions and units.<sup>[11][12]</sup> Consequently,

$$\frac{B_\lambda(T)}{B_\nu(T)} = \frac{c}{\lambda^2} = \frac{\nu^2}{c}.$$

Evidently, the location of the peak of the spectral distribution for Planck's law depends on the choice of spectral variable. Nevertheless, in a manner of speaking, this formula means that the shape of the spectral distribution is independent of temperature, according to Wien's displacement law, as detailed below in the sub-section **Percentiles** of the section **Properties**.

### Spectral energy density form

Planck's law can also be written in terms of the spectral energy density ( $u$ ) by multiplying  $B$  by  $4\pi/c$ :<sup>[13]</sup>

$$u_i(T) = \frac{4\pi}{c} B_i(T).$$

These distributions have units of energy per volume per spectral unit.

### First and second radiation constants

In the above variants of Planck's law, the *Wavelength* and *Wavenumber* variants use the terms  $2hc^2$  and  $hc/kB$  which comprise physical constants only. Consequently, these terms can be considered as physical constants themselves,<sup>[14]</sup> and are therefore referred to as the **first radiation constant  $c_1L$**  and the **second radiation constant  $c_2$**  with

$$c_1L = 2hc^2$$

and

$$c_2 = hc/kB.$$

Using the radiation constants, the *Wavelength* variant of Planck's law can be simplified to

$$L(\lambda, T) = \frac{c_1 L}{\lambda^5} \frac{1}{\exp\left(\frac{c_2}{\lambda T}\right) - 1}$$

and the *wavenumber* variant can be simplified correspondingly.

$L$  is used here instead of  $B$  because it is the SI symbol for *spectral radiance*. The  $L$  in  $c_1L$  refers to that. This reference is necessary because Planck's law can be reformulated to give *spectral radiant exitance*  $M(\lambda, T)$  rather than *spectral radiance*  $L(\lambda, T)$ , in which case  $c_1$  replaces  $c_1L$ , with

$$c_1 = 2\pi hc^2,$$

so that Planck's law for *spectral radiant exitance* can be written as

$$M(\lambda, T) = \frac{c_1}{\lambda^5} \frac{1}{\exp\left(\frac{c_2}{\lambda T}\right) - 1}$$

### 2.1.3 Derivation

See also: Gas in a box and Photon gas

Consider a cube of side  $L$  with conducting walls filled with electromagnetic radiation in thermal equilibrium at temperature  $T$ . If there is a small hole in one of the walls, the radiation emitted from the hole will be characteristic of a perfect **black body**. We will first calculate the spectral energy density within the cavity and then determine the spectral radiance of the emitted radiation.

At the walls of the cube, the parallel component of the electric field and the orthogonal component of the magnetic field must vanish. Analogous to the wave function of a **particle in a box**, one finds that the fields are superpositions of periodic functions. The three wavelengths  $\lambda_1$ ,  $\lambda_2$ , and  $\lambda_3$ , in the three directions orthogonal to the walls can be:

$$\lambda_i = \frac{2L}{n_i},$$

where the  $n_i$  are positive integers. For each set of integers  $n_i$  there are two linear independent solutions (modes). According to quantum theory, the energy levels of a mode are given by:

$$E_{n_1, n_2, n_3}(r) = \left(r + \frac{1}{2}\right) \frac{hc}{2L} \sqrt{n_1^2 + n_2^2 + n_3^2}. \quad (1)$$

The quantum number  $r$  can be interpreted as the number of photons in the mode. The two modes for each set of  $n_i$  correspond to the two polarization states of the photon which has a spin of 1. Note that for  $r = 0$  the energy of the mode is not zero. This vacuum energy of the electromagnetic field is responsible for the **Casimir effect**. In the following we will calculate the internal energy of the box at **absolute temperature  $T$** .

According to **statistical mechanics**, the probability distribution over the energy levels of a particular mode is given by:

$$P_r = \frac{\exp(-\beta E(r))}{Z(\beta)}.$$

Here

$$\beta \stackrel{\text{def}}{=} \frac{1}{k_B T}.$$

The denominator  $Z(\beta)$ , is the **partition function** of a single mode and makes  $P_r$  properly normalized:

$$Z(\beta) = \sum_{r=0}^{\infty} e^{-\beta E(r)} = \frac{e^{-\beta\varepsilon/2}}{1 - e^{-\beta\varepsilon}}.$$

Here we have implicitly defined

$$\varepsilon \stackrel{\text{def}}{=} \frac{hc}{2L} \sqrt{n_1^2 + n_2^2 + n_3^2},$$

which is the energy of a single photon. As explained [here](#), the average energy in a mode can be expressed in terms of the partition function:

$$\langle E \rangle = -\frac{d \log(Z)}{d\beta} = \frac{\varepsilon}{2} + \frac{\varepsilon}{e^{\beta\varepsilon} - 1}.$$

This formula, apart from the first vacuum energy term, is a special case of the general formula for particles obeying Bose–Einstein statistics. Since there is no restriction on the total number of photons, the chemical potential is zero.

If we measure the energy relative to the ground state, the total energy in the box follows by summing  $\langle E \rangle - \varepsilon/2$  over all allowed single photon states. This can be done exactly in the thermodynamic limit as  $L$  approaches infinity. In this limit,  $\varepsilon$  becomes continuous and we can then integrate  $\langle E \rangle - \varepsilon/2$  over this parameter. To calculate the energy in the box in this way, we need to evaluate how many photon states there are in a given energy range. If we write the total number of single photon states with energies between  $\varepsilon$  and  $\varepsilon + d\varepsilon$  as  $g(\varepsilon)d\varepsilon$ , where  $g(\varepsilon)$  is the density of states (which is evaluated below), then we can write:

$$U = \int_0^\infty \frac{\varepsilon}{e^{\beta\varepsilon} - 1} g(\varepsilon) d\varepsilon. \quad (2)$$

To calculate the density of states we rewrite equation (1) as follows:

$$\varepsilon \stackrel{\text{def}}{=} \frac{hc}{2L} n,$$

where  $n$  is the norm of the vector  $\mathbf{n} = (n_1, n_2, n_3)$ :

$$n = \sqrt{n_1^2 + n_2^2 + n_3^2}.$$

For every vector  $\mathbf{n}$  with integer components larger than or equal to zero, there are two photon states. This means that the number of photon states in a certain region of  $n$ -space is twice the volume of that region. An energy range of  $d\varepsilon$  corresponds to shell of thickness  $dn = 2L/hc d\varepsilon$  in  $n$ -space. Because the components of  $\mathbf{n}$  have to be positive, this shell spans an octant of a sphere. The number of photon states  $g(\varepsilon)d\varepsilon$ , in an energy range  $d\varepsilon$ , is thus given by:

$$g(\varepsilon) d\varepsilon = 2 \frac{1}{8} 4\pi n^2 dn = \frac{8\pi L^3}{h^3 c^3} \varepsilon^2 d\varepsilon.$$

Inserting this in Eq. (2) gives:

$$U = L^3 \frac{8\pi}{h^3 c^3} \int_0^\infty \frac{\varepsilon^3}{e^{\beta\varepsilon} - 1} d\varepsilon. \quad (3)$$

From this equation one can derive the spectral energy density as a function of frequency  $uv(T)$  and as a function of wavelength  $u\lambda(T)$ :

$$\frac{U}{L^3} = \int_0^\infty u_\nu(T) d\nu,$$

where

$$u_\nu(T) = \frac{8\pi h\nu^3}{c^3} \frac{1}{e^{h\nu/k_B T} - 1}.$$

And:

$$\frac{U}{L^3} = \int_0^\infty u_\lambda(T) d\lambda,$$

where

$$u_\lambda(T) = \frac{8\pi hc}{\lambda^5} \frac{1}{e^{hc/\lambda k_B T} - 1}.$$

This is also a spectral energy density function with units of energy per unit wavelength per unit volume. Integrals of this type for Bose and Fermi gases can be expressed in terms of polylogarithms. In this case, however, it is possible to calculate the integral in closed form using only elementary functions. Substituting

$$\varepsilon = k_B T x,$$

in Eq. (3), makes the integration variable dimensionless giving:

$$u(T) = \frac{8\pi (k_B T)^4}{(hc)^3} J,$$

where  $J$  is a Bose–Einstein integral given by:

$$J = \int_0^\infty \frac{x^3}{e^x - 1} dx = \frac{\pi^4}{15}.$$

The total electromagnetic energy inside the box is thus given by:

$$\frac{U}{V} = \frac{8\pi^5 (k_B T)^4}{15(hc)^3},$$

where  $V = L^3$  is the volume of the box.

The combination  $hc/kB$  has the value 14387.770  $\mu\text{m}\cdot\text{K}$ .

This is **not** the Stefan–Boltzmann law (which provides the total energy *radiated* by a black body per unit surface area per unit time), but it can be written more compactly using the Stefan–Boltzmann constant  $\sigma$ , giving

$$\frac{U}{V} = \frac{4\sigma T^4}{c}.$$

The constant  $4\sigma/c$  is sometimes called the radiation constant.

Since the radiation is the same in all directions, and propagates at the speed of light ( $c$ ), the spectral radiance of radiation exiting the small hole is

$$B_\nu(T) = \frac{u_\nu(T) c}{4\pi},$$

which yields

$$B_\nu(T) = \frac{2h\nu^3}{c^2} \frac{1}{e^{h\nu/k_B T} - 1}.$$

It can be converted to an expression for  $B\lambda(T)$  in wavelength units by substituting  $\nu$  by  $c/\lambda$  and evaluating

$$B_\lambda(T) = B_\nu(T) \left| \frac{d\nu}{d\lambda} \right|.$$

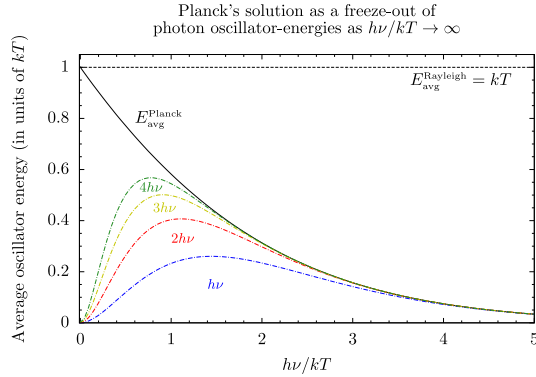
Note that dimensional analysis shows that the unit of steradians, shown in the denominator of left hand side of the equation above, is generated in and carried through the derivation but does not appear in any of the dimensions for any element on the left-hand-side of the equation.

This derivation is based on Brehm & Mullin 1989.

## 2.1.4 Physics

### Outline

Planck's law describes the unique and characteristic spectral distribution for electromagnetic radiation in thermodynamic equilibrium, when there is no net flow of matter or energy.<sup>[4]</sup> Its physics is most easily understood by considering the radiation in a cavity with rigid opaque walls. Motion of the walls can affect the radiation. If the walls are not opaque, then the thermodynamic equilibrium is not isolated. It is of interest to explain how the thermodynamic equilibrium is attained. There are two main cases: (a) when the approach to thermodynamic equilibrium is in the presence of matter, when the walls of the cavity are imperfectly reflective for every wavelength or when



*Freeze-out of high-energy oscillators.*

the walls are perfectly reflective while the cavity contains a small black body (this was the main case considered by Planck); or (b) when the approach to equilibrium is in the absence of matter, when the walls are perfectly reflective for all wavelengths and the cavity contains no matter. For matter not enclosed in such a cavity, thermal radiation can be approximately explained by appropriate use of Planck's law.

Classical physics led, via the **Equipartition theorem**, to the **Ultraviolet catastrophe**, a prediction that the total black-body radiation intensity was infinite. If supplemented by the classically unjustifiable assumption that for some reason the radiation is finite, classical thermodynamics provides an account of some aspects of the Planck distribution, such as the **Stefan–Boltzmann law**, and the **Wien displacement law**. For the case of the presence of matter, quantum mechanics provides a good account, as found below in the section headed **Einstein coefficients**. This was the case considered by Einstein, and is nowadays used for quantum optics.<sup>[15][16]</sup> For the case of the absence of matter, quantum field theory is necessary, because non-relativistic quantum mechanics with fixed particle numbers does not provide a sufficient account.

### Photons

Quantum theoretical explanation of Planck's law views the radiation as a gas of massless, uncharged, bosonic particles, namely photons, in **thermodynamic equilibrium**. Photons are viewed as the carriers of the electromagnetic interaction between electrically charged elementary particles. Photon numbers are not conserved. Photons are created or annihilated in the right numbers and with the right energies to fill the cavity with the Planck distribution. For a photon gas in thermodynamic equilibrium, the internal energy density is entirely determined by the temperature; moreover, the pressure is entirely determined by the internal energy density. This is unlike the case of thermodynamic equilibrium for material gases, for which the internal energy is determined not only by the temperature, but also, independently, by

the respective numbers of the different molecules, and independently again, by the specific characteristics of the different molecules. For different material gases at given temperature, the pressure and internal energy density can vary independently, because different molecules can carry independently different excitation energies.

Planck's law arises as a limit of the **Bose–Einstein distribution**, the energy distribution describing non-interacting bosons in thermodynamic equilibrium. In the case of massless bosons such as photons and gluons, the **chemical potential** is zero and the Bose-Einstein distribution reduces to the Planck distribution. There is another fundamental equilibrium energy distribution: the **Fermi–Dirac distribution**, which describes fermions, such as electrons, in thermal equilibrium. The two distributions differ because multiple bosons can occupy the same quantum state, while multiple fermions cannot. At low densities, the number of available quantum states per particle is large, and this difference becomes irrelevant. In the low density limit, the Bose-Einstein and the Fermi-Dirac distribution each reduce to the **Maxwell–Boltzmann distribution**.

### Kirchhoff's law of thermal radiation

Main article: Kirchhoff's law of thermal radiation

Kirchhoff's law of thermal radiation is a succinct and brief account of a complicated physical situation. The following is an introductory sketch of that situation, and is very far from being a rigorous physical argument. The purpose here is only to summarize the main physical factors in the situation, and the main conclusions.

**Spectral dependence of thermal radiation** There is a difference between conductive heat transfer and radiative heat transfer. Radiative heat transfer can be filtered to pass only a definite band of radiative frequencies.

It is generally known that the hotter a body becomes the more heat it radiates at every frequency.

In a cavity in an opaque body with rigid walls that are not perfectly reflective at any frequency, in thermodynamic equilibrium, there is only one temperature, and it must be shared in common by the radiation of every frequency.

One may imagine two such cavities, each in its own isolated radiative and thermodynamic equilibrium. One may imagine an optical device that allows radiative heat transfer between the two cavities, filtered to pass only a definite band of radiative frequencies. If the values of the spectral radiances of the radiations in the cavities differ in that frequency band, heat may be expected to pass from the hotter to the colder. One might propose to use such a filtered transfer of heat in such a band to drive a heat engine. If the two bodies are at the same temperature, the second law of thermodynamics does not allow

the heat engine to work. It may be inferred that for a temperature common to the two bodies, the values of the spectral radiances in the pass-band must also be common. This must hold for every frequency band.<sup>[17][18][19]</sup> This became clear to Balfour Stewart and later to Kirchhoff. Balfour Stewart found experimentally that of all surfaces, one of lamp-black emitted the greatest amount of thermal radiation for every quality of radiation, judged by various filters.

Thinking theoretically, Kirchhoff went a little further, and pointed out that this implied that the spectral radiance, as a function of radiative frequency, of any such cavity in thermodynamic equilibrium must be a unique universal function of temperature. He postulated an ideal black body that interfaces with its surrounds in just such a way as to absorb all the radiation that falls on it. By the Helmholtz reciprocity principle, radiation from the interior of such a body would pass unimpeded, directly to its surrounds without reflection at the interface. In thermodynamic equilibrium, the thermal radiation emitted from such a body would have that unique universal spectral radiance as a function of temperature. This insight is the root of Kirchhoff's law of thermal radiation.

**Relation between absorptivity and emissivity** One may imagine a small homogeneous spherical material body labeled  $X$  at a temperature  $T_X$ , lying in a radiation field within a large cavity with walls of material labeled  $Y$  at a temperature  $T_Y$ . The body  $X$  emits its own thermal radiation. At a particular frequency  $\nu$ , the radiation emitted from a particular cross-section through the centre of  $X$  in one sense in a direction normal to that cross-section may be denoted  $I_{\nu,X}(T_X)$ , characteristically for the material of  $X$ . At that frequency  $\nu$ , the radiative power from the walls into that cross-section in the opposite sense in that direction may be denoted  $I_{\nu,Y}(T_Y)$ , for the wall temperature  $T_Y$ . For the material of  $X$ , defining the absorptivity  $\alpha_{\nu,X,Y}(T_X, T_Y)$  as the fraction of that incident radiation absorbed by  $X$ , that incident energy is absorbed at a rate  $\alpha_{\nu,X,Y}(T_X, T_Y) I_{\nu,Y}(T_Y)$ .

The rate  $q(\nu, T_X, T_Y)$  of accumulation of energy in one sense into the cross-section of the body can then be expressed

$$q(\nu, T_X, T_Y) = \alpha_{\nu,X,Y}(T_X, T_Y) I_{\nu,Y}(T_Y) - I_{\nu,X}(T_X).$$

Kirchhoff's seminal insight, mentioned just above, was that, at thermodynamic equilibrium at temperature  $T$ , there exists a unique universal radiative distribution, nowadays denoted  $B\nu(T)$ , that is independent of the chemical characteristics of the materials  $X$  and  $Y$ , that leads to a very valuable understanding of the radiative exchange equilibrium of any body at all, as follows.

When there is thermodynamic equilibrium at temperature  $T$ , the cavity radiation from the walls has that unique universal value, so that  $I_{\nu,Y}(T_Y) = B\nu(T)$ . Further, one

may define the emissivity  $\varepsilon_{\nu,X}(TX)$  of the material of the body  $X$  just so that at thermodynamic equilibrium at temperature  $TX = T$ , one has  $I_{\nu,X}(TX) = I_{\nu,X}(T) = \varepsilon_{\nu,X}(T) B_{\nu}(T)$ .

When thermal equilibrium prevails at temperature  $T = TX = TY$ , the rate of accumulation of energy vanishes so that  $q(\nu, TX, TY) = 0$ . It follows that in thermodynamic equilibrium, when  $T = TX = TY$ ,

$$0 = \alpha_{\nu,X,Y}(T, T) B_{\nu}(T) - \epsilon_{\nu,X}(T) B_{\nu}(T).$$

Kirchhoff pointed out that it follows that in thermodynamic equilibrium, when  $T = TX = TY$ ,

$$\alpha_{\nu,X,Y}(T, T) = \epsilon_{\nu,X}(T).$$

Introducing the special notation  $\alpha_{\nu,X}(T)$  for the absorptivity of material  $X$  at thermodynamic equilibrium at temperature  $T$  (justified by a discovery of Einstein, as indicated below), one further has the equality

$$\alpha_{\nu,X}(T) = \epsilon_{\nu,X}(T)$$

at thermodynamic equilibrium.

The equality of absorptivity and emissivity here demonstrated is specific for thermodynamic equilibrium at temperature  $T$  and is in general not to be expected to hold when conditions of thermodynamic equilibrium do not hold. The emissivity and absorptivity are each separately properties of the molecules of the material but they depend differently upon the distributions of states of molecular excitation on the occasion, because of a phenomenon known as "stimulated emission", that was discovered by Einstein. On occasions when the material is in thermodynamic equilibrium or in a state known as local thermodynamic equilibrium, the emissivity and absorptivity become equal. Very strong incident radiation or other factors can disrupt thermodynamic equilibrium or local thermodynamic equilibrium. Local thermodynamic equilibrium in a gas means that molecular collisions far outweigh light emission and absorption in determining the distributions of states of molecular excitation.

Kirchhoff pointed out that he did not know the precise character of  $B_{\nu}(T)$ , but he thought it important that it should be found out. Four decades after Kirchhoff's insight of the general principles of its existence and character, Planck's contribution was to determine the precise mathematical expression of that equilibrium distribution  $B_{\nu}(T)$ .

## Black body

Main article: Black body

In physics, one considers an ideal black body, here labeled  $B$ , defined as one that completely absorbs all of the electromagnetic radiation falling upon it at every frequency  $\nu$  (hence the term "black"). According to Kirchhoff's law of thermal radiation, this entails that, for every frequency  $\nu$ , at thermodynamic equilibrium at temperature  $T$ , one has  $\alpha_{\nu,B}(T) = \epsilon_{\nu,B}(T) = 1$ , so that the thermal radiation from a black body is always equal to the full amount specified by Planck's law. No physical body can emit thermal radiation that exceeds that of a black body, since if it were in equilibrium with a radiation field, it would be emitting more energy than was incident upon it.

Though perfectly black materials do not exist, in practice a black surface can be accurately approximated.<sup>[4]</sup> As to its material interior, a body of condensed matter, liquid, solid, or plasma, with a definite interface with its surroundings, is completely black to radiation if it is completely opaque. That means that it absorbs all of the radiation that penetrates the interface of the body with its surroundings, and enters the body. This is not too difficult to achieve in practice. On the other hand, a perfectly black interface is not found in nature. A perfectly black interface reflects no radiation, but transmits all that falls on it, from either side. The best practical way to make an effectively black interface is to simulate an 'interface' by a small hole in the wall of a large cavity in a completely opaque rigid body of material that does not reflect perfectly at any frequency, with its walls at a controlled temperature. Beyond these requirements, the component material of the walls is unrestricted. Radiation entering the hole has almost no possibility of escaping the cavity without being absorbed by multiple impacts with its walls.<sup>[20]</sup>

## Lambert's cosine law

Main article: Lambert's cosine law

As explained by Planck,<sup>[21]</sup> a radiating body has an interior consisting of matter, and an interface with its contiguous neighbouring material medium, which is usually the medium from within which the radiation from the surface of the body is observed. The interface is not composed of physical matter but is a theoretical conception, a mathematical two-dimensional surface, a joint property of the two contiguous media, strictly speaking belonging to neither separately. Such an interface can neither absorb nor emit, because it is not composed of physical matter; but it is the site of reflection and transmission of radiation, because it is a surface of discontinuity of optical properties. The reflection and transmission of radiation at the interface obey the Stokes–Helmholtz reciprocity principle.

At any point in the interior of a black body located inside a cavity in thermodynamic equilibrium at temperature  $T$  the radiation is homogeneous, isotropic and unpolarized. A black body absorbs all and reflects none of the elec-

tromagnetic radiation incident upon it. According to the Helmholtz reciprocity principle, radiation from the interior of a black body is not reflected at its surface, but is fully transmitted to its exterior. Because of the isotropy of the radiation in the body's interior, the spectral radiance of radiation transmitted from its interior to its exterior through its surface is independent of direction.<sup>[22]</sup>

This is expressed by saying that radiation from the surface of a black body in thermodynamic equilibrium obeys Lambert's cosine law.<sup>[23][24]</sup> This means that the spectral flux  $d\Phi(dA, \theta, d\Omega, dv)$  from a given infinitesimal element of area  $dA$  of the actual emitting surface of the black body, detected from a given direction that makes an angle  $\theta$  with the normal to the actual emitting surface at  $dA$ , into an element of solid angle of detection  $d\Omega$  centred on the direction indicated by  $\theta$ , in an element of frequency bandwidth  $dv$ , can be represented as<sup>[25]</sup>

$$\frac{d\Phi(dA, \theta, d\Omega, dv)}{d\Omega} = L^0(dA, dv) dA dv \cos \theta$$

where  $L^0(dA, dv)$  denotes the flux, per unit area per unit frequency per unit solid angle, that area  $dA$  would show if it were measured in its normal direction  $\theta = 0$ .

The factor  $\cos \theta$  is present because the area to which the spectral radiance refers directly is the projection, of the actual emitting surface area, onto a plane perpendicular to the direction indicated by  $\theta$ . This is the reason for the name *cosine law*.

Taking into account the independence of direction of the spectral radiance of radiation from the surface of a black body in thermodynamic equilibrium, one has  $L^0(dA, dv) = B_\nu(T)$  and so

$$\frac{d\Phi(dA, \theta, d\Omega, dv)}{d\Omega} = B_\nu(T) dA dv \cos \theta.$$

Thus Lambert's cosine law expresses the independence of direction of the spectral radiance  $B_\nu(T)$  of the surface of a black body in thermodynamic equilibrium.

### Stefan–Boltzmann law

Main article: Stefan–Boltzmann law

The total power emitted per unit area at the surface of a black body ( $P$ ) may be found by integrating the black body spectral flux found from Lambert's law over all frequencies, and over the solid angles corresponding to a hemisphere ( $h$ ) above the surface.

$$P = \int_0^\infty d\nu \int_h d\Omega B_\nu \cos(\theta)$$

The infinitesimal solid angle can be expressed in spherical polar coordinates:

$$d\Omega = \sin(\theta) d\theta d\phi.$$

So that:

$$P = \int_0^\infty d\nu \int_0^{\frac{\pi}{2}} d\theta \int_0^{2\pi} d\phi B_\nu(T) \cos(\theta) \sin(\theta) = \sigma T^4$$

where

$$\sigma = \frac{2k_B^4 \pi^5}{15c^2 h^3} \approx 5.670400 \times 10^{-8} \text{ Js}^{-1} \text{ m}^{-2} \text{ K}^{-4}$$

is known as the Stefan–Boltzmann constant.<sup>[26]</sup>

### Radiative transfer

Main article: Radiative transfer

The equation of radiative transfer describes the way in which radiation is affected as it travels through a material medium. For the special case in which the material medium is in thermodynamic equilibrium in the neighborhood of a point in the medium, Planck's law is of special importance.

For simplicity, we can consider the linear steady state, without scattering. The equation of radiative transfer states that for a beam of light going through a small distance  $ds$ , energy is conserved: The change in the (spectral) radiance of that beam ( $I_\nu$ ) is equal to the amount removed by the material medium plus the amount gained from the material medium. If the radiation field is in equilibrium with the material medium, these two contributions will be equal. The material medium will have a certain emission coefficient and absorption coefficient.

The absorption coefficient  $\alpha$  is the fractional change in the intensity of the light beam as it travels the distance  $ds$ , and has units of length<sup>-1</sup>. It is composed of two parts, the decrease due to absorption and the increase due to stimulated emission. Stimulated emission is emission by the material body which is caused by and is proportional to the incoming radiation. It is included in the absorption term because, like absorption, it is proportional to the intensity of the incoming radiation. Since the amount of absorption will generally vary linearly as the density  $\rho$  of the material, we may define a "mass absorption coefficient"  $\kappa_\nu = \alpha/\rho$  which is a property of the material itself. The change in intensity of a light beam due to absorption as it traverses a small distance  $ds$  will then be<sup>[2]</sup>

$$dI_\nu = -\kappa_\nu \rho I_\nu ds$$

The "mass emission coefficient"  $j_\nu$  is equal to the radiance per unit volume of a small volume element divided

by its mass (since, as for the mass absorption coefficient, the emission is proportional to the emitting mass) and has units of power·solid angle<sup>-1</sup>·frequency<sup>-1</sup>·density<sup>-1</sup>. Like the mass absorption coefficient, it too is a property of the material itself. The change in a light beam as it traverses a small distance  $ds$  will then be<sup>[27]</sup>

$$dI_\nu = j_\nu \rho ds$$

The equation of radiative transfer will then be the sum of these two contributions:<sup>[28]</sup>

$$\frac{dI_\nu}{ds} = j_\nu \rho - \kappa_\nu \rho I_\nu.$$

If the radiation field is in equilibrium with the material medium, then the radiation will be homogeneous (independent of position) so that  $dI_\nu = 0$  and:

$$\kappa_\nu B_\nu = j_\nu$$

which is another statement of Kirchhoff's law, relating two material properties of the medium, and which yields the radiative transfer equation at a point around which the medium is in thermodynamic equilibrium:

$$\frac{dI_\nu}{ds} = \kappa_\nu \rho (B_\nu - I_\nu).$$

### Einstein coefficients

Main article: Atomic spectral line

The principle of detailed balance states that, at thermodynamic equilibrium, each elementary process is equilibrated by its reverse process.

In 1916, Albert Einstein applied this principle on an atomic level to the case of an atom radiating and absorbing radiation due to transitions between two particular energy levels,<sup>[29]</sup> giving a deeper insight into the equation of radiative transfer and Kirchhoff's law for this type of radiation. If level 1 is the lower energy level with energy  $E_1$ , and level 2 is the upper energy level with energy  $E_2$ , then the frequency  $\nu$  of the radiation radiated or absorbed will be determined by Bohr's frequency condition:<sup>[30][31]</sup>

$$E_2 - E_1 = h\nu$$

If  $n_1$  and  $n_2$  are the number densities of the atom in states 1 and 2 respectively, then the rate of change of these densities in time will be due to three processes:

where  $I\nu(T)$  is the spectral radiance of the radiation field. The three parameters  $A_{21}$ ,  $B_{21}$  and  $B_{12}$ , known as the Einstein coefficients, are associated with the photon frequency  $\nu$  produced by the transition between two energy levels (states). As a result, each line in a spectra has its own set of associated coefficients. When the atoms and the radiation field are in equilibrium, the radiance will be given by Planck's law and, by the principle of detailed balance, the sum of these rates must be zero:

$$0 = A_{21}n_2 + B_{21}n_2B_\nu(T) - B_{12}n_1B_\nu(T)$$

Since the atoms are also in equilibrium, the populations of the two levels are related by the Boltzmann factor:

$$\frac{n_2}{n_1} = \frac{g_2}{g_1} e^{-h\nu/k_B T}$$

where  $g_1$  and  $g_2$  are the multiplicities of the respective energy levels. Combining the above two equations with the requirement that they be valid at any temperature yields two relationships between the Einstein coefficients:

$$\frac{A_{21}}{B_{21}} = \frac{2h\nu^3}{c^2}$$

$$\frac{B_{21}}{B_{12}} = \frac{g_1}{g_2}$$

so that knowledge of one coefficient will yield the other two. For the case of isotropic absorption and emission, the emission coefficient ( $j_\nu$ ) and absorption coefficient ( $\kappa_\nu$ ) defined in the radiative transfer section above, can be expressed in terms of the Einstein coefficients. The relationships between the Einstein coefficients will yield the expression of Kirchhoff's law expressed in the *Radiative transfer* section above, namely that

$$j_\nu = \kappa_\nu B_\nu.$$

These coefficients apply to both atoms and molecules.

### 2.1.5 Properties

#### Peaks

The distributions  $B\nu$ ,  $B\omega$ ,  $B\tilde{\nu}$  and  $Bk$  peak at a photon energy of<sup>[32]</sup>

$$E = \left[ 3 + W \left( \frac{-3}{e^3} \right) \right] k_B T \approx 2.821 k_B T,$$

where  $W$  is the Lambert W function and  $e$  is Euler's number.

The distributions  $B\lambda$  and  $B\nu$  however, peak at a different energy<sup>[32]</sup>

$$E = \left[ 5 + W \left( \frac{-5}{e^5} \right) \right] k_B T \approx 4.965 k_B T,$$

The reason for this is that, as mentioned above, one cannot go from (for example)  $B\nu$  to  $B\lambda$  simply by substituting  $\nu$  by  $\lambda$ . In addition, one must also multiply the result of the substitution by

$$\left| \frac{d\nu}{d\lambda} \right| = c/\lambda^2$$

This  $1/\lambda^2$  factor shifts the peak of the distribution to higher energies.

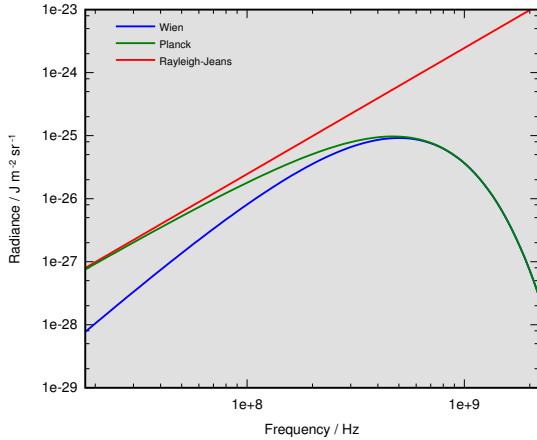
Dividing  $hc$  by this energy expression gives the wavelength of the peak. For this one can use  $hc/kB = 14387.770 \mu\text{m}\cdot\text{K}$ .

The spectral radiance at these peaks is given by:

$$B_{\nu,\max}(T) = \frac{2k_B^3 T^3 (3 + W(-3 \exp(-3))^3)}{h^2 c^2} \frac{1}{e^{3+W(-3 \exp(-3))} - 1}$$

$$B_{\lambda,\max}(T) = \frac{2k_B^5 T^5 (5 + W(-5 \exp(-5))^5)}{h^4 c^3} \frac{1}{e^{5+W(-5 \exp(-5))} - 1}$$

## Approximations



Log-log plots of radiance vs. frequency for Planck's law (green), compared with the Rayleigh-Jeans law (red) and the Wien approximation (blue) for a black body at 8 mK temperature.

In the limit of low frequencies (i.e. long wavelengths), Planck's law becomes the Rayleigh-Jeans law<sup>[33][34][35]</sup>

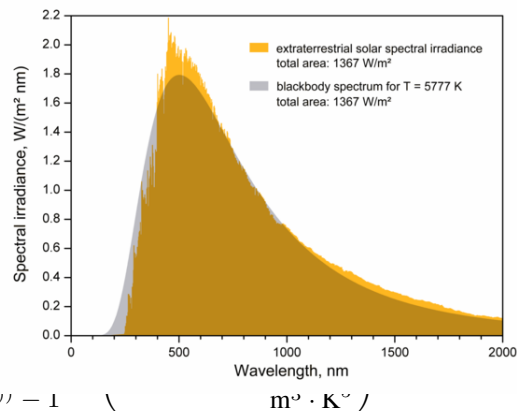
$$B_\nu(T) \approx \frac{2\nu^2}{c^2} k_B T \quad \text{or} \quad B_\lambda(T) \approx \frac{2c}{\lambda^4} k_B T.$$

The radiance increases as the square of the frequency, illustrating the **ultraviolet catastrophe**. In the limit of high frequencies (i.e. small wavelengths) Planck's law tends to the **Wien approximation**:<sup>[35][36][37]</sup>

$$B_\nu(T) \approx \frac{2h\nu^3}{c^2} e^{-\frac{h\nu}{k_B T}} \quad \text{or} \quad B_\lambda(T) \approx \frac{2hc^2}{\lambda^5} e^{-\frac{hc}{\lambda k_B T}}.$$

Both approximations were known to Planck before he developed his law. He was led by these two approximations to develop a law which incorporated both limits, which ultimately became Planck's law.

## Percentiles



The Sun is an excellent approximation of a black body. Its effective temperature is  $\sim 5777 \text{ K}$ .

Wien's displacement law in its stronger form states that the shape of Planck's law is independent of temperature. It is therefore possible to list the percentile points of the total radiation as well as the peaks for wavelength and frequency, in a form which gives the wavelength  $\lambda$  when divided by temperature  $T$ .<sup>[38]</sup> The second row of the following table lists the corresponding values of  $\lambda T$ , that is, those values of  $x$  for which the wavelength  $\lambda$  is  $x/T$  micrometers at the radiance percentile point given by the corresponding entry in the first row.

That is, 0.01% of the radiation is at a wavelength below  $910/T \mu\text{m}$ , 20% below  $2676/T \mu\text{m}$ , etc. The wavelength and frequency peaks are in bold and occur at 25.0% and 64.6% respectively. The 41.8% point is the wavelength-frequency-neutral peak. These are the points at which the respective Planck-law functions  $1/\lambda^5$ ,  $\nu^3$  and  $\nu^2/\lambda^2$  divided by  $\exp(h\nu/k_B T) - 1$  attain their maxima. Also note the much smaller gap in ratio of wavelengths between 0.1% and 0.01% ( $1110$  is 22% more than  $910$ ) than between 99.9% and 99.99% ( $113374$  is 120% more than  $51613$ ), reflecting the exponential decay of energy

at short wavelengths (left end) and polynomial decay at long.

Which peak to use depends on the application. The conventional choice is the wavelength peak at 25.0% given by Wien's displacement law in its weak form. For some purposes the median or 50% point dividing the total radiation into two halves may be more suitable. The latter is closer to the frequency peak than to the wavelength peak because the radiance drops exponentially at short wavelengths and only polynomially at long. The neutral peak occurs at a shorter wavelength than the median for the same reason.

For the Sun,  $T$  is 5778 K, allowing the percentile points of the Sun's radiation, in nanometers, to be tabulated as follows when modeled as a black body radiator, to which the Sun is a fair approximation. For comparison a planet modeled as a black body radiating at a nominal 288 K (15 °C) as a representative value of the Earth's highly variable temperature has wavelengths more than twenty times that of the Sun, tabulated in the third row in micrometers (thousands of nanometers).

That is, only 1% of the Sun's radiation is at wavelengths shorter than 251 nm, and only 1% at longer than 3961 nm. Expressed in micrometers this puts 98% of the Sun's radiation in the range from 0.251 to 3.961 μm. The corresponding 98% of energy radiated from a 288 K planet is from 5.03 to 79.5 μm, well above the range of solar radiation (or below if expressed in terms of frequencies  $\nu = c/\lambda$  instead of wavelengths  $\lambda$ ).

A consequence of this more-than-order-of-magnitude difference in wavelength between solar and planetary radiation is that filters designed to pass one and block the other are easy to construct. For example, windows fabricated of ordinary glass or transparent plastic pass at least 80% of the incoming 5778 K solar radiation, which is below 1.2 μm in wavelength, while blocking over 99% of the outgoing 288 K thermal radiation from 5 μm upwards, wavelengths at which most kinds of glass and plastic of construction-grade thickness are effectively opaque.

The Sun's radiation is that arriving at the top of the atmosphere (TOA). As can be read from the table, radiation below 400 nm, or **ultraviolet**, is about 12%, while that above 700 nm, or **infrared**, starts at about the 49% point and so accounts for 51% of the total. Hence only 37% of the TOA insolation is visible to the human eye. The atmosphere shifts these percentages substantially in favor of visible light as it absorbs most of the ultraviolet and significant amounts of infrared.

## 2.1.6 History

### Forerunners

**Balfour Stewart** In 1858, Balfour Stewart described his experiments on the thermal radiative emissive and absorptive powers of polished plates of various substances, compared with the powers of lamp-black surfaces, at the same temperature.<sup>[5]</sup> Stewart chose lamp-black surfaces as his reference because of various previous experimental findings, especially those of Pierre Prevost and of John Leslie. He wrote "Lamp-black, which absorbs all the rays that fall upon it, and therefore possesses the greatest possible absorbing power, will possess also the greatest possible radiating power."

Stewart measured radiated power with a thermo-pile and sensitive galvanometer read with a microscope. He was concerned with selective thermal radiation, which he investigated with plates of substances that radiated and absorbed selectively for different qualities of radiation rather than maximally for all qualities of radiation. He discussed the experiments in terms of rays which could be reflected and refracted, and which obeyed the Helmholtz reciprocity principle (though he did not use an eponym for it). He did not in this paper mention that the qualities of the rays might be described by their wavelengths, nor did he use spectrally resolving apparatus such as prisms or diffraction gratings. His work was quantitative within these constraints. He made his measurements in a room temperature environment, and quickly so as to catch his bodies in a condition near the thermal equilibrium in which they had been prepared by heating to equilibrium with boiling water. His measurements confirmed that substances that emit and absorb selectively respect the principle of selective equality of emission and absorption at thermal equilibrium.

Stewart offered a theoretical proof that this should be the case separately for every selected quality of thermal radiation, but his mathematics was not rigorously valid. According to historian D. M. Siegel: "He was not a practitioner of the more sophisticated techniques of nineteenth-century mathematical physics; he did not even make use of the functional notation in dealing with spectral distributions."<sup>[39]</sup> He made no mention of thermodynamics in this paper, though he did refer to conservation of *vis viva*. He proposed that his measurements implied that radiation was both absorbed and emitted by particles of matter throughout depths of the media in which it propagated. He applied the Helmholtz reciprocity principle to account for the material interface processes as distinct from the processes in the interior material. He concluded that his experiments showed that, in the interior of an enclosure in thermal equilibrium, the radiant heat, reflected and emitted combined, leaving any part of the surface, regardless of its substance, was the same as would have left that same portion of the surface if it had been composed of lamp-black. He did not mention the possibility of ideally perfectly reflective walls; in particular he noted that highly polished real physical metals absorb very slightly.

**Gustav Kirchhoff** In 1859, not knowing of Stewart's work, Gustav Robert Kirchhoff reported the coincidence of the wavelengths of spectrally resolved lines of absorption and of emission of visible light. Importantly for thermal physics, he also observed that bright lines or dark lines were apparent depending on the temperature difference between emitter and absorber.<sup>[40]</sup>

Kirchhoff then went on to consider bodies that emit and absorb heat radiation, in an opaque enclosure or cavity, in equilibrium at temperature  $T$ .

Here is used a notation different from Kirchhoff's. Here, the emitting power  $E(T, i)$  denotes a dimensioned quantity, the total radiation emitted by a body labeled by index  $i$  at temperature  $T$ . The total absorption ratio  $a(T, i)$  of that body is dimensionless, the ratio of absorbed to incident radiation in the cavity at temperature  $T$ . (In contrast with Balfour Stewart's, Kirchhoff's definition of his absorption ratio did not refer in particular to a lamp-black surface as the source of the incident radiation.) Thus the ratio  $E(T, i)/a(T, i)$  of emitting power to absorption ratio is a dimensioned quantity, with the dimensions of emitting power, because  $a(T, i)$  is dimensionless. Also here the wavelength-specific emitting power of the body at temperature  $T$  is denoted by  $E(\lambda, T, i)$  and the wavelength-specific absorption ratio by  $a(\lambda, T, i)$ . Again, the ratio  $E(\lambda, T, i)/a(\lambda, T, i)$  of emitting power to absorption ratio is a dimensioned quantity, with the dimensions of emitting power.

In a second report made in 1859, Kirchhoff announced a new general principle or law for which he offered a theoretical and mathematical proof, though he did not offer quantitative measurements of radiation powers.<sup>[41]</sup> His theoretical proof was and still is considered by some writers to be invalid.<sup>[39][42]</sup> His principle, however, has endured: it was that for heat rays of the same wavelength, in equilibrium at a given temperature, the wavelength-specific ratio of emitting power to absorption ratio has one and the same common value for all bodies that emit and absorb at that wavelength. In symbols, the law stated that the wavelength-specific ratio  $E(\lambda, T, i)/a(\lambda, T, i)$  has one and the same value for all bodies, that is for all values of index  $i$ . In this report there was no mention of black bodies.

In 1860, still not knowing of Stewart's measurements for selected qualities of radiation, Kirchhoff pointed out that it was long established experimentally that for total heat radiation, of unselected quality, emitted and absorbed by a body in equilibrium, the dimensioned total radiation ratio  $E(T, i)/a(T, i)$ , has one and the same value common to all bodies, that is, for every value of the material index  $i$ .<sup>[43]</sup> Again without measurements of radiative powers or other new experimental data, Kirchhoff then offered a fresh theoretical proof of his new principle of the universality of the value of the wavelength-specific ratio  $E(\lambda, T, i)/a(\lambda, T, i)$  at thermal equilibrium. His fresh theoretical proof was and still is considered by some writers

to be invalid.<sup>[39][42]</sup>

But more importantly, it relied on a new theoretical postulate of “perfectly black bodies”, which is the reason why one speaks of Kirchhoff's law. Such black bodies showed complete absorption in their infinitely thin most superficial surface. They correspond to Balfour Stewart's reference bodies, with internal radiation, coated with lamp-black. They were not the more realistic perfectly black bodies later considered by Planck. Planck's black bodies radiated and absorbed only by the material in their interiors; their interfaces with contiguous media were only mathematical surfaces, capable neither of absorption nor emission, but only of reflecting and transmitting with refraction.<sup>[44]</sup>

Kirchhoff's proof considered an arbitrary non-ideal body labeled  $i$  as well as various perfect black bodies labeled BB. It required that the bodies be kept in a cavity in thermal equilibrium at temperature  $T$ . His proof intended to show that the ratio  $E(\lambda, T, i)/a(\lambda, T, i)$  was independent of the nature  $i$  of the non-ideal body, however partly transparent or partly reflective it was.

His proof first argued that for wavelength  $\lambda$  and at temperature  $T$ , at thermal equilibrium, all perfectly black bodies of the same size and shape have the one and the same common value of emissive power  $E(\lambda, T, BB)$ , with the dimensions of power. His proof noted that the dimensionless wavelength-specific absorption ratio  $a(\lambda, T, BB)$  of a perfectly black body is by definition exactly 1. Then for a perfectly black body, the wavelength-specific ratio of emissive power to absorption ratio  $E(\lambda, T, BB)/a(\lambda, T, BB)$  is again just  $E(\lambda, T, BB)$ , with the dimensions of power. Kirchhoff considered, successively, thermal equilibrium with the arbitrary non-ideal body, and with a perfectly black body of the same size and shape, in place in his cavity in equilibrium at temperature  $T$ . He argued that the flows of heat radiation must be the same in each case. Thus he argued that at thermal equilibrium the ratio  $E(\lambda, T, i)/a(\lambda, T, i)$  was equal to  $E(\lambda, T, BB)$ , which may now be denoted  $B\lambda(\lambda, T)$ , a continuous function, dependent only on  $\lambda$  at fixed temperature  $T$ , and an increasing function of  $T$  at fixed wavelength  $\lambda$ , at low temperatures vanishing for visible but not for longer wavelengths, with positive values for visible wavelengths at higher temperatures, which does not depend on the nature  $i$  of the arbitrary non-ideal body. (Geometrical factors, taken into detailed account by Kirchhoff, have been ignored in the foregoing.)

Thus **Kirchhoff's law of thermal radiation** can be stated: *For any material at all, radiating and absorbing in thermodynamic equilibrium at any given temperature  $T$ , for every wavelength  $\lambda$ , the ratio of emissive power to absorptive ratio has one universal value, which is characteristic of a perfect black body, and is an emissive power which we here represent by  $B\lambda(\lambda, T)$ .* (For our notation  $B\lambda(\lambda, T)$ , Kirchhoff's original notation was simply e.)<sup>[2][43][45][46][47][48]</sup>

Kirchhoff announced that the determination of the function  $B\lambda(\lambda, T)$  was a problem of the highest importance, though he recognized that there would be experimental difficulties to be overcome. He supposed that like other functions that do not depend on the properties of individual bodies, it would be a simple function. That function  $B\lambda(\lambda, T)$  has occasionally been called 'Kirchhoff's (emission, universal) function',<sup>[49][50][51][52]</sup> though its precise mathematical form would not be known for another forty years, till it was discovered by Planck in 1900. The theoretical proof for Kirchhoff's universality principle was worked on and debated by various physicists over the same time, and later.<sup>[42]</sup> Kirchhoff stated later in 1860 that his theoretical proof was better than Balfour Stewart's, and in some respects it was so.<sup>[39]</sup> Kirchhoff's 1860 paper did not mention the second law of thermodynamics, and of course did not mention the concept of entropy which had not at that time been established. In a more considered account in a book in 1862, Kirchhoff mentioned the connection of his law with "Carnot's principle", which is a form of the second law.<sup>[53]</sup>

According to Helge Kragh, "Quantum theory owes its origin to the study of thermal radiation, in particular to the "blackbody" radiation that Robert Kirchhoff had first defined in 1859–1860."<sup>[54]</sup>

### Empirical and theoretical ingredients for the scientific induction of Planck's law

In 1860, Kirchhoff predicted experimental difficulties for the empirical determination of the function that described the dependence of the black-body spectrum as a function only of temperature and wavelength. And so it turned out. It took some forty years of development of improved methods of measurement of electromagnetic radiation to get a reliable result.<sup>[55]</sup>

In 1865, John Tyndall described radiation from electrically heated filaments and from carbon arcs as visible and invisible.<sup>[56]</sup> Tyndall spectrally decomposed the radiation by use of a rock salt prism, which passed heat as well as visible rays, and measured the radiation intensity by means of a thermopile.<sup>[57][58]</sup>

In 1880, André-Prosper-Paul Crova published a diagram of the three-dimensional appearance of the graph of the strength of thermal radiation as a function of wavelength and temperature.<sup>[59]</sup> He determined the spectral variable by use of prisms. He analyzed the surface through what he called "isothermal" curves, sections for a single temperature, with a spectral variable on the abscissa and a power variable on the ordinate. He put smooth curves through his experimental data points. They had one peak at a spectral value characteristic for the temperature, and fell either side of it towards the horizontal axis.<sup>[60][61]</sup> Such spectral sections are widely shown even today.

In a series of papers from 1881 to 1886, Langley reported measurements of the spectrum of heat radiation,

using diffraction gratings and prisms, and the most sensitive detectors that he could make. He reported that there was a peak intensity that increased with temperature, that the shape of the spectrum was not symmetrical about the peak, that there was a strong fall-off of intensity when the wavelength was shorter than an approximate cut-off value for each temperature, that the approximate cut-off wavelength decreased with increasing temperature, and that the wavelength of the peak intensity decreased with temperature, so that the intensity increased strongly with temperature for short wavelengths that were longer than the approximate cut-off for the temperature.<sup>[62]</sup>

Having read Langley, in 1888, Russian physicist V.A. Michelson published a consideration of the idea that the unknown Kirchhoff radiation function could be explained physically and stated mathematically in terms of "complete irregularity of the vibrations of ... atoms".<sup>[63][64]</sup> At this time, Planck was not studying radiation closely, and believed in neither atoms nor statistical physics.<sup>[65]</sup> Michelson produced a formula for the spectrum for temperature:

$$I_\lambda = B_1 \theta^{\frac{3}{2}} \exp\left(-\frac{c}{\lambda^2 \theta}\right) \lambda^{-6},$$

where  $I_\lambda$  denotes specific radiative intensity at wavelength  $\lambda$  and temperature  $\theta$ , and where  $B_1$  and  $c$  are empirical constants.

In 1898, Otto Lummer and Ferdinand Kurlbaum published an account of their cavity radiation source.<sup>[66]</sup> Their design has been used largely unchanged for radiation measurements to the present day. It was a platinum box, divided by diaphragms, with its interior blackened with iron oxide. It was an important ingredient for the progressively improved measurements that led to the discovery of Planck's law.<sup>[67]</sup> A version described in 1901 had its interior blackened with a mixture of chromium, nickel, and cobalt oxides.<sup>[68]</sup>

The importance of the Lummer and Kurlbaum cavity radiation source was that it was an experimentally accessible source of black-body radiation, as distinct from radiation from a simply exposed incandescent solid body, which had been the nearest available experimental approximation to black-body radiation over a suitable range of temperatures. The simply exposed incandescent solid bodies, that had been used before, emitted radiation with departures from the black-body spectrum that made it impossible to find the true black-body spectrum from experiments.<sup>[69][70]</sup>

### Planck's views before the empirical facts led him to find his eventual law

Planck first turned his attention to the problem of black body radiation in 1897.<sup>[71]</sup> Theoretical and empirical progress enabled Lummer and Pringsheim to write

in 1899 that available experimental evidence was approximately consistent with the specific intensity law  $C\lambda^{-5}e^{-c/\lambda T}$  where  $C$  and  $c$  denote empirically measurable constants, and where  $\lambda$  and  $T$  denote wavelength and temperature respectively.<sup>[72][73]</sup> For theoretical reasons, Planck at that time accepted this formulation, which has an effective cut-off of short wavelengths.<sup>[74][75][76]</sup>

### Finding the empirical law

Max Planck produced his law on 19 October 1900<sup>[77][78]</sup> as an improvement upon the Wien approximation, published in 1896 by Wilhelm Wien, which fit the experimental data at short wavelengths (high frequencies) but deviated from it at long wavelengths (low frequencies).<sup>[36]</sup> In June 1900, based on heuristic theoretical considerations, Rayleigh had suggested a formula<sup>[79]</sup> that he proposed might be checked experimentally. The suggestion was that the Stewart–Kirchhoff universal function might be of the form  $c_1 T \lambda^{-4} \exp(-c_2/\lambda T)$ . This was not the celebrated Rayleigh–Jeans formula  $8\pi k B T \lambda^{-4}$ , which did not emerge until 1905,<sup>[33]</sup> though it did reduce to the latter for long wavelengths, which are the relevant ones here. According to Klein,<sup>[71]</sup> one may speculate that it is likely that Planck had seen this suggestion though he did not mention it in his papers of 1900 and 1901. Planck would have been aware of various other proposed formulas which had been offered.<sup>[55][80]</sup> On 7 October 1900, Rubens told Planck that in the complementary domain (long wavelength, low frequency), and only there, Rayleigh's 1900 formula fitted the observed data well.<sup>[80]</sup>

For long wavelengths, Rayleigh's 1900 heuristic formula approximately meant that energy was proportional to temperature,  $U\lambda = \text{const.}$   $T$ .<sup>[71][80][81]</sup> It is known that  $dS/dU\lambda = 1/T$  and this leads to  $dS/dU\lambda = \text{const.}/U\lambda$  and thence to  $d^2S/dU\lambda^2 = -\text{const.}/U\lambda^2$  for long wavelengths. But for short wavelengths, the Wien formula leads to  $1/T = -\text{const.}$   $\ln U\lambda + \text{const.}$  and thence to  $d^2S/dU\lambda^2 = -\text{const.}/U\lambda$  for short wavelengths. Planck perhaps patched together these two heuristic formulas, for long and for short wavelengths,<sup>[80][82]</sup> to produce a formula

$$\frac{d^2S}{dU_\lambda^2} = \frac{\alpha}{U_\lambda(\beta+U_\lambda)}. \quad [77]$$

This led Planck to the formula

$$B_\lambda(T) = \frac{C\lambda^{-5}}{e^{\frac{c}{\lambda T}} - 1},$$

where Planck used the symbols  $C$  and  $c$  to denote empirical fitting constants.

Planck sent this result to Rubens, who compared it with his and Kurlbaum's observational data and found that it fitted for all wavelengths remarkably well. On 19 October 1900, Rubens and Kurlbaum briefly reported the fit to the data,<sup>[83]</sup> and Planck added a short presentation to give

a theoretical sketch to account for his formula.<sup>[77]</sup> Within a week, Rubens and Kurlbaum gave a fuller report of their measurements confirming Planck's law. Their technique for spectral resolution of the longer wavelength radiation was called the residual ray method. The rays were repeatedly reflected from polished crystal surfaces, and the rays that made it all the way through the process were 'residual', and were of wavelengths preferentially reflected by crystals of suitably specific materials.<sup>[84][85][86]</sup>

### Trying to find a physical explanation of the law

See also: Planck–Einstein relation

Once Planck had discovered the empirically fitting function, he constructed a physical derivation of this law. His thinking revolved around entropy rather than being directly about temperature. Planck considered a cavity with perfectly reflective walls; the cavity contained finitely many hypothetical well separated and recognizable but identically constituted, of definite magnitude, resonant oscillatory bodies, several such oscillators at each of finitely many characteristic frequencies. The hypothetical oscillators were for Planck purely imaginary theoretical investigative probes, and he said of them that such oscillators do not need to "really exist somewhere in nature, provided their existence and their properties are consistent with the laws of thermodynamics and electrodynamics."<sup>[87]</sup> Planck did not attribute any definite physical significance to his hypothesis of resonant oscillators, but rather proposed it as a mathematical device that enabled him to derive a single expression for the black body spectrum that matched the empirical data at all wavelengths.<sup>[88]</sup> He tentatively mentioned the possible connection of such oscillators with atoms. In a sense, the oscillators corresponded to Planck's speck of carbon; the size of the speck could be small regardless of the size of the cavity, provided the speck effectively transduced energy between radiative wavelength modes.<sup>[80]</sup>

Partly following a heuristic method of calculation pioneered by Boltzmann for gas molecules, Planck considered the possible ways of distributing electromagnetic energy over the different modes of his hypothetical charged material oscillators. This acceptance of the probabilistic approach, following Boltzmann, for Planck was a radical change from his former position, which till then had deliberately opposed such thinking proposed by Boltzmann.<sup>[89]</sup> Heuristically, Boltzmann had distributed the energy in arbitrary merely mathematical quanta  $\epsilon$ , which he had proceeded to make tend to zero in magnitude, because the finite magnitude  $\epsilon$  had served only to allow definite counting for the sake of mathematical calculation of probabilities, and had no physical significance. Referring to a new universal constant of nature,  $h$ ,<sup>[90]</sup> Planck supposed that, in the several oscillators of each of the finitely many characteristic frequencies, the total energy was distributed to each in an integer multi-

ple of a definite physical unit of energy,  $\epsilon$ , not arbitrary as in Boltzmann's method, but now for Planck, in a new departure, characteristic of the respective characteristic frequency.<sup>[78][91][92][93]</sup> His new universal constant of nature,  $h$ , is now known as Planck's constant.

Planck explained further<sup>[78]</sup> that the respective definite unit,  $\epsilon$ , of energy should be proportional to the respective characteristic oscillation frequency  $\nu$  of the hypothetical oscillator, and in 1901 he expressed this with the constant of proportionality  $h$ :<sup>[94][95]</sup>

$$\epsilon = h\nu.$$

Planck did not propose that light propagating in free space is quantized.<sup>[96][97][98]</sup> The idea of quantization of the free electromagnetic field was developed later, and eventually incorporated into what we now know as quantum field theory.<sup>[99]</sup>

In 1906 Planck acknowledged that his imaginary resonators, having linear dynamics, did not provide a physical explanation for energy transduction between frequencies.<sup>[100][101]</sup> Present-day physics explains the transduction between frequencies in the presence of atoms by their quantum excitability, following Einstein. Planck believed that in a cavity with perfectly reflecting walls and with no matter present, the electromagnetic field cannot exchange energy between frequency components.<sup>[102]</sup> This is because of the linearity of Maxwell's equations.<sup>[103]</sup> Present-day quantum field theory predicts that, in the absence of matter, the electromagnetic field obeys nonlinear equations and in that sense does self-interact.<sup>[104][105]</sup> Such interaction in the absence of matter has not yet been directly measured because it would require very high intensities and very sensitive and low-noise detectors, which are still in the process of being constructed.<sup>[104][106]</sup> Planck believed that a field with no interactions neither obeys nor violates the classical principle of equipartition of energy,<sup>[107][108]</sup> and instead remains exactly as it was when introduced, rather than evolving into a black body field.<sup>[109]</sup> Thus, the linearity of his mechanical assumptions precluded Planck from having a mechanical explanation of the maximization of the entropy of the thermodynamic equilibrium thermal radiation field. This is why he had to resort to Boltzmann's probabilistic arguments.<sup>[110][111]</sup>

Planck's law may be regarded as fulfilling the prediction of Gustav Kirchhoff that his law of thermal radiation was of the highest importance. In his mature presentation of his own law, Planck offered a thorough and detailed theoretical proof for Kirchhoff's law,<sup>[112]</sup> theoretical proof of which until then had been sometimes debated, partly because it was said to rely on unphysical theoretical objects, such as Kirchhoff's perfectly absorbing infinitely thin black surface.<sup>[113]</sup>

## Subsequent events

It was not till five years after Planck made his heuristic assumption of abstract elements of energy or of action that Albert Einstein conceived of really existing quanta of light in 1905<sup>[114]</sup> as a revolutionary explanation of black-body radiation, of photoluminescence, of the photoelectric effect, and of the ionization of gases by ultraviolet light. In 1905, "Einstein believed that Planck's theory could not be made to agree with the idea of light quanta, a mistake he corrected in 1906."<sup>[115]</sup> Contrary to Planck's beliefs of the time, Einstein proposed a model and formula whereby light was emitted, absorbed, and propagated in free space in energy quanta localized in points of space.<sup>[114]</sup> As an introduction to his reasoning, Einstein recapitulated Planck's model of hypothetical resonant material electric oscillators as sources and sinks of radiation, but then he offered a new argument, disconnected from that model, but partly based on a thermodynamic argument of Wien, in which Planck's formula  $\epsilon = h\nu$  played no role.<sup>[116]</sup> Einstein gave the energy content of such quanta in the form  $R\beta\nu/N$ . Thus Einstein was contradicting the undulatory theory of light held by Planck. In 1910, criticizing a manuscript sent to him by Planck, knowing that Planck was a steady supporter of Einstein's theory of special relativity, Einstein wrote to Planck: "To me it seems absurd to have energy continuously distributed in space without assuming an aether."<sup>[117]</sup>

According to Thomas Kuhn, it was not till 1908 that Planck more or less accepted part of Einstein's arguments for physical as distinct from abstract mathematical discreteness in thermal radiation physics. Still in 1908, considering Einstein's proposal of quantal propagation, Planck opined that such a revolutionary step was perhaps unnecessary.<sup>[118]</sup> Until then, Planck had been consistent in thinking that discreteness of action quanta was to be found neither in his resonant oscillators nor in the propagation of thermal radiation. Kuhn wrote that, in Planck's earlier papers and in his 1906 monograph,<sup>[119]</sup> there is no "mention of discontinuity, [nor] of talk of a restriction on oscillator energy, [nor of] any formula like  $U = nh\nu$ ".<sup>[120]</sup> Kuhn pointed out that his study of Planck's papers of 1900 and 1901, and of his monograph of 1906,<sup>[119]</sup> had led him to "heretical" conclusions, contrary to the widespread assumptions of others who saw Planck's writing only from the perspective of later, anachronistic, viewpoints.<sup>[121][122]</sup> Kuhn's conclusions, finding a period till 1908, when Planck consistently held his 'first theory', have been accepted by other historians.<sup>[123][124]</sup>

In the second edition of his monograph, in 1912, Planck sustained his dissent from Einstein's proposal of light quanta. He proposed in some detail that absorption of light by his virtual material resonators might be continuous, occurring at a constant rate in equilibrium, as distinct from quantal absorption. Only emission was

quantal.<sup>[103][125]</sup> This has at times been called Planck's "second theory".<sup>[126]</sup>

It was not till 1919 that Planck in the third edition of his monograph more or less accepted his 'third theory', that both emission and absorption of light were quantal.<sup>[127]</sup>

The colourful term "ultraviolet catastrophe" was given by Paul Ehrenfest in 1911 to the paradoxical result that the total energy in the cavity tends to infinity when the **equipartition theorem** of classical statistical mechanics is (mistakenly) applied to black body radiation.<sup>[128][129]</sup> But this had not been part of Planck's thinking, because he had not tried to apply the doctrine of equipartition: when he made his discovery in 1900, he had not noticed any sort of "catastrophe".<sup>[74][75][76][71][130]</sup> It was first noted by Lord Rayleigh in 1900,<sup>[79][131][132]</sup> and then in 1901<sup>[133]</sup> by Sir James Jeans; and later, in 1905, by Einstein when he wanted to support the idea that light propagates as discrete packets, later called 'photons', and by Rayleigh<sup>[34]</sup> and by Jeans.<sup>[33][134][135][136]</sup>

In 1913, Bohr gave another formula with a further different physical meaning to the quantity  $h\nu$ .<sup>[29][30][31][137][138][139]</sup> In contrast to Planck's and Einstein's formulas, Bohr's formula referred explicitly and categorically to energy levels of atoms. Bohr's formula was  $W\tau_2 - W\tau_1 = h\nu$  where  $W\tau_2$  and  $W\tau_1$  denote the energy levels of quantum states of an atom, with quantum numbers  $\tau_2$  and  $\tau_1$ . The symbol  $\nu$  denotes the frequency of a quantum of radiation that can be emitted or absorbed as the atom passes between those two quantum states. In contrast to Planck's model, the frequency  $\nu$  has no immediate relation to frequencies that might describe those quantum states themselves.

Later, in 1924, Satyendra Nath Bose developed the theory of the statistical mechanics of photons, which allowed a **theoretical derivation** of Planck's law. The actual word 'photon' was invented still later, by G.N. Lewis in 1926,<sup>[140]</sup> who mistakenly believed that photons were conserved, contrary to Bose–Einstein statistics; nevertheless the word 'photon' was adopted to express the Einstein postulate of the packet nature of light propagation. In an electromagnetic field isolated in a vacuum in a vessel with perfectly reflective walls, such as was considered by Planck, indeed the photons would be conserved according to Einstein's 1905 model, but Lewis was referring to a field of photons considered as a system closed with respect to ponderable matter but open to exchange of electromagnetic energy with a surrounding system of ponderable matter, and he mistakenly imagined that still the photons were conserved, being stored inside atoms.

Ultimately, Planck's law of black-body radiation contributed to Einstein's concept of quanta of light carrying linear momentum,<sup>[29][114]</sup> which became the fundamental basis for the development of **quantum mechanics**.

The above-mentioned linearity of Planck's mechanical assumptions, not allowing for energetic interactions between frequency components, was superseded in 1925

by Heisenberg's original quantum mechanics. In his paper submitted on 29 July 1925, Heisenberg's theory accounted for Bohr's above-mentioned formula of 1913. It admitted non-linear oscillators as models of atomic quantum states, allowing energetic interaction between their own multiple internal discrete Fourier frequency components, on the occasions of emission or absorption of quanta of radiation. The frequency of a quantum of radiation was that of a definite coupling between internal atomic meta-stable oscillatory quantum states.<sup>[141][142]</sup> At that time, Heisenberg knew nothing of matrix algebra, but Max Born read the manuscript of Heisenberg's paper and recognized the matrix character of Heisenberg's theory. Then Born and Jordan published an explicitly matrix theory of quantum mechanics, based on, but in form distinctly different from, Heisenberg's original quantum mechanics; it is the Born and Jordan matrix theory that is today called matrix mechanics.<sup>[143][144][145]</sup> Heisenberg's explanation of the Planck oscillators, as non-linear effects apparent as Fourier modes of transient processes of emission or absorption of radiation, showed why Planck's oscillators, viewed as enduring physical objects such as might be envisaged by classical physics, did not give an adequate explanation of the phenomena.

Nowadays, as a statement of the energy of a light quantum, often one finds the formula  $E = \hbar\omega$ , where  $\hbar = h/2\pi$ , and  $\omega = 2\pi\nu$  denotes angular frequency,<sup>[146][147][148][149][150]</sup> and less often the equivalent formula  $E = h\nu$ .<sup>[149][150][151][152][153]</sup> This statement about a really existing and propagating light quantum, based on Einstein's, has a physical meaning different from that of Planck's above statement  $\epsilon = h\nu$  about the abstract energy units to be distributed amongst his hypothetical resonant material oscillators.

An article by Helge Kragh published in *Physics World* gives an account of this history.<sup>[93]</sup>

### 2.1.7 See also

- Emissivity
- Radiance
- Sakuma–Hattori equation
- Wien's displacement law

### 2.1.8 References

- [1] Planck 1914, pp. 6, 168
- [2] Chandrasekhar 1960, p. 8
- [3] Rybicki & Lightman 1979, p. 22
- [4] Planck 1914, p. 42
- [5] Stewart 1858
- [6] Hapke 1993, pp. 362–373

- [7] Planck 1914
- [8] Loudon 2000, pp. 3–45
- [9] Caniou 1999, p. 117
- [10] Kramm & Mölders 2009, p. 10
- [11] Sharkov 2003, p. 210
- [12] Goody & Yung 1989, p. 16.
- [13] Fischer 2011
- [14] Mohr, Taylor & Newell 2012, p. 1591
- [15] Loudon 2000
- [16] Mandel & Wolf 1995
- [17] Wilson 1957, p. 182
- [18] Adkins 1983, pp. 147–148
- [19] Landsberg 1978, p. 208
- [20] Siegel & Howell 2002, p. 25
- [21] Planck 1914, pp. 9–11
- [22] Planck 1914, p. 35
- [23] Landsberg 1961, pp. 273–274
- [24] Born & Wolf 1999, pp. 194–199
- [25] Born & Wolf 1999, p. 195
- [26] Rybicki & Lightman 1979, p. 19
- [27] Chandrasekhar 1960, p. 7
- [28] Chandrasekhar 1960, p. 9
- [29] Einstein 1916
- [30] Bohr 1913
- [31] Jammer 1989, pp. 113, 115
- [32] Kittel & Kroemer 1980, p. 98
- [33] Jeans 1905a, p. 98
- [34] Rayleigh 1905
- [35] Rybicki & Lightman 1979, p. 23
- [36] Wien 1896, p. 667
- [37] Planck 1906, p. 158
- [38] Lowen & Blanch 1940
- [39] Siegel 1976
- [40] Kirchhoff 1860a
- [41] Kirchhoff 1860b
- [42] Schirrmacher 2001
- [43] Kirchhoff 1860c
- [44] Planck 1914, p. 11
- [45] Milne 1930, p. 80
- [46] Rybicki & Lightman 1979, pp. 16–17
- [47] Mihalas & Weibel-Mihalas 1984, p. 328
- [48] Goody & Yung 1989, pp. 27–28
- [49] Paschen, F. (1896), personal letter cited by Hermann 1971, p. 6
- [50] Hermann 1971, p. 7
- [51] Kuhn 1978, pp. 8, 29
- [52] Mehra and Rechenberg 1982, pp. 26, 28, 31, 39
- [53] Kirchhoff 1862/1882, p. 573
- [54] Kragh 1999, p. 58
- [55] Kangro 1976
- [56] Tyndall 1865a
- [57] Tyndall 1865b
- [58] Kangro 1976, pp. 8–10
- [59] Crova 1880
- [60] Crova 1880, p. 577, Plate I
- [61] Kangro 1976, pp. 10–15
- [62] Kangro 1976, pp. 15–26
- [63] Michelson 1888
- [64] Kangro 1976, pp. 30–36
- [65] Kangro 1976, pp. 122–123
- [66] Lummer & Kurlbaum 1898
- [67] Kangro 1976, p. 159
- [68] Lummer & Kurlbaum 1901
- [69] Kangro 1976, pp. 75–76
- [70] Paschen 1895, pp. 297–301
- [71] Klein 1962, p. 460.
- [72] Lummer & Pringsheim 1899, p. 225
- [73] Kangro 1976, p. 174
- [74] Planck 1900d
- [75] Rayleigh 1900, p. 539
- [76] Kangro 1976, pp. 181–183
- [77] Planck 1900a
- [78] Planck 1900b
- [79] Rayleigh 1900
- [80] Dougal 1976
- [81] Planck 1943, p. 156

- [82] Hettner 1922
- [83] Rubens & Kurlbaum 1900a
- [84] Rubens & Kurlbaum 1900b
- [85] Kangro 1976, p. 165
- [86] Mehra & Rechenberg 1982, p. 41
- [87] Planck 1914, p. 135
- [88] Kuhn 1978, pp. 117–118
- [89] Hermann 1971, p. 16
- [90] Planck 1900c
- [91] Kangro 1976, p. 214
- [92] Kuhn 1978, p. 106
- [93] Kragh 2000
- [94] Planck 1901
- [95] Planck 1915, p. 89
- [96] Ehrenfest & Kamerlingh Onnes 1914, p. 873
- [97] ter Haar 1967, p. 14
- [98] Stehle 1994, p. 128
- [99] Scully & Zubairy 1997, p. 21.
- [100] Planck 1906, p. 220
- [101] Kuhn 1978, p. 162
- [102] Planck 1914, pp. 44–45, 113–114
- [103] Stehle 1994, p. 150
- [104] Jauch & Rohrlich 1980, Chapter 13
- [105] Karplus & Neuman 1951
- [106] Tommasini et al. 2008
- [107] Jeffreys 1973, p. 223
- [108] Planck 1906, p. 178
- [109] Planck 1914, p. 26
- [110] Boltzmann 1878
- [111] Kuhn 1978, pp. 38–39
- [112] Planck 1914, pp. 1–45
- [113] Cotton 1899
- [114] Einstein 1905
- [115] Kragh 1999, p. 67
- [116] Stehle 1994, pp. 132–137
- [117] Einstein 1993, p. 143, letter of 1910.
- [118] Planck 1915, p. 95
- [119] Planck 1906
- [120] Kuhn 1984, p. 236
- [121] Kuhn 1978, pp. 196–202
- [122] Kuhn 1984
- [123] Darrigol 1992, p. 76
- [124] Kragh 1999, pp. 63–66
- [125] Planck 1914, p. 161
- [126] Kuhn 1978, pp. 235–253
- [127] Kuhn 1978, pp. 253–254
- [128] Ehrenfest 1911
- [129] Kuhn 1978, p. 152
- [130] Kuhn 1978, pp. 151–152
- [131] Kangro 1976, p. 190
- [132] Kuhn 1978, pp. 144–145
- [133] See footnote on p. 398 in Jeans 1901.
- [134] Jeans 1905b
- [135] Jeans 1905c
- [136] Jeans 1905d
- [137] Sommerfeld 1923, p. 43
- [138] Heisenberg 1925, p. 108
- [139] Brillouin 1970, p. 31
- [140] Lewis 1926
- [141] Heisenberg 1925
- [142] Razavy 2011, pp. 39–41
- [143] Born & Jordan 1925
- [144] Stehle 1994, p. 286
- [145] Razavy 2011, pp. 42–43
- [146] Messiah 1958, p. 14
- [147] Pauli 1973, p. 1
- [148] Feynman, Leighton & Sands 1963, p. 38-1
- [149] Schwinger 2001, p. 203
- [150] Bohren & Clothiaux 2006, p. 2
- [151] Schiff 1949, p. 2
- [152] Mihalas & Weibel-Mihalas 1984, p. 143
- [153] Rybicki & Lightman 1979, p. 20

## Bibliography

- Adkins, C. J. (1983). *Equilibrium Thermodynamics* (3rd ed.). Cambridge University Press. ISBN 0-521-25445-0.
- Bohr, N. (1913). "On the constitution of atoms and molecules" (PDF). *Philosophical Magazine*. **26** (153): 1–25. doi:10.1080/14786441308634993.
- Bohren, C. F.; Clothiaux, E. E. (2006). *Fundamentals of Atmospheric Radiation*. Wiley-VCH. ISBN 3-527-40503-8.
- Boltzmann, L. (1878). "Über die Beziehung zwischen dem zweiten Hauptsatze der mechanischen Wärmetheorie und der Wahrscheinlichkeitsrechnung, respective den Sätzen über das Wärmegleichgewicht". *Sitzungsberichte Mathematisch-Naturwissenschaftlichen Classe der kaiserlichen Akademie der Wissenschaften in Wien*. **76** (2): 373–435.
- Born, M.; Wolf, E. (1999). *Principles of Optics* (7th ed.). Cambridge University Press. ISBN 0-521-64222-1.
- Born, M.; Jordan, P. (1925). "Zur Quantenmechanik". *Zeitschrift für Physik*. **34**: 858–888. Bibcode:1925ZPhy..34..858B. doi:10.1007/BF01328531. Translated in part as "On quantum mechanics" in van der Waerden, B. L. (1967). *Sources of Quantum Mechanics*. North-Holland Publishing. pp. 277–306.
- Brehm, J. J.; Mullin, W. J. (1989). *Introduction to the Structure of Matter*. Wiley. ISBN 0-471-60531-X.
- Brillouin, L. (1970). *Relativity Reexamined*. Academic Press. ISBN 978-0-12-134945-5.
- Caniou, J. (1999). *Passive Infrared Detection: Theory and Applications*. Springer. ISBN 978-0-7923-8532-5.
- Chandrasekhar, S. (1960) [1950]. *Radiative Transfer* (Revised reprint ed.). Dover Publications. ISBN 978-0-486-60590-6.
- Cotton, A. (1899). "The present status of Kirchhoff's law". *The Astrophysical Journal*. **9**: 237–268. Bibcode:1899ApJ.....9..237C. doi:10.1086/140585.
- Crova, A. P. P. (1880). "Étude des radiations émises par les corps incandescents. Mesure optique des hautes températures". *Annales de chimie et de physique*. Série 5. **19**: 472–550.
- Dougal, R. C. (September 1976). "The presentation of the Planck radiation formula (tutorial)". *Physics Education*. **11** (6): 438–443. Bibcode:1976PhyEd..11..438D. doi:10.1088/0031-9120/11/6/008.
- Ehrenfest, P. (1911). "Welche Züge der Lichtquantenhypothese spielen in der Theorie der Wärmestrahlung eine wesentliche Rolle?". *Annalen der Physik*. **36** (11): 91–118. Bibcode:1911AnP...341...91E. doi:10.1002/andp.19113411106.
- Ehrenfest, P.; Kamerling Onnes, H. (1914). "Simplified deduction of the formula from the theory of combinations which Planck uses as the basis of his radiation theory". *Proceedings of the Royal Dutch Academy of Sciences in Amsterdam*. **17** (2): 870–873. Bibcode:1914KNAB...17..870E.
- Einstein, A. (1905). "Über einen die Erzeugung und Verwandlung des Lichtes betreffenden heuristischen Gesichtspunkt". *Annalen der Physik*. **17** (6): 132–148. Bibcode:1905AnP...322..132E. doi:10.1002/andp.19053220607. Translated in Arons, A. B.; Peppard, M. B. (1965). "Einstein's proposal of the photon concept: A translation of the *Annalen der Physik* paper of 1905" (PDF). *American Journal of Physics*. **33** (5): 367. Bibcode:1965AmJPh..33..367A. doi:10.1119/1.1971542.
- Einstein, A. (1916). "Zur Quantentheorie der Strahlung". *Mitteilungen der Physikalischen Gesellschaft Zürich*. **18**: 47–62. and a nearly identical version Einstein, A. (1917). "Zur Quantentheorie der Strahlung". *Physikalische Zeitschrift*. **18**: 121–128. Bibcode:1917PhyZ...18..121E. Translated in ter Haar, D. (1967). *The Old Quantum Theory*. Pergamon Press. pp. 167–183. LCCN 66029628. See also .
- Einstein, A. (1993). *The Collected Papers of Albert Einstein*. **3**. English translation by Beck, A. Princeton University Press. ISBN 0-691-10250-3.
- Feynman, R. P.; Leighton, R. B.; Sands, M. (1963). *The Feynman Lectures on Physics, Volume 1*. Addison-Wesley. ISBN 0-201-02010-6.
- Fischer, T. (1 November 2011). "Topics: Derivation of Planck's Law". ThermalHUB. Retrieved 2015-06-19.
- Goody, R. M.; Yung, Y. L. (1989). *Atmospheric Radiation: Theoretical Basis* (2nd ed.). Oxford University Press. ISBN 978-0-19-510291-8.
- Guggenheim, E. A. (1967). *Thermodynamics. An Advanced Treatment for Chemists and Physicists* (fifth revised ed.). North-Holland Publishing Company.
- Haken, H. (1981). *Light* (Reprint ed.). Amsterdam: North-Holland Publishing. ISBN 0-444-86020-7.

- Hapke, B. (1993). *Theory of Reflectance and Emissittance Spectroscopy*. Cambridge University Press, Cambridge UK. ISBN 0-521-30789-9.
- Heisenberg, W. (1925). "Über quantentheoretische Umdeutung kinematischer und mechanischer Beziehungen". *Zeitschrift für Physik*. **33**: 879–893. Bibcode:1925ZPhy...33..879H. doi:10.1007/BF01328377. Translated as "Quantum-theoretical Re-interpretation of kinematic and mechanical relations" in van der Waerden, B. L. (1967). *Sources of Quantum Mechanics*. North-Holland Publishing. pp. 261–276.
- Heisenberg, W. (1930). *The Physical Principles of the Quantum Theory*. Eckart, C.; Hoyt, F. C. (transl.). University of Chicago Press.
- Hermann, A. (1971). *The Genesis of Quantum Theory*. Nash, C.W. (transl.). MIT Press. ISBN 0-262-08047-8. a translation of *Friihgeschichte der Quantentheorie (1899–1913)*, Physik Verlag, Mosbach/Baden, 1969.
- Hettner, G. (1922). "Die Bedeutung von Rubens Arbeiten für die Plancksche Strahlungsformel". *Naturwissenschaften*. **10** (48): 1033–1038. Bibcode:1922NW.....10.1033H. doi:10.1007/BF01565205.
- Jammer, M. (1989). *The Conceptual Development of Quantum Mechanics* (second ed.). Tomash Publishers/American Institute of Physics. ISBN 0-88318-617-9.
- Jauch, J. M.; Rohrlich, F. (1980) [1955]. *The Theory of Photons and Electrons. The Relativistic Quantum Field Theory of Charged Particles with Spin One-half* (second printing of second ed.). Springer. ISBN 0-387-07295-0.
- Jeans, J. H. (1901). "The Distribution of Molecular Energy". *Philosophical Transactions of the Royal Society A*. **196** (274–286): 397. Bibcode:1901RSPTA.196..397J. JSTOR 90811. doi:10.1098/rsta.1901.0008.
- Jeans, J. H. (1905a). "XI. On the partition of energy between matter and æther". *Philosophical Magazine*. **10** (55): 91. doi:10.1080/14786440509463348.
- Jeans, J. H. (1905b). "On the Application of Statistical Mechanics to the General Dynamics of Matter and Ether". *Proceedings of the Royal Society A*. **76** (510): 296. Bibcode:1905RSPSA..76..296J. JSTOR 92714. doi:10.1098/rspa.1905.0029.
- Jeans, J. H. (1905c). "A Comparison between Two Theories of Radiation". *Nature*. **72** (1865): 293. Bibcode:1905Natur..72..293J. doi:10.1038/072293d0.
- Jeans, J. H. (1905d). "On the Laws of Radiation". *Proceedings of the Royal Society A*. **76** (513): 545. Bibcode:1905RSPSA..76..545J. JSTOR 92704. doi:10.1098/rspa.1905.0060.
- Jeffreys, H. (1973). *Scientific Inference* (3rd ed.). Cambridge University Press. ISBN 978-0-521-08446-8.
- Kangro, H. (1976). *Early History of Planck's Radiation Law*. Taylor & Francis. ISBN 0-85066-063-7.
- Karplus, R.; Neuman, M. (1951). "The Scattering of Light by Light". *Physical Review*. **83** (4): 776–784. Bibcode:1951PhRv...83..776K. doi:10.1103/PhysRev.83.776.
- Kirchhoff, G. R.; [27 October 1859] (1860a). "Über die Fraunhofer'schen Linien". *Monatsberichte der Königlich Preussischen Akademie der Wissenschaften zu Berlin*: 662–665.
- Kirchhoff, G. R.; [11 December 1859] (1860b). "Über den Zusammenhang zwischen Emission und Absorption von Licht und Wärme". *Monatsberichte der Königlich Preussischen Akademie der Wissenschaften zu Berlin*: 783–787.
- Kirchhoff, G. R. (1860c). "Über das Verhältniss zwischen dem Emissionsvermögen und dem Absorptionsvermögen der Körper für Wärme und Licht". *Annalen der Physik und Chemie*. **109** (2): 275–301. Bibcode:1860AnP...185..275K. doi:10.1002/andp.18601850205. Translated by Guthrie, F. as Kirchhoff, G. R. (1860). "On the relation between the radiating and absorbing powers of different bodies for light and heat". *Philosophical Magazine*. Series 4. **20**: 1–21.
- Kirchhoff, G. R. (1882) [1862], "Über das Verhältniss zwischen dem Emissionsvermögen und dem Absorptionsvermögen der Körper für Wärme und Licht", *Gessamte Abhandlungen*, Johann Ambrosius Barth, pp. 571–598
- Kittel, C.; Kroemer, H. (1980). *Thermal Physics* (2nd ed.). W. H. Freeman. ISBN 0-7167-1088-9.
- Klein, M. J. (1962). "Max Planck and the beginnings of the quantum theory". *Archive for History of Exact Sciences*. **1** (5): 459–479. doi:10.1007/BF00327765.
- Kragh, H. (1999). *Quantum Generations. A History of Physics in the Twentieth Century*. Princeton University Press. ISBN 0-691-01206-7.
- Kragh, H. (December 2000). "Max Planck: The reluctant revolutionary". *Physics World*.

- Kramm, Gerhard; Mölders, N. (2009). “Planck’s Blackbody Radiation Law: Presentation in Different Domains and Determination of the Related Dimensional Constant”. *Journal of the Calcutta Mathematical Society*. **5** (1–2): 27–61. Bibcode:2009arXiv0901.1863K. arXiv:0901.1863.
- Kuhn, T. S. (1978). *Black-Body Theory and the Quantum Discontinuity*. Oxford University Press. ISBN 0-19-502383-8.
- Landsberg, P. T. (1961). *Thermodynamics with Quantum Statistical Illustrations*. Interscience Publishers.
- Landsberg, P. T. (1978). *Thermodynamics and Statistical Mechanics*. Oxford University Press. ISBN 0-19-851142-6.
- Lewis, G. N. (1926). “The Conservation of Photons”. *Nature*. **118** (2981): 874. Bibcode:1926Natur.118..874L. doi:10.1038/118874a0.
- Loudon, R. (2000). *The Quantum Theory of Light* (3rd ed.). Oxford University Press. ISBN 0-19-850177-3.
- Lowen, A. N.; Blanch, G. (1940). “Tables of Planck’s radiation and photon functions”. *Journal of the Optical Society of America*. **30** (2): 70. Bibcode:1940JOSA...30...70L. doi:10.1364/JOSA.30.000070.
- Lummer, O.; Kurlbaum, F. (1898). “Der electrisch gegliühte “absolut schwarze” Körper und seine Temperaturmessung”. *Verhandlungen der Deutschen Physikalischen Gesellschaft*. **17**: 106–111.
- Lummer, O.; Pringsheim, E. (1899). “1. Die Vertheilung der Energie in Spectrum des schwarzen Körpers und des blanken Platins; 2. Temperaturbestimmung fester glühender Körper”. *Verhandlungen der Deutschen Physikalischen Gesellschaft*. **1**: 215–235.
- Lummer, O.; Kurlbaum, F. (1901). “Der elektrisch gegliühte “schwarze” Körper”. *Annalen der Physik*. **310** (8): 829–836. Bibcode:1901AnP...310..829L. doi:10.1002/andp.19013100809.
- Mandel, L.; Wolf, E. (1995). *Optical Coherence and Quantum Optics*. Cambridge University Press. ISBN 0-521-41711-2.
- Mehra, J.; Rechenberg, H. (1982). *The Historical Development of Quantum Theory*. **1**. Springer-Verlag. ISBN 0-387-90642-8.
- Messiah, A. (1958). *Quantum Mechanics*. Temmer, G. G. (transl.). Wiley.
- Michelson, V. A. (1888). “Theoretical essay on the distribution of energy in the spectra of solids”. *Philosophical Magazine*. Series 5. **25** (156): 425–435. doi:10.1080/14786448808628207.
- Mihalas, D.; Weibel-Mihalas, B. (1984). *Foundations of Radiation Hydrodynamics*. Oxford University Press. ISBN 0-19-503437-6.
- Milne, E. A. (1930). “Thermodynamics of the Stars”. *Handbuch der Astrophysik*. **3** (1): 63–255.
- Mohr, P. J.; Taylor, B. N.; Newell, D. B. (2012). “CODATA Recommended Values of the Fundamental Physical Constants: 2010” (PDF). *Reviews of Modern Physics*. **84** (4): 1527–1605. Bibcode:2012RvMP...84.1527M. doi:10.1103/RevModPhys.84.1527.
- Paltridge, G. W.; Platt, C. M. R. (1976). *Radiative Processes in Meteorology and Climatology*. Elsevier. ISBN 0-444-41444-4.
- Paschen, F. (1895). “Über Gesetzmäßigkeiten in den Spectren fester Körper und über ein neue Bestimmung der Sonnentemperatur”. *Nachrichten von der Königlichen Gesellschaft der Wissenschaften zu Göttingen (Mathematisch-Physikalische Klasse)*: 294–304.
- Pauli, W. (1973). Enz, C. P., ed. *Wave Mechanics*. Margulies, S.; Lewis, H. R. (transl.). MIT Press. ISBN 0-262-16050-1.
- Planck, M. (1900a). “Über eine Verbesserung der Wien’schen Spectralgleichung”. *Verhandlungen der Deutschen Physikalischen Gesellschaft*. **2**: 202–204. Translated in ter Haar, D. (1967). “On an Improvement of Wien’s Equation for the Spectrum”. *The Old Quantum Theory* (PDF). Pergamon Press. pp. 79–81. LCCN 66029628.
- Planck, M. (1900b). “Zur Theorie des Gesetzes der Energieverteilung im Normalspectrum”. *Verhandlungen der Deutschen Physikalischen Gesellschaft*. **2**: 237–245. Translated in ter Haar, D. (1967). “The Old Quantum Theory” (PDF). Pergamon Press: 82. LCCN 66029628.
- Planck, M. (1900c). “Entropie und Temperatur strahlender Wärme”. *Annalen der Physik*. **306** (4): 719–737. Bibcode:1900AnP...306..719P. doi:10.1002/andp.19003060410.
- Planck, M. (1900d). “Über irreversible Strahlungsvorgänge”. *Annalen der Physik*. **306** (1): 69–122. Bibcode:1900AnP...306...69P. doi:10.1002/andp.19003060105.
- Planck, M. (1901). “Über das Gesetz der Energieverteilung im Normalspektrum”. *Annalen der Physik*. **4** (3): 553. Bibcode:1901AnP...309..553P.

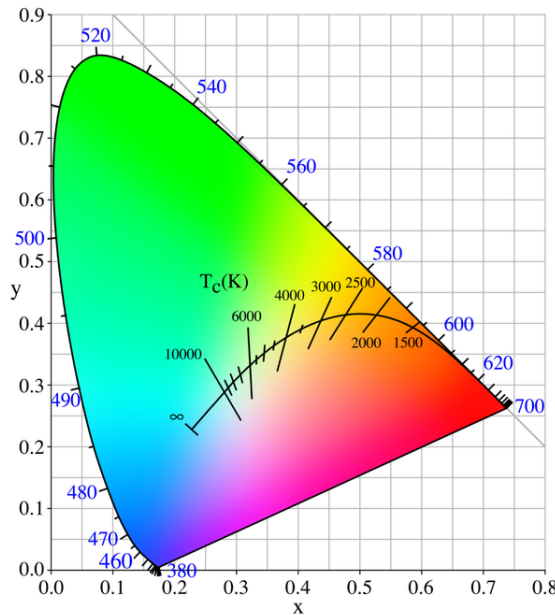
- doi:10.1002/andp.19013090310. Translated in Ando, K. "On the Law of Distribution of Energy in the Normal Spectrum" (PDF). Retrieved 2011-10-13.
- Planck, M. (1906). *Vorlesungen über die Theorie der Wärmestrahlung*. Johann Ambrosius Barth. LCCN 07004527.
  - Planck, M. (1914). *The Theory of Heat Radiation*. Masius, M. (transl.) (2nd ed.). P. Blakiston's Son & Co. OL 7154661M.
  - Planck, M. (1915). *Eight Lectures on Theoretical Physics*. Wills, A. P. (transl.). Dover Publications. ISBN 0-486-69730-4.
  - Planck, M. (1943). "Zur Geschichte der Auffindung des physikalischen Wirkungsquants". *Naturwissenschaften*. **31** (14–15): 153–159. Bibcode:1943NW.....31..153P. doi:10.1007/BF01475738.
  - Rayleigh, Lord (1900). "LIII. Remarks upon the law of complete radiation". *Philosophical Magazine*. Series 5. **49** (301): 539. doi:10.1080/14786440009463878.
  - Rayleigh, Lord (1905). "The Dynamical Theory of Gases and of Radiation". *Nature*. **72** (1855): 54–55. Bibcode:1905Natur..72...54R. doi:10.1038/072054c0.
  - Razavy, M. (2011). *Heisenberg's Quantum Mechanics*. World Scientific. ISBN 978-981-4304-10-8.
  - Rubens, H.; Kurlbaum, F. (1900a). "Über die Emission langer Wellen durch den schwarzen Körper". *Verhandlungen der Deutschen Physikalischen Gesellschaft*. **2**: 181.
  - Rubens, H.; Kurlbaum, F. (1900b). "Über die Emission langwelliger Wärmestrahlen durch den schwarzen Körper bei verschiedenen Temperaturen". *Sitzungsberichte der Königlich Preussischen Akademie der Wissenschaften zu Berlin*: 929–941. Translated in Rubens, H.; Kurlbaum, F. (1901). "On the heat-radiation of long wave-length emitted by black bodies at different temperatures". *The Astrophysical Journal*. **14**: 335–348. Bibcode:1901ApJ....14..335R. doi:10.1086/140874.
  - Rybicki, G. B.; Lightman, A. P. (1979). *Radiative Processes in Astrophysics*. John Wiley & Sons. ISBN 0-471-82759-2.
  - Sharkov, E. A. (2003). "Black-body radiation". *Passive Microwave Remote Sensing of the Earth* (PDF). Springer. ISBN 978-3-540-43946-2.
  - Schiff, L. I. (1949). *Quantum Mechanics*. McGraw-Hill.
  - Schirrmacher, A. (2001). *Experimenting theory: the proofs of Kirchhoff's radiation law before and after Planck*. Münchner Zentrum für Wissenschafts und Technikgeschichte.
  - Schwinger, J. (2001). Englert, B.-G., ed. *Quantum Mechanics: Symbolism of Atomic Measurements*. Springer. ISBN 3-540-41408-8.
  - Scully, M. O.; Zubairy, M. S. (1997). *Quantum Optics*. Cambridge University Press. ISBN 0-521-43458-0.
  - Siegel, D. M. (1976). "Balfour Stewart and Gustav Robert Kirchhoff: two independent approaches to "Kirchhoff's radiation law"". *Isis*. **67** (4): 565–600. doi:10.1086/351669.
  - Siegel, R.; Howell, J. R. (2002). *Thermal Radiation Heat Transfer, Volume 1* (4th ed.). Taylor & Francis. ISBN 978-1-56032-839-1.
  - Sommerfeld, A. (1923). *Atomic Structure and Spectral Lines*. Brose, H. L. (transl.) (from 3rd German ed.). Methuen.
  - Stehle, P. (1994). *Order, Chaos, Order. The Transition from Classical to Quantum Physics*. Oxford University Press. ISBN 0-19-507513-7.
  - Stewart, B. (1858). "An account of some experiments on radiant heat". *Transactions of the Royal Society of Edinburgh*. **22**: 1–20.
  - ter Haar, D. (1967). *The Old Quantum Theory*. Pergamon Press. LCCN 66-029628.
  - Thornton, S. T.; Rex, A. F. (2002). *Modern Physics*. Thomson Learning. ISBN 0-03-006049-4.
  - Tisza, L. (1966). *Generalized Thermodynamics*. MIT Press.
  - Tommasini, D.; Ferrando, F.; Michinel, H.; Seco, M. (2008). "Detecting photon-photon scattering in vacuum at exawatt lasers". *Physical Review A*. **77**: 042101. Bibcode:2008PhRvA..77a2101M. arXiv:quant-ph/0703076. doi:10.1103/PhysRevA.77.012101.
  - Tyndall, J. (1865a). "Über leuchtende und dunkle Strahlung". *Annalen der Physik und Chemie*. **200**: 36–53. Bibcode:1865AnP...200...36T. doi:10.1002/andp.18652000103.
  - Tyndall, J. (1865b). *Heat considered as a Mode of Motion* (PDF). D. Appleton & Company.
  - Wien, W. (1896). "Über die Energievertheilung im Emissionsspectrum eines schwarzen Körpers". *Annalen der Physik und Chemie*. **294** (8): 662–669. Bibcode:1896AnP...294..662W. doi:10.1002/andp.18962940803.

- Wilson, A. H. (1957). *Thermodynamics and Statistical Mechanics*. Cambridge University Press.
- YAN Kun(2011). Research on adaptive connection equation in discontinuous area of data curve( Extended form of Einstein-Stern equation, zero-point energy step and average energy equation at negative absolute temperature), doi:10.3969/j.issn.1004-2903.2011.01.018.

### 2.1.9 External links

- Summary of Radiation
- Radiation of a Blackbody – interactive simulation to play with Planck's law
- Scienceworld entry on Planck's Law

## 2.2 Planckian locus



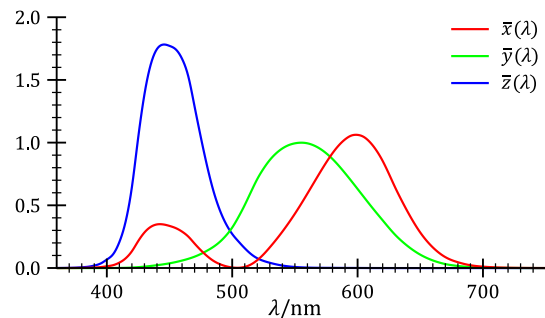
Planckian locus in the CIE 1931 chromaticity diagram

In physics and color science, the **Planckian locus** or **black body locus** is the path or *locus* that the color of an incandescent black body would take in a particular chromaticity space as the blackbody temperature changes. It goes from deep red at low temperatures through orange, yellowish white, white, and finally bluish white at very high temperatures.

A color space is a three-dimensional space; that is, a color is specified by a set of three numbers (the CIE coordinates  $X$ ,  $Y$ , and  $Z$ , for example, or other values such as hue, colorfulness, and luminance) which specify the color and brightness of a particular homogeneous visual

stimulus. A chromaticity is a color projected into a two-dimensional space that ignores brightness. For example, the standard CIE XYZ color space projects directly to the corresponding chromaticity space specified by the two chromaticity coordinates known as  $x$  and  $y$ , making the familiar chromaticity diagram shown in the figure. The Planckian locus, the path that the color of a black body takes as the blackbody temperature changes, is often shown in this standard chromaticity space.

### 2.2.1 The Planckian locus in the XYZ color space



CIE 1931 Standard Colorimetric Observer functions used to map blackbody spectra to XYZ coordinates

In the CIE XYZ color space, the three coordinates defining a color are given by  $X$ ,  $Y$ , and  $Z$ :<sup>[1]</sup>

$$X_T = \int_0^\infty X(\lambda) M(\lambda, T) d\lambda$$

$$Y_T = \int_0^\infty Y(\lambda) M(\lambda, T) d\lambda$$

$$Z_T = \int_0^\infty Z(\lambda) M(\lambda, T) d\lambda$$

where  $M(\lambda, T)$  is the spectral radiant exitance of the light being viewed, and  $X(\lambda)$ ,  $Y(\lambda)$  and  $Z(\lambda)$  are the color matching functions of the CIE standard colorimetric observer, shown in the diagram on the right, and  $\lambda$  is the wavelength. The Planckian locus is determined by substituting into the above equations the black body spectral radiant exitance, which is given by Planck's law:

$$M(\lambda, T) = \frac{c_1}{\lambda^5} \frac{1}{\exp\left(\frac{c_2}{\lambda T}\right) - 1}$$

where:

$c_1 = 2\pi hc^2$  is the first radiation constant

$c_2 = hc/k$  is the second radiation constant

and:

$M$  is the black body spectral radiant exitance (power per unit area per unit wavelength: watt per square meter per meter ( $\text{W/m}^3$ ))

$T$  is the temperature of the black body

$h$  is Planck's constant

$c$  is the speed of light

$k$  is Boltzmann's constant

This will give the Planckian locus in CIE XYZ color space. If these coordinates are  $XT$ ,  $YT$ ,  $ZT$  where  $T$  is the temperature, then the CIE chromaticity coordinates will be

$$x_T = \frac{XT}{XT + YT + ZT}$$

$$y_T = \frac{YT}{XT + YT + ZT}$$

Note that in the above formula for Planck's Law, you might as well use  $c1L = 2hc^2$  (the first radiation constant for spectral radiance) instead of  $c_1$  (the "regular" first radiation constant), in which case the formula would give the spectral radiance  $L(\lambda, T)$  of the black body instead of the spectral radiant exitance  $M(\lambda, T)$ . However, this change only affects the absolute values of  $XT$ ,  $YT$  and  $ZT$ , not the values relative to each other. Since  $XT$ ,  $YT$  and  $ZT$  are usually normalized to  $YT = 1$  (or  $YT = 100$ ) and are normalized when  $xT$  and  $yT$  are calculated, the absolute values of  $XT$ ,  $YT$  and  $ZT$  do not matter. For practical reasons,  $c_1$  might therefore simply be replaced by 1.

## Approximation

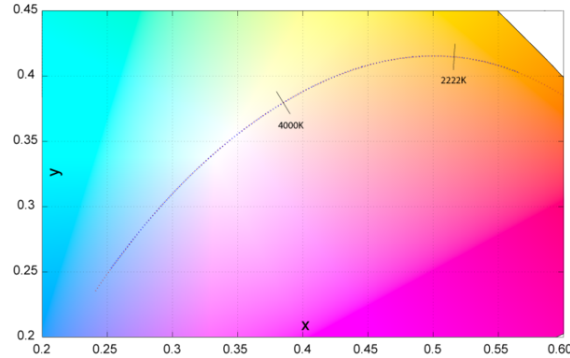
The Planckian locus in  $xy$  space is depicted as a curve in the chromaticity diagram above. While it is possible to compute the CIE  $xy$  co-ordinates exactly given the above formulas, it is faster to use approximations. Since the mired scale changes more evenly along the locus than the temperature itself, it is common for such approximations to be functions of the reciprocal temperature. Kim *et al.* uses a cubic spline:<sup>[2][3]</sup>

$$x_c = \begin{cases} -0.2661239 \frac{10^9}{T^3} - 0.2343580 \frac{10^6}{T^2} + 0.8776956 \frac{10^3}{T} + 0.179 & \text{for } 1000\text{K} \leq T \leq 1966\text{K} \\ -3.0258469 \frac{10^9}{T^3} + 2.1070379 \frac{10^6}{T^2} + 0.2226347 \frac{10^3}{T} + 0 & \text{for } 1966\text{K} \leq T \leq 2222\text{K} \end{cases}$$

$$y_c = \begin{cases} -1.1063814x_c^3 - 1.34811020x_c^2 + 2.18555832x_c - 0.20210683 & \text{for } 1000\text{K} \leq T \leq 1966\text{K} \\ -0.9549476x_c^3 - 1.37418593x_c^2 + 2.09137015x_c - 0.167880 & \text{for } 1966\text{K} \leq T \leq 2222\text{K} \\ +3.0817580x_c^3 - 5.87338670x_c^2 + 3.75112997x_c - 0.37001483 & \text{for } 2222\text{K} \leq T \leq 2500\text{K} \end{cases}$$

The inverse calculation, from chromaticity co-ordinates ( $x, y$ ) on or near the Planckian locus to correlated color temperature, is discussed in [Color temperature#Approximation](#).

The Planckian locus can also be approximated in the CIE 1960 UCS, which is used to compute CCT and CRI, using the following expressions:<sup>[4]</sup>



Kim et al.'s approximation to the Planckian locus (shown in red). The notches demarcate the three splines (shown in blue).

$$\bar{u}(T) = \frac{0.860117757 + 1.54118254 \times 10^{-4}T + 1.28641212 \times 10^{-7}T^2}{1 + 8.42420235 \times 10^{-4}T + 7.08145163 \times 10^{-7}T^2}$$

$$\bar{v}(T) = \frac{0.317398726 + 4.22806245 \times 10^{-5}T + 4.20481691 \times 10^{-8}T^2}{1 - 2.89741816 \times 10^{-5}T + 1.61456053 \times 10^{-7}T^2}$$

This approximation is accurate to within  $|u - \bar{u}| < 8 \times 10^{-5}$  and  $|v - \bar{v}| < 9 \times 10^{-5}$  for  $1000\text{K} < T < 15,000\text{K}$

## 2.2.2 Correlated color temperature

The **correlated color temperature** ( $T_{cp}$ ) is the temperature

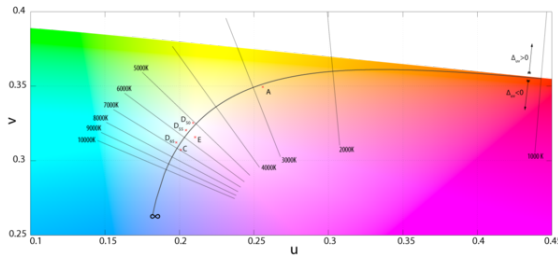
of the Planckian radiator whose perceived colour most closely resembles that of a given stimulus at the same brightness and under specified viewing conditions

— CIE/IEC 17.4:1987, International Lighting Vocabulary (ISBN 3900734070)<sup>[5]</sup>

The mathematical procedure for determining the correlated color temperature involves finding the closest point to the light source's white point on the Planckian locus. Since the CIE's 1959 meeting in Brussels, the Planckian locus has been computed using the **CIE 1960 color space**, also known as MacAdam's ( $u, v$ ) diagram.<sup>[6]</sup> Today, the CIE 1960 color space is deprecated for other purposes:<sup>[7]</sup>

The 1960 CIE color space was declared obsolete in 1986, but has been retained for calculating color rendering index and correlated color temperature. The 1976 CIE 13.3-1985 Method of Measuring and Specifying Colour Rendering Properties of Light Sources

Owing to the perceptual inaccuracy inherent to the concept, it suffices to calculate to within 2K at lower CCTs and 10K at higher CCTs to reach the threshold of imperceptibility.<sup>[8]</sup>



*Close up of the CIE 1960 UCS. The isotherms are perpendicular to the Planckian locus, and are drawn to indicate the maximum distance from the locus that the CIE considers the correlated color temperature to be meaningful:  $\Delta_{uv} = \pm 0.05$*

### International Temperature Scale

The Planckian locus is derived by determining the chromaticity values of a Planckian radiator using the standard colorimetric observer. The relative spectral power distribution (SPD) of a Planckian radiator follows Planck's law, and depends on the second radiation constant,  $c_2 = hc/k$ . As measuring techniques have improved, the General Conference on Weights and Measures has revised its estimate of this constant, with the International Temperature Scale (and briefly, the *International Practical Temperature Scale*). These successive revisions caused a shift in the Planckian locus and, as a result, the correlated color temperature scale. Before ceasing publication of standard illuminants, the CIE worked around this problem by explicitly specifying the form of the SPD, rather than making references to black bodies and a color temperature. Nevertheless, it is useful to be aware of previous revisions in order to be able to verify calculations made in older texts.<sup>[9][10]</sup>

- $c_2 = 1.432 \times 10^{-2} \text{ m}\cdot\text{K}$  (ITS-27). Note: Was in effect during the standardization of Illuminants A, B, C (1931), however the CIE used the value recommended by the U.S. National Bureau of Standards,  $1.435 \times 10^{-2}$ <sup>[11][12]</sup>
- $c_2 = 1.4380 \times 10^{-2} \text{ m}\cdot\text{K}$  (IPTS-48). In effect for Illuminant series D (formalized in 1967).
- $c_2 = 1.4388 \times 10^{-2} \text{ m}\cdot\text{K}$  (ITS-68), (ITS-90). Often used in recent papers.
- $c_2 = 1.4387770(13) \times 10^{-2} \text{ m}\cdot\text{K}$  (CODATA, 2006). Current value, as of 2010.<sup>[13]</sup>

### 2.2.3 References

- [1] Wyszecki, Günter & Stiles, Walter Stanley (2000). *Color Science: Concepts and Methods, Quantitative Data and Formulae* (2E ed.). Wiley-Interscience. ISBN 0-471-39918-3.
- [2] US patent 7024034, Kim *et al.*, "Color Temperature Conversion System and Method Using the Same", issued 2006-04-04

[3] Bongsoon Kang; Ohak Moon; Changhee Hong; Honam Lee; Bonghwan Cho; Youngsun Kim (December 2002). "Design of Advanced Color Temperature Control System for HDTV Applications". *Journal of the Korean Physical Society*. **41** (6): 865–871.

[4] Krystek, Michael P. (January 1985). "An algorithm to calculate correlated colour temperature". *Color Research & Application*. **10** (1): 38–40. doi:10.1002/col.5080100109. A new algorithm to calculate correlated colour temperature is given. This algorithm is based on a rational Chebyshev approximation of the Planckian locus in the CIE 1960 UCS diagram and a bisection procedure. Thus time-consuming search procedures in tables or charts are no longer necessary.

[5] Borbély, Ákos; Sámos, Árpád; Schanda, János (December 2001). "The concept of correlated colour temperature revisited". *Color Research & Application*. **26** (6): 450–457. doi:10.1002/col.1065.

[6] Kelly, Kenneth L. (August 1963). "Lines of constant correlated color temperature based on MacAdam's (u,v) Uniform chromaticity transformation of the CIE diagram" (abstract). *JOSA*. **53** (8): 999. doi:10.1364/JOSA.53.000999.

[7] Simons, Ronald Harvey; Bean, Arthur Robert (2001). *Lighting Engineering: Applied Calculations*. Architectural Press. ISBN 0-7506-5051-6.

[8] Ohno, Yoshi; Jergens, Michael (19 June 1999). "Results of the Intercomparison of Correlated Color Temperature Calculation" (PDF). CORM.

[9] Janos Schanda (2007). "3: CIE Colorimetry". *Colorimetry: Understanding the CIE System*. Wiley Interscience. pp. 37–46. ISBN 978-0-470-04904-4.

#### 10 The ITS-90 Resource Site

[11] Hall, J.A. (January 1967). "The Early History of the International Practical Scale of Temperature". *Metrologia*. **3** (1): 25–28. doi:10.1088/0026-1394/3/1/006.

[12] Moon, Parry (March 1948). "A table of Planckian radiation" (abstract). *JOSA*. **38** (3): 291–294. doi:10.1364/JOSA.38.000291.

[13] Mohr, Peter J.; Taylor, Barry N.; Newell, David B. (2012). "CODATA Recommended Values of the Fundamental Physical Constants: 2010" (PDF).

### 2.2.4 External links

- Numerical table of color temperature and the corresponding xy and sRGB coordinates for both the 1931 and 1964 CMFs, by Mitchell Charity.

### 2.3 Planck–Einstein relation

The **Planck–Einstein relation**<sup>[1][2][3]</sup> is also referred to as the **Einstein relation**,<sup>[1][4][5]</sup> **Planck's energy–frequency relation**,<sup>[6]</sup> the **Planck relation**,<sup>[7]</sup> and the

**Planck equation.**<sup>[8]</sup> Also the eonym 'Planck formula'<sup>[9]</sup> belongs on this list, but also often refers instead to Planck's law<sup>[10][11]</sup> These various eonyms are far from standard; they are used only sporadically, neither regularly nor very widely. They refer to a formula integral to quantum mechanics, which states that the energy of a photon,  $E$ , known as **photon energy**, is proportional to its frequency,  $\nu$ :

$$E = h\nu$$

The constant of proportionality,  $h$ , is known as the **Planck constant**. Several equivalent forms of the relation exist.

The relation accounts for quantized nature of light, and plays a key role in understanding phenomena such as the photoelectric effect, and Planck's law of black body radiation. See also the Planck postulate.

### 2.3.1 Spectral forms

Light can be characterized using several **spectral quantities**, such as **frequency**  $\nu$ , **wavelength**  $\lambda$ , **wavenumber**  $\tilde{\nu}$ , and their angular equivalents (**angular frequency**  $\omega$ , **angular wavelength**  $y$ , and **angular wavenumber**  $k$ ). These quantities are related through

$$\nu = \frac{c}{\lambda} = c\tilde{\nu} = \frac{\omega}{2\pi} = \frac{c}{2\pi y} = \frac{ck}{2\pi},$$

so the Planck relation can take the following 'standard' forms

$$E = h\nu = \frac{hc}{\lambda} = hc\tilde{\nu},$$

as well as the following 'angular' forms,

$$E = \hbar\omega = \frac{\hbar c}{y} = \hbar ck.$$

The standard forms make use of the Planck constant  $h$ . The angular forms make use of the reduced Planck constant  $\hbar = h/2\pi$ . Here  $c$  is the **speed of light**.

### 2.3.2 de Broglie relation

See also: Matter wave § de Broglie relations

The de Broglie relation,<sup>[5][12][13]</sup> also known as the de Broglie's momentum–wavelength relation,<sup>[6]</sup> generalizes the Planck relation to matter waves. Louis de Broglie argued that if particles had a wave nature, the relation  $E = h\nu$  would also apply to them, and postulated that particles

would have a wavelength equal to  $\lambda = h/p$ . Combining de Broglie's postulate with the Planck–Einstein relation leads to

$$p = h\tilde{\nu}$$

$$p = \hbar k.$$

The de Broglie's relation is also often encountered in vector form

$$\mathbf{p} = \hbar \mathbf{k},$$

where  $\mathbf{p}$  is the momentum vector, and  $\mathbf{k}$  is the angular wave vector.

### 2.3.3 Bohr's frequency condition

Bohr's frequency condition states that the frequency of a photon absorbed or emitted during an **electronic transition** is related to the energy difference ( $\Delta E$ ) between the two **energy levels** involved in the transition:<sup>[14]</sup>

$$\Delta E = h\nu.$$

This is a direct consequence of the Planck–Einstein relation.

### 2.3.4 References

- [1] French & Taylor (1978), pp. 24, 55.
- [2] Cohen-Tannoudji, Diu & Laloë (1973/1977), pp. 10–11.
- [3] Kalckar 1985, p. 39.
- [4] Messiah (1958/1961), p. 72.
- [5] Weinberg (1995), p. 3.
- [6] Schwinger (2001), p. 203.
- [7] Landsberg (1978), p. 199.
- [8] Landé (1951), p. 12.
- [9] Griffiths, D.J. (1995), pp. 143, 216.
- [10] Griffiths, D.J. (1995), pp. 217, 312.
- [11] Weinberg (2013), pp. 24, 28, 31.
- [12] Messiah (1958/1961), p. 14.
- [13] Cohen-Tannoudji, Diu & Laloë (1973/1977), p. 27.
- [14] van der Waerden (1967), p. 5.

### 2.3.5 Cited bibliography

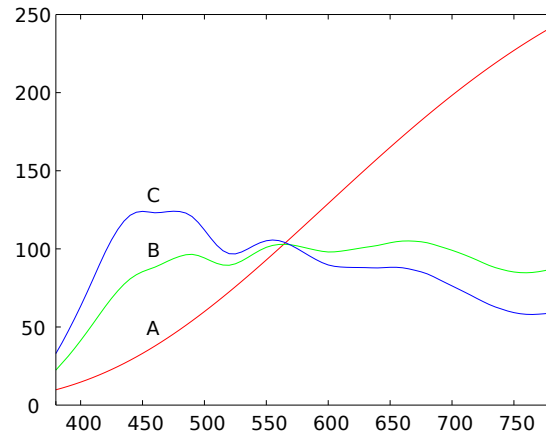
- Cohen-Tannoudji, C., Diu, B., Laloë, F. (1973/1977). *Quantum Mechanics*, translated from the French by S.R. Hemley, N. Ostrowsky, D. Ostrowsky, second edition, volume 1, Wiley, New York, ISBN 0471164321.
- French, A.P., Taylor, E.F. (1978). *An Introduction to Quantum Physics*, Van Nostrand Reinhold, London, ISBN 0-442-30770-5.
- Griffiths, D.J. (1995). *Introduction to Quantum Mechanics*, Prentice Hall, Upper Saddle River NJ, ISBN 0-13-124405-1.
- Landé, A. (1951). *Quantum Mechanics*, Sir Isaac Pitman & Sons, London.
- Landsberg, P.T. (1978). *Thermodynamics and Statistical Mechanics*, Oxford University Press, Oxford UK, ISBN 0-19-851142-6.
- Messiah, A. (1958/1961). *Quantum Mechanics*, volume 1, translated from the French by G.M. Temmer, North-Holland, Amsterdam.
- Schwinger, J. (2001). *Quantum Mechanics: Symbolism of Atomic Measurements*, edited by B.-G. Englert, Springer, Berlin, ISBN 3-540-41408-8.
- van der Waerden, B.L. (1967). *Sources of Quantum Mechanics*, edited with a historical introduction by B.L. van der Waerden, North-Holland Publishing, Amsterdam.
- Weinberg, S. (1995). *The Quantum Theory of Fields*, volume 1, *Foundations*, Cambridge University Press, Cambridge UK, ISBN 978-0-521-55001-7.
- Weinberg, S. (2013). *Lectures on Quantum Mechanics*, Cambridge University Press, Cambridge UK, ISBN 978-1-107-02872-2.

## 2.4 Standard illuminant

A **standard illuminant** is a theoretical source of **visible light** with a profile (its **spectral power distribution**) which is published. Standard illuminants provide a basis for comparing images or colors recorded under different lighting.

### 2.4.1 CIE illuminants

The **International Commission on Illumination** (usually abbreviated **CIE** for its French name) is the body responsible for publishing all of the well-known standard illuminants. Each of these is known by a letter or by a letter-number combination.



*Relative spectral power distributions (SPDs) of CIE illuminants A, B, and C from 380 nm to 780 nm.*

Illuminants A, B, and C were introduced in 1931, with the intention of respectively representing average incandescent light, direct sunlight, and average daylight. Illuminants D represent phases of daylight, Illuminant E is the equal-energy illuminant, while Illuminants F represent fluorescent lamps of various composition.

There are instructions on how to experimentally produce light sources (“standard sources”) corresponding to the older illuminants. For the relatively newer ones (such as series D), experimenters are left to measure to profiles of their sources and compare them to the published spectra.<sup>[1]</sup>

At present no artificial source is recommended to realize CIE standard illuminant D65 or any other illuminant D of different CCT. It is hoped that new developments in light sources and filters will eventually offer sufficient basis for a CIE recommendation.

—CIE, Technical Report (2004) Colorimetry, 3rd ed., Publication 15:2004, CIE Central Bureau, Vienna

Nevertheless, they do provide a measure, called the **Metamerism Index**, to assess the quality of daylight simulators.<sup>[2][3]</sup> The **Metamerism Index** tests how well five sets of metamerous samples match under the test and reference illuminant. In a manner similar to the **color rendering index**, the average difference between the metamers is calculated.<sup>[4]</sup>

### Illuminant A

The CIE defines illuminant A in these terms:

CIE standard illuminant A is intended to represent typical, domestic, tungsten-filament lighting. Its relative spectral power distribution

is that of a Planckian radiator at a temperature of approximately 2856 K. CIE standard illuminant A should be used in all applications of colorimetry involving the use of incandescent lighting, unless there are specific reasons for using a different illuminant.

— CIE, CIE Standard Illuminants for Colorimetry

The spectral radiant exitance of a black body follows Planck's law:

$$M_{e,\lambda}(\lambda, T) = \frac{c_1 \lambda^{-5}}{\exp\left(\frac{c_2}{\lambda T}\right) - 1}.$$

At the time of standardizing illuminant A, both  $c_1 = 2\pi \cdot h \cdot c^2$  (which does not affect the relative SPD) and  $c_2 = h \cdot c/k$  were different. In 1968, the estimate of  $c_2$  was revised from 0.01438 m·K to 0.014388 m·K (and before that, it was 0.01435 m·K when illuminant A was standardized). This difference shifted the Planckian locus, changing the color temperature of the illuminant from its nominal 2848 K to 2856 K:

$$T_{new} = T_{old} \times \frac{1.438,8}{1.435} = 2,848 \text{ K} \times 1.002,648 = 2,855.54 \text{ K}.$$

In order to avoid further possible changes in the color temperature, the CIE now specifies the SPD directly, based on the original (1931) value of  $c_2$ :<sup>[1]</sup>

$$S_A(\lambda) = 100 \left( \frac{560}{\lambda} \right)^5 \frac{\exp \frac{1.435 \times 10^7}{2,848 \times 560} - 1}{\exp \frac{1.435 \times 10^7}{2,848 \lambda} - 1}.$$

The coefficients have been selected to achieve a peak SPD of 100 nm at 560 nm. The tristimulus values are  $(X, Y, Z) = (109.85, 100.00, 35.58)$ , and the chromaticity coordinates using the standard observer are  $(x, y) = (0.447, 58, 0.407, 45)$ .

### Illuminants B and C

Illuminants B and C are daylight simulators. They are derived from Illuminant A by using liquid filters. B served as a representative of noon sunlight, with a correlated color temperature (CCT) of 4874 K, while C represented average day light with a CCT of 6774 K. They are poor approximations of any phase of natural daylight, particularly in the short-wave visible and in the ultraviolet spectral ranges. Still, the lighting cabinets, such as the Spectralight III, that use filtered incandescent lamps have better fits to the D illuminants in the 400 nm to 700 nm range than do the fluorescent daylight simulators.<sup>[5]</sup> As a result, these illuminants have been deprecated in favor of the D series:<sup>[1]</sup>

Illuminant C does not have the status of a CIE standard but its relative spectral power distribution, tristimulus values and chromaticity coordinates are given in Table T.1 and Table T.3, as many practical measurement instruments and calculations still use this illuminant.

— CIE, Publication 15:2004<sup>[6]</sup>

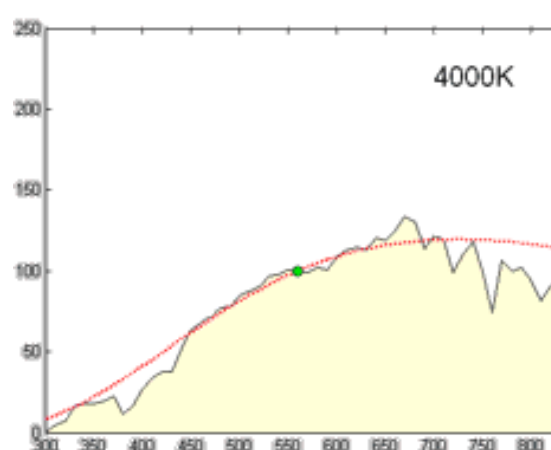
The liquid filters, designed by Raymond Davis, Jr. and Kasson S. Gibson in 1931,<sup>[7]</sup> have a relatively high absorbance at the red end of the spectrum, effectively increasing the CCT of the gas lamp to daylight levels. This is similar in function to a CTO color gel that photographers and cinematographers use today, albeit much less convenient.

Each filter uses a pair of solutions, comprising specific amounts of distilled water, copper sulfate, mannite, pyridine, sulfuric acid, cobalt, and ammonium sulfate. The solutions are separated by a sheet of uncolored glass. The amounts of the ingredients are carefully chosen so that their combination yields a color temperature conversion filter; that is, the filtered light is still white.

### Illuminant series D

See also: CIE Standard Illuminant D65

Derived by Judd, MacAdam, and Wyszecki,<sup>[8]</sup> the D se-



*Relative spectral power distribution of illuminant D and a black body of the same correlated color temperature (in red), normalized about 560 nm.*

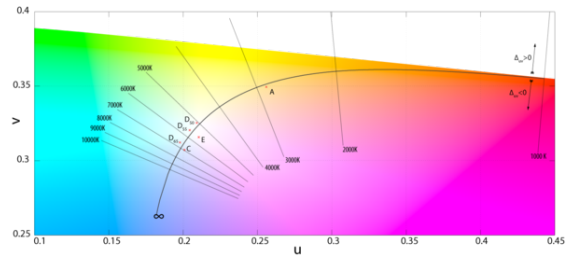
ries of illuminants are constructed to represent natural daylight. They are difficult to produce artificially, but are easy to characterize mathematically.

H. W. Budde of the National Research Council of Canada in Ottawa, H. R. Condit and F. Grum of the Eastman Kodak Company in Rochester, New York,<sup>[9]</sup> and S. T. Henderson and D. Hodgkiss of Thorn Electrical Industries in Enfield<sup>[10]</sup> had independently measured the spectral power distribution (SPD) of daylight from 330 nm

to 700 nm, totaling among them 622 samples. Judd *et al.* analyzed these samples and found that the  $(x, y)$  chromaticity coordinates had a simple, quadratic relation:

$$y = 2.870x - 3.000x^2 - 0.275.$$

Simonds supervised the characteristic vector analysis of the SPDs.<sup>[11][12]</sup> Application of his method revealed that the SPDs could be satisfactorily approximated by using the mean ( $S_0$ ) and first two characteristic vectors ( $S_1$  and  $S_2$ ):



*Kelly's figures depicted the lines of constant correlated color temperature on the CIE 1960 UCS, as shown here, as well as the familiar xy diagram.*

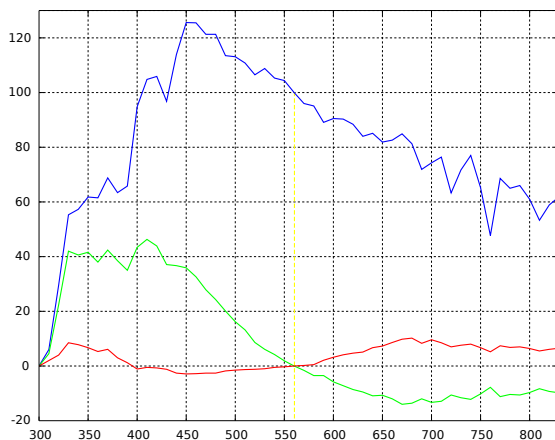
$$M_2 = \frac{0.030, 0 - 31.442, 4x + 30.071, 7y}{0.024, 1 + 0.256, 2x - 0.734, 1y}.$$

The only problem is that this left unsolved the computation of the coordinate  $(x, y)$  for a particular phase of daylight. Judd *et al.* simply tabulated the values of certain chromaticity coordinates, corresponding to commonly used correlated color temperatures, such as 5500 K, 6500 K, and 7500 K. For other color temperatures, one could consult figures made by Kelly.<sup>[13]</sup> This problem was addressed in the CIE report that formalized illuminant D, with an approximation of the x coordinate in terms of the reciprocal color temperature, valid from 4000 K to 25,000 K.<sup>[14]</sup> The y coordinate trivially followed from Judd's quadratic relation.

Judd *et al.* then extended the reconstituted SPDs to 300 nm–330 nm and 700 nm–830 nm by using Moon's spectral absorbance data of the Earth's atmosphere.<sup>[15]</sup>

The tabulated SPDs presented by the CIE today are derived by linear interpolation of the 10 nm data set down to 5 nm. The limited nature of the photometric data is not an impediment to the calculation of the **CIEXYZ** tristimulus values since the CIE standard colorimetric observer's color matching functions are only tabulated from 380 to 780 nm in increments of 5 nm.<sup>[16]</sup>

Similar studies have been undertaken in other parts of the world, or repeating Judd *et al.*'s analysis with modern computational methods. In several of these studies, the daylight locus is notably closer to the Planckian locus than in Judd *et al.*<sup>[17]</sup>



*Characteristic vectors of illuminant D; component SPDs S0 (blue), SI (green), S2 (red).*

Expressing the chromaticities x and y as:

$$x = \frac{X_0 + M_1 X_1 + M_2 X_2}{S_0 + M_1 S_1 + M_2 S_2},$$

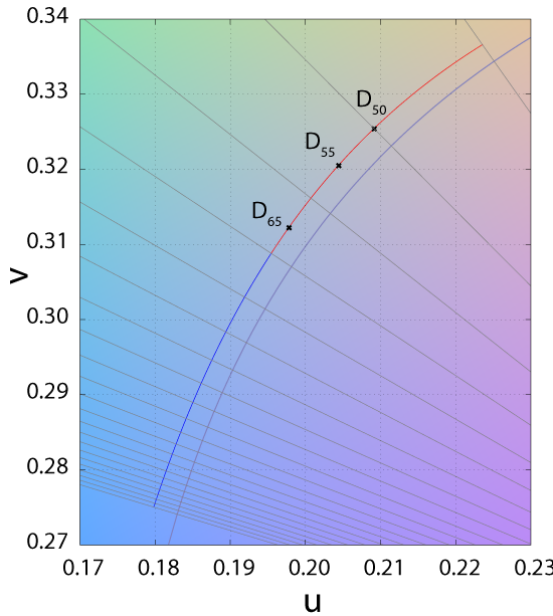
$$y = \frac{Y_0 + M_1 Y_1 + M_2 Y_2}{S_0 + M_1 S_1 + M_2 S_2}$$

and making use of known tristimulus values for the mean vectors, they were able to express  $M_1$  and  $M_2$  as follows:

Computation

The relative spectral power distribution (SPD)  $S_D(\lambda)$  of a D series illuminant can be derived from its chromaticity coordinates in the CIE 1931 color space,  $(x_D, y_D)$ :<sup>[18]</sup>

$$x_D = \begin{cases} 0.244,063 + 0.09911 \frac{10^3}{T} + 2.967,8 \frac{10^6}{T^2} - 4.607,0 \frac{10^9}{T^3} & 4,000 \text{ K} \\ 0.237,040 + 0.24748 \frac{10^3}{T} + 1.901,8 \frac{10^6}{T^2} - 2.006,4 \frac{10^9}{T^3} & 7,000 \text{ K} \end{cases}$$



*Daylight locus in the CIE 1960 UCS. The isotherms are perpendicular to the Planckian locus. The two sections of the daylight locus, from 4000–7000 K and 7000–25000 K, are color-coded. Note that the two loci are separated by a fairly even distance, of around  $\Delta_{uv} = 0.003$ .*

$$y_D = -3.000x_D^2 + 2.870x_D - 0.275$$

where  $T$  is the illuminant's CCT. The chromaticity coordinates of the Illuminants D are said to form the *CIE Daylight Locus*. The relative SPD is given by:

$$S_D(\lambda) = S_0(\lambda) + M_1 S_1(\lambda) + M_2 S_2(\lambda),$$

$$M_1 = (-1.351, 5 - 1.770, 3x_D + 5.911, 4y_D)/M,$$

$$M_2 = (0.030, 00 - 31.442, 4x_D + 30.071, 7y_D)/M,$$

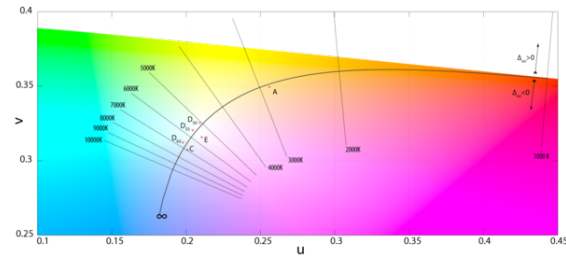
$$M = 0.024, 1 + 0.256, 2x_D - 0.734, 1y_D$$

where  $S_0(\lambda), S_1(\lambda), S_2(\lambda)$  are the mean and first two eigenvector SPDs, depicted above.<sup>[18]</sup> The characteristic vectors both have a zero at 560 nm, since all the relative SPDs have been normalized about this point.

The CCTs of the canonical illuminants,  $D_{50}$ ,  $D_{55}$ ,  $D_{65}$ , and  $D_{75}$ , differ slightly from what their names suggest. For example,  $D_{50}$  has a CCT of 5003 K (“horizon” light), while  $D_{65}$  has a CCT of 6504 K (noon light). As explained in a previous section, this is because the value of the constants in Planck’s law have been slightly changed since the definition of these canonical illuminants, whose SPDs are based on the original values in Planck’s law. In order to match all significant digits of the published data of the canonical illuminants the values of  $M_1$  and  $M_2$  have to be rounded to three decimal places before calculation of  $SD$ .<sup>[1]</sup>

## Illuminant E

Illuminant E is an equal-energy radiator; it has a constant SPD inside the visible spectrum. It is useful as a theoretical reference; an illuminant that gives equal weight to all wavelengths, presenting an even color. It also has equal CIE XYZ tristimulus values, thus its chromaticity coordinates are  $(x,y)=(1/3,1/3)$ . This is by design; the XYZ color matching functions are normalized such that their integrals over the visible spectrum are the same.<sup>[1]</sup>



*Illuminant E is beneath the Planckian locus, and roughly isothermal with  $D_{55}$ .*

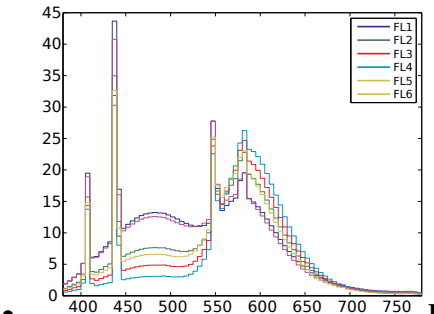
Illuminant E is not a black body, so it does not have a color temperature, but it can be approximated by a D series illuminant with a CCT of 5455 K. (Of the canonical illuminants,  $D_{55}$  is the closest.) Manufacturers sometimes compare light sources against Illuminant E to calculate the *excitation purity*.<sup>[19]</sup>

## Illuminant series F

The **F** series of illuminants represent various types of fluorescent lighting.

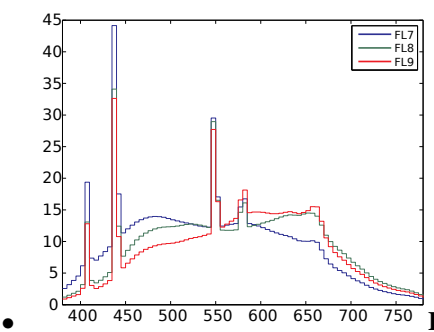
F1–F6 “standard” fluorescent lamps consist of two semi-broadband emissions of antimony and manganese activations in calcium halophosphate phosphor.<sup>[20]</sup> F4 is of particular interest since it was used for calibrating the CIE color rendering index (the CRI formula was chosen such that F4 would have a CRI of 51). F7–F9 are “broadband” (full-spectrum light) fluorescent lamps with multiple phosphors, and higher CRIs. Finally, F10–F12 are narrow triband illuminants consisting of three “narrowband” emissions (caused by ternary compositions of rare-earth phosphors) in the R,G,B regions of the visible spectrum. The phosphor weights can be tuned to achieve the desired CCT.

The spectra of these illuminants are published in Publication 15:2004.<sup>[6][21]</sup>



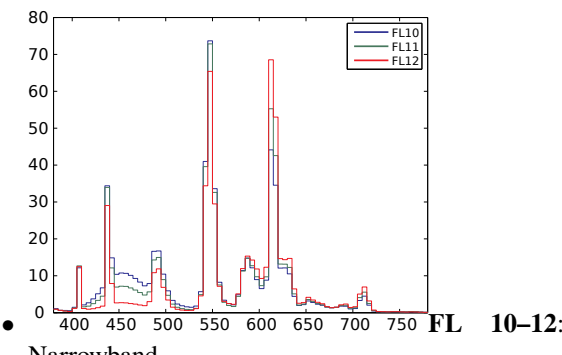
Standard

1-6:



Broadband

7-9:



Narrowband

10-12:

### Illuminant series L

Publication of an **L** series of illuminants is expected in 2017. It will represent various types of **LED** lighting.

#### 2.4.2 White point

Main article: [White point](#)

The spectrum of a standard illuminant, like any other profile of light, can be converted into **tristimulus values**. The set of three tristimulus coordinates of an illuminant is called a *white point*. If the profile is **normalized**, then the white point can equivalently be expressed as a pair of chromaticity coordinates.

If an image is recorded in tristimulus coordinates (or in values which can be converted to and from them), then

the white point of the illuminant used gives the maximum value of the tristimulus coordinates that will be recorded at any point in the image, in the absence of **fluorescence**. It is called the white point of the image.

The process of calculating the white point discards a great deal of information about the profile of the illuminant, and so although it is true that for every illuminant the exact white point can be calculated, it is not the case that knowing the white point of an image alone tells you a great deal about the illuminant that was used to record it.

#### White points of standard illuminants

A list of standardized illuminants, their CIE chromaticity coordinates ( $x, y$ ) of a perfectly reflecting (or transmitting) diffuser, and their **correlated color temperatures** (CCTs) are given below. The CIE chromaticity coordinates are given for both the 2 degree field of view (1931) and the 10 degree field of view (1964). The color swatches represent the **hue** of each white point, calculated with **luminance**  $Y=0.54$  and the standard observer, assuming correct **sRGB** display calibration.

#### 2.4.3 References

- [1] Schanda, János (2007). “3: CIE Colorimetry”. *Colorimetry: Understanding the CIE System*. Wiley Interscience. pp. 37–46. ISBN 978-0-470-04904-4.
- [2] CIE Technical Report (1999). *A Method for Assessing the Quality of Daylight Simulators for Colorimetry*. 51.2-1999 (including Supplement 1-1999). Paris: Bureau central de la CIE. ISBN 92-9034-051-7. A method is provided for evaluating the suitability of a test source as a simulator of CIE Standard Illuminants D55, D65, or D75. The Supplement, prepared in 1999, adds the CIE Illuminant D50 to the line of illuminants where the method can be applied to. For each of these standard illuminants, spectral radiance factor data are supplied for five pairs of nonfluorescent samples that are metamerically matched. The colorimetric differences of the five pairs are computed for the test illuminant; the average of these differences is taken as the visible range metamerism index and is used as a measure of the quality of the test illuminant as a simulator for nonfluorescent samples. For fluorescent samples, the quality is further assessed in terms of an ultraviolet range metamerism index, defined as the average of the colorimetric differences computed with the test illuminant for three further pairs of samples, each pair consisting of a fluorescent and a nonfluorescent sample which are metamerically matched under the standard illuminant.
- [3] CIE Standard (2004). *Standard Method of Assessing the Spectral Quality of Daylight Simulators for Visual Appraisal and Measurement of Colour*. S012/E:2004. Prepared by TC 1-53 “A Standard Method for Assessing the Quality of Daylight Simulators”. ISO Standard 23603:2005(E).
- [4] Lam, Yuk-Ming; Xin, John H. (August 2002). “Evaluation of the quality of different D65 simulators for visual

- assessment". *Color Research & Application*. **27** (4): 243–251. doi:10.1002/col.10061.
- [5] Wyszecki, Gunter (1970). "Development of New CIE Sources for Colorimetry". *Die Farbe*. **19**: 43–.
- [6] CIE Technical Report (2004). *Colorimetry*. Publication 15:2004 (3rd ed.). CIE Central Bureau, Vienna. ISBN 3-901906-33-9.
- [7] Davis, Raymond; Gibson, Kasson S. (January 21, 1931). "Filters for the reproduction of sunlight and daylight and the determination of color temperature". *Precision Measurement and Calibration*. National Bureau of Standards. **10**: 641–805.
- [8] Judd, Deane B.; MacAdam, David L.; Wyszecki, Günter (August 1964). "Spectral Distribution of Typical Daylight as a Function of Correlated Color Temperature". *JOSA*. **54** (8): 1031–1040. doi:10.1364/JOSA.54.001031.
- [9] Condit, Harold R.; Grum, Frank (July 1964). "Spectral energy distribution of daylight". *JOSA*. **54** (7): 937–944. doi:10.1364/JOSA.54.000937. Retrieved 2008-05-13.
- [10] Henderson, Stanley Thomas; Hodgkiss, D. (1963). "The spectral energy distribution of daylight". *British Journal of Applied Physics*. **14** (3): 125–131. doi:10.1088/0508-3443/14/3/307.  
Henderson, Stanley Thomas; Hodgkiss, D. (1964). "The spectral energy distribution of daylight". *British Journal of Applied Physics*. **15** (8): 947–952. doi:10.1088/0508-3443/15/8/310.
- [11] Simonds, John L. (August 1963). "Application of Characteristic Vector Analysis to Photographic and Optical Response Data". *JOSA*. **53** (8): 968–974. doi:10.1364/JOSA.53.000968.
- [12] Tzeng, Di-Yuan; Berns, Roy S. (April 2005). "A review of principal component analysis and its applications to color technology". *Color Research & Application*. **30** (2): 84–98. doi:10.1002/col.20086.
- [13] Kelly, Kenneth L. (August 1963). "Lines of Constant Correlated Color Temperature Based on MacAdam's (u,v) Uniform Chromaticity Transformation of the CIE Diagram". *JOSA*. **53** (8): 999–1002. doi:10.1364/JOSA.53.000999.
- [14] Commission Internationale de l'Eclairage (1964). *Proceedings of the 15th Session, Vienna*.
- [15] Moon, Parry (November 1940). "Proposed standard solar-radiation curves for engineering use". *Journal of the Franklin Institute*. **230** (5): 583–617. doi:10.1016/S0016-0032(40)90364-7.
- [16] CIE 1931 and 1964 Standard Colorimetric Observers from 380 nm to 780 nm in increments of 5 nm.
- [17] Studies from the 1960s and 1970s include:
- G. T. Winch; M. C. Boshoff; C. J. Kok & A. G. du Toit (April 1966). "Spectroradiometric and Colorimetric Characteristics of Daylight in the Southern Hemisphere: Pretoria, South Africa". *JOSA*. **56** (4): 456–464. doi:10.1364/JOSA.56.000456.
- The derived chromaticities were found to be much closer to the full radiator locus than those previously published, which had been obtained in the northern hemisphere.
- Das, S.R.; Sastri, V.D.P. (March 1965). "Spectral Distribution and Color of Tropical Daylight". *JOSA*. **55** (3): 319–323. doi:10.1364/JOSA.55.000319.
  - Sastri, V.D.P.; Das, S.R. (March 1968). "Typical Spectral Distributions and Color for Tropical Daylight". *JOSA*. **58** (3): 391–398. doi:10.1364/JOSA.58.000391.
  - Sastri, V.D.P. (January 11, 1976). "Locus of daylight chromaticities in relation to atmospheric conditions". *Journal of Physics D: Applied Physics*. **9** (1): L1–L3. doi:10.1088/0022-3727/9/1/001.
  - Dixon, E.R. (April 1978). "Spectral distribution of Australian daylight". *JOSA*. **68** (4): 437–450. doi:10.1364/JOSA.68.000437.
  - Analyses using the faster computation of the 1990s and 2000s include:
  - Hernández-Andrés, Javier; Javier Romero; Antonio García-Beltrán; Juan L. Nieves (February 20, 1998). "Testing Linear Models on Spectral Daylight Measurements". *Applied Optics*. **37** (6): 971–977. PMID 18268673. doi:10.1364/AO.37.000971.
  - Hernández-Andrés, Javier; Javier Romero; Juan L. Nieves; Raymond L. Lee Jr (June 2001). "Color and spectral analysis of daylight in southern Europe". *JOSA A*. **18** (6): 1325–1335. doi:10.1364/JOSAA.18.001325.
  - Thanh Hai Bui; Reiner Lenz; Tomas Landelius (2004). *Group theoretical investigations of daylight spectra* (PDF). CGIV (European Conference on Colour Graphics, Imaging and Vision). pp. 437–442. Retrieved 2008-05-13.
  - [18] The coefficients differ from those in the original paper due to the change in the constants in Planck's law. See Lindbloom for the current version, and Planckian locus for details.
  - [19] Philips. "Optical Testing for SuperFlux, SnapLED and LUXEON Emitters" (PDF). CIE has defined the color coordinates of several different white Illuminants, but within Lumileds, CIE Illuminant E is used for all color calculations
  - [20] For commercial examples of calcium halophosphate fluorescents, see for example US 5447660 Method for making a calcium halophosphate phosphor or US 6666993 Single component calcium halophosphate phosphor
  - [21] Spectral power distribution of Illuminants Series F (Excel), in 5 nm increments from 380 nm to 780 nm.
  - [22] Danny Pascale. "A Review of RGB color spaces" (PDF). Babel Color.
  - [23] Equivalent White Light Sources, and CIE Illuminants
  - [24] CIE F-series Spectral Data, CIE 15.2:1986

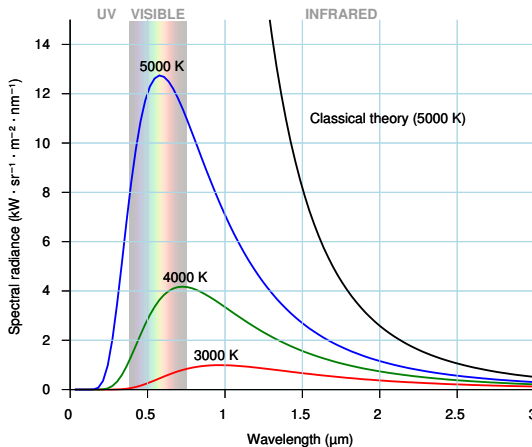
#### 2.4.4 External links

- Selected colorimetric tables in Excel, as published in CIE 15:2004
- Konica Minolta Sensing: Light sources & Illuminants

### 2.5 Black body

For the radiation from a black body in thermal equilibrium, see [Black-body radiation](#).

A **black body** is an idealized physical body that absorbs



As the temperature of a black body decreases, its intensity also decreases and its peak moves to longer wavelengths. Shown for comparison is the classical Rayleigh–Jeans law and its ultraviolet catastrophe.

all incident electromagnetic radiation, regardless of frequency or angle of incidence. A **white body** is one with a “rough surface [that] reflects all incident rays completely and uniformly in all directions.”<sup>[1]</sup>

A black body in thermal equilibrium (that is, at a constant temperature) emits electromagnetic radiation called **black-body radiation**. The radiation is emitted according to Planck’s law, meaning that it has a **spectrum** that is determined by the **temperature** alone (see figure at right), not by the body’s shape or composition.

A black body in thermal equilibrium has two notable properties:<sup>[2]</sup>

1. It is an ideal emitter: at every frequency, it emits as much energy as – or more energy than – any other body at the same temperature.
2. It is a diffuse emitter: the energy is radiated isotropically, independent of direction.

An approximate realization of a black surface is a hole in the wall of a large enclosure. Any light entering the hole is reflected indefinitely or absorbed inside and is unlikely

to re-emerge, making the hole a nearly perfect absorber. The radiation confined in such an enclosure may or may not be in thermal equilibrium, depending upon the nature of the walls and the other contents of the enclosure.<sup>[3][4]</sup>

Real materials emit energy at a fraction—called the **emissivity**—of black-body energy levels. By definition, a black body in thermal equilibrium has an emissivity of  $\epsilon = 1.0$ . A source with lower emissivity independent of frequency often is referred to as a **gray body**.<sup>[5][6]</sup> Construction of black bodies with emissivity as close to one as possible remains a topic of current interest.<sup>[7]</sup>

In astronomy, the radiation from stars and planets is sometimes characterized in terms of an **effective temperature**, the temperature of a black body that would emit the same total flux of electromagnetic energy.

#### 2.5.1 Definition

The idea of a black body originally was introduced by Gustav Kirchhoff in 1860 as follows:

...the supposition that bodies can be imagined which, for infinitely small thicknesses, completely absorb all incident rays, and neither reflect nor transmit any. I shall call such bodies *perfectly black*, or, more briefly, *black bodies*.<sup>[8]</sup>

A more modern definition drops the reference to “infinitely small thicknesses”:<sup>[9]</sup>

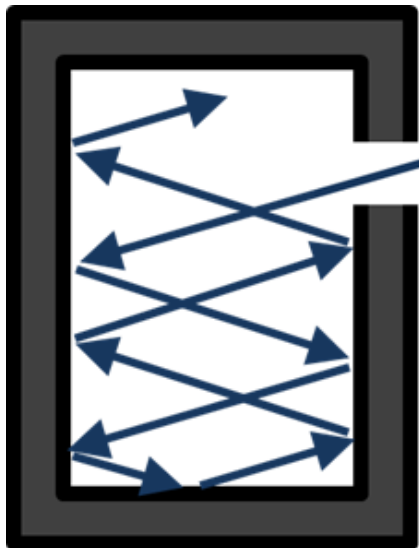
An ideal body is now defined, called a *blackbody*. A *blackbody* allows *all* incident radiation to pass into it (no reflected energy) and internally absorbs *all* the incident radiation (no energy transmitted through the body). This is true for radiation of all wavelengths and for all angles of incidence. Hence the blackbody is a *perfect absorber for all incident radiation*.<sup>[10]</sup>

#### 2.5.2 Idealizations

This section describes some concepts developed in connection with black bodies.

##### Cavity with a hole

A widely used model of a black surface is a small hole in a cavity with walls that are opaque to radiation.<sup>[10]</sup> Radiation incident on the hole will pass into the cavity, and is very unlikely to be re-emitted if the cavity is large. The hole is not quite a perfect black surface — in particular, if the wavelength of the incident radiation is longer than the diameter of the hole, part will be reflected. Similarly, even in perfect thermal equilibrium, the radiation inside a



*An approximate realization of a black body as a tiny hole in an insulated enclosure*

finite-sized cavity will not have an ideal Planck spectrum for wavelengths comparable to or larger than the size of the cavity.<sup>[11]</sup>

Suppose the cavity is held at a fixed temperature  $T$  and the radiation trapped inside the enclosure is at **thermal equilibrium** with the enclosure. The hole in the enclosure will allow some radiation to escape. If the hole is small, radiation passing in and out of the hole has negligible effect upon the equilibrium of the radiation inside the cavity. This escaping radiation will approximate **black-body radiation** that exhibits a distribution in energy characteristic of the temperature  $T$  and does not depend upon the properties of the cavity or the hole, at least for wavelengths smaller than the size of the hole.<sup>[11]</sup> See the figure in the Introduction for the **spectrum** as a function of the frequency of the radiation, which is related to the energy of the radiation by the equation  $E=hf$ , with  $E$  = energy,  $h$  = Planck's constant,  $f$  = frequency.

At any given time the radiation in the cavity may not be in thermal equilibrium, but the **second law of thermodynamics** states that if left undisturbed it will eventually reach equilibrium,<sup>[12]</sup> although the time it takes to do so may be very long.<sup>[13]</sup> Typically, equilibrium is reached by continual absorption and emission of radiation by matter in the cavity or its walls.<sup>[3][4][14][15]</sup> Radiation entering the cavity will be "thermalized"; by this mechanism: the energy will be redistributed until the ensemble of photons achieves a **Planck distribution**. The time taken for thermalization is much faster with condensed matter present than with rarefied matter such as a dilute gas. At temperatures below billions of Kelvin, direct **photon-photon interactions**<sup>[16]</sup> are usually negligible compared to interactions with matter.<sup>[17]</sup> Photons are an example of an interacting boson gas,<sup>[18]</sup> and as described by the **H-theorem**,<sup>[19]</sup> under very general conditions any interacting boson gas will approach thermal equilibrium.

### Transmission, absorption, and reflection

A body's behavior with regard to thermal radiation is characterized by its transmission  $\tau$ , absorption  $\alpha$ , and reflection  $\rho$ .

The boundary of a body forms an interface with its surroundings, and this interface may be rough or smooth. A nonreflecting interface separating regions with different refractive indices must be rough, because the laws of reflection and refraction governed by the **Fresnel equations** for a smooth interface require a reflected ray when the refractive indices of the material and its surroundings differ.<sup>[20]</sup> A few idealized types of behavior are given particular names:

An opaque body is one that transmits none of the radiation that reaches it, although some may be reflected.<sup>[21][22]</sup> That is,  $\tau=0$  and  $\alpha+\rho=1$

A transparent body is one that transmits all the radiation that reaches it. That is,  $\tau=1$  and  $\alpha=\rho=0$ .

A gray body is one where  $\alpha$ ,  $\rho$  and  $\tau$  are uniform for all wavelengths. This term also is used to mean a body for which  $\alpha$  is temperature and wavelength independent.

A white body is one for which all incident radiation is reflected uniformly in all directions:  $\tau=0$ ,  $\alpha=0$ , and  $\rho=1$ .

For a black body,  $\tau=0$ ,  $\alpha=1$ , and  $\rho=0$ . Planck offers a theoretical model for perfectly black bodies, which he noted do not exist in nature: besides their opaque interior, they have interfaces that are perfectly transmitting and non-reflective.<sup>[23]</sup>

### Kirchhoff's perfect black bodies

Kirchhoff in 1860 introduced the theoretical concept of a perfect black body with a completely absorbing surface layer of infinitely small thickness, but Planck noted some severe restrictions upon this idea. Planck noted three requirements upon a black body: the body must (i) allow radiation to enter but not reflect; (ii) possess a minimum thickness adequate to absorb the incident radiation and prevent its re-emission; (iii) satisfy severe limitations upon scattering to prevent radiation from entering and bouncing back out. As a consequence, Kirchhoff's perfect black bodies that absorb all the radiation that falls on them cannot be realized in an infinitely thin surface layer, and impose conditions upon scattering of the light within the black body that are difficult to satisfy.<sup>[24][25]</sup>

### 2.5.3 Realizations

A realization of a black body is a real world, physical embodiment. Here are a few.

### Cavity with a hole

In 1898, Otto Lummer and Ferdinand Kurlbaum published an account of their cavity radiation source.<sup>[26]</sup> Their design has been used largely unchanged for radiation measurements to the present day. It was a hole in the wall of a platinum box, divided by diaphragms, with its interior blackened with iron oxide. It was an important ingredient for the progressively improved measurements that led to the discovery of Planck's law.<sup>[27][28]</sup> A version described in 1901 had its interior blackened with a mixture of chromium, nickel, and cobalt oxides.<sup>[29]</sup> See also Hohlraum.

### Near-black materials

There is interest in blackbody-like materials for camouflage and radar-absorbent materials for radar invisibility.<sup>[30][31]</sup> They also have application as solar energy collectors, and infrared thermal detectors. As a perfect emitter of radiation, a hot material with black body behavior would create an efficient infrared heater, particularly in space or in a vacuum where convective heating is unavailable.<sup>[32]</sup> They are also useful in telescopes and cameras as anti-reflection surfaces to reduce stray light, and to gather information about objects in high-contrast areas (for example, observation of planets in orbit around their stars), where blackbody-like materials absorb light that comes from the wrong sources.

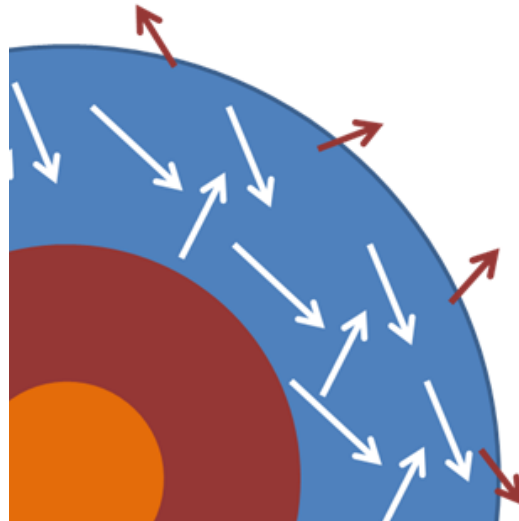
It has long been known that a lamp-black coating will make a body nearly black. An improvement on lamp-black is found in manufactured carbon nanotubes. Nanoporous materials can achieve refractive indices nearly that of vacuum, in one case obtaining average reflectance of 0.045%.<sup>[7][33]</sup> In 2009, a team of Japanese scientists created a material called nanoblack which is close to an ideal black body, based on vertically aligned single-walled carbon nanotubes. This absorbs between 98% and 99% of the incoming light in the spectral range from the ultraviolet to the far-infrared regions.<sup>[32]</sup>

Other examples of nearly perfect black materials are super black, prepared by chemically etching a nickel-phosphorus alloy,<sup>[34]</sup> and vantablack made of carbon nanotubes; both absorb 99.9% of light or more.

### Stars and planets

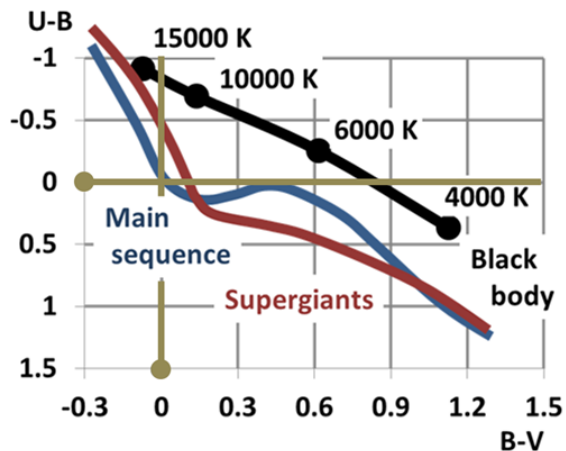
For more about the UBV color index, see Photometric system.

A star or planet often is modeled as a black body, and electromagnetic radiation emitted from these bodies as black-body radiation. The figure shows a highly schematic cross-section to illustrate the idea. The photosphere of the star, where the emitted light is generated, is idealized as a layer within which the photons



An idealized view of the cross-section of a star. The photosphere contains photons of light nearly in thermal equilibrium, and some escape into space as near-black-body radiation.

of light interact with the material in the photosphere and achieve a common temperature  $T$  that is maintained over a long period of time. Some photons escape and are emitted into space, but the energy they carry away is replaced by energy from within the star, so that the temperature of the photosphere is nearly steady. Changes in the core lead to changes in the supply of energy to the photosphere, but such changes are slow on the time scale of interest here. Assuming these circumstances can be realized, the outer layer of the star is somewhat analogous to the example of an enclosure with a small hole in it, with the hole replaced by the limited transmission into space at the outside of the photosphere. With all these assumptions in place, the star emits black-body radiation at the temperature of the photosphere.<sup>[35]</sup>



Effective temperature of a black body compared with the B-V and U-B color index of main sequence and super giant stars in what is called a color-color diagram.<sup>[36]</sup>

Using this model the effective temperature of stars is es-

timated, defined as the temperature of a black body that yields the same surface flux of energy as the star. If a star were a black body, the same effective temperature would result from any region of the spectrum. For example, comparisons in the *B* (blue) or *V* (visible) range lead to the so-called *B-V* color index, which increases the redder the star,<sup>[37]</sup> with the Sun having an index of  $+0.648 \pm 0.006$ .<sup>[38]</sup> Combining the *U* (ultraviolet) and the *B* indices leads to the *U-B* index, which becomes more negative the hotter the star and the more the UV radiation. Assuming the Sun is a type G2 V star, its *U-B* index is  $+0.12$ .<sup>[39]</sup> The two indices for two types of stars are compared in the figure with the effective surface temperature of the stars assuming they are black bodies. It can be seen that there is only a rough correlation. For example, for a given *B-V* index from the blue-visible region of the spectrum., the curves for both types of star lie below the corresponding black-body *U-B* index that includes the ultraviolet spectrum, showing that both types of star emit less ultraviolet light than a black body with the same *B-V* index. It is perhaps surprising that they fit a black body curve as well as they do, considering that stars have greatly different temperatures at different depths.<sup>[40]</sup> For example, the Sun has an effective temperature of 5780 K,<sup>[41]</sup> which can be compared to the temperature of the photosphere of the Sun (the region generating the light), which ranges from about 5000 K at its outer boundary with the chromosphere to about 9500 K at its inner boundary with the convection zone approximately 500 km (310 mi) deep.<sup>[42]</sup>

## Black holes

See also: Hawking radiation

A black hole is a region of spacetime from which nothing escapes. Around a black hole there is a mathematically defined surface called an event horizon that marks the point of no return. It is called “black” because it absorbs all the light that hits the horizon, reflecting nothing, making it almost an ideal black body<sup>[43]</sup> (radiation with a wavelength equal to or larger than the radius of the hole may not be absorbed, so black holes are not perfect black bodies).<sup>[44]</sup> Physicists believe that to an outside observer, black holes have a non-zero temperature and emit radiation with a nearly perfect black-body spectrum, ultimately evaporating.<sup>[45]</sup> The mechanism for this emission is related to vacuum fluctuations in which a virtual pair of particles is separated by the gravity of the hole, one member being sucked into the hole, and the other being emitted.<sup>[46]</sup> The energy distribution of emission is described by Planck’s law with a temperature  $T$ :

$$T = \frac{\hbar c^3}{8\pi G k_B M},$$

where  $c$  is the speed of light,  $\hbar$  is the reduced Planck con-

stant,  $kB$  is Boltzmann’s constant,  $G$  is the gravitational constant and  $M$  is the mass of the black hole.<sup>[47]</sup> These predictions have not yet been tested either observationally or experimentally.<sup>[48]</sup>

## Cosmic microwave background radiation

See also: Big Bang and Cosmic microwave background radiation

The big bang theory is based upon the cosmological principle, which states that on large scales the Universe is homogeneous and isotropic. According to theory, the Universe approximately a second after its formation was a near-ideal black body in thermal equilibrium at a temperature above  $10^{10}$  K. The temperature decreased as the Universe expanded and the matter and radiation in it cooled. The cosmic microwave background radiation observed today is “the most perfect black body ever measured in nature”.<sup>[49]</sup> It has a nearly ideal Planck spectrum at a temperature of about 2.7 K. It departs from the perfect isotropy of true black-body radiation by an observed anisotropy that varies with angle on the sky only to about one part in 100,000.

## 2.5.4 Radiative cooling

See also: Radiative cooling and Radiosity (heat transfer)

The integration of Planck’s law over all frequencies provides the total energy per unit of time per unit of surface area radiated by a black body maintained at a temperature  $T$ , and is known as the Stefan–Boltzmann law:

$$P/A = \sigma T^4,$$

where  $\sigma$  is the Stefan–Boltzmann constant,  $\sigma \approx 5.67 \times 10^{-8} \text{ W}/(\text{m}^2\text{K}^4)$ .<sup>[50]</sup> To remain in thermal equilibrium at constant temperature  $T$ , the black body must absorb or internally generate this amount of power  $P$  over the given area  $A$ .

The cooling of a body due to thermal radiation is often approximated using the Stefan–Boltzmann law supplemented with a “gray body” emissivity  $\epsilon \leq 1$  ( $P/A = \epsilon\sigma T^4$ ). The rate of decrease of the temperature of the emitting body can be estimated from the power radiated and the body’s heat capacity.<sup>[51]</sup> This approach is a simplification that ignores details of the mechanisms behind heat redistribution (which may include changing composition, phase transitions or restructuring of the body) that occur within the body while it cools, and assumes that at each moment in time the body is characterized by a single temperature. It also ignores other possible complications, such as changes in the emissivity with temperature,<sup>[52][53]</sup>

and the role of other accompanying forms of energy emission, for example, emission of particles like neutrinos.<sup>[54]</sup>

If a hot emitting body is assumed to follow the Stefan-Boltzmann law and its power emission  $P$  and temperature  $T$  are known, this law can be used to estimate the dimensions of the emitting object, because the total emitted power is proportional to the area of the emitting surface. In this way it was found that X-ray bursts observed by astronomers originated in neutron stars with a radius of about 10 km, rather than black holes as originally conjectured.<sup>[55]</sup> It should be noted that an accurate estimate of size requires some knowledge of the emissivity, particularly its spectral and angular dependence.<sup>[56]</sup>

## 2.5.5 See also

- Kirchhoff's law of thermal radiation
- Vantablack, a substance produced in 2014 and the blackest known
- Planckian locus, black body incandescence in a given chromaticity space

## 2.5.6 References

### Citations

- [1] Planck 1914, pp. 9–10
- [2] Mahmoud Massoud (2005). "§2.1 Blackbody radiation". *Engineering thermofluids: thermodynamics, fluid mechanics, and heat transfer*. Springer. p. 568. ISBN 3-540-22292-8.
- [3] The approach to thermal equilibrium of the radiation in the cavity can be catalyzed by adding a small piece of matter capable of radiating and absorbing at all frequencies. See Peter Theodore Landsberg. *Thermodynamics and statistical mechanics* (Reprint of Oxford University Press 1978 ed.). Courier Dover Publications. p. 209. ISBN 0-486-66493-7.
- [4] Planck 1914, p. 44, §52
- [5] The emissivity of a surface in principle depends upon frequency, angle of view, and temperature. However, by definition, the radiation from a *gray body* is simply proportional to that of a black body at the same temperature, so its emissivity does not depend upon frequency (or, equivalently, wavelength). See Massoud Kaviany (2002). "Figure 4.3(b): Behaviors of a gray (no wavelength dependence), diffuse (no directional dependence) and opaque (no transmission) surface". *Principles of heat transfer*. Wiley-IEEE. p. 381. ISBN 0-471-43463-9. and Ronald G. Driggers (2003). *Encyclopedia of optical engineering, Volume 3*. CRC Press. p. 2303. ISBN 0-8247-4252-4.
- [6] Some authors describe sources of infrared radiation with emissivity greater than approximately 0.99 as a black body. See "What is a Blackbody and Infrared Radiation?". *Education/Reference tab*. Electro Optical Industries, Inc. 2008.
- [7] Ai Lin Chun (25 Jan 2008). "Carbon nanotubes: Blacker than black". *Nature Nanotechnology*. doi:10.1038/nnano.2008.29.
- [8] Translated by F. Guthrie from *Annalen der Physik*: **109**, 275-301 (1860); G. Kirchhoff (July 1860). "On the relation between the radiating and absorbing powers of different bodies for light and heat". *The London, Edinburgh and Dublin philosophical magazine and journal of science*. Taylor & Francis. **20** (130).
- [9] The notion of an infinitely thin layer was dropped by Planck. See Planck 1914, p. 10, footnote 2, .
- [10] Siegel, Robert; Howell, John R. (2002). *Thermal Radiation Heat Transfer; Volume 1* (4th ed.). Taylor & Francis. p. 7. ISBN 1-56032-839-8.
- [11] Corrections to the spectrum do arise related to boundary conditions at the walls, curvature, and topology, particularly for wavelengths comparable to the cavity dimensions; see Roger Dale Van Zee; J. Patrick Looney (2002). *Cavity-enhanced spectroscopies*. Academic Press. p. 202. ISBN 0-12-475987-4.
- [12] Clement John Adkins (1983). "§4.1 The function of the second law". *Equilibrium thermodynamics* (3rd ed.). Cambridge University Press. p. 50. ISBN 0-521-27456-7.
- [13] In simple cases the approach to equilibrium is governed by a relaxation time. In others, the system may 'hang up' in a metastable state, as stated by Adkins (1983) on page 10. For another example, see Michel Le Bellac; Fabrice Mortessagne; Ghassan George Batrouni (2004). *Equilibrium and non-equilibrium statistical thermodynamics*. Cambridge University Press. p. 8. ISBN 0521821436.
- [14] Loudon 2000, Chapter 1
- [15] Mandel & Wolf 1995, Chapter 13
- [16] Robert Karplus\* and Maurice Neuman , "The Scattering of Light by Light", Phys. Rev. 83, 776–784 (1951)
- [17] Ludwig Bergmann; Clemens Schaefer; Heinz Niedrig (1999). *Optics of waves and particles*. Walter de Gruyter. p. 595. ISBN 3-11-014318-6. Because the interaction of the photons with each other is negligible, a small amount of matter is necessary to establish thermodynamic equilibrium of heat radiation.
- [18] The fundamental bosons are the photon, the vector bosons of the weak interaction, the gluon, and the graviton. See Allan Griffin; D. W. Srolovitz; S. Stringari (1996). *Bose-Einstein condensation*. Cambridge University Press. p. 4. ISBN 0-521-58990-8.
- [19] Richard Chace Tolman (2010). "§103: Change of  $H$  with time as a result of collisions". *The principles of statistical mechanics* (Reprint of 1938 Oxford University Press ed.). Dover Publications. pp. 455 ff. ISBN 0-486-63896-0.

- ...we can define a suitable quantity  $H$  to characterize the condition of a gas which [will exhibit] a tendency to decrease with time as a result of collisions, unless the distribution of the molecules [is already that of] equilibrium. (p. 458)
- [20] Paul A. Tipler (1999). "Relative intensity of reflected and transmitted light". *Physics for Scientists and Engineers, Parts 1-35; Part 39* (4th ed.). Macmillan. p. 1044. ISBN 0-7167-3821-X.
- [21] Massoud Kaviany (2002). "Figure 4.3(b) Radiation properties of an opaque surface". *Principles of heat transfer*. Wiley-IEEE. p. 381. ISBN 0-471-43463-9.
- [22] BA Venkanna (2010). "§10.3.4 Absorptivity, reflectivity, and transmissivity". *Fundamentals of heat and mass transfer*. PHI Learning Pvt. Ltd. pp. 385–386. ISBN 81-203-4031-0.
- [23] Planck 1914, p. 10
- [24] Planck 1914, pp. 9–10, §10
- [25] Kirchhoff 1860c
- [26] Lummer & Kurlbaum 1898
- [27] An extensive historical discussion is found in Jagdish Mehra; Helmut Rechenberg (2000). *The historical development of quantum theory*. Springer. pp. 39 ff. ISBN 0-387-95174-1.
- [28] Kangro 1976, p. 159
- [29] Lummer & Kurlbaum 1901
- [30] CF Lewis (June 1988). "Materials keep a low profile" (PDF). *Mech. Eng.*: 37–41.
- [31] Bradley Quinn (2010). *Textile Futures*. Berg. p. 68. ISBN 1-84520-807-2.
- [32] K. Mizuno; et al. (2009). "A black body absorber from vertically aligned single-walled carbon nanotubes". *Proceedings of the National Academy of Sciences*. **106** (15): 6044–6077. Bibcode:2009PNAS..106.6044M. PMC 2669394. PMID 19339498. doi:10.1073/pnas.0900155106.
- [33] Zu-Po Yang; et al. (2008). "Experimental observation of an extremely dark material made by a low-density nanotube array". *Nano Letters*. American Chemical Society. **8**: 446–451. Bibcode:2008NanoL...8..446Y. PMID 18181658. doi:10.1021/nl072369t.
- [34] See description of work by Richard Brown and his colleagues at the UK's National Physical Laboratory: Mick Hamer (correspondent) (6 February 2003). "Mini craters key to 'blackest ever black'". *New Scientist Magazine online*.
- [35] Simon F. Green; Mark H. Jones; S. Jocelyn Burnell (2004). *An introduction to the sun and stars*. Cambridge University Press. pp. 21–22, 53. ISBN 0-521-54622-2. A source in which photons are much more likely to interact with the material within the source than to escape is a condition for the formation of a black-body spectrum
- [36] Figure modeled after E. Böhm-Vitense (1989). "Figure 4.9". *Introduction to Stellar Astrophysics: Basic stellar observations and data*. Cambridge University Press. p. 26. ISBN 0-521-34869-2.
- [37] David H. Kelley; Eugene F. Milone; Anthony F. (FRW) Aveni (2011). *Exploring Ancient Skies: A Survey of Ancient and Cultural Astronomy* (2nd ed.). Springer. p. 52. ISBN 1-4419-7623-X.
- [38] David F Gray (February 1995). "Comparing the sun with other stars along the temperature coordinate". *Publications of the Astronomical Society of the Pacific*. **107**: 120–123. Bibcode:1995PASP..107..120G. doi:10.1086/133525. Retrieved 2012-01-26.
- [39] M Golay (1974). "Table IX: U-B Indices". *Introduction to astronomical photometry*. Springer. p. 82. ISBN 90-277-0428-7.
- [40] Lawrence Hugh Aller (1991). *Atoms, stars, and nebulae* (3rd ed.). Cambridge University Press. p. 61. ISBN 0-521-31040-7.
- [41] Kenneth R. Lang (2006). *Astrophysical formulae, Volume I* (3rd ed.). Birkhäuser. p. 23. ISBN 3-540-29692-1.
- [42] B. Bertotti; Paolo Farinella; David Vokrouhlický (2003). "Figure 9.2: The temperature profile in the solar atmosphere". *New Views of the Solar System*. Springer. p. 248. ISBN 1-4020-1428-7.
- [43] Schutz, Bernard (2004). *Gravity From the Group Up: An Introductory Guide to Gravity and General Relativity* (1st ed.). Cambridge University Press. p. 304. ISBN 0-521-45506-5.
- [44] PCW Davies (1978). "Thermodynamics of black holes" (PDF). *Rep Prog Phys.* **41** (8): 1313 ff. Bibcode:1978RPPh...41.1313D. doi:10.1088/0034-4885/41/8/004.
- [45] Robert M Wald (2005). "The thermodynamics of black holes". In Andrés Gomberoff; Donald Marolf. *Lectures on quantum gravity*. Springer. pp. 1 ff. ISBN 0-387-23995-2.
- [46] Bernard J Carr & Steven B Giddings (2008). "Chapter 6: Quantum black holes". *Beyond Extreme Physics: Cutting-edge science*. Rosen Publishing Group, Scientific American (COR). p. 30. ISBN 1-4042-1402-X.
- [47] Valeri P. Frolov; Andrei Zelnikov (2011). "Equation 9.7.1". *Introduction to Black Hole Physics*. Oxford University Press. p. 321. ISBN 0-19-969229-7.
- [48] Robert M Wald. "The thermodynamics of black holes". *cited work*. p. 28. ISBN 0-387-23995-2. ... no results on black hole thermodynamics have been subject to any experimental or observational tests, ...
- [49] White, M. (1999). "Anisotropies in the CMB" (PDF). *Proceedings of the Los Angeles Meeting, DPF 99*. UCLA. See also arXive.org.
- [50] "Stefan–Boltzmann constant". *NIST reference on constants, units, and uncertainty*. Retrieved 2012-02-02.

- [51] A simple example is provided by Srivastava M. K. (2011). “Cooling by radiation”. *The Person Guide to Objective Physics for the IIT-JEE*. Pearson Education India. p. 610. ISBN 81-317-5513-4.
- [52] M Vollmer; K-P Möllmann (2011). “Figure 1.38: Some examples for temperature dependence of emissivity for different materials”. *Infrared Thermal Imaging: Fundamentals, Research and Applications*. John Wiley & Sons. p. 45. ISBN 3-527-63087-2.
- [53] Robert Osiander; M. Ann Garrison Darrin; John Champion (2006). *MEMS and Microstructures in aerospace applications*. CRC Press. p. 187. ISBN 0-8247-2637-5.
- [54] Neutrino emission is a mechanism of cooling in neutron stars, for example; see Mikhail A. Shifman (2001). “Cooling by neutrino emission”. In B. L. Ioffe; Mikhail A. Shifman. World Scientific. p. 2135. ISBN 981-02-4969-1 [https://books.google.com/books?id=2yhBnW\\_CtLIC&pg=PA2135](https://books.google.com/books?id=2yhBnW_CtLIC&pg=PA2135). Missing or empty title= (help)
- [55] Walter Lewin; Warren Goldstein (2011). “X-ray bursters!”. *For the love of physics*. Simon and Schuster. pp. 251 ff. ISBN 1-4391-0827-7.
- [56] TE Strohmayer (2006). “Neutron star structure and fundamental physics”. In John W. Mason. *Astrophysics update, Volume 2*. Birkhäuser. p. 41. ISBN 3-540-30312-X.
- Kirchhoff, G. (1860c). “Ueber das Verhältniss zwischen dem Emissionsvermögen und dem Absorptionsvermögen der Körper für Wärme und Licht”. *Annalen der Physik und Chemie*. **109**: 275–301. Bibcode:1860AnP...185..275K. doi:10.1002/andp.18601850205. Translated by Guthrie, F. as Kirchhoff, G. (1860). “On the relation between the radiating and absorbing powers of different bodies for light and heat”. *Philosophical Magazine*. Series 4, volume 20: 1–21.
  - Kirchhoff, G. (1882) [1862], “Ueber das Verhältniss zwischen dem Emissionsvermögen und dem Absorptionsvermögen der Körper für Wärme und Licht”, *Gessamte Abhandlungen*, Leipzig: Johann Ambrosius Barth, pp. 571–598
  - Kondepudi, D.; Prigogine, I. (1998). *Modern Thermodynamics. From Heat Engines to Dissipative Structures*. John Wiley & Sons. ISBN 0-471-97393-9.
  - Krugh, H. (1999). *Quantum Generations: a History of Physics in the Twentieth Century*. Princeton University Press. ISBN 0-691-01206-7.
  - Kuhn, T. S. (1978). *Black-Body Theory and the Quantum Discontinuity*. Oxford University Press. ISBN 0-19-502383-8.
  - Loudon, R. (2000) [1973]. *The Quantum Theory of Light* (third ed.). Cambridge University Press. ISBN 0-19-850177-3.
  - Lummer, O.; Kurlbaum, F. (1898). “Der elektrisch geglühte ‘absolut schwarze’ Körper und seine Temperaturmessung”. *Verhandlungen der Deutschen Physikalischen Gesellschaft*. **17**: 106–111.
  - Lummer, O.; Kurlbaum, F. (1901). “Der elektrisch geglühte ‘schwarze’ Körper”. *Annalen der Physik*. **310** (8): 829–836. Bibcode:1901AnP...310..829L. doi:10.1002/andp.19013100809.
  - Mandel, L.; Wolf, E. (1995). *Optical Coherence and Quantum Optics*. Cambridge University Press. ISBN 0-521-41711-2.
  - Mehra, J.; Rechenberg, H. (1982). *The Historical Development of Quantum Theory*. volume 1, part 1. Springer-Verlag. ISBN 0-387-90642-8.
  - Mihalas, D.; Weibel-Mihalas, B. (1984). *Foundations of Radiation Hydrodynamics*. Oxford University Press. ISBN 0-19-503437-6.
  - Milne, E.A. (1930). “Thermodynamics of the Stars”. *Handbuch der Astrophysik*. 3, part 1: 63–255.
  - Planck, M. (1914). *The Theory of Heat Radiation* (PDF). Masius, M. (transl.) (2nd ed.). P. Blakiston’s Son & Co. OL 7154661M.

## Bibliography

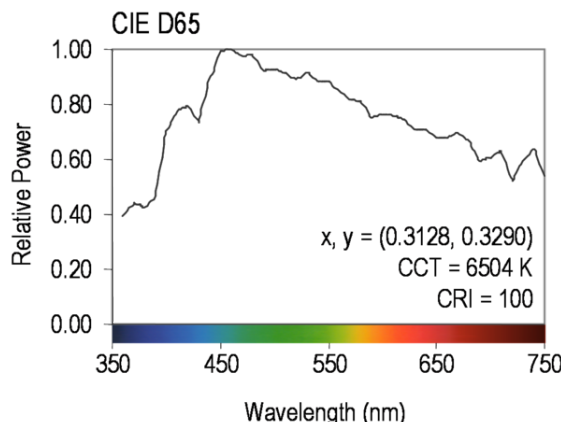
- Chandrasekhar, S. (1950). *Radiative Transfer*. Oxford University Press.
- Goody, R. M.; Yung, Y. L. (1989). *Atmospheric Radiation: Theoretical Basis* (2nd ed.). Oxford University Press. ISBN 978-0-19-510291-8.
- Hermann, A. (1971). *The Genesis of Quantum Theory*. Nash, C.W. (transl.). MIT Press. ISBN 0-262-08047-8. a translation of *Friihgeschichte der Quantentheorie (1899–1913)*, Physik Verlag, Mosbach/Baden.
- Kangro, H. (1976). *Early History of Planck’s Radiation Law*. Taylor and Francis. ISBN 0-85066-063-7.
- Kirchhoff, G.; [27 October 1859] (1860a). “Über die Fraunhofer’schen Linien”. *Monatsberichte der Königlich Preussischen Akademie der Wissenschaften zu Berlin*: 662–665.
- Kirchhoff, G.; [11 December 1859] (1860b). “Über den Zusammenhang zwischen Emission und Absorption von Licht und Wärme”. *Monatsberichte der Königlich Preussischen Akademie der Wissenschaften zu Berlin*: 783–787.

- Rybicki, G. B.; Lightman, A. P. (1979). *Radiative Processes in Astrophysics*. John Wiley & Sons. ISBN 0-471-82759-2.
- Schirrmacher, A. (2001). *Experimenting theory: the proofs of Kirchhoff's radiation law before and after Planck*. Münchner Zentrum für Wissenschafts und Technikgeschichte.
- Stewart, B. (1858). "An account of some experiments on radiant heat". *Transactions of the Royal Society of Edinburgh*. 22: 1–20.

### 2.5.7 External links

- Keesey, Lori J. (Dec 12, 2010). "Blacker than black". NASA. Engineers now developing a blacker-than pitch material that will help scientists gather hard-to-obtain scientific measurements... nanotech-based material now being developed by a team of 10 technologists at the NASA Goddard Space Flight Center

## 2.6 Illuminant D65



*Spectral power distribution of D65.*

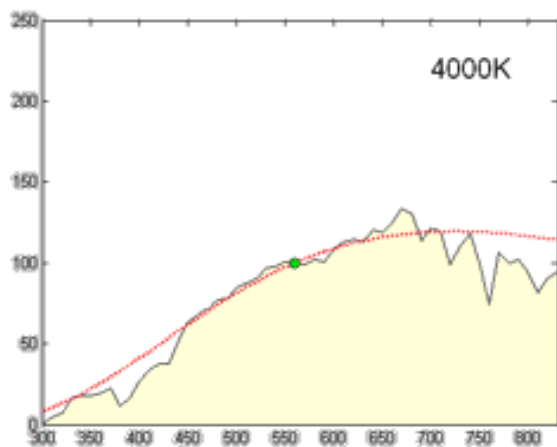
**CIE Standard Illuminant D65** (sometimes written **D<sub>65</sub>**<sup>[1][2]</sup>) is a commonly used standard illuminant defined by the International Commission on Illumination (CIE).<sup>[3]</sup> It is part of the **D** series of illuminants that try to portray standard illumination conditions at open-air in different parts of the world.

D65 corresponds roughly to the average midday light in **Western Europe / Northern Europe** (comprising both direct sunlight and the light diffused by a clear sky), hence it is also called a **daylight** illuminant. As any standard illuminant is represented as a table of averaged **spectrophotometric** data, any light source which statistically has the same relative **spectral power distribution** (SPD) can be considered a D65 light source. There are no actual D65 light sources, only simulators. The quality

of a simulator can be assessed with the **CIE Metamerism Index**.<sup>[4][5]</sup>

The CIE positions D65 as the standard daylight illuminant:

[D65] is intended to represent average daylight and has a correlated colour temperature of approximately 6500 K. CIE standard illuminant D65 should be used in all colorimetric calculations requiring representative daylight, unless there are specific reasons for using a different illuminant. Variations in the relative spectral power distribution of daylight are known to occur, particularly in the ultraviolet spectral region, as a function of season, time of day, and geographic location.  
— ISO 10526:1999/CIE S005/E-1998, **CIE Standard Illuminants for Colorimetry**



*Relative spectral power distribution of illuminant D and a black body of the same correlated color temperature, normalized about 560nm.*

### 2.6.1 History

For more details on this topic, see **Standard illuminant § Illuminant series D**.

The CIE introduced three standard illuminants in 1931:

- A: Incandescent bulb simulator
- B: Daylight simulator (direct)
- C: Daylight simulator (shade)

B and C were derived from A by using liquid filters. The approximation to real light this provided was found lacking, so in 1967 the CIE accepted a proposal by Judd, MacAdam, and Wyszecki for a new series of daylight simulators, bearing the initial D.<sup>[6][7][8]</sup>

## 2.6.2 Definition

D65 is a tabulated SPD in increments of 5 nm from 300 nm to 830 nm, using linear interpolation on the original data binned at 10 nm.<sup>[9][10]</sup> The CIE recommends using linear interpolation of the component SPDs,  $S_0$ ,  $S_1$ , and  $S_2$  if the application requires greater precision, but there is a proposal to use spline interpolation instead.<sup>[11]</sup>

The CIE 1931 color space chromaticity coordinates of D65 are

$$x = 0.31271,$$

$$y = 0.32902$$

using the standard  $2^\circ$  observer.

Normalizing for relative luminance (i.e. set  $Y = 100$ ), the XYZ tristimulus values are

$$X = 95.047,$$

$$Y = 100.00,$$

$$Z = 108.883$$

For the supplementary  $10^\circ$  observer,

$$x = 0.31382,$$

$$y = 0.33100$$

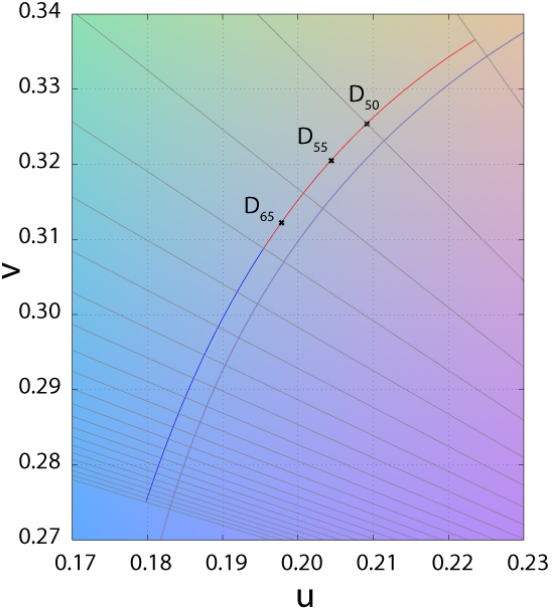
Since D65 represents white light, its co-ordinates are also a white point, corresponding to a correlated color temperature of 6504 K. Rec. 709, used in HDTV systems, truncates the CIE 1931 coordinates to  $x=0.3127$ ,  $y=0.329$ .

## 2.6.3 Why 6504 K?

The name D<sub>65</sub> suggests that the correlated color temperature (CCT) should be 6500 K, while in truth it is closer to 6504 K. This discrepancy is due to the scientific community's revision of the constants in Planck's law after the definition of the illuminant.<sup>[3]</sup> This shifted the Planckian locus, affecting all CCTs, which are calculated by finding the nearest point on the locus to the white point. The same discrepancy applies to all standard illuminants in the D series—D<sub>50</sub>, D<sub>55</sub>, D<sub>65</sub>, D<sub>75</sub>—and can be “rectified” by multiplying the nominal color temperature by  $\frac{1.4388}{1.438}$ ; for example  $6500\text{ K} \times \frac{1.4388}{1.438} = 6503.6\text{ K}$  for D<sub>65</sub>.

## 2.6.4 References

- [1] Noboru, Ohta; Robertson, Alan R. (2005). “3.9: Standard and Supplementary Illuminants”. *Colorimetry*. Wiley. pp. 92–96. ISBN 0-470-09472-9. doi:10.1002/0470094745.ch3.



*Chromaticity of D<sub>50</sub>, D<sub>55</sub>, and D<sub>65</sub> as points on the daylight locus in the CIE 1960 UCS.*

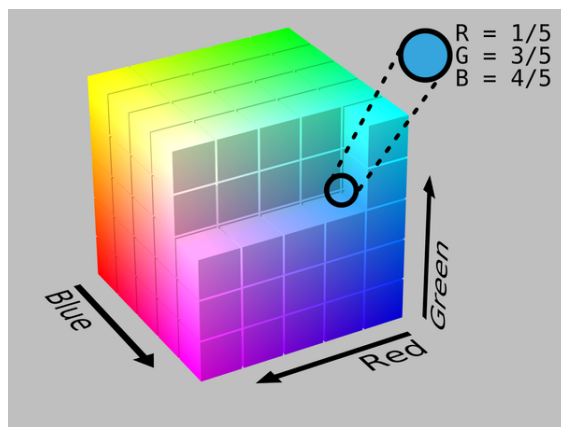
- [2] Poynton, Charles A. (2003). *Digital Video and HDTV: Algorithms and Interfaces*. Morgan Kaufmann. p. 224. ISBN 1-55860-792-7. The CIE D illuminants are properly denoted with a two-digit subscript.
- [3] Schanda, János (2007). “3. CIE Colorimetry”. *Colorimetry: Understanding the CIE System*. Wiley. pp. 43, 44. ISBN 978-0-470-04904-4. doi:10.1002/9780470175637.ch3. In 1967 the International Practical Temperature Scale, 1948, amended 1960 was in use. With that temperature scale c<sub>2</sub> was  $1.438 \times 10^{-2}\text{ m}\cdot\text{K}$ . In 1968, the International Practical Temperature Scale changed the value of c<sub>2</sub> to  $1.4388 \times 10^{-2}\text{ m}\cdot\text{K}$ . Because of this fact the CCT of a daylight phase of T K on the 1948/1960 scale changed to  $1.4388/1.4380 \times T$ , thus D65 with its “nominal CCT” has now a CCT of approximately 6504 K, and this temperature has to be set into the Equations (3.17) and (3.18) to get to the SPD as defined in 1967.
- [4] CIE Technical Report (1999). *A Method for Assessing the Quality of Daylight Simulators for Colorimetry*. Paris: Bureau central de la CIE. ISBN 92-9034-051-7. A method is provided for evaluating the suitability of a test source as a simulator of CIE Standard Illuminants D55, D65, or D75. The Supplement, prepared in 1999, adds the CIE Illuminant D50 to the line of illuminants where the method can be applied to. For each of these standard illuminants, spectral radiance factor data are supplied for five pairs of nonfluorescent samples that are metamerically matched. The colorimetric differences of the five pairs are computed for the test illuminant; the average of these differences is taken as the visible range metamerism index and is used as a measure of the quality of the test illuminant as a simulator for nonfluorescent samples. For fluorescent samples, the quality is further assessed in terms of an ultraviolet range metamerism index, defined as the average of the colorimetric differences computed with the test illu-

- minant for three further pairs of samples, each pair consisting of a fluorescent and a nonfluorescent sample which are metameric under the standard illuminant.
- [5] Lam, Yuk-Ming; Xin, John H. (August 2002). "Evaluation of the quality of different D65 simulators for visual assessment". *Color Research & Application*. **27** (4): 243–251. doi:10.1002/col.10061.
- [6] Judd, Deane B.; MacAdam, David L; Wyszecki, Günter (August 1964). "Spectral Distribution of Typical Daylight as a Function of Correlated Color Temperature" (abstract). *JOSA*. **54** (8): 1031–1040. doi:10.1364/JOSA.54.001031.
- [7] Wyszecki, Günter (February 1968). "Recent Agreements Reached by the Colorimetry Committee of the Commission Internationale de l'Eclairage" (abstract). *JOSA*. **58** (2): 290–292.
- [8] Committee E-1.3.1 (Colorimetry) (June 19–28, 1967). *Proceedings of the 16th session*. Washington, D.C. Paris: CIE.
- [9] CIE. Relative SPD of D65, 300–780nm in 5nm increments.
- [10] Relative SPD of D65, 300–830nm in 1nm increments. Derived by linear interpolation of the 5nm table.
- [11] Kránicz, Balázs; Schanda, János (August 2000). "Re-evaluation of daylight spectral distributions". *Color Research & Application*. **25** (4): 250–259. doi:10.1002/1520-6378(200008)25:4<250::AID-COL5>3.0.CO;2-D. Later the  $S_0(\lambda)$ ,  $S_1(\lambda)$  and  $S_2(\lambda)$  functions have been linearly interpolated at 5 nm steps and for even finer step-size also a linear interpolation has been recommended

## 2.6.5 External links

- Selected colorimetric tables in Excel. CIE.

## 2.7 RGB color space

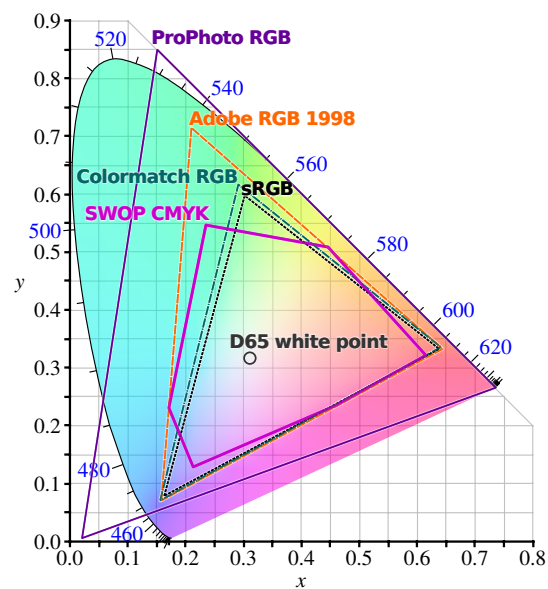


RGB-Cube

An **RGB color space** is any additive color space based on the **RGB color model**.<sup>[1]</sup> A particular RGB color space is defined by the three chromaticities of the red, green, and blue additive primaries, and can produce any chromaticity that is the triangle defined by those primary colors.<sup>[2]</sup> The complete specification of an RGB color space also requires a white point chromaticity and a gamma correction curve. As of 2007, sRGB is by far the most commonly used RGB color space.

**RGB** is an abbreviation for red–green–blue.

### 2.7.1 Intuition



Comparison of some RGB and CMYK colour gamuts on a CIE 1931 xy chromaticity diagram

An RGB color space can be understood by thinking of it as all possible colors that can be made from three colored lights for red, green, and blue. Imagine, for example, shining three lights together onto a white wall in a dark room: one red light, one green light, and one blue light, each with dimmers. If only the red light is on, the wall will be red. If only the green light is on, the wall will look green. If the red and green lights are on together, the wall will look yellow. Dim the red light and the wall will become more of a yellow-green. Dim the green light instead, and the wall will become more orange. Bringing up the blue light a bit will cause the orange to become less saturated and more whitish. In all, each setting of the three dimmers will produce a different result, either in color or in brightness or both. The set of all possible results is the **gamut** defined by those particular color lamps. Swap the red lamp for one of a different brand that is slightly more orange, and there will be a slightly different gamut, since the set of all colors that can be produced with the three lights will be changed.

A computer LCD display can be thought of as a grid of

millions of little red, green, and blue lamps, each with their own dimmers. The gamut of the display will depend on the three colors used for the red, green, and blue lights. A wide-gamut display will have very saturated, “pure” light colors, and thus be able to display very saturated, deep colors.

## 2.7.2 Applications

RGB is a convenient color model for computer graphics because the **human visual system** works in a way that is similar – though not quite identical – to an RGB color space. The most commonly used RGB color spaces are **sRGB** and **Adobe RGB** (which has a significantly larger gamut). Adobe has recently developed another color space called **Adobe Wide Gamut RGB**, which is even larger, in detriment to gamut density.

As of 2007, **sRGB** is by far the most commonly used RGB color space, particularly in consumer grade digital cameras, HD video cameras, and computer monitors. HDTVs use a similar space, commonly called Rec. 709, sharing the sRGB primaries. The sRGB space is considered adequate for most consumer applications. Having all devices use the same color space is convenient in that an image does not need to be converted from one color space to another before being displayed. However, sRGB’s limited gamut leaves out many highly saturated colors that can be produced by printers or in film, and thus is not ideal for some high quality applications. The wider gamut Adobe RGB is being built into more medium-grade digital cameras, and is favored by many professional graphic artists for its larger gamut.

## 2.7.3 Specifications

RGB spaces are generally specified by defining three primary colors and a **white point**. In the table below the three primary colors and white points for various RGB spaces are given. The primary colors are specified in terms of their **CIE 1931 color space** chromaticity coordinates (x,y).

The **CIE 1931 color space** standard defines both the CIE RGB space, which is an RGB color space with monochromatic **primaries**, and the CIE XYZ color space, which works like an RGB color space except that it has non-physical primaries that cannot be said to be red, green, and blue.

## 2.7.4 See also

- **CIE L\*a\*b\*** color space
- **Web colors**
- **RGB color model**
- **RGBA color space**

## 2.7.5 References

- [1] Poynton, Charles A. (2003). *Digital Video and HDTV: Algorithms and Interfaces*. Morgan Kaufmann. ISBN 1-55860-792-7.
- [2] Hunt, R. W. G (2004). *The Reproduction of Colour (6th ed.)*. Chichester UK: Wiley-IS&T Series in Imaging Science and Technology. ISBN 0-470-02425-9.

## 2.7.6 External links

- Pascale, Danny. “A Review of RGB color spaces...from xyY to R’G’B'” (PDF). Retrieved 2008-01-21.
- Sussstrunk, Buckley and Swen. “Standard RGB Color Spaces” (PDF). Retrieved November 18, 2005.
- Lindbloom, Bruce. “RGB Working Space Information”. Retrieved November 18, 2005.
- Colantoni, Philippe. “RGB cube transformation in different color spaces”.

## 2.8 sRGB

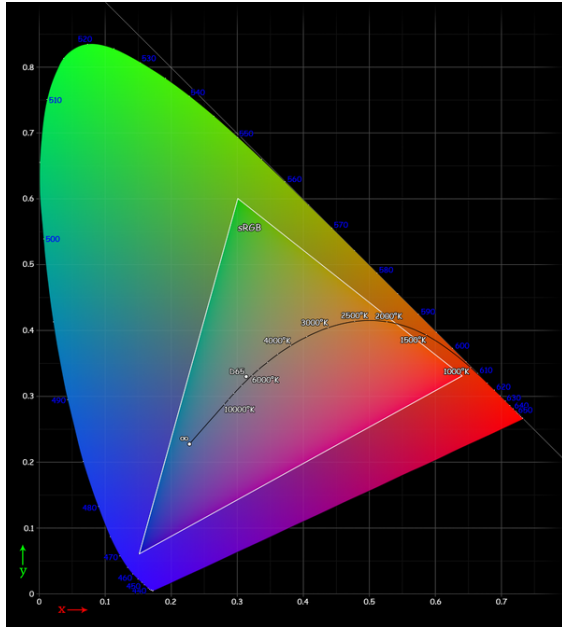
**sRGB** (standard Red Green Blue) is an RGB color space created cooperatively by **HP** and **Microsoft** in 1996 for use on monitors, printers and the **Internet**, and subsequently standardized by the **IEC** as IEC 61966-2-1:1999.<sup>[1]</sup> It is often used as the “default” color space for images that do not contain any color space information, especially if the images are stored as 8-bit integers.

sRGB uses the **ITU-R BT.709** primaries, the same as are used in studio monitors and **HDTV**,<sup>[2]</sup> a transfer function (**gamma curve**) typical of **CRTs**, and a viewing environment designed to match typical home and office viewing conditions. This specification allowed sRGB to be directly displayed on typical CRT monitors of the time, a factor which greatly aided its acceptance.

### 2.8.1 The sRGB gamut

sRGB defines the chromaticities of the red, green, and blue **primaries**, the colors where one of the three channels is nonzero and the other two are zero. The **gamut** of chromaticities that can be represented in sRGB is the **color triangle** defined by these primaries. As with any RGB color space, for non-negative values of R, G, and B it is not possible to represent colors outside this triangle, which is well inside the range of colors visible to a human with normal trichromatic vision.

sRGB is sometimes avoided by high-end print publishing professionals because its color gamut is not big enough,



*CIE 1931 xy chromaticity diagram showing the gamut of the sRGB color space and location of the primaries. The D65 white point is shown in the center. The Planckian locus is shown with color temperatures labeled in kelvins. The outer curved boundary is the spectral (or monochromatic) locus, with wavelengths shown in nanometers (labeled in blue). Note that the colors in this displayed file are being specified using sRGB. Areas outside the triangle cannot be accurately colored because they are out of the gamut of sRGB therefore they have been interpreted. Also note how the D65 label is not an ideal 6500-kelvin blackbody because it is based on atmospheric filtered daylight.*

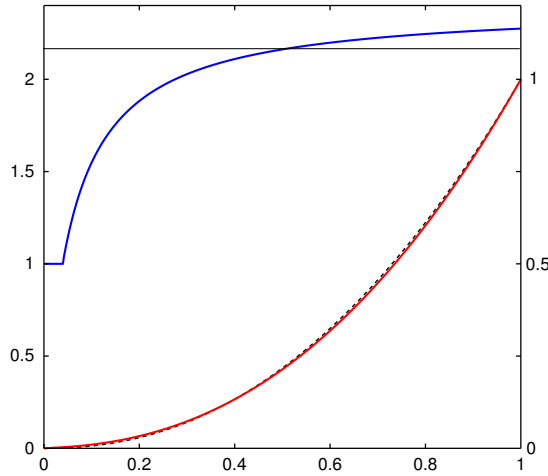
especially in the blue-green colors, to include all the colors that can be reproduced in CMYK printing.

## 2.8.2 The sRGB transfer function (“gamma”)

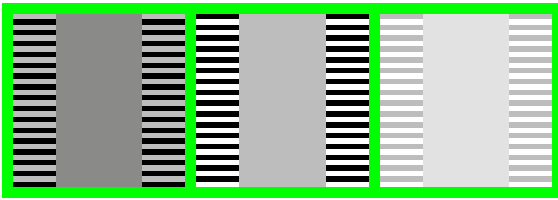
sRGB also defines a nonlinear transformation between the intensity of these primaries and the actual number stored. The curve is similar to the gamma response of a CRT display. This nonlinear conversion means that sRGB is a reasonably efficient use of the values in an integer-based image file to display human-discriminable light levels.

Unlike most other RGB color spaces, the sRGB gamma cannot be expressed as a single numerical value. The overall gamma is approximately 2.2, consisting of a linear (gamma 1.0) section near black, and a non-linear section elsewhere involving a 2.4 exponent and a gamma (slope of log output versus log input) changing from 1.0 through about 2.3. The purpose of the linear section is so the curve does not have an infinite slope at zero, it is not for matching CRT behavior.

## 2.8.3 Specification of the transformation



*Plot of the sRGB intensities versus sRGB numerical values (red), and this function’s slope in log-log space (blue) which is the effective gamma at each point. Below a compressed value of 0.04045 or a linear intensity of 0.00313, the curve is linear so the gamma is 1. Behind the red curve is a dashed black curve showing an exact gamma = 2.2 power law.*



*On an sRGB display, each solid bar should look as bright as the surrounding striped dither. (Note: must be viewed at original, 100% size)*

## The forward transformation (CIE XYZ to sRGB)

The CIE XYZ values must be scaled so that the Y of D65 (“white”) is 1.0 ( $X, Y, Z = 0.9505, 1.0000, 1.0890$ ). This is usually true but some color spaces use 100 or other values (such as in the Lab article).

The first step in the calculation of sRGB from CIE XYZ is a linear transformation, which may be carried out by a matrix multiplication. (The numerical values below match those in the official sRGB specification<sup>[1]</sup> which corrected some small rounding errors in the original publication<sup>[3]</sup> by sRGB’s creators, and assume the 2° standard colorimetric observer for CIE XYZ<sup>[3]</sup>)

$$\begin{bmatrix} R_{\text{linear}} \\ G_{\text{linear}} \\ B_{\text{linear}} \end{bmatrix} = \begin{bmatrix} 3.2406 & -1.5372 & -0.4986 \\ -0.9689 & 1.8758 & 0.0415 \\ 0.0557 & -0.2040 & 1.0570 \end{bmatrix} \begin{bmatrix} X \\ Y \\ Z \end{bmatrix}$$

**It is important to note that these linear RGB values are *not* the final result as they have not been adjusted for the gamma correction.** The following formula transforms the linear values into sRGB:

$$C_{\text{srgb}} = \begin{cases} 12.92C_{\text{linear}}, & C_{\text{linear}} \leq 0.0031308 \\ (1+a)C_{\text{linear}}^{1/2.4} - a, & C_{\text{linear}} > 0.0031308 \end{cases}$$

- where  $a = 0.055$  and where  $C$  is  $R$ ,  $G$ , or  $B$ .

These gamma-corrected values are in the range 0 to 1. If values in the range 0 to 255 are required, e.g. for video display or 8-bit graphics, the usual technique is to multiply by 255 and round to an integer.

The values are usually clipped to the 0 to 1 range. This clipping can be done before or after the gamma calculation, or done as part of converting to 8 bits.

### The reverse transformation

Again the sRGB component values  $R_{\text{srgb}}$ ,  $G_{\text{srgb}}$ ,  $B_{\text{srgb}}$  are in the range 0 to 1. (A range of 0 to 255 can simply be divided by 255.0).

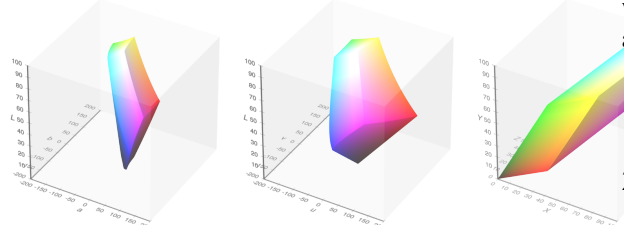
$$C_{\text{linear}} = \begin{cases} \frac{C_{\text{srgb}}}{12.92}, & C_{\text{srgb}} \leq 0.04045 \\ \left(\frac{C_{\text{srgb}}+a}{1+a}\right)^{2.4}, & C_{\text{srgb}} > 0.04045 \end{cases}$$

- where  $a = 0.055$  and where  $C$  is  $R$ ,  $G$ , or  $B$ .

Followed by a matrix multiplication of the linear values to get XYZ:

$$\begin{bmatrix} X \\ Y \\ Z \end{bmatrix} = \begin{bmatrix} 0.4124 & 0.3576 & 0.1805 \\ 0.2126 & 0.7152 & 0.0722 \\ 0.0193 & 0.1192 & 0.9505 \end{bmatrix} \begin{bmatrix} R_{\text{linear}} \\ G_{\text{linear}} \\ B_{\text{linear}} \end{bmatrix}$$

### 2.8.4 Theory of the transformation



sRGB gamut projected into other color spaces. Clockwise from top-left: CIELAB, CIELUV, CIExyY, CIEXYZ.

It is often casually stated that the decoding gamma for sRGB data is 2.2, yet the above transform shows an exponent of 2.4. This is because the net effect of the piecewise decomposition is necessarily a changing instantaneous gamma at each point in the range: it goes from gamma = 1 at zero to a gamma of 2.4 at maximum intensity with a median value being close to 2.2. The transformation was designed to approximate a gamma of about

2.2, but with a linear portion near zero to avoid having an infinite slope at  $K = 0$ , which can cause numerical problems. The continuity condition for the curve  $C_{\text{linear}}$  which is defined above as a piecewise function of  $C_{\text{srgb}}$ , is

$$\left( \frac{K_0 + a}{1 + a} \right)^\gamma = \frac{K_0}{\phi}.$$

Solving with  $\gamma = 2.4$  and the standard value  $\phi = 12.92$  yields two solutions,  $K_0 \approx 0.0381548$  or  $K_0 \approx 0.0404482$ . The IEC 61966-2-1 standard uses the rounded value  $K_0 = 0.04045$ . However, if we impose the condition that the slopes match as well then we must have

$$\gamma \left( \frac{K_0 + a}{1 + a} \right)^{\gamma-1} \left( \frac{1}{1 + a} \right) = \frac{1}{\phi}.$$

We now have two equations. If we take the two unknowns to be  $K_0$  and  $\phi$  then we can solve to give

$$K_0 = \frac{a}{\gamma - 1}, \quad \phi = \frac{(1+a)^\gamma (\gamma - 1)^{\gamma-1}}{(a^{\gamma-1})(\gamma^\gamma)}.$$

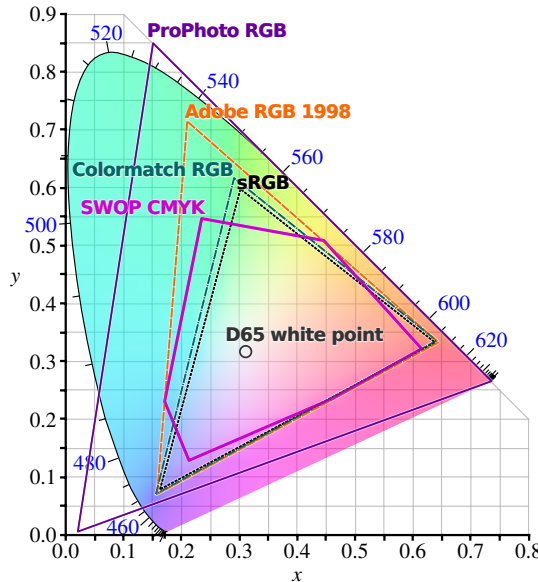
Substituting  $a = 0.055$  and  $\gamma = 2.4$  gives  $K_0 \approx 0.0392857$  and  $\phi \approx 12.9232102$ , with the corresponding linear-domain threshold at  $K_0/\phi \approx 0.00303993$ . These values, rounded to  $K_0 = 0.03928$ ,  $\phi = 12.92321$ , and  $K_0/\phi = 0.00304$ , are sometimes used to describe sRGB conversion.<sup>[4]</sup> Publications by sRGB's creators<sup>[3]</sup> rounded to  $K_0 = 0.03928$  and  $\phi = 12.92$ , resulting in a small discontinuity in the curve. Some authors adopted these values in spite of the discontinuity.<sup>[5]</sup> For the standard, the rounded value  $\phi = 12.92$  was kept and the  $K_0$  value was recomputed to make the resulting curve continuous, as described above, resulting in a slope discontinuity from 12.92 below the intersection to 12.70 above.

### 2.8.5 Viewing environment

The

The sRGB specification assumes a dimly lit encoding (creation) environment with an ambient correlated color temperature (CCT) of 5000 K. It is interesting to note that this differs from the CCT of the illuminant (D65). Using D50 for both would have made the white point of most photographic paper appear excessively blue.<sup>[6]</sup> The other parameters, such as the luminance level, are representative of a typical CRT monitor.

For optimal results, the ICC recommends using the encoding viewing environment (i.e., dim, diffuse lighting) rather than the less-stringent typical viewing environment.<sup>[3]</sup>



*Comparison of some RGB and CMYK colour gamuts on a CIE 1931 xy chromaticity diagram*

## 2.8.6 Usage

Due to the standardization of sRGB on the Internet, on computers, and on printers, many low- to medium-end consumer digital cameras and scanners use sRGB as the default (or only available) working color space. As the sRGB gamut meets or exceeds the gamut of a low-end inkjet printer, an sRGB image is often regarded as satisfactory for home use. However, consumer-level CCDs are typically uncalibrated, meaning that even though the image is being labeled as sRGB, one can't conclude that the image is color-accurate sRGB.

If the color space of an image is unknown and it is an 8- to 16-bit image format, assuming it is in the sRGB color space is a safe choice. This allows a program to identify a color space for all images, which may be much easier and more reliable than trying to track the “unknown” color space. An ICC profile may be used; the ICC distributes three such profiles:<sup>[7]</sup> a profile conforming to version 4 of the ICC specification, which they recommend, and two profiles conforming to version 2, which is still commonly used.

Images intended for professional printing via a fully color-managed workflow, e.g. prepress output, sometimes use another color space such as Adobe RGB (1998), which allows for a wider gamut. If such images are to be used on the Internet they may be converted to sRGB using color management tools that are usually included with software that works in these other color spaces.

The two dominant programming interfaces for 3D graphics, OpenGL and Direct3D, have both incorporated support for the sRGB gamma curve. OpenGL supports textures with sRGB gamma encoded color components (first introduced with EXT\_texture\_sRGB ex-

tension, added to the core in OpenGL 2.1) and rendering into sRGB gamma encoded framebuffers (first introduced with EXT\_FRAMEBUFFER\_SRGB extension, added to the core in OpenGL 3.0). Direct3D supports sRGB gamma textures and rendering into sRGB gamma surfaces starting with DirectX 9. Correct mipmapping and interpolation of sRGB gamma textures has direct hardware support in texturing units of most modern GPUs (for example nVidia GeForce 8 performs conversion from 8-bit texture to linear values before interpolating those values), and does not have any performance penalty.<sup>[8]</sup>

## 2.8.7 See also

- RGB color space
- scRGB

## 2.8.8 References

- [1] “IEC 61966-2-1:1999”. *IEC Webstore*. International Electrotechnical Commission. Retrieved 3 March 2017.
- [2] Charles A. Poynton (2003). *Digital Video and HDTV: Algorithms and Interfaces*. Morgan Kaufmann. ISBN 1-55860-792-7.
- [3] Michael Stokes; Matthew Anderson; Srinivasan Chandrasekar; Ricardo Motta (November 5, 1996). “A Standard Default Color Space for the Internet – sRGB, Version 1.10”.
- [4] Phil Green & Lindsay W. MacDonald (2002). *Colour Engineering: Achieving Device Independent Colour*. John Wiley and Sons. ISBN 0-471-48688-4.
- [5] Jon Y. Hardeberg (2001). *Acquisition and Reproduction of Color Images: Colorimetric and Multispectral Approaches*. Universal-Publishers.com. ISBN 1-58112-135-0.
- [6] Rodney, Andrew (2005). *Color Management for Photographers*. Focal Press. p. 121. ISBN 978-0-240-80649-5. Why Calibrate Monitor to D50 When Light Booth is D50
- [7] sRGB profiles, ICC
- [8] “GPU Gems 3: Chapter 24. The Importance of Being Linear, section 24.4.1”. NVIDIA Corporation. Retrieved 3 March 2017.

## Standards

- IEC 61966-2-1:1999 is the official specification of sRGB. It provides viewing environment, encoding, and colorimetric details.
- Amendment A1:2003 to IEC 61966-2-1:1999 describes an analogous sYCC encoding for YCbCr color spaces, an extended-gamut RGB encoding, and a CIELAB transformation.

- sRGB on [www.color.org](http://www.color.org)
- The fourth working draft of IEC 61966-2-1 is available online, but is not the complete standard. It can be downloaded from [www2.units.it](http://www2.units.it).

## 2.8.9 External links

- International Color Consortium
- Archive copy of <http://www.srgb.com>, now unavailable, containing much information on the design, principles and use of sRGB
- A Standard Default Color Space for the Internet – sRGB at [w3.org](http://w3.org)
- OpenGL extension for sRGB gamma textures at [sgi.com](http://sgi.com)
- Conversion matrices for RGB vs. XYZ conversion
- Will the Real sRGB Profile Please Stand Up?

## 2.9 rg chromaticity

The **rg chromaticity** space, two dimensions of the *normalized RGB* space,<sup>[1]</sup> is a **chromaticity space**, a two-dimensional color space in which there is no intensity information.

In the **RGB** color space a pixel is identified by the intensity of red, green, and blue **primary colors**. Therefore, a bright red can be represented as (R,G,B) (255,0,0), while a dark red may be (40,0,0). In the normalized rg space or rg space, a color is represented by the proportion of red, green, and blue in the color, rather than by the intensity of each. Since these proportions must always add up to a total of 1, we are able to quote just the red and green proportions of the color, and can calculate the blue value if necessary.

### 2.9.1 Conversion between RGB and rg chromaticity

Given a color (R,G,B) where R, G, B = intensity of Red, Green and Blue, this can be converted to color ( $r, g, b$ ) where  $r, g, b$  imply the proportion of red, green and blue in the original color:<sup>[2]</sup>

$$\begin{aligned} r &= \frac{R}{R+G+B} \\ g &= \frac{G}{R+G+B} \\ b &= \frac{B}{R+G+B} \\ r + g + b &= 1 \end{aligned}$$

The sum of  $rgb$  will always equal one, because of this property the  $b$  dimension can be thrown away without causing any loss in information. The reverse conversion is not possible with only two dimensions, as the intensity information is lost during the conversion to rg chromaticity, e.g. (1/3, 1/3, 1/3) has equal proportions of each color, but it is not possible to determine whether this corresponds to dark gray, light gray, or white. If R, G, B, is normalized to r, g, G color space the conversion can be computed by the following:

$$\begin{aligned} R &= \frac{rG}{g} \\ G &= G \\ B &= \frac{(1-r-g)G}{g} \end{aligned}$$

The conversion from rgG to RGB, is the same as the conversion from xyY to XYZ.<sup>[3]</sup> The conversion requires at least some information relative to the intensity of the scene. For this reason if the G is persevered then the inverse is possible.

### 2.9.2 Pixel-Based Photometric Invariance

Although rg chromaticity contains less information than RGB or **HSV** color spaces, it has a number of useful properties for computer vision applications. Notably, where a scene viewed by a camera is not lit evenly – for example if lit by a spotlight – then an object of a given color will change in apparent color as it moves across the scene. Where color is being used to track an object in an RGB image, this can cause problems. The lack of intensity information in rg chromaticity images removes this problem, and the apparent color remains constant. Note that in the case where different parts of the image are lit by different colored light sources, problems can still emerge.

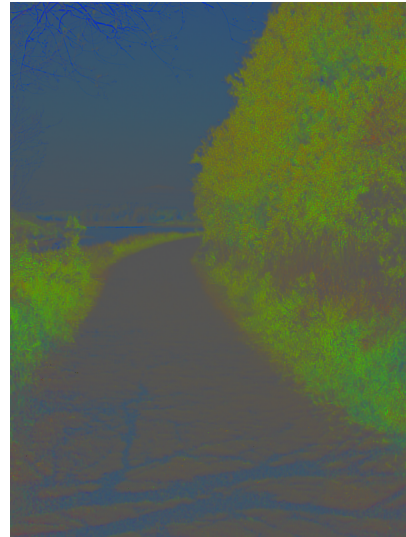
Computer vision algorithms tend to suffer from varying imaging conditions. To make more robust computer vision algorithms it is important to use a color invariant color space. Color invariant color spaces are desensitized to disturbances in the image. One common problem in computer vision is varying light source (color and intensity) between multiple images and within a single image.<sup>[4]</sup> To properly perform image segmentation and object detection requires an increased need for images that are stable to variations in imaging conditions. Normalizing RGB color space to rg color system performs a linear transform. Normalized rg space eliminates the effect of varying intensities from the light source. Uniform surfaces of color with varying geometric features are affected by the angle and intensity of the light source. Where a uniform red surface with a uniform green object placed on top, should easily be segmented. Due to the shape of the 3D object shades are formed preventing uniform fields of color. Normalizing intensity out removes the shadow. A lambertian reflector under a white illumination is defined by the equation below:

$$f^c(x) = m^b(x) \int_{\omega} s(\lambda, x) \rho^c(\lambda) d\lambda$$

When the r,g,b normalized equations are substituted into the equation above the equations below are derived, which define the invariant properties of the rg color system.

$$\begin{aligned} r &= \frac{m^b(x)k_R}{m^b(x)(k_R+k_G+k_B)} = \frac{k_R}{k_R+k_G+k_B} \\ g &= \frac{m^b(x)k_G}{m^b(x)(k_R+k_G+k_B)} = \frac{k_G}{k_R+k_G+k_B} \\ b &= \frac{m^b(x)k_B}{m^b(x)(k_R+k_G+k_B)} = \frac{k_B}{k_R+k_G+k_B} \end{aligned}$$

Where  $k_c = \int_{\omega} s(\lambda, x) \rho^c(\lambda) d\lambda$  and  $c \in \{R, G, B\}$ . The  $m^b(x)$  coefficient which denotes the relationship between the white light source and the surface reflectance. This coefficient is cancelled out, assuming a lambertian reflection and white illumination the rg color space only depends on  $k_c$ . The normalized image is free from shadow and shading effects. The rg color space is dependent on the color of the light source. The color space is only dependent on  $k_c$  which is made up of  $\rho^c(\lambda)$  and  $s(\lambda, x)$ ,  $\rho$  and  $s$  are determined by the sensor and surface of object.



A visual representation of the chromaticity of the image. Each pixel has been scaled so the total red, green, and blue coordinates sum to 1. Notice the effect on the foliage and shadowed regions.



A visual representation of the average value of red, green, and blue coordinates for each pixel in the original image. This information can be combined with the rg chromaticity information to reconstruct the original image.

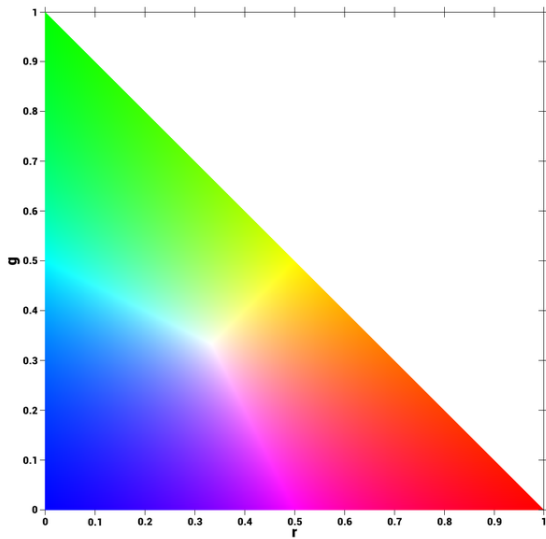
### Illustration



A photograph with varying illumination levels.

### rg color space

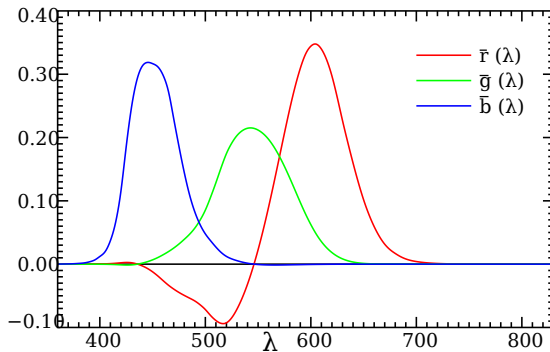
r, g, and b chromaticity coordinates are ratios of the one tristimulus value over the sum of all three tristimulus values. A neutral object infers equal values of red, green and blue stimulus. The lack of luminance information in rg prevents having more than 1 neutral point where all three coordinates are of equal value. The white point of the rg chromaticity diagram is defined by the point (1/3,1/3). The white point has one third red, one third green and the final third blue. On an rg chromaticity diagram the first quadrant where all values of r and g are positive forms a right triangle. With max r equals 1 unit along the x and max g equals 1 unit along the y axis. Connecting a line



Normalized rg Color Space

from the max r (1,0) to max g (0,1) from a straight line with slope of negative 1. Any sample that falls on this line has no blue. Moving along the line from max r to max g, shows a decrease in red and an increase of green in the sample, without blue changing. The further a sample moves from this line the more blue is present in the sample trying to be matched.

### 2.9.3 RGB Color specification System



The CIE 1931 RGB Color matching functions. The color matching functions are the amounts of primaries needed to match the monochromatic test primary at the wavelength shown on the horizontal scale.

RGB is a color mixture system. Once the color matching function are determined the tristimulus values can be determined easily. Since standardization is required to compare results, CIE established standards to determine color matching function.<sup>[5]</sup>

1. The reference stimuli must be monochromatic lights R, G, B. With wavelengths  $\lambda_R = 700.0\text{nm}$ ,  $\lambda_G = 546.1\text{nm}$ ,  $\lambda_B = 435.8\text{nm}$  respectively.

2. The basic stimulus is white with equal energy spectrum. Require a ratio of 1.000:4.5907:0.0601 (RGB) to match white point.

Therefore, a white with equi-energy lights of  $1.000 + 4.5907 + 0.0601 = 5.6508 \text{ lm}$  can be matched by mixing together R, G and B. Guild and Wright used 17 subjects to determine RGB color matching functions.<sup>[6]</sup> RGB color matching serve as the base for rg chromaticity. The RGB color matching functions are used to determine the tristimulus RGB values for a spectrum. Normalizing the RGB tristimulus values converts the tristimulus into rg. Normalized RGB tristimulus value can be plotted on an rg chromaticity diagram.

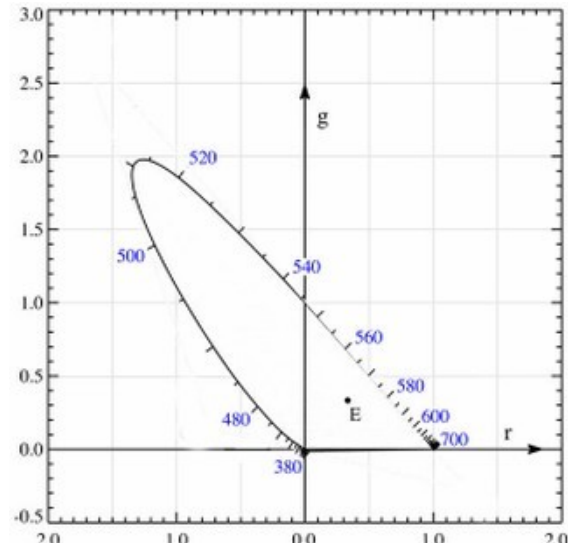
An example of color matching function below.  $[F_\lambda]$  is any monochromatic. Any monochromatic can be matched by adding reference stimuli  $R[R]$ ,  $G[G]$  and  $B[B]$ . The test light is also to bright to account for this reference stimuli is added to the target to dull the saturation. Thus  $R$  is negative.  $[R]$ ,  $[G]$  and  $[B]$  can be defined as a vector in a three-dimensional space. This three-dimensional space is defined as the color space. Any color  $[F]$  can be reached by matching a given amount of  $[R]$ ,  $[G]$  and  $[B]$ .

$$[F_\lambda] + R[R] = G[G] + B[B]$$

$$[F_\lambda] = -R[R] + G[G] + B[B]$$

The negative  $[R]$  calls for color matching functions that are negative at certain wavelengths. This is evidence of why the  $\bar{r}$  color matching function appears to have negative tristimulus values.

### rg Chromaticity Diagram



rg Chromaticity Diagram

The figure to the side is a plotted rg chromaticity diagram. Noting the importance of the E which is defined as the

white point where rg are equal and have a value of  $1/3$ . Next notice the straight line from  $(0,1)$  to  $(1,0)$ , follows the expression  $y = -x + 1$ . As the x (red) increases the y (green) decreases by the same amount. Any point on the line represents the limit in rg, and can be defined by a point that has no b information and formed by some combination of r and g. Moving of the linear line towards E represents a decrease in r and g and an increase in b. In computer vision and digital imagery only use the first quadrant because a computer cannot display negative RGB values. The range of RGB is 0-255 for most displays. But when trying to form color matches using real stimuli negative values are needed according to Grassmann's Laws to match all possible colors. This is why the rg chromaticity diagram extends in the negative r direction.

#### 2.9.4 Conversion xyY color system

Avoid negative color coordinate values prompted the change from to rg to xy. Negative coordinates are used in rg space because when making a spectral sample match can be created by adding stimulus to the sample. The color matching functions r, g, and b are negative at certain wavelengths to allow for any monochromatic sample to be matched. This is why in the rg chromaticity diagram the spectral locus extends into the negative r direction and ever so slightly into the negative g direction. On an xy chromaticity diagram the spectral locus if formed by all positive values of x and y.

#### 2.9.5 See also

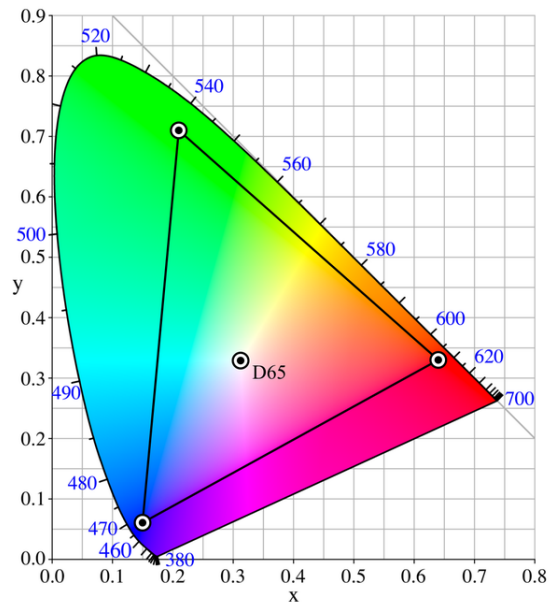
- RG color space
- CIE 1931 color space
- Trichromacy
- Imaginary color
- Grassmann's law
- Chromaticity
- Chrominance
- Image segmentation
- Computer vision

#### 2.9.6 References

- [1] J. B. Martinkuuppi & M. Pietikäinen (2005). "Facial Skin Color Modeling". In S. Z. Li & Anil K. Jain. *Handbook of face recognition*. Springer Science & Business. p. 117. ISBN 978-0-387-40595-7.

- [2] W. T. Wintringham (1951). "Color Television and Colorimetry". In D L. MacAdam. *Selected Papers on Colorimetry Fundamentals*. SPIE - The International Society for Optical Engineering. p. 343. ISBN 0-8194-1296-1.
- [3] Lindloom, Bruce (13 March 2009). "xyY to XYZ". <http://www.brucelindbloom.com/>. Retrieved 7 December 2013. External link in `lwebsite=` (help)
- [4] T. Gevers; A. Gijsenij; J. van de Weijer & J. Geusebroek (2012). "Pixel-Based Photometric Invariance". In M. A. Kriss. *Color in Computer Vision Fundamentals and Applications*. Wiley - IS&T Series. p. 50. ISBN 978-0-470-89084-4.
- [5] N. Ohto & A. R. Robertson (2005). "CIE Standard Colorimetric System". In M. A. Kriss. *Colorimetry Fundamentals and Applications*. Wiley - IS&T Series. p. 65. ISBN 978-0-470-09472-3.
- [6] R. W. G. Hunt (2004). "The Colour Triangle". In M. A. Kriss. *The Reproduction of Colour*. Wiley - IS&T Series. p. 71. ISBN 0-470-02425-9.

#### 2.10 Adobe RGB color space



The CIE 1931 xy chromaticity diagram showing the primaries of the Adobe RGB (1998) color space. The CIE Standard Illuminant D65 white point is shown in the center.

The **Adobe RGB (1998) color space** is an RGB color space developed by Adobe Systems, Inc. in 1998. It was designed to encompass most of the colors achievable on CMYK color printers, but by using RGB primary colors on a device such as a computer display. The Adobe RGB (1998) color space encompasses roughly 50% of the visible colors specified by the CIELAB color space – improving upon the gamut of the sRGB color space, primarily in cyan-green hues.

### 2.10.1 Historical background

Beginning in 1997, Adobe Systems was looking into creating **ICC profiles** that its consumers could use in conjunction with **Photoshop's** new color management features. Since not many applications at the time had any **ICC color management**, most **operating systems** did not ship with useful profiles.

Lead developer of Photoshop, **Thomas Knoll** decided to build an **ICC profile** around specifications he found in the documentation for the **SMPTE 240M** standard, the precursor to **Rec. 709**. SMPTE 240M's gamut was wider than that of the sRGB color space, but not by much. However, with the release of **Photoshop 5.0** nearing, Adobe made the decision to include the profile within the software.

Although users loved the wider range of reproducible colors, those familiar with the SMPTE 240M specifications contacted Adobe, informing the company that it had copied the values that described idealized primaries, not actual standard ones. The real values were much closer to sRGB's, which avid Photoshop consumers did not enjoy as a working environment. To make matters worse, an engineer had made an error when copying the red primary chromaticity coordinates, resulting in an even more inaccurate representation of the SMPTE standard.

Adobe tried numerous tactics to correct the profile, such as correcting the red primary and changing the white point to match that of the **CIE Standard Illuminant D50**, yet all of the adjustments made CMYK conversion worse than before. In the end, Adobe decided to keep the "incorrect" profile, but changed the name to **Adobe RGB (1998)** in order to avoid a trademark search or infringement.<sup>[1]</sup>

### 2.10.2 Specifications

#### Reference viewing conditions

In **Adobe RGB (1998)**, colors are specified as  $[R, G, B]$  triplets, where each of the  $R$ ,  $G$ , and  $B$  components have values ranging between 0 and 1. When displayed on a monitor, the exact **chromaticities** of the reference **white point** [1,1,1], the reference black point [0,0,0], and the primaries ([1,0,0], [0,1,0], and [0,0,1]) are specified. To meet the color appearance requirements of the color space, the **luminance** of the monitor must be 160.00 cd/m<sup>2</sup> at the white point, and 0.5557 cd/m<sup>2</sup> at the black point, which implies a **contrast ratio** of 287.9. Moreover, the black point shall have the same chromaticity as the white point, yet with a luminance equal to 0.34731% of the white point luminance.<sup>[2]</sup> The ambient **illumination** level at the monitor faceplate when the monitor is turned off must be 32 **lx**.

As with sRGB, the **RGB** component values in **Adobe RGB (1998)** are not proportional to the luminances.

Rather, a gamma of 2.2 is assumed, without the linear segment near zero that is present in sRGB. The precise gamma value is 563/256, or 2.19921875. In coverage of the **CIE 1931 color space** the **Adobe RGB (1998)** color space covers 52.1%.<sup>[3]</sup>

The chromaticities of the primary colors and the white point, both of which correspond to the **CIE Standard Illuminant D65**, are as follows:<sup>[2]</sup>

The corresponding absolute **XYZ tristimulus** values for the reference display white and black points are as follows:<sup>[2]</sup>

Normalized **XYZ tristimulus** values can be obtained from absolute luminance  $X_a Y_a Z_a$  tristimulus values as follows:<sup>[2]</sup>

$$X = \frac{X_a - X_K}{X_W - X_K} \frac{X_W}{Y_W}$$

$$Y = \frac{Y_a - Y_K}{Y_W - Y_K}$$

$$Z = \frac{Z_a - Z_K}{Z_W - Z_K} \frac{Z_W}{Y_W}$$

where  $X_K Y_K Z_K$  and  $X_W Y_W Z_W$  are reference display black and white points in the table above.

The conversion between normalized **XYZ** to and from **Adobe RGB tristimulus** values can be done as follows:<sup>[2]</sup>

$$\begin{bmatrix} R \\ G \\ B \end{bmatrix} = \begin{bmatrix} 2.04159 & -0.56501 & -0.34473 \\ -0.96924 & 1.87597 & 0.04156 \\ 0.01344 & -0.11836 & 1.01517 \end{bmatrix} \begin{bmatrix} X \\ Y \\ Z \end{bmatrix}$$

$$\begin{bmatrix} X \\ Y \\ Z \end{bmatrix} = \begin{bmatrix} 0.57667 & 0.18556 & 0.18823 \\ 0.29734 & 0.62736 & 0.07529 \\ 0.02703 & 0.07069 & 0.99134 \end{bmatrix} \begin{bmatrix} R \\ G \\ B \end{bmatrix}$$

#### ICC PCS color image encoding

An image in the **ICC Profile Connection Space (PCS)** is encoded in 24-bit **Adobe RGB (1998)** color image encoding. Through the application of the 3x3 matrix below (derived from the inversion of the color space chromaticity coordinates and a **chromatic adaptation** to **CIE Standard Illuminant D50** using the Bradford transformation matrix), the input image's normalized **XYZ tristimulus** values are transformed into **RGB tristimulus** values. The component values would be **clipped** to the range [0, 1].<sup>[2]</sup>

$$\begin{bmatrix} R \\ G \\ B \end{bmatrix} = \begin{bmatrix} 1.96253 & -0.61068 & -0.34137 \\ -0.97876 & 1.91615 & 0.03342 \\ 0.02869 & -0.14067 & 1.34926 \end{bmatrix} \begin{bmatrix} X \\ Y \\ Z \end{bmatrix}$$

The **RGB tristimulus** values are then converted to **Adobe RGB R'G'B'** component values through the use of the following component transfer functions:

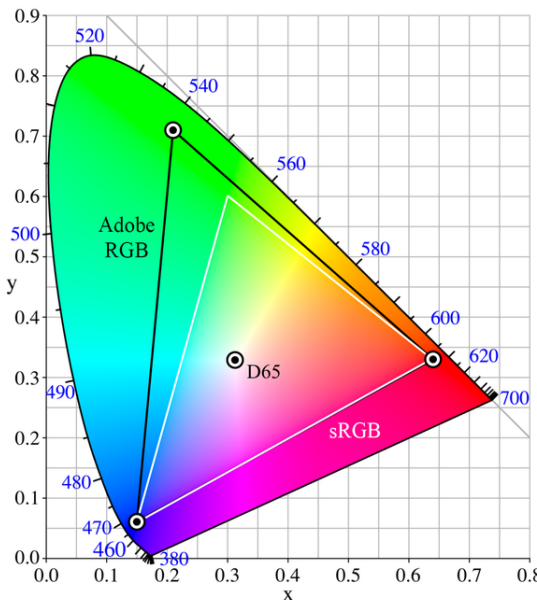
$$R' = R^{\frac{1}{2.19921875}}, G' = G^{\frac{1}{2.19921875}}, B' = B^{\frac{1}{2.19921875}}$$

The resulting component values would be then represented in floating point or integer encodings. If it is necessary to encode values from the PCS back to the input device space, the following matrix can be implemented:

$$\begin{bmatrix} X \\ Y \\ Z \end{bmatrix} = \begin{bmatrix} 0.60974 & 0.20528 & 0.14919 \\ 0.31111 & 0.62567 & 0.06322 \\ 0.01947 & 0.06087 & 0.74457 \end{bmatrix} \begin{bmatrix} R \\ G \\ B \end{bmatrix}$$

### 2.10.3 Comparison to sRGB

#### Gamut



A comparison of the Adobe RGB (1998) color space and sRGB color gamut space within the CIE 1931 xy chromaticity diagram. The sRGB gamut is lacking in cyan-green hues.

sRGB is an RGB color space proposed by HP and Microsoft in 1996 to approximate the color gamut of the most common computer display devices. Since sRGB serves as a “best guess” metric for how another person’s monitor produces color, it has become the standard color space for displaying images on the Internet. sRGB’s color gamut encompasses just 35% of the visible colors specified by CIE, whereas Adobe RGB (1998) encompasses slightly more than 50% of all visible colors. Adobe RGB (1998) extends into richer cyans and greens than does sRGB – for all levels of luminance. The two gamuts are often compared in mid-tone values (~50% luminance), but clear differences are evident in shadows (~25% luminance) and highlights (~75% luminance) as well. In fact, Adobe RGB (1998) expands its advantages to areas of intense orange, yellow, and magenta regions.<sup>[4]</sup>

It should be noted that while there is a significant difference between gamut ranges in the CIE xy chromaticity diagram, if the coordinates were to be transformed to fit on the CIE  $u'$  $v'$  chromaticity diagram, which illustrates the eye’s perceived variance in hue more closely, the difference in the green region is far less exaggerated. Also, although Adobe RGB (1998) can *theoretically* represent a wider gamut of colors, the color space requires special software and a complex workflow in order to utilize its full range. Otherwise, the produced colors would be squeezed into a smaller range (making them appear duller) in order to match sRGB’s more widely used gamut.

#### Bit depth distribution

Although the Adobe RGB (1998) working space clearly provides more colors to utilize, another factor to consider when choosing between color spaces is how each space influences the distribution of the image’s bit depth. Color spaces with larger gamuts “stretch” the bits over a broader region of colors, whereas smaller gamuts concentrate these bits within a narrow region.

A similar, yet not as dramatic concentration of bit depth occurs with Adobe RGB (1998) versus sRGB, except in three dimensions rather than one. The Adobe RGB (1998) color space occupies roughly 40% more volume than the sRGB color space, which concludes that one would only be exploiting 70% of the available bit depth if the colors in Adobe RGB (1998) are unnecessary.<sup>[4]</sup> On the contrary, one may have plenty of “spare” bits if using a 16-bit image, thus negating any reduction due to the choice of working space.

### 2.10.4 See also

- International Electrotechnical Commission (IEC)
- Society for Imaging Science and Technology (IS&T)
- Society for Information Display (SID)

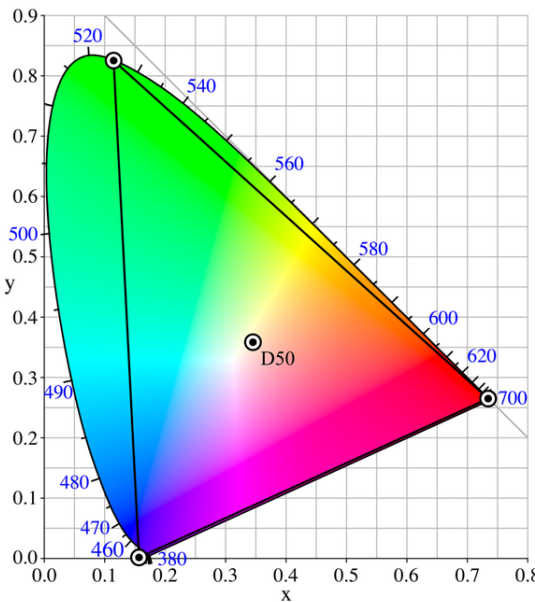
### 2.10.5 References

- [1] “2011 Color and Imaging Conference, Part VI: Special Session”. *Real-Time Rendering*. 21 December 2011.
- [2] *Adobe RGB (1998) Color Image Encoding* (PDF) (Technical report). Adobe Systems Incorporated. 13 May 2005.
- [3] Yamashita, Takayuki; Masuda, Hiroyasu; Masaoka, Kenichiro; Ohmura, Kohei; Emoto, Masaki; Nishida, Yukihiko; Sugawara, Masayuki (November–December 2012). “”Super Hi-Vision” as Next-Generation Television and Its Video Parameters” (PDF). *Information Display*. Society for Information Display. **28** (11 & 12): 12–17.
- [4] “sRGB vs. Adobe RGB 1998”. *Cambridge in Colour*.

## 2.10.6 External links

- *Adobe Magazine* discussion of Photoshop 5.0's new RGB working spaces
- Adobe RGB (1998) Color Image Encoding
- Color Management in Practice – Advantages of the Adobe RGB Color Space
- ICC Adobe RGB (1998) Encoding Characteristics

## 2.11 Wide-gamut RGB color space



*CIE 1931 xy chromaticity diagram showing the gamut of the wide-gamut RGB color space and location of the primaries. The D50 white point is shown in the center.*

The **wide-gamut RGB color space** (or **Adobe Wide Gamut RGB**) is an RGB color space developed by **Adobe Systems**, that offers a large gamut by using pure spectral primary colors.<sup>[1]</sup> It is able to store a wider range of color values than sRGB or Adobe RGB color spaces. As a comparison, the wide-gamut RGB color space encompasses 77.6% of the visible colors specified by the Lab color space, while the standard Adobe RGB color space covers just 52.1%<sup>[2]</sup> and sRGB covers only 35.9%.<sup>[3]</sup>

When working in color spaces with such a large gamut, it is recommended to work in 16-bit per channel color depth to avoid posterization effects. This will occur more frequently in 8-bit per channel modes as the gradient steps are much larger.<sup>[4]</sup>

As with sRGB, the color component values in wide-gamut RGB are not proportional to the luminances. Similar to Adobe RGB, a **gamma** of 2.2 is assumed, without

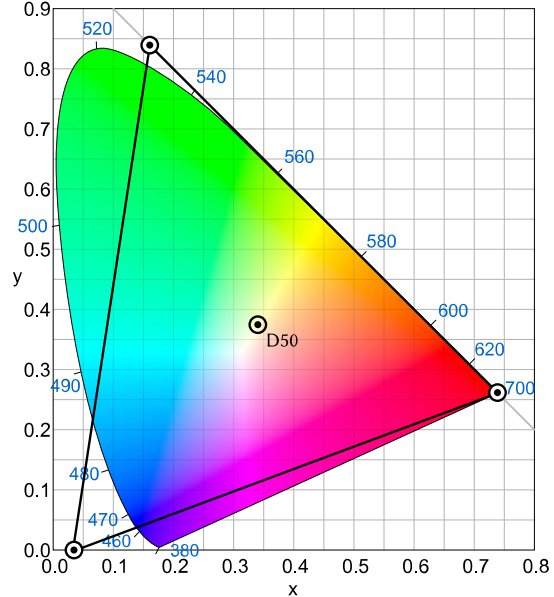
the linear segment near zero that is present in sRGB. The precise gamma value is 563/256, or 2.19921875.

The white point corresponds to D50. The chromaticities of the primary colors and the white point are as follows:

## 2.11.1 References

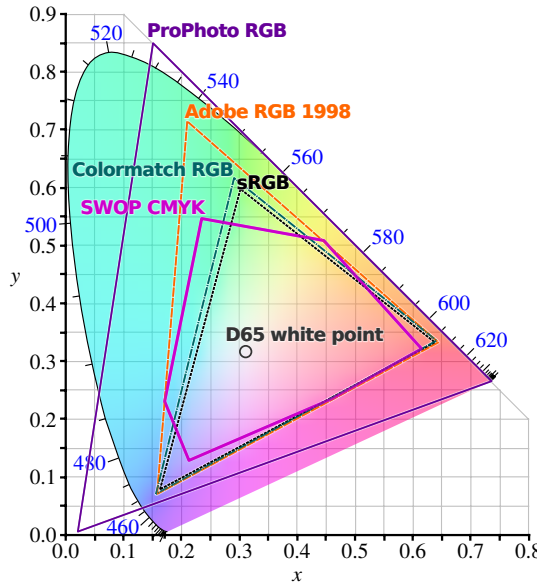
- [1] Pascale, Danny. "A Review of RGB Color Spaces ...from xyY to R'G'B'" (PDF). Retrieved 2010-02-12.
- [2] Adobe RGB color space
- [3] Rec. 709
- [4] Rodney, Andrew. "The role of working spaces in Adobe applications" (PDF). Retrieved 2010-02-12.

## 2.12 ProPhoto RGB color space



*CIE 1931 xy chromaticity diagram showing the chromaticities enclosed by the ProPhoto RGB color space and location of the primaries. The D50 white point is shown in the center. The areas of the triangle that are outside the colored area are imaginary colors.*

The **ProPhoto RGB color space**, also known as **ROMM RGB** (Reference Output Medium Metric), is an output referred RGB color space developed by **Kodak**. It offers an especially large **gamut** designed for use with photographic output in mind. The ProPhoto RGB color space encompasses over 90% of possible surface colors in the CIE L\*a\*b\* color space, and 100% of likely occurring real-world surface colors documented by Pointer in 1980,<sup>[1][2]</sup> making ProPhoto even larger than the **Wide-gamut RGB color space**. The ProPhoto RGB primaries were also chosen in order to minimize hue rotations associated with non-linear tone scale operations. One of the



*Comparison of some RGB and CMYK colour gamuts on a CIE 1931 xy chromaticity diagram*

downsides to this color space is that approximately 13% of the representable colors are **imaginary colors** that do not exist and are not visible colors.

When working in **color spaces** with such a large gamut, it is recommended to work in 16-bit color depth to avoid posterization effects. This will occur more frequently in 8-bit modes as the gradient steps are much larger.

There are two corresponding scene space color encodings known as **RIMM RGB** intended to encode standard dynamic range scene space images, and **ERIMM RGB** intended to encode extended dynamic-range scene space images.

## 2.12.1 Development

The development of ProPhoto RGB and other color spaces is documented in an article<sup>[3]</sup> summarizing a presentation by one of its developers Dr. Geoff Wolfe at Kodak, now Senior Research Manager at Canon Information Systems Research Australia, at the SPIE Color Imaging Conference in 2011.

## 2.12.2 ProPhoto RGB (ROMM RGB) Encoding Primaries

### 2.12.3 Viewing Environment

- Luminance level is in the range of 160–640 cd/m<sup>2</sup>.
- Viewing surround is average.
- There is 0.5–1.0% viewing flare.

- The adaptive white point is specified by the chromaticity values for CIE Standard Illuminant D50 ( $x = 0.3457$ ,  $y = 0.3585$ ).

- The image color values are assumed to be encoded using flareless (or flare corrected) colorimetric measurements based on the CIE 1931 Standard Colorimetric Observer.

## 2.12.4 Encoding Function

$$X'_{\text{ROMM}} = I_{\text{MAX}} \cdot \begin{cases} 0; & X_{\text{ROMM}} < 0.0 \\ 16 \cdot X_{\text{ROMM}}; & 0.0 \leq X_{\text{ROMM}} < E_t \\ X_{\text{ROMM}}^{1/1.8}; & E_t \leq X_{\text{ROMM}} < 1.0 \\ 1; & X_{\text{ROMM}} \geq 1.0 \end{cases}$$

where

$X = R, G, \text{ or } B$

and

$I_{\text{MAX}}$

and

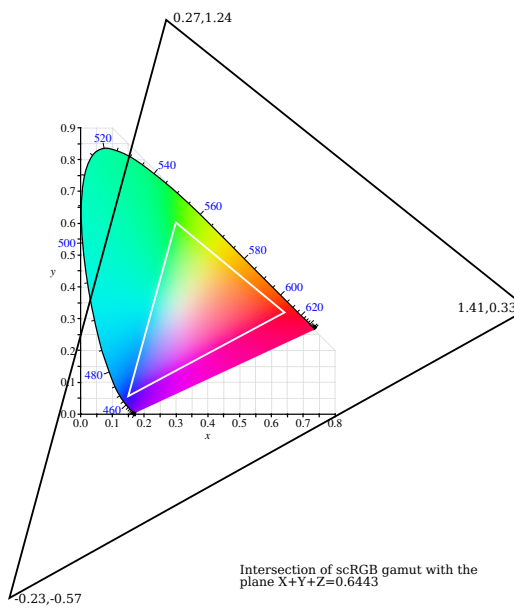
$$E_t = 16^{1.8/(1-1.8)} = 2^{-9} = 1/512 = 0.001953125$$

## 2.12.5 References

- [1] Pointer, M. R. (1980), The Gamut of Real Surface Colours. *Color Res. Appl.*, 5: 145–155. doi: 10.1002/col.5080050308
- [2] [http://www.tftcentral.co.uk/articles/pointers\\_gamut.htm](http://www.tftcentral.co.uk/articles/pointers_gamut.htm)
- [3] <http://www.realtimerendering.com/blog/2011-color-and-imaging-conference-part-vi-special-session/>

## 2.12.6 External links

- Specification of ROMM RGB
- Information page about ROMM RGB including a downloadable ICC format profile.
- Understanding ProPhoto RGB
- Color Spaces: Beyond Adobe RGB
- Why Use the ProPhoto RGB Color Space?



*Intersection of the scRGB gamut with the  $X+Y+Z=.6443$  plane (the gamut varies depending on the intensity as it is a cube with a non-zero origin).*

## 2.13 scRGB

**scRGB** is a wide color gamut RGB (Red Green Blue) color space created by Microsoft and HP that uses the same color primaries and white/black points as the sRGB color space but allows coordinates below zero and greater than one. The full range is  $-0.5$  through just less than  $+7.5$ .

Negative numbers enables scRGB to encompass most of the CIE 1931 color space while maintaining simplicity and backward compatibility with sRGB without the complexity of **color management**. The cost of maintaining compatibility with sRGB is that approximately 80% of the scRGB color space consists of **imaginary colors**.

Large positive numbers allow **high dynamic range** images to be represented, though the range is inferior to that of some other high dynamic range formats such as OpenEXR.<sup>[1]</sup>

### 2.13.1 Encoding

Two encodings are defined for the individual primaries: a linear 16 bit per channel encoding and a nonlinear 12 bit per channel encoding.

The 16 bit **scRGB(16)** encoding is the *linear* RGB channels converted by  $8192x + 4096$ . Compared to 8-bit sRGB this ranges from almost  $2\frac{1}{2}$  times the color resolution near 0.0 to more than 14 times the color resolution near 1.0. Storage as 16 bits clamps the linear range to  $-0.5..7.4999$ .

The 12-bit **scRGB-nl** encoding is the linear RGB chan-

nels passed through the same opto-electric conversion function as sRGB (for negative numbers use  $-f(-x)$ ) and then converted by  $1280x + 1024$ . This is exactly 5 times the color resolution of 8-bit sRGB, and 8-bit sRGB can be converted directly with  $5x + 1024$ . The linear range is clamped to the slightly larger  $-0.6038..7.5913$

A 12-bit encoding called **scYCC-nl** is the conversion of the non-linear sRGB levels to JFIF-Y'CbCr and then converted by  $1280Y' + 1024$  and  $1280C_x + 2048$ . This form can allow greater compression and direct conversion to/from JPEG files and video hardware.

With the addition of an alpha channel with the same number of bits the 16-bit encoding may be seen referred to as 64 bit and the 12-bit encoding referred to as 48-bit. Alpha is not encoded as above, however. Alpha is instead a linear 0-1 range multiplied by  $2^n - 1$  where  $n$  is 12 or 16.

### 2.13.2 Usage

The first implementation of scRGB was the **GDI+** API in Windows Vista. At WinHEC 2008 Microsoft announced that Windows 7 would support 48-bit scRGB (which for HDMI can be converted and output as xvYCC). The components in Windows 7 that support 48-bit scRGB are Direct3D, the Windows Imaging Component, and the Windows Color System and they support it in both full screen exclusive mode and in video overlays.<sup>[2][3]</sup>

### 2.13.3 Origin of sc in scRGB

The origin of the sc in scRGB is shrouded in mystery. Officially it stands for nothing. According to Michael Stokes (the national and international leader of the International Electrotechnical Commission, or IEC, group working on scRGB), the name appeared when the Japanese national committee requested a name change from the earlier XsRGB (excess RGB). The two leading candidates for meaning are “specular RGB” because scRGB supports whites greater than the diffuse 1.0 values, and “standard compositing RGB” because the linearity, floating-point support, HDR (high dynamic range) support, and wide gamut support are ideally suited for compositing. This meaning also implicitly emphasizes that scRGB is not intended to be directly supported in devices or formats, since by definition scRGB encompasses values that are beyond both the human visual system and (even theoretically) realizable physical devices.<sup>[4]</sup>

### 2.13.4 See also

### 2.13.5 References

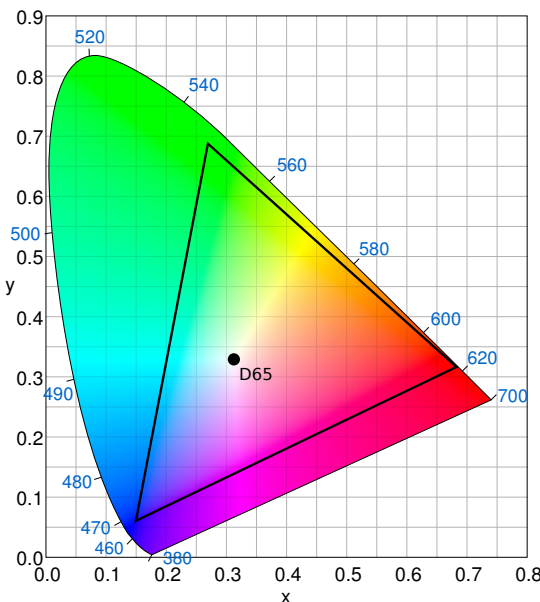
[1] “High Dynamic Range Image Encodings”. Greg Ward. Retrieved 2010-10-25.

- [2] “WinHEC 2008 GRA-583: Display Technologies”. Microsoft. 2008-11-06. Retrieved 2008-12-06.
- [3] “Windows 7 High Color Support”. Softpedia. 2008-11-26. Retrieved 2008-12-06.
- [4] Essential Windows Presentation Foundation (WPF), by Chris Anderson, p.227

## 2.13.6 External links

- The standard IEC 61966-2-2
- Annex B: Non-linear encoding for scRGB : scRGB-nl
- A working draft of IEC 61966-2-2 is available online.
- PCMag.com: Defining scRGB

## 2.14 DCI-P3



The CIE 1931 chromaticity diagram with the spectral colors and purple line along the rim. The corners of the triangle are the primary colors of the DCI-P3 color space. DCI-P3 D65 uses Illuminant D65 for the white point.

**DCI-P3**, or **DCI/P3**, is a common RGB color space for digital movie projection from the US-American film industry.<sup>[1]</sup> In the CIE 1931 xy chromaticity diagram the DCI-P3 color space covers 45.5% of all chromaticities and 86.9% of Pointer's gamut. In the CIE 1976 u'v' chromaticity diagram the coverage is 41.7% and 85.5% respectively.<sup>[2]</sup> The blue primary color is the same as sRGB and Adobe RGB;<sup>[1]</sup> the red primary color is a monochromatic light source and has a wavelength of 615

nm. DCI-P3 was defined by the Digital Cinema Initiatives (DCI) organization and published by the Society of Motion Picture and Television Engineers (SMPTE) in **SMPTE EG 432-1** and **SMPTE RP 431-2**.<sup>[3]</sup> As a step towards the implementation of the significantly wider Rec. 2020 it is expected to see adoption in television systems and in the home cinema domain.<sup>[4]</sup>

### 2.14.1 History

#### 2010-2011

On November 10, 2010, SMPTE published SMPTE EG 432-1:2010.<sup>[5]</sup>

On April 6, 2011, SMPTE published SMPTE RP 431-2:2011.<sup>[6]</sup>

#### 2015-2016

In September 2015, Apple's iMac desktop became the first consumer computer with a built-in wide-gamut display, supporting the P3 color space.

On January 4, 2016, the UHD Alliance announced their specifications for **Ultra HD Premium** which requires devices to display at least 90% of the DCI P3 color space.<sup>[7][8]</sup>

In August 2016, the Phablet Samsung Galaxy Note 7 shipped with an **HDR** display<sup>[9]</sup> with 100% DCI-P3 color gamut.<sup>[10]</sup>

In September 2016, Apple's 9.7-inch iPad Pro shipped with a display supporting P3 color.

In September 2016, Apple's iPhone 7 shipped with a wide-gamut display, supporting P3.<sup>[11]</sup>

In October 2016, Microsoft's Surface Studio desktop computer.

Also in October, Apple's new MacBook Pro notebook computers were released with P3 displays.

#### 2017

In April 2017, Samsung released the Galaxy S8, the first phone to cover 113% of the DCI-P3 Color Gamut, 102% AdobeRGB and 142% of sRGB / Rec.709 Gamuts.<sup>[12]</sup>

### 2.14.2 System colorimetry

DCI-P3 has a 25% larger Color Gamut than sRGB.<sup>[15]</sup>

### 2.14.3 References

- [1] “Color spaces”. Technicolor SA. Retrieved 2016-02-01.
- [2] Kid Jansen (2014-02-19). “The Pointer's Gamut”. tftcentral. Retrieved 2017-01-06.
- [3] The Society of Motion Picture and Television Engineers, 2011, New York: *RP 431-2, D-Cinema Quality – Refer-*

- ence Projector and Environment for the Display of DCDM in Review Rooms and Theaters*
- [4] Geoffrey Morrison (2015-04-12). “Ultra HD 4K TV color, part II: The (near) future”. CNET. Retrieved 2016-02-01.
  - [5] “EG 432-1:2010 - Digital Source Processing — Color Processing for D-Cinema”. Institute of Electrical and Electronics Engineers. 2010-11-10. Retrieved 2016-02-01.
  - [6] “RP 431-2:2011 - D-Cinema Quality — Reference Projector and Environment”. Institute of Electrical and Electronics Engineers. 2011-04-06. Retrieved 2016-02-01.
  - [7] “UHD Alliance Defines Premium Home Entertainment Experience”. Business Wire. 2016-01-04. Retrieved 2016-02-01.
  - [8] Andy Vandervell (2016-01-06). “What is Ultra HD Premium? New HDR standard explained”. TrustedReviews. Time Inc. UK. Retrieved 2016-09-19.
  - [9] “The HDR screen of the Galaxy Note 7 could be the next big thing for phones”. CNET. Retrieved 2017-04-09.
  - [10] “Galaxy Note7 OLED Display Technology Shoot-Out”. [www.displaymate.com](http://www.displaymate.com). Retrieved 2017-04-09.
  - [11] Mike Wuerthele (2016-09-09). “Apple’s Wide Color screen on the iPhone 7 will lead to more faithful color reproduction”. AppleInsider. Retrieved 2016-09-19.
  - [12] Soneira, Raymond. “Galaxy S8 OLED Display Technology Shoot-Out”. *DisplayMate*. Retrieved 4 April 2017.
  - [13] Kid Jansen. “The Pointer’s Gamut”. TFT Central. Retrieved 2016-01-30.
  - [14] Rajan Joshi; Shan Liu; Gary Sullivan; Gerhard Tech; Ye-Kui Wang; Jizheng Xu; Yan Ye (2016-01-31). “HEVC Screen Content Coding Draft Text 5”. JCT-VC. Retrieved 2016-01-31.
  - [15] Dean Jackson (2016-07-01). “Improving Color on the Web”. *WebKit*. Retrieved 2016-09-19.

## 2.15 Rec. 709

**ITU-R Recommendation BT.709**, more commonly known by the abbreviations **Rec. 709** or **BT.709**, standardizes the format of high-definition television, having 16:9 (widescreen) aspect ratio. The first edition of the standard was approved in 1990.

### 2.15.1 Technical details

#### Pixel count

Rec. 709 refers to HDTV systems having roughly two million luma samples per frame. Rec. 709 has two parts:

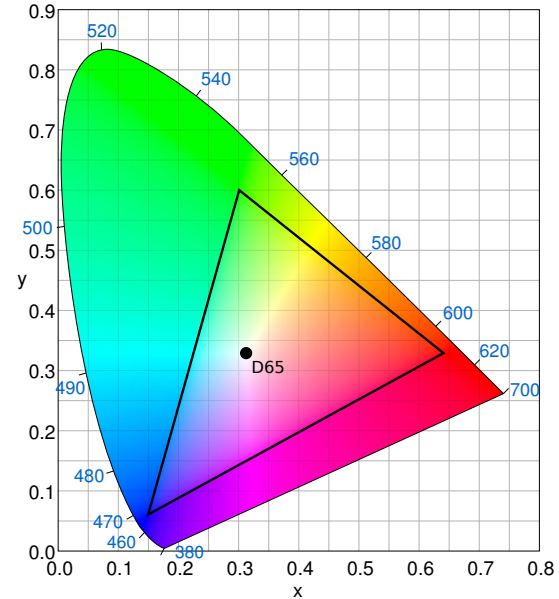


Diagram of the CIE 1931 color space that shows the Rec. 709 (HDTV) color space in the triangle and the location of the primary colors. Rec. 709 uses Illuminant D65 for the white point.

Part 2 codifies current and prospective 1080i and 1080p systems with square sampling. In an attempt to unify 1080-line HDTV standards, part 2 defines a *common image format* (CIF) with picture parameters independent of the picture rate.

Part 1 codifies what are now referred to as 1035i30 and 1152i25 HDTV systems. The 1035i30 system is now obsolete, having been superseded by 1080i and 1080p square-sampled (“square-pixel”) systems. The 1152i25 system was used for experimental equipment in Europe and was never commercially deployed.

#### Frame rate

Rec. 709 specifies the following picture rates: 60 Hz, 50 Hz, 30 Hz, 25 Hz and 24 Hz. “Fractional” rates having the above values divided by 1.001 are also permitted.

Initial acquisition is possible in either progressive or interlaced form. Video captured as progressive can be transported with either progressive transport or *progressive segmented frame* (PsF) transport. Video captured as interlaced can be transported with interlace transport. In cases where a progressive captured image is transported as a segmented frame, segment/field frequency must be twice the frame rate.

In practice, the above requirements result in the following frame rates (“fractional” rates are specified in commonly used “decimal” form): 25i, 25PsF, 25p, 50p for 50 Hz systems; 23.976p, 23.976PsF, 24p, 24PsF, 29.97i, 29.97p, 29.97PsF, 30PsF, 30p, 59.94p, 60p for 60 Hz systems.

## Digital representation

Rec. 709 defines an  $R'G'B'$  encoding and a  $Y'CbCr$  encoding, each with either 8 bits or 10 bits per sample in each color channel. In the 8-bit encoding, the  $R'$ ,  $B'$ ,  $G'$ , and  $Y'$  channels have a nominal range of [16..235], and the  $CB$  and  $CR$  channels have a nominal range of [16..240] with 128 as the neutral value. So in  $R'G'B'$ , reference black is (16, 16, 16) and reference white is (235, 235, 235), and in  $Y'CbCr$ , reference black is (16, 128, 128), and reference white is (235, 128, 128). Values outside the nominal ranges are allowed, but typically they would be clamped for broadcast or for display. Values 0 and 255 are reserved as timing references, and may not contain color data. Rec. 709's 10-bit encoding uses nominal values four times those of the 8-bit encoding. Rec. 709's nominal ranges are the same as those defined in ITU Rec. 601.<sup>[1]</sup>

## Primary chromaticities

Note that red and blue are the same as the EBU Tech 3213 primaries while green is halfway between EBU Tech 3213 and SMPTE C (two types of Rec.601). In coverage of the CIE 1931 color space the Rec. 709 color space (and the derivative sRGB color space) is almost identical to Rec. 601 and covers 35.9%.<sup>[3]</sup>

**Standards Conversion** When converting between the various HD and SD formats, it would be correct to compensate for the differences in the primaries (e.g. between the Rec. 709, EBU Tech 3213, and SMPTE C primaries). In practice, this conversion is rarely performed and such a conversion would create a liability for post production facilities as they would need to ensure that the color bars on all the new masters are redone. Correcting for differences in the primaries would cause the resulting color bars on the converted tape to be inaccurate. Incorrect color bars will cause a (sub)master to be rejected by quality control checks.<sup>[4]</sup>

## Luma coefficients

HDTV according to Rec. 709 forms luma ( $Y'$ ) using  $R'G'B'$  coefficients 0.2126, 0.7152, and 0.0722. This means that unlike Rec. 601, the coefficients match the primaries and white points, so luma corresponds more closely to luminance. Some experts feel that the advantages of correct matrix coefficients do not justify the change from Rec. 601 coefficients.<sup>[5]</sup>

## Transfer characteristics

Rec. 709 is written as if it specifies the capture and transfer characteristics of HDTV encoding - that is, as

if it were scene-referred. However, in practice it is output (display) referred with the convention of a 2.4-power function display [2.35 power function in EBU recommendations has also been changed to power function 2.4 since October 2014, according to EBU Tech 3320]. (Rec. 709 and sRGB share the same primary chromaticities and white point chromaticity; however, sRGB is explicitly output (display) referred with an average gamma of 2.2.)<sup>[6]</sup>

The Rec. 709 transfer function from the linear signal (luminance) to the nonlinear (voltage) is, similar to sRGB's transfer function, linear in the bottom part and then transfers to a power function for the rest of the [0..1] range:<sup>[7]</sup>

$$V = \begin{cases} 4.500L & L < 0.018 \\ 1.099L^{0.45} - 0.099 & L \geq 0.018 \end{cases}$$

The conversion to linear is as follows.

$$L = \begin{cases} \frac{V}{4.5} & V < 0.081 \\ \left(\frac{V + 0.099}{1.099}\right)^{\frac{1}{0.45}} & V \geq 0.081 \end{cases}$$

## 2.15.2 See also

- Rec. 601, a comparable standard for standard-definition television (SDTV)
- Rec. 2020, a standard for ultra high definition television (UHDTV) with standard dynamic range
- Rec. 2100, a standard for HDTV and UHDTV with high dynamic range
- sRGB, a standard color space for web/computer graphics, based on the Rec. 709 primaries and white point

## 2.15.3 References

- ITU-R BT.709-6: *Parameter values for the HDTV standards for production and international programme exchange*. June, 2015. Note that the -6 is the current version; previous versions were -1 through to -5.
- : Poynton, Charles, *Perceptual uniformity, picture rendering, image state, and Rec. 709*. May, 2008.
- sRGB: IEC 61966-2-1:1999

[1] ITU-R Rec. BT.601-5, 1995

[2] ITU-R Rec. BT.709-5 page 18, items 1.3 and 1.4

[3] ""Super Hi-Vision" as Next-Generation Television and Its Video Parameters". Information Display. Retrieved 2013-01-01.

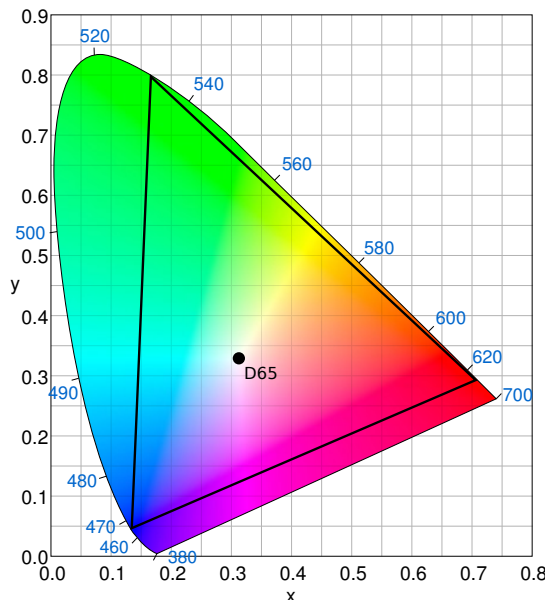
[4] : Chan, Glenn, "HD versus SD Color Space".

- [5] : Poynton, Charles, "Luminance, luma, and the migration to DTV" (Feb. 6, 1998)
- [6] Poynton, Charles (2012). *Digital Video and HD Algorithms and Interfaces*. Burlington, Mass.: Elsevier/Morgan Kaufmann. p. 321. ISBN 978-0-12-391926-7.
- [7] ITU-R Rec. BT.709-5 page 2, item 1.2

### 2.15.4 External links

- ITU-R Recommendation BT.709

## 2.16 Rec. 2020



*CIE 1931 chromaticity diagram showing the Rec. 2020 (UHDTV) color space in the triangle and the location of the primary colors. Rec. 2020 uses Illuminant D65 for the white point.*

**ITU-R Recommendation BT.2020**, more commonly known by the abbreviations **Rec. 2020** or **BT.2020**, defines various aspects of ultra-high-definition television (UHDTV) with standard dynamic range (SDR) and wide color gamut (WCG), including picture resolutions, frame rates with progressive scan, bit depths, color primaries, RGB and luma-chroma color representations, chroma subsamplings, and an opto-electronic transfer function.<sup>[1]</sup> The first version of Rec. 2020 was posted on the International Telecommunication Union (ITU) website on August 23, 2012, and two further editions have been published since then.<sup>[1][2][3][4][5]</sup>

### 2.16.1 Technical details

#### Resolution

Rec. 2020 defines two resolutions of  $3840 \times 2160$  ("4K") and  $7680 \times 4320$  ("8K").<sup>[1]</sup> These resolutions have an aspect ratio of 16:9 and use square pixels.<sup>[1]</sup>

#### Frame rate

Rec. 2020 specifies the following frame rates: 120p, 119.88p, 100p, 60p, 59.94p, 50p, 30p, 29.97p, 25p, 24p, 23.976p.<sup>[1]</sup> Only progressive scan frame rates are allowed.<sup>[1]</sup>

#### Digital representation

Rec. 2020 defines a bit depth of either 10-bits per sample or 12-bits per sample.<sup>[1]</sup>

10-bits per sample Rec. 2020 uses video levels where the **black level** is defined as code 64 and the nominal peak is defined as code 940.<sup>[1]</sup> Codes 0–3 and 1,020–1,023 are used for the timing reference.<sup>[1]</sup> Codes 4 through 63 provide video data below the black level while codes 941 through 1,019 provide video data above the nominal peak.<sup>[1]</sup>

12-bits per sample Rec. 2020 uses video levels where the black level is defined as code 256 and the nominal peak is defined as code 3760.<sup>[1]</sup> Codes 0–15 and 4,080–4,095 are used for the timing reference.<sup>[1]</sup> Codes 16 through 255 provide video data below the black level while codes 3,761 through 4,079 provide video data above the nominal peak.<sup>[1]</sup>

#### System colorimetry

The Rec. 2020 (UHDTV/UHD-1/UHD-2) color space can reproduce colors that cannot be shown with the Rec. 709 (HDTV) color space.<sup>[6][7]</sup> The RGB primaries used by Rec. 2020 are equivalent to monochromatic light sources on the CIE 1931 spectral locus.<sup>[7][8]</sup> The wavelength of the Rec. 2020 primary colors is 630 nm for the red primary color, 532 nm for the green primary color, and 467 nm for the blue primary color.<sup>[8][9]</sup> In coverage of the CIE 1931 color space the Rec. 2020 color space covers 75.8%, the DCI-P3 digital cinema color space covers 53.6%, the Adobe RGB color space covers 52.1%, and the Rec. 709 color space covers 35.9%.<sup>[6]</sup>

During the development of the Rec. 2020 color space it was decided that it would use real colors, instead of imaginary colors, so that it would be possible to show the Rec. 2020 color space on a display without the need for conversion circuitry.<sup>[10]</sup> Since a larger color space increases the difference between colors an increase of 1-bit per sample is needed for Rec. 2020 to equal or exceed the color precision of Rec. 709.<sup>[10]</sup>

The NHK measured contrast sensitivity for the Rec. 2020 color space using Barten's equation which had previously been used to determine the bit depth for digital cinema.<sup>[6]</sup> 11-bits per sample for the Rec. 2020 color space is below the visual modulation threshold, the ability to discern a one value difference in luminance, for the entire luminance range.<sup>[6]</sup> The NHK is planning for their UHDTV system, Super Hi-Vision, to use 12-bits per sample RGB.<sup>[6][11]</sup>

### Transfer characteristics

Rec. 2020 defines a nonlinear transfer function for gamma correction that is the same nonlinear transfer function that is used by Rec. 709, except that its parameters are given with higher precision:<sup>[1][12]</sup>

$$E' = \begin{cases} 4.5E & 0 \leq E < \beta \\ \alpha E^{0.45} - (\alpha - 1) & \beta \leq E \leq 1 \end{cases}$$

- where  $E$  is the signal proportional to camera-input light intensity and  $E'$  is the corresponding nonlinear signal
- where  $\alpha \approx 1.09929682680944$  and  $\beta \approx 0.018053968510807$  (values chosen to achieve a continuous function with a continuous slope)

The standard says that for practical purposes, the following values of  $\alpha$  and  $\beta$  can be used:

- $\alpha = 1.099$  and  $\beta = 0.018$  for 10-bits per sample system (the values given in Rec. 709)
- $\alpha = 1.0993$  and  $\beta = 0.0181$  for 12-bits per sample system

While the Rec. 2020 transfer function can be used for encoding, it is expected that most productions will use a reference monitor that has an appearance of using Gamma 2.4 transfer function as defined in Rec. ITU-R BT.1886 and that the reference monitor will be evaluated as defined in Rec. ITU-R BT.2035.<sup>[1][13][14]</sup>

### RGB and luma-chroma formats

Rec. 2020 allows for RGB and luma-chroma signal formats with 4:4:4 full-resolution sampling and luma-chroma signal formats with 4:2:2 and 4:2:0 chroma subsampling.<sup>[1]</sup> It supports two types of luma-chroma signals, called YCbCr and YcCbcCrc.

YCbCr may be used when the top priority is compatibility with existing SDTV and HDTV operating practices.<sup>[1][10]</sup> The luma ( $Y'$ ) signal for YCbCr is calculated as the weighted average  $Y' = KR \cdot R' + (1-KR-KB) \cdot G' + KB \cdot B'$ , using the gamma-corrected RGB values (denoted  $R'G'B'$ ) and the weighting coefficients  $KR =$

0.2627 and  $KB = 0.0593$ .<sup>[1]</sup> As in similar schemes, the chroma components in YCbCr are calculated as  $C'B = 2 \cdot (B' - Y') / (1 - KB)$  and  $C'R = 2 \cdot (R' - Y') / (1 - KR)$ , and for digital representation the  $Y'$ ,  $C'B$ , and  $C'R$  signals are scaled, offset by constants, and rounded to integers.

The YcCbcCrc scheme is a “constant luminance” luma-chroma representation.<sup>[1]</sup> YcCbcCrc may be used when the top priority is the most accurate retention of luminance information.<sup>[1]</sup> The luma component in YcCbcCrc is calculated using the same coefficient values as for YCbCr, but it is calculated from linear RGB and then gamma corrected, rather than being calculated from gamma-corrected  $R'G'B'$ .<sup>[10]</sup> The chroma components in YcCbcCrc are calculated from the  $Y'$ ,  $B'$ , and  $R'$  signals with equations that depend on the range of values of  $B' - Y'$  and  $R' - Y'$ .

## 2.16.2 Implementations

HDMI 2.0 supports the Rec. 2020 color space.<sup>[15]</sup> HDMI 2.0 can transmit 12-bit per sample RGB at a resolution of 2160p and a frame rate of 24/25/30 fps or it can transmit 12-bits per sample 4:2:2/4:2:0 YCbCr at a resolution of 2160p and a frame rate of 50/60 fps.<sup>[15]</sup>

The Rec. 2020 color space is supported by H.264/MPEG-4 AVC and H.265/High Efficiency Video Coding (HEVC).<sup>[16][17][18]</sup> The Main 10 profile in HEVC was added based on proposal JCTVC-K0109 which proposed that a 10-bit profile be added to HEVC for consumer applications.<sup>[19]</sup> The proposal stated that this was to allow for improved video quality and to support the Rec. 2020 color space that will be used by UHDTV.<sup>[19]</sup>

On September 11, 2013, ViXS Systems announced the XCode 6400 SoC which supports 4K resolution at 60 fps, the Main 10 profile of HEVC, and the Rec. 2020 color space.<sup>[20]</sup>

## 2014

On May 22, 2014, Nanosys announced that using a quantum dot enhancement film (QDEF) a current LCD TV was modified so that it could cover 91% of the Rec. 2020 color space.<sup>[21]</sup> Nanosys engineers believe that with improved LCD color filters it is possible to make a LCD that covers 97% of the Rec. 2020 color space.<sup>[21]</sup>

On September 4, 2014, Canon Inc. released a firmware upgrade, that added support for the Rec. 2020 color space, to their EOS C500 and EOS C500 PL camera models and their DP-V3010 4K display.<sup>[22][23]</sup>

On September 5, 2014, the Blu-ray Disc Association revealed that the future 4K Blu-ray Disc format will support 4K UHD (3840x2160 resolution) video at frame rates up to 60 frames per second.<sup>[24]</sup> The standard will encode videos under the High Efficiency Video Coding

standard.<sup>[24]</sup> 4K Blu-ray Discs will support both a higher dynamic range by increasing the color depth to 10-bit per color, and a greater color gamut by using the Rec. 2020 color space.<sup>[24]</sup> The 4K-Blu-ray specification allows for three disc sizes, each with their own data rate: 50 GB with 82 Mbit/s, 66 GB with 108 Mbit/s, and 100 GB with 128 Mbit/s.<sup>[24]</sup> The first Ultra HD Blu-ray titles were officially released from four studios on March 1, 2016.<sup>[25]</sup>

On November 6, 2014, Google added support for the Rec. 2020 color space to VP9.<sup>[26]</sup>

On November 7, 2014, DivX developers announced that DivX265 version 1.4.21 has added support for the Main 10 profile of HEVC and the Rec. 2020 color space.<sup>[27]</sup>

On December 22, 2014, Avid Technology released an update for Media Composer that added support for 4K resolution, the Rec. 2020 color space, and a bit rate of up to 3,730 Mbit/s with the DNxHD codec.<sup>[28][29]</sup>

## 2015

On January 6, 2015, the MHL Consortium announced the release of the superMHL specification which will support 8K resolution at 120 fps, 48-bit video, the Rec. 2020 color space, high dynamic range support, a 32-pin reversible superMHL connector, and power charging of up to 40 watts.<sup>[30][31][32]</sup>

On January 7, 2015, Ateme added support for the Rec. 2020 color space to their TITAN File video platform.<sup>[33]</sup>

On March 18, 2015, Arri announced the SXT line of Arri Alexa cameras which will support Apple ProRes recording at 4K resolution and the Rec. 2020 color space.<sup>[34][35]</sup>

On April 8, 2015, Canon Inc. announced the DP-V2410 4K display and EOS C300 Mark II camera with support for the Rec. 2020 color space.<sup>[36][37]</sup>

On May 26, 2015, the NHK announced a 4K LCD with a laser diode backlight that covers 98% of the Rec. 2020 color space.<sup>[38][39]</sup> The NHK stated that at the time it was announced this 4K LCD has the widest color gamut of any display in the world.<sup>[40]</sup>

On June 17, 2015, Digital Projection International presented a 4K LED projector with support for the Rec. 2020 color space.<sup>[41]</sup>

## 2016

On January 4, 2016, the UHD Alliance announced their specifications for Ultra HD Premium which includes support for the Rec. 2020 color space.<sup>[42]</sup>

On January 27, 2016, VESA announced that DisplayPort version 1.4 will support the Rec. 2020 color space.<sup>[43]</sup>

On April 17, 2016, Sony presented a 55 in (140 cm) 4K OLED display with the support of Rec. 2020 color space.<sup>[44]</sup>

On April 18, 2016, the Ultra HD Forum announced industry guidelines for UHD Phase A which includes support for the Rec. 2020 color space.<sup>[45][46]</sup>

### 2.16.3 Rec. 2100

Rec. 2100 is an ITU-R Recommendation released in July 2016 that defines high dynamic range (HDR) formats for both HDTV 1080p and 4K/8K UHDTV resolutions.<sup>[47]</sup> These formats use the same color primaries as Rec. 2020, but with different transfer functions for HDR use. Rec. 2100 includes two such transfer function definitions that may be used for HDR:<sup>[47][48]</sup>

- Perceptual Quantizer (PQ), which was previously standardized as SMPTE ST 2084, and
- Hybrid Log-Gamma (HLG), which was previously standardized as ARIB STD-B67.

The PQ scheme with 10 bits of color bit depth has also been called HDR10.<sup>[49]</sup> Similarly, the HLG scheme with 10 bits of color bit depth has been called HLG10.<sup>[45]</sup> The Ultra HD Forum guidelines for UHD Phase A include support for SDR formats with 10 bits of color bit depth based on both Rec. 709 and Rec. 2020 color gamuts and also both the HDR10 and HLG10 formats of Rec. 2100.<sup>[45]</sup>

In addition to defining RGB and YCbCr color representations that are the same as in Rec. 2020 except for the transfer functions, Rec. 2100 also defines an approach known as ICtCp. Rec. 2100 does not support the Yc-CbcCrc scheme of Rec. 2020.

### 2.16.4 See also

- **UHDTV** – Digital video formats with resolutions of 4K ( $3840 \times 2160$ ) and 8K ( $7680 \times 4320$ )
- **High Efficiency Video Coding (HEVC)** – Video standard that supports 4K/8K UHDTV and resolutions up to  $8192 \times 4320$
- **Rec. 709** – ITU-R Recommendation for HDTV
- **Rec. 601** – ITU-R Recommendation for SDTV
- **Rec. 2100** – ITU-R Recommendation for HDR HDTV and UHD

### 2.16.5 References

- [1] “BT.2020: Parameter values for ultra-high definition television systems for production and international programme exchange”. International Telecommunication Union. 2014-07-17. Retrieved 2014-08-31.

- [2] "BT.2020: Parameter values for ultra-high definition television systems for production and international programme exchange". International Telecommunication Union. 2012-08-23. Retrieved 2014-08-31.
- [3] "The international standard for Super Hi-Vision TV". NHK. 2012-08-23. Retrieved 2012-08-30.
- [4] "8K Ultra High Def TV Format Opens Options for TV Viewing". The Hollywood Reporter. 2012-08-28. Retrieved 2012-08-30.
- [5] "ITU approves NHK's Super Hi-Vision as 8K standard, sets the UHDTV ball rolling very slowly". Engadget. 2012-08-25. Retrieved 2012-08-30.
- [6] ""Super Hi-Vision" as Next-Generation Television and Its Video Parameters". Information Display. Retrieved 2012-12-27.
- [7] "Super Hi-Vision format". NHK. Retrieved 2012-08-24.
- [8] "Wide-color-gamut Super Hi-Vision System". NHK. Retrieved 2013-05-18.
- [9] David Wood (2012-03-08). "Deciding Tomorrow's Television Parameters" (PDF). European Broadcasting Union. Retrieved 2013-05-02.
- [10] "BT.2246-2(2012): The present state of ultra-high definition television". International Telecommunication Union. 2013-01-16. Retrieved 2013-04-30.
- [11] "Super Hi-Vision Production Devices for Mobile". NHK. Retrieved 2013-05-18.
- [12] "BT.709: Parameter values for the HDTV standards for production and international programme exchange". International Telecommunication Union. 2009-08-27. Retrieved 2012-09-15.
- [13] "BT.1886: Reference electro-optical transfer function for flat panel displays used in HDTV studio production". International Telecommunication Union. 2011-04-06. Retrieved 2014-08-31.
- [14] "BT.2035: A reference viewing environment for evaluation of HDTV program material or completed programmes". International Telecommunication Union. 2013-08-13. Retrieved 2014-11-05.
- [15] "FAQ for HDMI 2.0". HDMI.org. Retrieved 2014-01-25.
- [16] "H.264: Advanced video coding for generic audiovisual services". ITU. 2013-06-07. Retrieved 2013-06-16.
- [17] G.J. Sullivan; J.-R. Ohm; W.-J. Han; T. Wiegand (2012-05-25). "Overview of the High Efficiency Video Coding (HEVC) Standard" (PDF). IEEE Transactions on Circuits and Systems for Video Technology. Retrieved 2013-06-16.
- [18] "H.265: High efficiency video coding". ITU. 2013-06-12. Retrieved 2013-06-16.
- [19] Alberto Dueñas; Adam Malamy (2012-10-18). "On a 10-bit consumer-oriented profile in High Efficiency Video Coding (HEVC)". JCT-VC. Retrieved 2013-06-16.
- [20] "ViXS Announces XCode 6400, the World's First System-on-Chip (SoC) with Native Support for 10-bit High Efficiency Video Coding (HEVC) and Ultra High Definition (HD) 4K". PRNewswire. 2013-09-11. Retrieved 2013-09-15.
- [21] "Is the rec.2020 UHD color broadcast spec really practical?". Nanosys. 2014-05-22. Retrieved 2014-07-21.
- [22] "Free Canon Firmware for Cinema EOS System Cameras Delivers Improved Basic Performance, Including Support for ITU-R BT.2020 Color Space". MarketWatch. September 4, 2014. Retrieved September 6, 2014.
- [23] "Free Canon Firmware Upgrade for DP-V3010 30-Inch 4K Professional Display Enables Confirmation of ITU-R BT.2020 Color Gamut Video Content". Business Wire. September 4, 2014. Retrieved September 6, 2014.
- [24] "4K Blu-ray discs arriving in 2015 to fight streaming media". CNET. September 5, 2014. Retrieved October 18, 2014.
- [25] "Upcoming Fox 4K Blu-ray Titles". Retrieved January 12, 2016.
- [26] "Change the use of a reserved color space entry". Chromium (*web browser*). Google. 2014-11-06. Retrieved 2014-11-07.
- [27] "DivX HEVC Community Encoder" (Press release). DivX. 2014-11-04. Retrieved 2014-11-15.
- [28] Wim Van den Broeck (2014-12-22). "Editing 4K and Beyond in Media Composer Now Available with Avid Resolution Independence Update". Avid Technology. Retrieved 2014-12-23.
- [29] Bryant Frazer (2014-12-22). "Starting Today, You Can Finally Edit 4K Natively in the Avid". studiodaily. Retrieved 2014-12-23.
- [30] "MHL Consortium Announces superMHL – the First Audio/Video Specification With Support Up to 8K". Yahoo Finance. 2015-01-06. Retrieved 2015-01-10.
- [31] Ryan Smith (2015-01-06). "MHL Consortium Announces superMHL: New Standard & New Cable To Drive 8K TV". AnandTech. Retrieved 2015-01-10.
- [32] "Introducing superMHL". MHL. Retrieved 2015-01-10.
- [33] "High Fidelity Pixels Enhance Ultra HD Video On Demand". PR Newswire. 2015-01-07. Retrieved 2015-01-10.
- [34] Deborah D. McAdams (2015-03-18). "Arri Rolls Out Alexa With 4K ProRes Recording". TVTechnology. Retrieved 2015-03-19.
- [35] "ALEXA SXT". Arri. Retrieved 2015-03-19.
- [36] Jose Antunes (2015-04-08). "New 24-inch 4K Reference Display from Canon". Pro Video Coalition. Retrieved 2015-04-08.
- [37] Jose Antunes (2015-04-08). "The EOS C300 Mark II Has Arrived". Pro Video Coalition. Retrieved 2015-04-08.

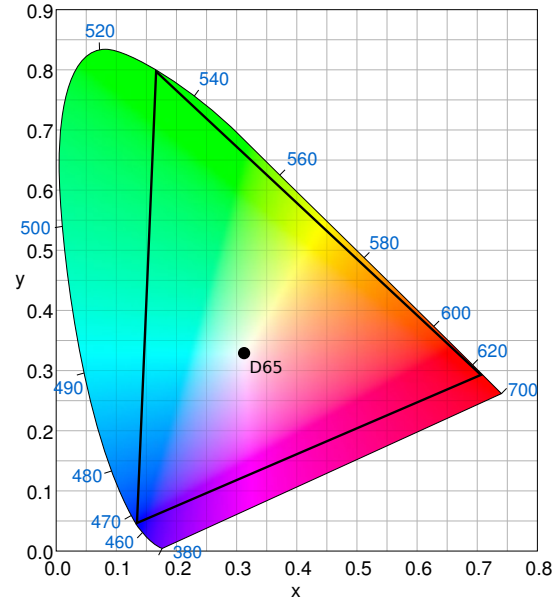
- [38] “NHK Showcases Latest 8K Super Hi-Vision Technologies”. cdrinfo. 2015-05-26. Retrieved 2015-05-26.
- [39] “Laser-backlit Wide-gamut LCD and Color Gamut Mapping”. NHK. Retrieved 2015-05-26.
- [40] Tetsuo Nozawa (2015-06-01). “STRL Announces 4k Display With World’s Widest Color Gamut”. Nikkei Business Publications. Retrieved 2015-06-01.
- [41] “Digital Projection Launches World’s Brightest LED Projector at InfoComm” (Press release). AVNetwork. June 16, 2015. Retrieved May 8, 2016.
- [42] “UHD Alliance Defines Premium Home Entertainment Experience”. Business Wire. 2016-01-04. Retrieved 2016-01-13.
- [43] “VESA Updates Display Stream Compression Standard to Support New Applications and Richer Display Content”. PRNewswire. 2016-01-27. Retrieved 2016-01-29.
- [44] “Sony introduces the PVM-X550, a 55” quad-view large screen Trimaster EL 4K OLED monitor” (Press release). Sony. 2016-04-17. Retrieved 2016-05-08.
- [45] “End-to-end guidelines for phase A implementation”. Ultra HD Forum. 2016-04-18. Retrieved 2016-04-18.
- [46] “Ultra HD Forum Releases First Industry Guidelines for Deploying End-to-End Live & Pre-Recorded UHD Services in 2016”. Business Wire. 2016-04-18. Retrieved 2016-04-18.
- [47] “BT.2100: Image parameter values for high dynamic range television for use in production and international programme exchange”. International Telecommunication Union. 2016-07-04. Retrieved 2016-07-04.
- [48] Adam Wilt (2014-02-20). “HPA Tech Retreat 2014 – Day 4”. DV Info Net. Retrieved 2014-11-01.
- [49] Rachel Cericola (2015-08-27). “What Makes a TV HDR-Compatible? The CEA Sets Guidelines”. Big Picture Big Sound. Retrieved 2015-09-21.

## 2.16.6 External links

- ITU-R Recommendation BT.2020

## 2.17 Rec. 2100

**ITU-R Recommendation BT.2100**, more commonly known by the abbreviations **Rec. 2100** or **BT.2100**, defines various aspects of high dynamic range (HDR) video such as display resolution (HDTV and UHDTV), frame rate, chroma subsampling, bit depth, color space, and optical transfer function.<sup>[1][2]</sup> It was posted on the International Telecommunication Union (ITU) website on July 4, 2016.<sup>[1][2]</sup> Rec. 2100 expands on several aspects of Rec. 2020.<sup>[2]</sup>



*CIE 1931 chromaticity diagram showing the Rec. 2100 color space in the triangle and the location of the primary colors. Rec. 2100 uses Illuminant D65 for the white point.*

### 2.17.1 Resolution

Rec. 2100 defines three resolutions of 1080p, 3840 × 2160 (“4K”), and 7680 × 4320 (“8K”).<sup>[1]</sup> These resolutions have an aspect ratio of 16:9 and use square pixels.<sup>[1]</sup>

### 2.17.2 Frame rate

Rec. 2100 specifies the following frame rates: 120p, 119.88p, 100p, 60p, 59.94p, 50p, 30p, 29.97p, 25p, 24p, 23.976p.<sup>[1]</sup> Only progressive scan frame rates are allowed.<sup>[1]</sup>

### 2.17.3 Digital representation

Rec. 2100 defines a bit depth of either 10-bits per sample or 12-bits per sample, with either narrow range or full range color values.<sup>[1]</sup>

For narrow range color, 10-bits per sample use video levels where the **black level** is defined as 64, **achromatic gray level** as 512 and the nominal peak as 940 in RGB encoding and 960 in YCbCr encoding. Codes 0–3 and 1,020–1,023 can be used for the timing reference and should be avoided.<sup>[1]</sup> 12-bits per sample use 256 as the black level, 2048 as the **achromatic gray level** and the nominal peak is 3760 in RGB encoding and 3840 in YCbCr encoding.<sup>[1]</sup> Codes 0–15 and 4,080–4,095 can be used for the timing reference and should be avoided.<sup>[1]</sup>

For full range color, 10-bit levels are 0 for the black level, 512 for the grey level and 1023 for the nominal peak, and 12-bit levels are 0, 2048 and 4092 (values 4093–4095 are

avoided to exclude clipping errors on 10-bit ADC/DAC circuits which have 1023 steps).<sup>[1]</sup>

#### 2.17.4 System colorimetry

Further information: Rec. 2020 § System colorimetry

Rec. 2100 has the same color space as Rec. 2020.<sup>[1][2]</sup>

#### 2.17.5 Luma coefficients

Rec. 2100 allows for RGB, YCbCr, and ICtCp signal formats with 4:4:4, 4:2:2, and 4:2:0 chroma subsampling.<sup>[1]</sup> Rec. 2100 specifies that if a luma (Y') signal is made that it uses the R'G'B' coefficients 0.2627 for red, 0.6780 for green, and 0.0593 for blue.<sup>[1]</sup>

#### 2.17.6 Signal formats

Rec. 2100 defines the use of RGB, YCbCr, and ICtCp.<sup>[1]</sup> ICtCp provides an improved color representation that is designed for high dynamic range (HDR) and wide color gamut signals (WCG).<sup>[1][3]</sup>

#### 2.17.7 Optical Transfer functions

Rec. 2100 defines two sets of HDR optical transfer functions which are perceptual quantization (PQ) and Hybrid Log-Gamma (HLG).<sup>[1]</sup> HLG is supported in Rec. 2100 with a nominal peak luminance of 1,000 cd/m<sup>2</sup> and a system gamma value that can be adjusted depending on background luminance.<sup>[1]</sup> For a reference viewing environment the peak luminance should be 1,000 cd/m<sup>2</sup> or more and the black level should be 0.005 cd/m<sup>2</sup> or less.<sup>[1]</sup> The surround light should be 5 cd/m<sup>2</sup> and be neutral grey at standard illuminant D<sub>65</sub>.<sup>[1]</sup>

Within each set, the documented transfer functions include an:

- electro-optical transfer function (EOTF) which maps the non-linear signal value into display light
- opto-optical transfer function (OOTF) which maps relative scene linear light to display linear light
- opto-electronic transfer function (OETF) which maps relative scene linear light into the non-linear signal value

#### 2.17.8 See also

- Rec. 2020 - ITU-R Recommendation for UHDTV

#### 2.17.9 References

- [1] “BT.2100-0 : Image parameter values for high dynamic range television for use in production and international programme exchange”. International Telecommunication Union. 2016-07-04. Retrieved 2016-07-04.
- [2] “ITU announces BT.2100 HDR TV standard”. Rasmus Larsen. 2016-07-05. Retrieved 2016-07-26.
- [3] “ICtCp Dolby White Paper” (PDF). Dolby. Retrieved 2016-04-20.

#### 2.17.10 External links

- ITU-R Recommendation BT.2100

# Chapter 3

## Text and image sources, contributors, and licenses

### 3.1 Text

- **CIE 1931 color space** *Source:* [https://en.wikipedia.org/wiki/CIE\\_1931\\_color\\_space?oldid=783325742](https://en.wikipedia.org/wiki/CIE_1931_color_space?oldid=783325742) *Contributors:* AxelBoldt, Michael Hardy, SebastianHelm, Cherkash, Mulad, Random832, Gutza, Birkett, BenRG, Phil Boswell, Ghouston, BenFrantzDale, Macrakis, Maneesh, Yamavu, Marco Polo, Eric Kvaalen, Katana, PAR, Alai, Joriki, Mindmatrix, Jacobolus, Lantic, SiriusB, NekoDaemon, Chobot, Adoniscik, YurikBot, Shawn81, Gaius Cornelius, ENeville, Malcolma, AdiJapan, Voidxor, Mareklug, Tonywalton, SmackBot, Direvus, Axd, Matveims, Eskimbot, Mhss, Hgrosser, VMS Mosaic, Fuzzypeg, Acdx, Ligulembot, Ohconfucius, Paulschou, Dicklyon, Optakeover, LandruBek, George100, Sakurambo, Cxw, Pumbaa80, Shandris, Ahalda, Thijs!bot, Epbr123, Keraunos, Headbomb, Pvjpjv, Glennchan, Escarbot, Robthbot, Moggie2002, R'n'B, Nono64, Cinnamon colbert, SharkD, Circular17, Lloydic, Fylwind, Dcouzin, Bababoef, Forlornturtle, Michael Frind, TSRL, Addbot, DOI bot, Fieldday-sunday, Da5nsy, Yobot, Adelpine, Andrzejkosz, Aboalbiss, AnomieBOT, Efa, Materialscientist, Citation bot, Xqbot, Capricorn42, RobotBOT, Elrofivjxhsudghhgd, Some standardized rigour, Yusungchang, Mfwitten, Dcah1, Citation bot 1, Maggyero, Spidey104, Duoquoduo, Gzorg, Weedwhacker128, Stryn, Dilbert36, Tommy2010, Westley Turner, Musormenyadostal, ClueBot NG, Monsieurpiggy, KlappCK, BarrelProof, Antiqueight, ThatAMan, Helpful Pixie Bot, Curb Chain, KonicaMinoltaSA, LCarulli, BG19bot, Austinprince, Lololo555, JuFo, AUllrich, BattyBot, Jhdewitt, Bercier, Titojoya, Physicsx-uxiao, Monkbot, Hoogamaphone, Burque Photophile, Me-in-nk, Dr Micko, Yihkrys, Jordan-daniel 20161227, Bender the Bot, Jhs12 and Anonymous: 102
- **CIE 1960 color space** *Source:* [https://en.wikipedia.org/wiki/CIE\\_1960\\_color\\_space?oldid=747624327](https://en.wikipedia.org/wiki/CIE_1960_color_space?oldid=747624327) *Contributors:* Bearcat, Hankwang, Eric Kvaalen, Jacobolus, ChKnoflach~enwiki, Adoniscik, Malcolma, SmackBot, Lambiam, R'n'B, SharkD, Echohunter, Addbot, DOI bot, Luckas-bot, AnomieBOT, Citation bot, Citation bot 1, Tom.Reding, Helpful Pixie Bot, Monkbot, Bender the Bot and Anonymous: 3
- **CIE 1964 color space** *Source:* [https://en.wikipedia.org/wiki/CIE\\_1964\\_color\\_space?oldid=785400745](https://en.wikipedia.org/wiki/CIE_1964_color_space?oldid=785400745) *Contributors:* Bearcat, Rich Farmbrough, Jacobolus, Rjwilmis, ChKnoflach~enwiki, Adoniscik, Malcolma, Cedar101, SmackBot, Dicklyon, Paul Foxworthy, MystBot, Addbot, DOI bot, Citation bot, Citation bot 1, Trappist the monk, KonicaMinoltaSA, LCarulli, Monkbot and Anonymous: 1
- **CIELUV** *Source:* <https://en.wikipedia.org/wiki/CIELUV?oldid=772914786> *Contributors:* Crissov, Bearcat, Kpalion, Jacobolus, Adoniscik, Boivie, Incnis Mrsi, Tim macready, Marcuscalabresus, Epbr123, Lovibond, JAnDbot, SharkD, Korey2ThaLee, PipepBot, Owirjadi, MystBot, Addbot, DOI bot, Matěj Grabovský, AnomieBOT, Efa, Maulucion, Citation bot 1, DrilBot, Weedwhacker128, EmausBot, Es-kandari.ar, ZéroBot, Atcold, Xkr47, KlappCK, Ulidtko, Ruby Murray, Monkbot and Anonymous: 11
- **LMS color space** *Source:* [https://en.wikipedia.org/wiki/LMS\\_color\\_space?oldid=766870394](https://en.wikipedia.org/wiki/LMS_color_space?oldid=766870394) *Contributors:* Bearcat, Dissident, Stuarteates, Jacobolus, Srleffler, Adoniscik, Dicklyon, Nthep, Nono64, Philip Trueman, SieBot, VVVBot, Addbot, Yobot, Atcold, Uli Zappe, Helpful Pixie Bot, BattyBot, Monkbot, Bender the Bot, Lift management services and Anonymous: 9
- **Lab color space** *Source:* [https://en.wikipedia.org/wiki/Lab\\_color\\_space?oldid=786728807](https://en.wikipedia.org/wiki/Lab_color_space?oldid=786728807) *Contributors:* Michael Hardy, SebastianHelm, Ellywa, Ahoerstemeier, Cherkash, Mulad, Crissov, Dysprosia, Gutza, Omegatron, Samsara, Mina86, Bearcat, Fredrik, 75th Trombone, Connelly, Dmmaus, Zeimusu, Tybruce, Kelson, Richie, Notinasmaid, Kjoonlee, Lysdexia, Varuna, PAR, Kdau, Kelly Martin, Mindmatrix, Jacobolus, Spike0xFF, Tabletop, Waldir, TAKASUGI Shinji, Mlewan, NekoDaemon, Adoniscik, Wavelength, IByte, Marcus Cyron, ENeville, Inike, Nick, Anetode, Jaysbro, Burton Radons, SmackBot, Slashme, Mhss, Chris the speller, Konstable, Tsca.bot, VMS Mosaic, Aelffin, Derek farn, SilkTork, Dicklyon, Mfield, LandruBek, Paul Foxworthy, Twas Now, Aoleson, Docreddi, Cxw, Thijs!bot, Glennchan, PhiLiP, Lovibond, CrizCraig, Magioladitis, STBot, UnknownVT, Nono64, Normankoren, Slow Riot, SharkD, Clerks, Dskluz, Motine, Serge925, Nourani~enwiki, Fylwind, STBotD, Remember the dot, Ann McCarthy, Ajfweb, A4bot, Jamelan, Ericeee10, Flyer22 Reborn, Tronic2, VanishedUser sdu9aya9fs787sads, Copyeditor42, Dhoerl, Alexbot, Resoru, Ost316, Addbot, MrOllie, Alpalfour, Yobot, Aboalbiss, AnomieBOT, Efa, Citation bot, Nadia arty, Ll1324, Nagualdesign, FrescoBot, Jiansia, Citation bot 1, Maggyero, Redrose64, Zink Dawg, EmausBot, TuHan-Bot, Bamyers99, Spiritworld, ClueBot NG, Parcly Taxel, Helpful Pixie Bot, Chevreul, Umeshksingla, NotWith, Leonorek, JYBot, Ruby Murray, John.cumings, Ibrahim Husain Meraj, AndyThe, Brainiacal, Sphonasepal, Monkbot, Ying.l.xiong, YdJ, Catclaw666, Farbenprofi, JosephSlomka, InternetArchiveBot, Bender the Bot and Anonymous: 115
- **CIECAM02** *Source:* <https://en.wikipedia.org/wiki/CIECAM02?oldid=785400387> *Contributors:* Robbot, Auric, Chowbok, Jacobolus, Adoniscik, Cedar101, SmackBot, C.Fred, Chris the speller, VMS Mosaic, Ohconfucius, Darkinquirer, Quibik, Fayenatic london, Squids and Chips, TXiKiBoT, XEmacs, Svick, Addbot, DOI bot, Ben Ben, Citation bot, Citation bot 1, Weedwhacker128, LoPiCompri, Helpful Pixie Bot, BattyBot, Mogism, RichardRegal, Monkbot, Bender the Bot, Fullout puppy wee and Anonymous: 14

- **Primary color** *Source:* [https://en.wikipedia.org/wiki/Primary\\_color?oldid=780524326](https://en.wikipedia.org/wiki/Primary_color?oldid=780524326) *Contributors:* Damian Yerrick, AxelBoldt, Lee Daniel Crocker, Bryan Derksen, Waveguy, Heron, Ram-Man, Wapcaplet, Elywa, Ahoerstemeier, ToastyKen, Vzbs34, Arteitle, BenRG, Northgrove, Chuunen Baka, Robbot, DHN, Hadal, Bryno, Bkonrad, Niteowlneils, Chinasaurs, Erdal Ronahi, Yekrads, Jackol, LiDaobing, Beland, MFNickster, Maneesh, Melonhead, Tsemii, Quota, Discospinster, Rhobite, Supercoop, YUL89YYZ, Triskaideka, Chewie, Dkroll2, Hayabusa future, Mqduck, Army1987, Myria, La goutte de pluie, Vanished user 19794758563875, Haham hanuka, Alansohn, Trjumpet, Carioca, Bsadowski1, Kazvorpal, Nuno Tavares, Georgia guy, Jacobolus, Cruccone, Tabletop, Kelisi, Dysespion, Mandarax, Glempling, Graham87, Rjwilmsi, MWAK, Margosbot-enwiki, Nihiltres, TheMidnighters, NekoDaemon, Gurch, Addesso, Themissinglint, Glenn L, Chobot, Citizen Premier, Bgwhite, Adoniscik, YurikBot, RussBot, ENeville, DAJF, Mysid, DeadEyeArrow, Cavan, Bmju, FF2010, Thelb4, JDspeeder1, SkerHawx, Sycthos, SmackBot, Moeron, C.Fred, Jab843, Trystan, Gilliam, Chris the speller, Bluebot, DHN-bot-enwiki, Brianhill, Darth Panda, Egsan Bacon, Chlewwbot, VMS Mosaic, Nahum Reduta, Dreadstar, Crd721, Tactik, Drc79, Lukeoz, JunCTionS, Kuru, Stale2000, Butko, Stratadrake, Dicklyon, AEMoreira042281, Avant Guard, Iridescent, Alchav, Shoeofdeath, CapitalR, Freelance Intellectual, Tawkerbot2, Jh12, JForget, Deon, Cxw, WeggeBot, Daveoh, Myasuda, Laura S, Meighan, Mjjj, Christian75, UberScienceNerd, Ohnjaynb, Epr123, Keraunos, AgentPeppermint, Nick Number, Mjad-enwiki, Mentifisto, AntiVandalBot, Luna Santin, Seaphoto, AxiomShell, MikeLynch, MER-C, Arch dude, PaleAqua, PhilKnight, Acroterion, Magioladitis, Connormah, Bong-warrior, VoABot II, Soulbot, 28421u2232nfencenc, Vssun, DerHexer, Nopira, GreggEdwards, MartinBot, Jim.henderson, Neodynamion, Glossando, LedgedGamer, J.delanoy, Lucaswilkins, Singularitarian, Javawizard, Onhm, Mrob27, Katalaveno, Thatotherperson, Velps, NewEnglandYankee, DadaNeem, Mike902, Koobmeej, Cmichael, KylieTastic, Cometstyles, EXCEPTION NOT HANDLED, Funandtrvl, VolkovBot, Davidmc64, TXiKiBoT, Oshawah, The Original Wildbear, Sarenne, Wiikipedian, Ferengi, LeaveSleaves, Fists, Steve3849, Feudonym, Ziphon, Enviroboy, RingWars2007, DrVenture, Chack Jadson, Pi is 3.14159, Keilana, Roosterrulez, Oda Mari, Man It's So Loud In Here, Shaheenjim, JSpong, KoshVorlon, Paulhiphop, Manway, Cult of the Sacred Or nge, Sunrise, OKBot, Anchor Link Bot, 48states, ClueBot, TransporterMan, The Thing That Should Not Be, Kathartic, Maggiewoo, Doyleb23, ChandlerMapBot, Monster boy1, Resoru, VRBones, Jotterbot, Ertemplin, Porridgebowl, Crowsnest, DumZiBoT, I\*Rok\*U\*Dont, InternetMeme, Matta96, Ost316, Avoided, WikHead, Joyonicity, MystBot, Tayste, Addbot, Some jerk on the Internet, DOI bot, Wsvlqc, Aitreia, West.andrew.g, Emrdgreg, Tide rolls, Ben Ben, આશીષ મનનગર, Luckas-bot, TheSuave, Yobot, Fraggie81, AnomieBOT, DemocraticLuntz, 1exec1, Götz, Jim1138, Materialscientist, Citation bot, Raven1977, Andrewmc123, Xqbot, HN45, Avicek, J04n, RibotBOT, Kickyandfun, Gerge125, CES1596, VS6507, Mfwitten, Citation bot 1, Javert, Pinethicket, I dream of horses, Captain Virtue, Jmmmmmm, White Shadows, Ticklewicks-leukulele, Jonkerz, SDLarsen, Weedwhacker128, Jhendersson777, Fastilysock (usurped), Minimac, RjwilmsiBot, P Aculeius, EmausBot, Orphan Wiki, Dcirovic, Fa, Sicklounge, Lacain247, Ocean Shores, TyA, L Kensington, VictorianMutant, TYelliot, Helpsome, ClueBot NG, Chocolate beans69, Snotbot, Widr, Helpful Pixie Bot, Strike Eagle, BG19bot, GreyAlien502, Whatthehell123, Max Ijzersteen, Fer408, Rockgirl745, BabyD1994, Wannabemodel, Jossian, Krystaleen, Mogism, Cerabot-enwiki, AkashBedi12, GranChi, Hpugh123, Me, Myself, and I are Here, Jeremy.usman33, ZIADMAJ, DavidLeighEllis, CensoredScribe, Kharkiv07, Atotalstranger, Noyster, Monkbot, KH-1, Grami210, MrGesham, Lolkittyfish123, Jimbo.sheffield, Shauny6983, CAPTAIN RAJU, CitrusEllipsis, Bigbluesky88, The liar2, Dorae-monGamer, Karlfonza, Carilchasens, Bender the Bot, L3X1, Evildrprokchop, Jefjulia40, Dfsafdsafdas, Podrick Payne and Anonymous: 485
- **Cone cell** *Source:* [https://en.wikipedia.org/wiki/Cone\\_cell?oldid=782264895](https://en.wikipedia.org/wiki/Cone_cell?oldid=782264895) *Contributors:* Kpj, DrBob, JohnOwens, Iluvcapra, Jimfbleak, Emperorbma, Sander123, RedWolf, Fuelbottle, Mfc, Jfdwolff, Christopherlin, Alexf, Maneesh, Icairns, Quota, JTN, Discospinster, Cacycle, Diomidis Spinellis, Jpgordon, Arcadian, La goutte de pluie, Shehal, Helix84, Lysdexia, Jeltz, Axl, Stillnotelf, Japanese Searobin, Jacobolus, WadeSimMiser, Deltabeignet, Rjwilmsi, Fred Hsu, Quiddity, Ligulem, AED, RexNL, Srleffler, DVdm, Adoniscik, YurikBot, RussBot, Hellbus, Shawn81, NawlinWiki, Janet13, Blitterbug, StuRat, Allens, SmackBot, Jwmillerusa, Chelmite, Delldot, Eskimbot, Notch, Gilliam, TimBentley, EncMstr, The359, Adamantios, Youragain, Abmac, Richard001, Ligulembot, MadCow257, Gobonobo, Beetstra, Dicklyon, Fangfufu, Daniel5127, Slmader, Tanthalas39, Ale jrb, L'œuf, Cahk, Kgbeer, Dr.enh, Thijis!bot, Epr123, Jaxsonjo, KrakatoaKatie, AntiVandalBot, Sluzzelin, Ph.eyes, Chagai, Arno Matthias, SwiftBot, LookingGlass, Wikianon, FisherQueen, VanessaEzekowitz, Akulo, Nono64, Pekaje, Hodja Nasreddin, Mdugvneaud, Paskari, ReddyVarun, TXiKiBoT, Tameeria, A4bot, GcSwRhIc, Madhero88, PAntoni, SieBot, WereSpielChequers, Jjw, HendrixEesti, Nn123645, ClueBot, Drmies, CounterVandalismBot, Michal Sobkowski, Ex-cirial, Muro Bot, CogitoErgoCogitoSum, Phynicen, ClanCC, InternetMeme, Delt01, Fastily, Vojtěch Dostál, Addbot, MXVN, Da5nsy, Diptanshu Das, ChenzwBot, LinkFA-Bot, 5 albert square, Tyw7, Tide rolls, OlEnglish, Luckas-bot, Aboalbiss, Jim1138, Materialscientist, Citation bot, Lucas718, Nagualdesign, Metalman94, NifCurator1, ChConnor, Citation bot 1, Pinethicket, Tom.Reding, RedBot, Meaghan, Callanecc, Ace of Clubs and Spades, Stefan.loska, EmausBot, John of Reading, RA0808, Wikipelli, Dcirovic, K6ka, AMAN-WithNoPlan, Drzank, ChuispastonBot, Peter Karlens, Sonicyouth86, ClueBot NG, Tideflat, Frietjes, KLBot2, Strutron, MusikAnimal, Mark Arsten, Anusan.rasalingam, ShellbyF, Kittyblue101, IF025, Amber.mccallum, Xiaoxuey, BattyBot, Abumkim, Alammagh, Dexbot, FoCuSandLeArN, LightandDark2000, Clopsywiki12, Jochen Burghardt, Thirumaran13, Loladee91, Nisar.a.shaik, Anetta773, Gideon-MarkCabanban, UTScholar, Yossofz, SMA2012, Soccer1818, Dinisoe, Monkbot, XU Hua, Kjerish, Appable, CV9933, Uwe Hartwig, CLCStudent, Savageboylol, Launch the Lunch, Mortee and Anonymous: 175
- **Spectral sensitivity** *Source:* [https://en.wikipedia.org/wiki/Spectral\\_sensitivity?oldid=774549218](https://en.wikipedia.org/wiki/Spectral_sensitivity?oldid=774549218) *Contributors:* Michael Devore, Ferried, Rjwilmsi, Kibibu, Adoniscik, Dicklyon, Nono64, Uncle Dick, Moonksy29, Sean.hoyland, SchreiberBike, Fgnievinski, KDS4444, Tom.Reding, Helpful Pixie Bot, BG19bot, ChrisGualtieri, Zor spec, Wren15, Bender the Bot, Snurggling!, Nielsnjr and Anonymous: 8
- **Planck's law** *Source:* [https://en.wikipedia.org/wiki/Planck%7Bs%7d\\_law?oldid=786697492](https://en.wikipedia.org/wiki/Planck%7Bs%7d_law?oldid=786697492) *Contributors:* XJaM, Jdpipe, Patrick, Michael Hardy, Tim Starling, SebastianHelm, Looxix-enwiki, Jordi Burguet Castell, Charles Matthews, Reddi, Choster, Chuunen Baka, Han-kwang, Peak, Marc Venot, Giftlite, Dratman, Pne, Delta G, DemonThing, Unquantum, JimWae, Mschlindwein, Rich Farmbrough, Paul August, Nabla, Guidod, Kjkolb, Photoniique, Eric Kvaalen, Keflavich, PAR, Jheald, Count Iblis, Lerduwa, Gene Nygaard, Dennis Bratland, Falcorian, Stemonitis, Simetrical, Linas, Mindmatrix, Rpanson, Johan Lont, Li-sung, Eteq, Nanite, Drbogdan, Rjwilmsi, R.e.b., Dugegalea, The wub, Alejo2083, Ground Zero, Srleffler, Chobot, DVdm, Unc.hbar, Bgwhite, Adoniscik, Roboto de Ajvol, YurikBot, Gaius Cornelius, Ojcit, R'son-W, Moe Epsilon, Light current, Enormousdude, 2over0, Reyk, Fram, Katieh5584, Bo Jacoby, SmackBot, Varunbhalerao, Bggoldie-enwiki, Anthony Liguori, Robin Whittle, Njerseyguy, Metacomet, Rizzardi, DaveFoster110@hotmail.com, Cybercobra, Daniel.o.jenkins, Clean Copy, Sadi Carnot, Andrei Stroe, SashatoBot, Jaganath, Kreuzfeld, IronGargoyle, Loadmaster, Dicklyon, Vaughan Pratt, Mikiemike, Thermochap, Diegueins, Gtxfrance, Michael C Price, Dchristle, Mikewax, Markus Pössel, HappyInGeneral, Headbomb, Jojan, Second Quantization, Dr. Submillimeter, Naturalnumber, Magioladitis, Bongwarrior, Ethanminot, Necrofear, Mbweissman, HEL, C. Trifle, Martyjmch, Drphysics, Cmelsheimer, Inwind, VolkovBot, Pasquale.Carelli, Suprcel, Aborghgr, Wiae, Maxim, Q Science, Andy Dingley, Dmcq, Mike4ty4, AlleborgoBot, IIZuhg3n1u5, Damorbrel, Yintan, Texliebmann, Jm smits, Pac72, Agu bar Jacé, StewartMH, ClueBot, EoGuy, R000t, Djr32, Francisco Albani, Muro Bot, Wnt, DumZiBoT, TimothyRias, Nathan Johnson, Salam32, MaizeAndBlue86, Phidus, Addbot, Iceblock, Jkastrup, Favonian, Lightbot, Zorrobot, Luckas-bot, Yobot, Gigaphd, AnomieBOT, טויקיון, Muhalii, Materialscientist, Citation bot, Xqbot, Tornado79, Spancek, Liberty821, Waleswatcher, Amaury, Chjoaygame, FrescoBot, Omniscientest, D'ohBot, Pythagoras0, Citation bot 1, Pinethicket, Holy Masamune, Bookerj, FoxBot, Trappist the monk, Wdanbae, PleaseStand,

Joseph449008, Jiffles1, RjwilmsiBot, John of Reading, Kosta Dean, Dewritech, GoingBatty, Robertuckles, Hhippo, ZéroBot, GianniG46, HCPotter, Toomuchrockcankill, 28bot, ClueBot NG, Uli Zappe, Bernhlav, Helpful Pixie Bot, Bibcode Bot, Lowercase sigmabot, BG19bot, Skarmenadius, Happyboy2011, Sparkie82, BattyBot, Ariaveeg, Mdann52, Jimw338, ChrisGualtieri, AK456, Dexbot, Planetree, Webclient101, Enyokoyama, Ruby Murray, Haohalihao, Monkbot, Ashwiniyengar, Rupeshec0440, 33wantittrue, Arunisaac, Isambard Kingdom, CV9933, Boehm, Nertuoop, Nlebed32, Chemistry1111, Bender the Bot, Rahul Mahanot and Anonymous: 198

- **Planckian locus** *Source:* [https://en.wikipedia.org/wiki/Planckian\\_locus?oldid=787524652](https://en.wikipedia.org/wiki/Planckian_locus?oldid=787524652) *Contributors:* Michael Hardy, Vadmium, Rich Farmbrough, PAR, Gene Nygaard, Jacobolus, TAKASUGI Shinji, SeanMack, NekoDaemon, Cyun, Srleffler, Nucleardave, Adoniscik, Thorseth, Bluebot, Acdx, Dicklyon, Futurebird, Jayron32, Leyo, DOI bot, Citation bot, Citation bot 1, Trappist the monk, HumblePiero, Dcirovic, Uli Zappe, Helpful Pixie Bot, Ushakaron, Monkbot, Krebs49, Bender the Bot, PrimeBOT and Anonymous: 12
- **Planck–Einstein relation** *Source:* [https://en.wikipedia.org/wiki/Planck%E2%80%99Einstein\\_relation?oldid=787524647](https://en.wikipedia.org/wiki/Planck%E2%80%99Einstein_relation?oldid=787524647) *Contributors:* Bearcat, Waldir, Kri, DVdm, A.R., Headbomb, Steelpillow, Favonian, Yobot, Materialscientist, ຂ່າຍ, Chjoaygame, MarioGL, Dtheobald, JSquish, Lightex, Lupiogh, PrimeBOT and Anonymous: 9
- **Standard illuminant** *Source:* [https://en.wikipedia.org/wiki/Standard\\_illuminant?oldid=784405161](https://en.wikipedia.org/wiki/Standard_illuminant?oldid=784405161) *Contributors:* Cherkash, Graeme Bartlett, TomViza, Chowbok, Rich Farmbrough, Jacobolus, Rjwilmsi, SiriusB, Srleffler, Adoniscik, Crystallina, RDBury, Chris the speller, Bluebot, VMS Mosaic, Dicklyon, DrSeehas, R'n'B, Nono64, Lamro, Winchelsea, Copyeditor42, Sun Creator, Scog, Addbot, DOI bot, AkhtaBot, Luckas-bot, Citation bot, Anon423, FrescoBot, Maggyero, Tom, Reding, RedBot, Trappist the monk, RjwilmsiBot, Dewritech, Dcirovic, Ό όστρος, ClueBot NG, Helpful Pixie Bot, BG19bot, BattyBot, Khazar2, ACUllrich, Monkbot, DRcolor and Anonymous: 15
- **Black body** *Source:* [https://en.wikipedia.org/wiki/Black\\_body?oldid=782705419](https://en.wikipedia.org/wiki/Black_body?oldid=782705419) *Contributors:* Carey Evans, Mav, Bryan Derksen, AstroNomer, Ed Poor, Andre Engels, LA2, XJaM, PierreAbbat, DrBob, Jdpipe, Heron, Youandme, Stevertigo, Edward, Lir, Patrick, JohnOwens, Michael Hardy, Wapcaplet, CesarB, Egil, StevenJ, William M. Conolley, Reddi, The Anomebot, Omegatron, Ed g2s, Betterworld, Hankwang, Cdang, Bkell, Wereon, HaeB, Xanzibar, Cyrus, Enochlau, Marc Venot, Giftlite, Niel Malan, Poszwa-enwiki, Shaun-MacPherson, Wolfkeeper, BenFrantzDale, MSGJ, Herbee, Monedula, Anville, TomViza, Solipsist, Thij\$, StuartH, LiDaobing, Zeimus, Pcarbonn, Rdsmith4, DragonflySixtyseven, Icairns, Lumidek, Gleam-enwiki, Deglrf6328, Talkstosocks, Eryian, Guanabot, Vsmith, ArnoldReinhold, Bender235, Nabla, Kaszeta, CanisRufus, El C, Femto, Casual3, Clawson, R. S. Shaw, 9SGjOSfyHJaQVsEmy9NS, Blinken, Nihil-enwiki, Helix84, Lysdexia, LutzL, Eric Kvaalen, Keenan Pepper, Keflavich, PAR, Batmanand, Hammertime, Hgrenbor, Aliencam, Count Iblis, Lerdsuwa, DV8 2XL, Gene Nygaard, Adrian.benko, Stemonitis, ChrisJ Moor, Woohookitty, Xover, Rparson, StradivariusTV, Kzollman, Yougotavirus, Duncan.france, Firien, Waldir, Xiong, Graham87, Li-sung, Adxm, Rjwilmsi, Vary, Hathawayc, AySz88, Maxim Razin, Mahlum-enwiki, Kevmitch, FayssalF, FlaBot, Ian Pitchford, SchuminWeb, Maustrauer, Goudzovski, SteveBaker, Srleffler, Da-Gizza, Deklund, Mhking, The Rambling Man, YurikBot, Cyferx, Brandmeister (old), JabberWok, Gaius Cornelius, Ethan, SEWilcoBot, Speedevil, AdiJapan, E2mb0t~enwiki, Bota47, JustAddPeter, Stefan Udrea, Light current, 2over0, Maddog Battie, Modify, CWenger, Argo Navis, RG2, GrinBot~enwiki, SmackBot, RDBury, FocalPoint, Baodo, Tuxkhan-enwiki, KnowledgeOfSelf, InvictaHOG, Bob Armstrong, Yamaguchi[], Skizzik, Reza1615, Bluebot, Notyouravgjoe, Complexica, Tianxiaozhang-enwiki, Metacomet, DHN-bot~enwiki, Colonies Chris, Daniel Böling, Can't sleep, clown will eat me, Andyparkins, VMS Mosaic, Huon, Kalexander, Thomas Palm, Ligulembot, Sadi Carnot, Esrever, Mouse Nightshirt, Jaganath, Frokor, BillFlis, Dicklyon, Hypnosifl, Chimical05~enwiki, Nialsh, JMK, Aeternus, LethargicParasite, Tawkerbot2, Vaughan Pratt, Friendly Neighbour, Domanix, Joelholdsworth, CumbiaDude, Cydebot, Kanags, Gogo Dodo, Wikipediарules2221, Michael C Price, Tawkerbot4, Bob Stein - VisiBone, Thrrapper, Dragonflare82, Pinky sl, CieloEstrellado, Thij\$!bot, Headbomb, Aquishix, EdJohnston, Natalie Erin, Northumbrian, AntiVandalBot, Wang ty87916, Orionus, Peter Harriman, JAnDbot, TV4Fun, Andonic, TAnthony, Kerotan, VoABot II, Jackmass, Ling.Nut, Brusegadi, KConWiki, LorenzoB, Freddy945, Aszostak, NatureA16, The Ubik, Keith D, BigrTex, Grim Revenant, Martyjmch, Barts1a, Aqwis, BobEnyart, Drphysics, Nwbeeson, SJP, Geekdiva, Vanished user 39948282, Grey Knight 1ce, VolkovBot, TreasuryTag, Pleasantville, AlnoktaBOT, Stou, Mortimer'sdad, Mathwhiz 29, Acjohns, Q Science, Kbrose, SieBot, Jim77742, Damorbel, Caltas, Texliebmann, Likebox, OKBot, Adaptardar, Adam Cuerden, Hamilton-daniel, Seth Bresnett, StewartMH, ImageRemovalBot, ClueBot, WurmWoode, Mad031683, Djr32, -Midorihana-, Mihaiam~enwiki, Brews ohare, DeltaQuad, Muro Bot, BOTarate, HannonRJ, Thingg, Aitias, Crnorizec, LieAfterLie, Darth Kule, EphemeralNecrosis, Petedskier, Addbot, ToolmakerSteve, DOI bot, Zawy1, Jkastrup, Jim10701, Download, Ginosbot, Tide rolls, Lightbot, Luckas-bot, Yobot, Fraggle81, PMLawrence, Quasar1826, AnomieBOT, The Lamb of God, Materialscientist, Citation bot, LilHelpa, Xqbot, Hanberke, Anna Frodesiak, GrouchoBot, Jhbdel, Omnipaedista, RibotBOT, Waleswatcher, Astatine-210, Itaygal, A. di M., Chjoaygame, FrescoBot, Rckrone, Citation bot 1, Pinethicket, Tom, Reding, RedBot, MastiBot, Toolnut, Trappist the monk, Amirhdzr 91, Weedwhacker128, RjwilmsiBot, Azure777, Noommos, Kevanhashem, John of Reading, Dewritech, 8digits, Jrockers, Dcirovic, Andres.felipe, ordonez, ZéroBot, Josve05a, 1howardsr1, BodkinDesign1968, GianniG46, AlphaPikachu578, Erianna, HCPotter, Hang Li Po, Tls60, Toomuchrockcankill, Semantic-Mantis, Mehdi, Disaster958, ClueBot NG, Spjrodrigues, Manubot, Ichka Ckmirindie Hos, GoldenGlory84, Tideflat, Fkhwang, Helpful Pixie Bot, Art and Muscle, Shivasgadharam, Bibcode Bot, Happyboy2011, ElphiBot, தடெங்காசி சுய்பிரமணியன், Snow Rise, Absconditus, BattyBot, MatthewIreland, Webclient101, Saehry, TwoTwoHello, Mcousino, Chronomentro, Monkbot, Puru Pandit, Koitus~nlwiki, Chrissymad and Anonymous: 316
- **Illuminant D65** *Source:* [https://en.wikipedia.org/wiki/Illuminant\\_D65?oldid=748568798](https://en.wikipedia.org/wiki/Illuminant_D65?oldid=748568798) *Contributors:* TomViza, Dmmaus, PAR, Serename, Ketiltrout, Ian Dunster, Srleffler, Adoniscik, KJBracey, SmackBot, Elonka, Chris the speller, Ohconfucius, Dicklyon, Cxw, Anthony Bradbury, Jayron32, Nono64, Leyo, Fylwind, Addbot, DOI bot, Yobot, Ptbotgourou, Citation bot, Hairypeanut, Citation bot 1, Trappist the monk, ZéroBot, Ό όστρος, Ivokabel, BabbaQ, 28bot, Helpful Pixie Bot, Dexbot, Monkbot, Bender the Bot and Anonymous: 14
- **RGB color space** *Source:* [https://en.wikipedia.org/wiki/RGB\\_color\\_space?oldid=785413317](https://en.wikipedia.org/wiki/RGB_color_space?oldid=785413317) *Contributors:* Michael Hardy, Gmalivuk, Meekohi, Wapcaplet, CesarB, Crissov, Gutza, Ed g2s, Samsara, Bevo, Finlay McWalter, Robbot, DemonThing, Bumm13, DmitryKo, Ta bu shi da yu, Smyth, Notinasnaid, Hugewolf, PAR, Cburnett, Mindmatrix, Nuggetboy, Jacobolus, Ma Baker, Yurik, Rjwilmsi, Ligulem, Ground Zero, Adoniscik, Gaius Cornelius, Entirety, Fourohfour, David Biddulph, Cmglee, That Guy, From That Show!, Incnis Mrsi, Bluebot, Nbarth, Zom-B, DO11.10, Stratadrake, Dicklyon, CRGreathouse, Cxw, Eric Le Bigot, Neelix, Keraunos, Rotundo, Stormie823, Ramurf, LookingGlass, Ashishbhatnagar72, Aurow, Loukreu, Nono64, SharkD, Cuddlyable3, Ricardo Cancho Niemietz, Tronic2, M4gnom0n, Addbot, Willking1979, ErJStarks, Debresser, KaiKemmann, Splodgeness, Yobot, Moyasta, Efa, Jan olieslagers, EmausBot, Blas3nik, BG19bot, Eyesnore, Dynamicdispatch, Averoess, Srednua Lenoroc, MisterZeus and Anonymous: 47
- **SRGB** *Source:* <https://en.wikipedia.org/wiki/SRGB?oldid=780144321> *Contributors:* Damian Yerrick, Zundark, Leandrod, Yann, Julesd, Cherkash, Ehn, Charles Matthews, Gutza, Traal, Furrykef, Fibonacci, BenRG, Frazzydee, Hankwang, Pjedice, Pengo, Grincho, Frencheigh, PenguiN42, Sam Hocevar, Ta bu shi da yu, Poccil, Vsmith, Smyth, Notinasnaid, ESkog, Spitzak, Army1987, Panjasan, Neon-umbers, Danog, PAR, Wdfarmer, Gene Nygaard, NantonosAedui, Jacobolus, Ruud Koot, GregorB, Quiddity, Ian Dunster, Ian Pitchford, SiriusB, Bgwhite, Adoniscik, YurikBot, Wavelength, Gaius Cornelius, Pseudomonas, Marcus Cyron, Mipadi, Janke, Mysid, Mareklug,

Ppanzini, BorgQueen, Femmina, KJBracey, DCEvoCE, Cmglee, SmackBot, Cryptor3, Mihai cartoaje, Davepape, KaiUwe, Unyoyega, Betacommand, Bugloaf, Nbarth, Pandora Xero, VMS Mosaic, Adcx, Charivari, Adam Nohejl, Deadcode, Stratadrake, Dicklyon, Di2000, Chris319, Elharo, CmdrObot, Cxw, Thijs!bot, Lovibond, JAnDbot, DanRuderman, Sterrys, DrSeehas, Tercer, Non064, BigrTex, SharkD, JensRex, ArdenD, Fylwind, Totsugeki, Dcouzin, Rebornsoldier, One half 3544, SieBot, RichardKirk, COnanPayne, WurmWoode, Fnordware, PixelBot, SpikeToronto, Ogat, Skarebo, Emry-d, Addbot, Olli Niemitalo, Zacao, ພິເນັດໜ້າ, Luckas-bot, Efa, Redbubblehat, Lijiacigreat, Citation bot, Martnym, Lainestl, E-t172, LMLB, Dcirovic, ZéroBot, Ida Shaw, DavidBrainard, Smgraphitech, Mikhail Ryazanov, Helpful Pixie Bot, Warmonk, Zyxwv99, CitationCleanerBot, Kakao 6e3 ra3a, Mntbat, Unixatwp, TCMemoire, Mattghali, Sizeofint, GreenC bot, Bender the Bot, Hal9kXPS and Anonymous: 71

- **Rg chromaticity** *Source:* [https://en.wikipedia.org/wiki/Rg\\_chromaticity?oldid=747514483](https://en.wikipedia.org/wiki/Rg_chromaticity?oldid=747514483) *Contributors:* Zundark, Asc99c, D6, Rich Farmbrough, Notinasnaid, Quiddity, Adoniscik, Wavelength, Wangi, Vampyrium, SmackBot, VMS Mosaic, Dicklyon, Magioladitis, QrczakMK, Rebornsoldier, WereSpielChequers, Dlrhrer2003, Erik9bot, Dcirovic, Augurar, Helpful Pixie Bot, CitationCleanerBot, Chris-Gaultieri, Brian3030, Antoine Morin-Paulhus, Naeschdy, Njm7203, Bender the Bot and Anonymous: 7
- **Adobe RGB color space** *Source:* [https://en.wikipedia.org/wiki/Adobe\\_RGB\\_color\\_space?oldid=787707240](https://en.wikipedia.org/wiki/Adobe_RGB_color_space?oldid=787707240) *Contributors:* Ixfd64, CesarB, Doug Pardee, Cherkash, Ehn, Finlay McWalter, Francs2000, Hankwang, Slowking Man, Perey, Poccil, Notinasnaid, Minghong, Grutness, Jacobolus, Eclektus, Cambridgeincolour, Adoniscik, YurikBot, Entirety, Xaje, BOT-Superzerocool, Cmglee, SmackBot, Betacommand, Einemmet, Ohconfucius, KeyJ-enwiki, Di2000, Thijs!bot, Lovibond, Sinoue@yahoo.com, MaxPont, Non064, KylieTastic, Cnilep, Svick, GrandDrake, Glenrrp, Wikit2007, Ogat, SilvonenBot, Addbot, Favonian, Lightbot, ພິເນັດໜ້າ, Efa, FrescoBot, Gunarta, BG19bot, BattyBot, OccultZone, Mbearnsstein37, Ying.I.xiong, InternetArchiveBot, ພິເນັດໜ້າ and Anonymous: 14
- **Wide-gamut RGB color space** *Source:* [https://en.wikipedia.org/wiki/Wide-gamut\\_RGB\\_color\\_space?oldid=768772660](https://en.wikipedia.org/wiki/Wide-gamut_RGB_color_space?oldid=768772660) *Contributors:* CesarB, Cherkash, Rvollmert, Slowking Man, Ta bu shi da yu, Notinasnaid, Rufus210, Jacobolus, Ucucha, Entirety, SmackBot, EntiretyToo, VMS Mosaic, Dicklyon, Eshouthe, Ogat, Skarebo, Lightbot, Yobot, Efa, Magicxcian, FrescoBot, Emmarbee, BarrelProof, CarlyCerque, ພິເນັດໜ້າ and Anonymous: 8
- **ProPhoto RGB color space** *Source:* [https://en.wikipedia.org/wiki/ProPhoto\\_RGB\\_color\\_space?oldid=778164833](https://en.wikipedia.org/wiki/ProPhoto_RGB_color_space?oldid=778164833) *Contributors:* Cherkash, Gifflite, Hugowolf, Jacobolus, GregorB, Entirety, Cmglee, Egilizard, EntiretyToo, VMS Mosaic, Stratadrake, AstroPig7, Lovibond, Fallschirmjäger, Forlornturtle, Michael Frind, Fnordware, Eshouthe, XLinkBot, Ogat, Skarebo, Addbot, Favonian, OlEnglish, Yobot, AnomieBOT, Efa, Obersachsebot, Dr RobH, Leolokey, BG19bot, ColeLoki, ພິເນັດໜ້າ and Anonymous: 13
- **ScRGB** *Source:* <https://en.wikipedia.org/wiki/ScRGB?oldid=738513754> *Contributors:* Behnam, Imroy, Spitzak, Mindmatrix, Jacobolus, Panoptical, Mysid, Rwalker, SmackBot, Tobias Schmidbauer, PetesGuide, Snogglethorpe, Smhanov, Philipp Kern, Cydebot, Lovibond, Dougher, Magioladitis, B. Wolterding, Little Professor, ArdenD, OrenT, St.Isaiah, Fuddle, GrandDrake, Yobot, Efa, Christoph hausner, GreenC bot and Anonymous: 3
- **DCI-P3** *Source:* <https://en.wikipedia.org/wiki/DCI-P3?oldid=781597669> *Contributors:* AxelBoldt, QuantumShadow, Quantum7, Lovibond, Magioladitis, TheHoax, Eamon Nerbonne, GrandDrake, Yobot, AnomieBOT, LilHelpa, Lonaowna, Jasonanaggie, BG19bot, Flugaal, Aidanbeardsley, Dialga 20, Kenji Gunawan, Itsquietuptown, Avtarrekhi and Anonymous: 17
- **Rec. 709** *Source:* [https://en.wikipedia.org/wiki/Rec.\\_709?oldid=780068529](https://en.wikipedia.org/wiki/Rec._709?oldid=780068529) *Contributors:* Ciphergoth, Cherkash, Gutza, Boffy b, DmitryKo, Rapscallion, Jacobolus, Mulligatawny, Cat5nap, Adoniscik, Mysid, Mikus, KJBracey, Farski, J Milburn, Cxw, Balazer, Thijs!bot, Glennchan, Davidhorman, Alissovski, DjScrawl, RingtailedFox, Cpoynont, GrandDrake, Copyeditor42, Addbot, Lemmusdk, Yobot, AnomieBOT, Jrosdahl, BroderickAU, Major Eleven, Helpful Pixie Bot, Bruno.uy and Anonymous: 28
- **Rec. 2020** *Source:* [https://en.wikipedia.org/wiki/Rec.\\_2020?oldid=780055806](https://en.wikipedia.org/wiki/Rec._2020?oldid=780055806) *Contributors:* Cherkash, Chrisdolan, DmitryKo, Alis-tair1978, Dan100, Mulligatawny, Zimbabweed, C.Fred, Onejaguar, Wikien2009, Lovibond, Fuddle, GrandDrake, Addbot, Yobot, Jsharp-minor, Jonorza, Lonaowna, LiberatorG, S-1-5-7, Jasonanaggie, Kokken Tor, Senator2029, Harizotoh9, Jodosma, Avieshek, Skyfall, Dust-ingreer, Bender the Bot and Anonymous: 21
- **Rec. 2100** *Source:* [https://en.wikipedia.org/wiki/Rec.\\_2100?oldid=776794689](https://en.wikipedia.org/wiki/Rec._2100?oldid=776794689) *Contributors:* GrandDrake, Yobot, Smoro100 and Anonymous: 2

## 3.2 Images

- **File:5-cell.gif** *Source:* <https://upload.wikimedia.org/wikipedia/commons/d/d8/5-cell.gif> *License:* Public domain *Contributors:* Transferred from en.wikipedia to Commons. *Original artist:* JasonHise at English Wikipedia
- **File:Ambox\_important.svg** *Source:* [https://upload.wikimedia.org/wikipedia/commons/b/b4/Ambox\\_important.svg](https://upload.wikimedia.org/wikipedia/commons/b/b4/Ambox_important.svg) *License:* Public domain *Contributors:* Own work, based off of Image:Ambox scales.svg *Original artist:* Dsmurat (talk · contribs)
- **File:BirdCone.png** *Source:* <https://upload.wikimedia.org/wikipedia/commons/2/29/BirdCone.png> *License:* Public domain *Contributors:* Own work *Original artist:* Jimfbleak
- **File:Black-body\_realization.png** *Source:* [https://upload.wikimedia.org/wikipedia/commons/0/08/Black-body\\_realization.png](https://upload.wikimedia.org/wikipedia/commons/0/08/Black-body_realization.png) *License:* CC BY-SA 3.0 *Contributors:* Own work *Original artist:* Brews ohare
- **File:Black\_body.svg** *Source:* [https://upload.wikimedia.org/wikipedia/commons/1/19/Black\\_body.svg](https://upload.wikimedia.org/wikipedia/commons/1/19/Black_body.svg) *License:* Public domain *Contributors:* Own work *Original artist:* Darth Kule
- **File:BlackbodyEnergies.svg** *Source:* <https://upload.wikimedia.org/wikipedia/commons/1/1d/BlackbodyEnergies.svg> *License:* CC BY-SA 4.0 *Contributors:* <https://systemreboot.net/post/black-body-energy-as-a-sum-of-photon-oscillator-energies> *Original artist:* Arun Isaac
- **File:CIE-1931\_diagram\_in\_LAB\_space.svg** *Source:* [https://upload.wikimedia.org/wikipedia/commons/5/5f/CIE-1931\\_diagram\\_in\\_LAB\\_space.svg](https://upload.wikimedia.org/wikipedia/commons/5/5f/CIE-1931_diagram_in_LAB_space.svg) *License:* CC BY-SA 3.0 *Contributors:* File:Chromaticity diagram full.pdf *Original artist:* User:Fuzzypeg at en.wikipedia, derived from a work by User:Paulschou at en.wikipedia
- **File:CIE1931\_RGBCMF.svg** *Source:* [https://upload.wikimedia.org/wikipedia/commons/6/69/CIE1931\\_RGBCMF.svg](https://upload.wikimedia.org/wikipedia/commons/6/69/CIE1931_RGBCMF.svg) *License:* Public domain *Contributors:* Transferred from en.wikipedia to Commons by Kanie. *Original artist:* Marco Polo at English Wikipedia
- **File:CIE1931\_rgxy.png** *Source:* [https://upload.wikimedia.org/wikipedia/commons/1/16/CIE1931\\_rgxy.png](https://upload.wikimedia.org/wikipedia/commons/1/16/CIE1931_rgxy.png) *License:* Public domain *Contributors:* ? *Original artist:* ?

- **File:CIE1931simple.png** *Source:* <https://upload.wikimedia.org/wikipedia/commons/6/67/CIE1931simple.png> *License:* CC-BY-SA-3.0 *Contributors:* ? *Original artist:* ?
- **File:CIE1931xy\_CIERGB.svg** *Source:* [https://upload.wikimedia.org/wikipedia/commons/6/60/CIE1931xy\\_CIERGB.svg](https://upload.wikimedia.org/wikipedia/commons/6/60/CIE1931xy_CIERGB.svg) *License:* Public domain *Contributors:* Own work, inspired by File:CIExy1931.png *Original artist:* BenRG
- **File:CIE1931xy\_blank.svg** *Source:* [https://upload.wikimedia.org/wikipedia/commons/3/3b/CIE1931xy\\_blank.svg](https://upload.wikimedia.org/wikipedia/commons/3/3b/CIE1931xy_blank.svg) *License:* Public domain *Contributors:* File:CIExy1931.svg *Original artist:* BenRG
- **File:CIE1931xy\_gamut\_comparison.svg** *Source:* [https://upload.wikimedia.org/wikipedia/commons/1/1e/CIE1931xy\\_gamut\\_comparison.svg](https://upload.wikimedia.org/wikipedia/commons/1/1e/CIE1931xy_gamut_comparison.svg) *License:* CC BY-SA 3.0 *Contributors:* [http://commons.wikimedia.org/wiki/File:CIE1931xy\\_blank.svg](http://commons.wikimedia.org/wiki/File:CIE1931xy_blank.svg) *Original artist:* BenRG and cmgtee
- **File:CIECAM02\_inputs.svg** *Source:* [https://upload.wikimedia.org/wikipedia/commons/0/0e/CIECAM02\\_inputs.svg](https://upload.wikimedia.org/wikipedia/commons/0/0e/CIECAM02_inputs.svg) *License:* Public domain *Contributors:* Own work *Original artist:* Adoniscik
- **File:CIELAB\_color\_space\_front\_view.png** *Source:* [https://upload.wikimedia.org/wikipedia/commons/7/7d/CIELAB\\_color\\_space\\_front\\_view.png](https://upload.wikimedia.org/wikipedia/commons/7/7d/CIELAB_color_space_front_view.png) *License:* CC BY-SA 4.0 *Contributors:* Own work *Original artist:* Holger Everding
- **File:CIELAB\_color\_space\_top\_view.png** *Source:* [https://upload.wikimedia.org/wikipedia/commons/0/06/CIELAB\\_color\\_space\\_top\\_view.png](https://upload.wikimedia.org/wikipedia/commons/0/06/CIELAB_color_space_top_view.png) *License:* CC BY-SA 4.0 *Contributors:* Own work *Original artist:* Holger kkk Everding
- **File:CIE\_1931\_XYZ\_Color\_Matching\_Functions.svg** *Source:* [https://upload.wikimedia.org/wikipedia/commons/8/8f/CIE\\_1931\\_XYZ\\_Color\\_Matching\\_Functions.svg](https://upload.wikimedia.org/wikipedia/commons/8/8f/CIE_1931_XYZ_Color_Matching_Functions.svg) *License:* GFDL *Contributors:* Own work *Original artist:* User:Acdx
- **File:CIE\_1976\_UCS.png** *Source:* [https://upload.wikimedia.org/wikipedia/commons/8/83/CIE\\_1976\\_UCS.png](https://upload.wikimedia.org/wikipedia/commons/8/83/CIE_1976_UCS.png) *License:* Public domain *Contributors:* Own work *Original artist:* Adoniscik
- **File:CIE\_UVW\_Diagramme\_de\_chromaticité\_002.png** *Source:* [https://upload.wikimedia.org/wikipedia/commons/3/38/CIE\\_UVW\\_Diagramme\\_de\\_chromaticit%C3%A9\\_002.png](https://upload.wikimedia.org/wikipedia/commons/3/38/CIE_UVW_Diagramme_de_chromaticit%C3%A9_002.png) *License:* CC BY-SA 3.0 *Contributors:* Own work *Original artist:* Alasjourn
- **File:CIE\_illuminants\_A,B,C.svg** *Source:* [https://upload.wikimedia.org/wikipedia/commons/2/27/CIE\\_illuminants\\_A%2CB%2CC.svg](https://upload.wikimedia.org/wikipedia/commons/2/27/CIE_illuminants_A%2CB%2CC.svg) *License:* Public domain *Contributors:* Own work *Original artist:* Adoniscik
- **File:CIE\_illuminants\_D\_and\_blackbody\_small.gif** *Source:* [https://upload.wikimedia.org/wikipedia/commons/2/21/CIE\\_illuminants\\_D\\_and\\_blackbody\\_small.gif](https://upload.wikimedia.org/wikipedia/commons/2/21/CIE_illuminants_D_and_blackbody_small.gif) *License:* CC BY 3.0 *Contributors:* Own work *Original artist:* Adoniscik
- **File:CIE\_illuminants\_D\_components.svg** *Source:* [https://upload.wikimedia.org/wikipedia/commons/5/51/CIE\\_illuminants\\_D\\_components.svg](https://upload.wikimedia.org/wikipedia/commons/5/51/CIE_illuminants_D_components.svg) *License:* Public domain *Contributors:* Own work *Original artist:* Adoniscik
- **File:CIE\_illuminants\_F\_10-12.svg** *Source:* [https://upload.wikimedia.org/wikipedia/commons/c/cb/CIE\\_illuminants\\_F\\_10-12.svg](https://upload.wikimedia.org/wikipedia/commons/c/cb/CIE_illuminants_F_10-12.svg) *License:* CC BY-SA 3.0 *Contributors:* Own work *Original artist:* Adoniscik
- **File:CIE\_illuminants\_F\_1\_to\_6.svg** *Source:* [https://upload.wikimedia.org/wikipedia/commons/4/46/CIE\\_illuminants\\_F\\_1\\_to\\_6.svg](https://upload.wikimedia.org/wikipedia/commons/4/46/CIE_illuminants_F_1_to_6.svg) *License:* CC BY-SA 3.0 *Contributors:* Own work *Original artist:* Adoniscik
- **File:CIE\_illuminants\_F\_7-9.svg** *Source:* [https://upload.wikimedia.org/wikipedia/commons/a/a7/CIE\\_illuminants\\_F\\_7-9.svg](https://upload.wikimedia.org/wikipedia/commons/a/a7/CIE_illuminants_F_7-9.svg) *License:* CC BY-SA 3.0 *Contributors:* Own work *Original artist:* Adoniscik
- **File:CIE\_rg\_Diagram.jpg** *Source:* [https://upload.wikimedia.org/wikipedia/en/8/8d/CIE\\_rg\\_Diagram.jpg](https://upload.wikimedia.org/wikipedia/en/8/8d/CIE_rg_Diagram.jpg) *License:* Fair use *Contributors:* <http://home.btconnect.com/mike.flemming/technical/colour2.htm> *Original artist:* mike flemming
- **File:CIExy1931\_AdobeRGB.png** *Source:* [https://upload.wikimedia.org/wikipedia/commons/5/53/CIExy1931\\_AdobeRGB.png](https://upload.wikimedia.org/wikipedia/commons/5/53/CIExy1931_AdobeRGB.png) *License:* CC-BY-SA-3.0 *Contributors:* ? *Original artist:* ?
- **File:CIExy1931\_AdobeRGB\_vs\_sRGB.png** *Source:* [https://upload.wikimedia.org/wikipedia/commons/0/0f/CIExy1931\\_AdobeRGB\\_vs\\_sRGB.png](https://upload.wikimedia.org/wikipedia/commons/0/0f/CIExy1931_AdobeRGB_vs_sRGB.png) *License:* CC BY-SA 3.0 *Contributors:* Own work *Original artist:* Mbearnstein37
- **File:CIExy1931\_AdobeWGRGB.png** *Source:* [https://upload.wikimedia.org/wikipedia/commons/1/1d/CIExy1931\\_AdobeWGRGB.png](https://upload.wikimedia.org/wikipedia/commons/1/1d/CIExy1931_AdobeWGRGB.png) *License:* Public domain *Contributors:* Transferred from en.wikipedia to Commons by Wadester16 using CommonsHelper. *Original artist:* Entirety at English Wikipedia
- **File:CIExy1931\_ProPhoto.svg** *Source:* [https://upload.wikimedia.org/wikipedia/commons/e/eb/CIExy1931\\_ProPhoto.svg](https://upload.wikimedia.org/wikipedia/commons/e/eb/CIExy1931_ProPhoto.svg) *License:* Public domain *Contributors:* en:File:CIExy1931 ProPhoto.png *Original artist:* Fred the Oyster
- **File:CIExy1931\_Rec\_2020.svg** *Source:* [https://upload.wikimedia.org/wikipedia/commons/b/b6/CIExy1931\\_Rec\\_2020.svg](https://upload.wikimedia.org/wikipedia/commons/b/b6/CIExy1931_Rec_2020.svg) *License:* CC BY-SA 3.0 *Contributors:*
- CIExy1931.svg *Original artist:* CIExy1931.svg: Sakurambo
- **File:CIExy1931\_Rec\_709.svg** *Source:* [https://upload.wikimedia.org/wikipedia/commons/e/ef/CIExy1931\\_Rec\\_709.svg](https://upload.wikimedia.org/wikipedia/commons/e/ef/CIExy1931_Rec_709.svg) *License:* CC BY-SA 3.0 *Contributors:*
- CIExy1931.svg *Original artist:* CIExy1931.svg: Sakurambo
- **File:CRT\_phosphors.png** *Source:* [https://upload.wikimedia.org/wikipedia/commons/2/29/CRT\\_phosphors.png](https://upload.wikimedia.org/wikipedia/commons/2/29/CRT_phosphors.png) *License:* CC-BY-SA-3.0 *Contributors:* Transferred from en.wikipedia Transfer was stated to be made by User:Nopira. *Original artist:* Original uploader was Deglr6328 at en.wikipedia
- **File:Canon\_S520\_ink\_jet\_printer\_-\_opened\_(cropped).jpg** *Source:* [https://upload.wikimedia.org/wikipedia/commons/8/85/Canon\\_S520\\_ink\\_jet\\_printer\\_-\\_opened\\_%28cropped%29.jpg](https://upload.wikimedia.org/wikipedia/commons/8/85/Canon_S520_ink_jet_printer_-_opened_%28cropped%29.jpg) *License:* CC BY-SA 2.5 *Contributors:* Own work *Original artist:* André Karwath aka Aka
- **File:Cie\_Chart\_with\_sRGB\_gamut\_by\_spigget.png** *Source:* [https://upload.wikimedia.org/wikipedia/commons/6/60/Cie\\_Chart\\_with\\_sRGB\\_gamut\\_by\\_spigget.png](https://upload.wikimedia.org/wikipedia/commons/6/60/Cie_Chart_with_sRGB_gamut_by_spigget.png) *License:* CC BY-SA 3.0 *Contributors:* Own work *Original artist:* Spigget
- **File:Ciecam02\_degree\_of\_adaptation.svg** *Source:* [https://upload.wikimedia.org/wikipedia/commons/1/1a/Ciecam02\\_degree\\_of\\_adaptation.svg](https://upload.wikimedia.org/wikipedia/commons/1/1a/Ciecam02_degree_of_adaptation.svg) *License:* Public domain *Contributors:* Own work *Original artist:* Adoniscik
- **File:Ciecam02\_luminance\_level\_adaptation\_factor.svg** *Source:* [https://upload.wikimedia.org/wikipedia/commons/8/8e/Ciecam02\\_luminance\\_level\\_adaptation\\_factor.svg](https://upload.wikimedia.org/wikipedia/commons/8/8e/Ciecam02_luminance_level_adaptation_factor.svg) *License:* Public domain *Contributors:* MATLAB *Original artist:* Myself

- **File:Ciecat02\_response\_compression.svg** *Source:* [https://upload.wikimedia.org/wikipedia/commons/1/11/Ciecat02\\_response\\_compression.svg](https://upload.wikimedia.org/wikipedia/commons/1/11/Ciecat02_response_compression.svg) *License:* Public domain *Contributors:* Own work *Original artist:* Adoniscik
- **File:Colouring\_pencils.jpg** *Source:* [https://upload.wikimedia.org/wikipedia/commons/b/b1/Colouring\\_pencils.jpg](https://upload.wikimedia.org/wikipedia/commons/b/b1/Colouring_pencils.jpg) *License:* CC BY-SA 3.0 *Contributors:* Own work *Original artist:* MichaelMaggs
- **File:Comparison\_between\_CIE\_luminosity\_function\_and\_M\_cone\_response.svg** *Source:* [https://upload.wikimedia.org/wikipedia/commons/6/65/Comparison\\_between\\_CIE\\_luminosity\\_function\\_and\\_M\\_cone\\_response.svg](https://upload.wikimedia.org/wikipedia/commons/6/65/Comparison_between_CIE_luminosity_function_and_M_cone_response.svg) *License:* CC0 *Contributors:* Drawn up in Inkscape, following the traces contained in File:CIE 1931 XYZ Color Matching Functions.svg and File:Cones SMJ2 E.svg *Original artist:* Fuzzytype
- **File:Cone\_cell\_eng.png** *Source:* [https://upload.wikimedia.org/wikipedia/commons/4/48/Cone\\_cell\\_eng.png](https://upload.wikimedia.org/wikipedia/commons/4/48/Cone_cell_eng.png) *License:* CC BY-SA 3.0 *Contributors:* Own work *Original artist:* Ivo Kruusamägi
- **File:Cones\_SMJ2\_E.svg** *Source:* [https://upload.wikimedia.org/wikipedia/commons/1/1e/Cones\\_SMJ2\\_E.svg](https://upload.wikimedia.org/wikipedia/commons/1/1e/Cones_SMJ2_E.svg) *License:* CC BY-SA 3.0 *Contributors:* Based on Dicklyon's PNG version, itself based on data from Stockman, MacLeod & Johnson (1993) Journal of the Optical Society of America A, 10, 2491-2521d <http://psy.ucsd.edu/~{}dmacleod/publications/61StockmanMacLeodJohnson1993.pdf> (log E human cone response, via <http://www.cvrl.org/database/text/cones/smj2.htm>) *Original artist:* Vanessazekowitz at en.wikipedia / Later version uploaded by BenRG.
- **File:DCI-P3\_D65.svg** *Source:* [https://upload.wikimedia.org/wikipedia/commons/e/e4/DCI-P3\\_D65.svg](https://upload.wikimedia.org/wikipedia/commons/e/e4/DCI-P3_D65.svg) *License:* CC BY-SA 3.0 *Contributors:*
- CIExy1931.svg *Original artist:* CIExy1931.svg: Sakurambo
- **File:Daylight-locus-in-CIE-1960-UCS.png** *Source:* <https://upload.wikimedia.org/wikipedia/commons/3/39/Daylight-locus-in-CIE-1960-UCS.png> *License:* GFDL *Contributors:* Own work *Original artist:* Adoniscik
- **File>Edit-clear.svg** *Source:* <https://upload.wikimedia.org/wikipedia/en/f/f2/Edit-clear.svg> *License:* Public domain *Contributors:* The Tango! Desktop Project. *Original artist:*  
The people from the Tango! project. And according to the meta-data in the file, specifically: "Andreas Nilsson, and Jakub Steiner (although minimally.)"
- **File:EffectiveTemperature\_300dpi\_e.png** *Source:* [https://upload.wikimedia.org/wikipedia/commons/0/0d/EffectiveTemperature\\_300dpi\\_e.png](https://upload.wikimedia.org/wikipedia/commons/0/0d/EffectiveTemperature_300dpi_e.png) *License:* CC-BY-SA-3.0 *Contributors:* Drawn by myself. The solar spectrum is the WRC spectrum provided by M. Iqbal: *An Introduction to Solar Radiation*, Academic Press 1983, Table C1. The black body spectral irradiance has been computed from a black-body spectrum for T equal 5777 K and assuming a solid angle of 6.8e-5 steradian for the source (the solar disk). *Original artist:* Sch
- **File:Effective\_temperature\_and\_color\_index.png** *Source:* [https://upload.wikimedia.org/wikipedia/commons/e/e9/Effective\\_temperature\\_and\\_color\\_index.png](https://upload.wikimedia.org/wikipedia/commons/e/e9/Effective_temperature_and_color_index.png) *License:* CC BY-SA 3.0 *Contributors:* Own work *Original artist:* Brews ohare
- **File:Elkhorn\_Slough.jpg** *Source:* [https://upload.wikimedia.org/wikipedia/commons/c/c7/Elkhorn\\_Slough.jpg](https://upload.wikimedia.org/wikipedia/commons/c/c7/Elkhorn_Slough.jpg) *License:* CC BY-SA 3.0 *Contributors:* Own work *Original artist:* Augurar
- **File:Example\_of\_LAB\_color\_enhancement.jpg** *Source:* [https://upload.wikimedia.org/wikipedia/commons/f/f3/Example\\_of\\_LAB\\_color\\_enhancement.jpg](https://upload.wikimedia.org/wikipedia/commons/f/f3/Example_of_LAB_color_enhancement.jpg) *License:* CCO *Contributors:* Own work *Original artist:* Ll1324
- **File:Folder\_Hexagonal\_Icon.svg** *Source:* [https://upload.wikimedia.org/wikipedia/en/4/48/Folder\\_Hexagonal\\_Icon.svg](https://upload.wikimedia.org/wikipedia/en/4/48/Folder_Hexagonal_Icon.svg) *License:* Cc-by-sa-3.0 *Contributors:* ? *Original artist:* ?
- **File:Idealized\_photosphere.png** *Source:* [https://upload.wikimedia.org/wikipedia/commons/7/74/Idealized\\_photosphere.png](https://upload.wikimedia.org/wikipedia/commons/7/74/Idealized_photosphere.png) *License:* CC BY-SA 3.0 *Contributors:* Own work *Original artist:* Brews ohare
- **File:Image\_without\_chromaticity.png** *Source:* [https://upload.wikimedia.org/wikipedia/commons/4/47/Image\\_without\\_chromaticity.png](https://upload.wikimedia.org/wikipedia/commons/4/47/Image_without_chromaticity.png) *License:* CC BY-SA 3.0 *Contributors:* Own work *Original artist:* Augurar
- **File:Judd'{}s-UCS.png** *Source:* <https://upload.wikimedia.org/wikipedia/commons/2/26/Judd%27s-UCS.png> *License:* CC BY 3.0 *Contributors:* Own work *Original artist:* Adoniscik
- **File:LCD\_pixels\_RGB\_(cropped).jpg** *Source:* [https://upload.wikimedia.org/wikipedia/commons/5/53/LCD\\_pixels\\_RGB\\_%28cropped%29.jpg](https://upload.wikimedia.org/wikipedia/commons/5/53/LCD_pixels_RGB_%28cropped%29.jpg) *License:* Public domain *Contributors:* Own work *Original artist:* Robin01
- **File:Lab\_color\_space.png** *Source:* [https://upload.wikimedia.org/wikipedia/commons/2/21/Lab\\_color\\_space.png](https://upload.wikimedia.org/wikipedia/commons/2/21/Lab_color_space.png) *License:* CC BY-SA 3.0 *Contributors:* Own work *Original artist:* Jacob Rus
- **File:Laser\_Pointer.jpg** *Source:* [https://upload.wikimedia.org/wikipedia/commons/8/8f/Laser\\_Pointer.jpg](https://upload.wikimedia.org/wikipedia/commons/8/8f/Laser_Pointer.jpg) *License:* GFDL *Contributors:* Own work *Original artist:* Pang Kakit
- **File:Lock-green.svg** *Source:* <https://upload.wikimedia.org/wikipedia/commons/6/65/Lock-green.svg> *License:* CC0 *Contributors:* en:File:Free-to-read\_lock\_75.svg *Original artist:* User:Trappist the monk
- **File:Opponent\_colors.svg** *Source:* [https://upload.wikimedia.org/wikipedia/commons/7/71/Opponent\\_colors.svg](https://upload.wikimedia.org/wikipedia/commons/7/71/Opponent_colors.svg) *License:* CC-BY-SA-3.0 *Contributors:* Own work *Original artist:* User:Spooky
- **File:Planckian-locus-approximation.png** *Source:* <https://upload.wikimedia.org/wikipedia/commons/5/57/Planckian-locus-approximation.png> *License:* Public domain *Contributors:* Own work *Original artist:* Adoniscik
- **File:Planckian-locus.png** *Source:* <https://upload.wikimedia.org/wikipedia/commons/d/d7/Planckian-locus.png> *License:* Public domain *Contributors:* Own work *Original artist:* Adoniscik
- **File:PlanckianLocus.png** *Source:* <https://upload.wikimedia.org/wikipedia/commons/b/ba/PlanckianLocus.png> *License:* Public domain *Contributors:* en:User:PAR *Original artist:* en:User:PAR
- **File:Portal-puzzle.svg** *Source:* <https://upload.wikimedia.org/wikipedia/en/f/fd/Portal-puzzle.svg> *License:* Public domain *Contributors:* ? *Original artist:* ?
- **File:Question\_book-new.svg** *Source:* [https://upload.wikimedia.org/wikipedia/en/9/99/Question\\_book-new.svg](https://upload.wikimedia.org/wikipedia/en/9/99/Question_book-new.svg) *License:* Cc-by-sa-3.0 *Contributors:*  
Created from scratch in Adobe Illustrator. Based on Image:Question book.png created by User:Equazcion *Original artist:* Tkgd2007

- **File:RBG\_color\_wheel.svg** *Source:* [https://upload.wikimedia.org/wikipedia/commons/a/ab/RBG\\_color\\_wheel.svg](https://upload.wikimedia.org/wikipedia/commons/a/ab/RBG_color_wheel.svg) *License:* CC BY-SA 3.0 *Contributors:* Own work (Original text: *self-made*) *Original artist:* DanPMK
- **File:RGB\_Cube\_Show\_lowgamma\_cutout\_b.png** *Source:* [https://upload.wikimedia.org/wikipedia/commons/8/83/RGB\\_Cube\\_Show\\_lowgamma\\_cutout\\_b.png](https://upload.wikimedia.org/wikipedia/commons/8/83/RGB_Cube_Show_lowgamma_cutout_b.png) *License:* CC BY-SA 3.0 *Contributors:*
- RGB\_farbwuerfel.jpg *Original artist:* RGB\_farbwuerfel.jpg; Horst Frank
- **File:RG\_Chromaticity\_Example.png** *Source:* [https://upload.wikimedia.org/wikipedia/commons/0/09/RG\\_Chromaticity\\_Example.png](https://upload.wikimedia.org/wikipedia/commons/0/09/RG_Chromaticity_Example.png) *License:* CC BY-SA 3.0 *Contributors:* Own work *Original artist:* Augurar
- **File:RWP-comparison.svg** *Source:* <https://upload.wikimedia.org/wikipedia/commons/7/72/RWP-comparison.svg> *License:* CC-BY-SA-3.0 *Contributors:* Own work *Original artist:* sfu
- **File:Rg\_normalized\_color\_coordinates.png** *Source:* [https://upload.wikimedia.org/wikipedia/en/7/7b/Rg\\_normalized\\_color\\_coordinates.png](https://upload.wikimedia.org/wikipedia/en/7/7b/Rg_normalized_color_coordinates.png) *License:* CC-BY-SA-3.0 *Contributors:*  
Plot generated with an Object Pascal program I written myself  
*Original artist:*  
Vampyrium
- **File:SPD\_D65.png** *Source:* [https://upload.wikimedia.org/wikipedia/commons/d/d0/SPD\\_D65.png](https://upload.wikimedia.org/wikipedia/commons/d/d0/SPD_D65.png) *License:* Public domain *Contributors:* The raw spectral data are from CIE Publication 15.2 Colorimetry. Values for (x, y), CCT, and CRI were computed using software developed by me as a teaching tool for AE 9200 Color Theory, which I teach at the University of Nebraska *Original artist:* Kevin Houser (Loucetios)
- **File:SRGB\_gamma.svg** *Source:* [https://upload.wikimedia.org/wikipedia/commons/e/ef/SRGB\\_gamma.svg](https://upload.wikimedia.org/wikipedia/commons/e/ef/SRGB_gamma.svg) *License:* Public domain *Contributors:* Transferred from en.wikipedia to Commons by Shizhao using CommonsHelper. *Original artist:* Dicklyon at English Wikipedia
- **File:SRGB\_gamut\_within\_CIELAB\_color\_space\_isosurface.png** *Source:* [https://upload.wikimedia.org/wikipedia/commons/7/70/SRGB\\_gamut\\_within\\_CIELAB\\_color\\_space\\_isosurface.png](https://upload.wikimedia.org/wikipedia/commons/7/70/SRGB_gamut_within_CIELAB_color_space_isosurface.png) *License:* CC BY-SA 4.0 *Contributors:* Own work. Download the source code here and animation frames here. *Original artist:* Michael Horvath (SharkD), Christoph Lipka
- **File:SRGB\_gamut\_within\_CIELUV\_color\_space\_isosurface.png** *Source:* [https://upload.wikimedia.org/wikipedia/commons/e/e8/SRGB\\_gamut\\_within\\_CIELUV\\_color\\_space\\_isosurface.png](https://upload.wikimedia.org/wikipedia/commons/e/e8/SRGB_gamut_within_CIELUV_color_space_isosurface.png) *License:* CC BY-SA 4.0 *Contributors:* Own work. Download the source code here and animation frames here. *Original artist:* Michael Horvath (SharkD), Christoph Lipka
- **File:SRGB\_gamut\_within\_CIEXYZ\_color\_space\_isosurface.png** *Source:* [https://upload.wikimedia.org/wikipedia/commons/1/13/SRGB\\_gamut\\_within\\_CIEXYZ\\_color\\_space\\_isosurface.png](https://upload.wikimedia.org/wikipedia/commons/1/13/SRGB_gamut_within_CIEXYZ_color_space_isosurface.png) *License:* CC BY-SA 4.0 *Contributors:* Own work. Download the source code here and animation frames here. *Original artist:* Michael Horvath (SharkD), Christoph Lipka
- **File:SRGB\_gamut\_within\_CIExY\_color\_space\_isosurface.png** *Source:* [https://upload.wikimedia.org/wikipedia/commons/f/f1/SRGB\\_gamut\\_within\\_CIExY\\_color\\_space\\_isosurface.png](https://upload.wikimedia.org/wikipedia/commons/f/f1/SRGB_gamut_within_CIExY_color_space_isosurface.png) *License:* CC BY-SA 4.0 *Contributors:* Own work. Download the source code here and animation frames here. *Original artist:* Michael Horvath (SharkD), Christoph Lipka
- **File:ScRGB.svg** *Source:* <https://upload.wikimedia.org/wikipedia/en/4/46/ScRGB.svg> *License:* PD *Contributors:* ? *Original artist:* ?
- **File:Självporträtt\_av\_Anders\_Zorn\_1896.jpg** *Source:* [https://upload.wikimedia.org/wikipedia/commons/b/ba/Sj%C3%A4lvportr%C3%A4tt\\_av\\_Anders\\_Zorn\\_1896.jpg](https://upload.wikimedia.org/wikipedia/commons/b/ba/Sj%C3%A4lvportr%C3%A4tt_av_Anders_Zorn_1896.jpg) *License:* Public domain *Contributors:* Unknown *Original artist:* Anders Zorn
- **File:Spectral\_sensibilities.png** *Source:* [https://upload.wikimedia.org/wikipedia/commons/c/c0/Spectral\\_sensibilities.png](https://upload.wikimedia.org/wikipedia/commons/c/c0/Spectral_sensibilities.png) *License:* Public domain *Contributors:* Light and shade and their applications *Original artist:* Matthew Luckiesh
- **File:Srgbnonlinearity.png** *Source:* <https://upload.wikimedia.org/wikipedia/commons/c/c9/Srgbnonlinearity.png> *License:* CC-BY-SA-3.0 *Contributors:* English Wikipedia *Original artist:* Army1987 (talk) and Dicklyon (talk)
- **File:Stockmansharpe10degCMFadj2000\_popconsens.svg** *Source:* [https://upload.wikimedia.org/wikipedia/commons/5/52/Stockmansharpe10degCMFadj2000\\_popconsens.svg](https://upload.wikimedia.org/wikipedia/commons/5/52/Stockmansharpe10degCMFadj2000_popconsens.svg) *License:* CC0 *Contributors:* ? *Original artist:* ?
- **File:Symbol\_template\_class.svg** *Source:* [https://upload.wikimedia.org/wikipedia/en/5/5c/Symbol\\_template\\_class.svg](https://upload.wikimedia.org/wikipedia/en/5/5c/Symbol_template_class.svg) *License:* Public domain *Contributors:* ? *Original artist:* ?

### 3.3 Content license

- Creative Commons Attribution-Share Alike 3.0